

Timber on Top

A parametric exploration of CLT vertical extensions in the Rotterdamse Laag

R.A.A. Kwakman | 10 January 2024



 **TU Delft**
—
**VAN
ROSSUM**

Timber on Top

A Parametric Exploration of CLT Vertical Extension Potential in the Rotterdamse Laag

by

R.A.A. Kwakman

in partial fulfilment of the requirements for the degree of

Master of Science
in Civil Engineering

at the Delft University of Technology,
to be defended publicly on Friday January 19, 2024 at 10:00 AM.

Student number: 4577922
Graduation Company: Van Rossum Raadgevende Ingenieurs

Thesis committee

Supervisor:	Prof. dr. ir. P.C. Louter	TU Delft
Thesis committee:	Ir. A.C.B. Schuurman	TU Delft
	Ir. M. Felicita	TU Delft
	Ir. D. Bresser	Van Rossum

An electronic version of this thesis is available at <http://repository.tudelft.nl/>

Abstract

The Netherlands is currently experiencing a significant housing crisis with an estimated housing shortage of 380.000 houses. In order to combat this shortage, it is estimated that 100.000 new housing units need to be created yearly. At the time of writing, however, the amount of new houses that is constructed annually is only around 70.000, which means that this housing crisis is nowhere near being solved. Taking note of the fact that urban densification is universally seen as a good way to create more housing, in combination with the fact that one very effective way of urban densification is vertical extension. Sustainable vertical extension can be achieved when using CLT as the main construction material. Two problems arise, however. On the one hand, the process of vertical extension is often approached as a unique problem, which works against a general approach. On the other hand, CLT, while proven to be sustainable and lightweight, is less strong than other construction materials like concrete and can therefore posit more of a design challenge. The following research goal was defined:

Identifying CLT vertical extension potential in existing buildings by creating a parametric tool that considers different types of structural constraints. Ultimately, contributing to informed decision-making practices in the sustainable and effective structural design of vertical extensions.

The methodology of this thesis consists of four parts: the analysis, synthesis, simulation and evaluation phases. In the analysis phase, existing vertical extensions are analyzed, as well as the structural context and the concept of spare capacity, which together form the basis for the synthesis phase. Here, a parametric tool was created using Grasshopper and Karamba. This tool was then utilized in the simulation phase, where a parameter study was carried out using the parameters that were found in the analysis phase. This phase is split into two parts: first the effects of the base geometry of the original structure on the spare capacity found in the structure is assessed, parameters assessed here are the position of the stability core, the base construction grid and the building height. In the second part, the focus shifts to the design of the extension itself and its effect on the utilization of spare capacity in the original building and the utilization of the extension elements. Here, the parameters looked at are the shear wall layout of the extension and the extension grid.

Finally, in the evaluation phase the results are discussed and the report is concluded, furthermore, recommendations are made.

In the parameter study it was found that the presence of a stability core shows the largest effect on the spare capacity found in the existing building. The placement of the stability core also shows a significant effect on the distribution of spare capacity in the original structure. The original construction grid and the original height of the building also have a significant effect on the spare capacity in the building, however, they have less influence on the distribution of spare capacity within the structure.

Furthermore, this study found that large differences in spare capacity utilization of specific elements in the original structure, as well as regular utilization of specific

elements in the extension, can be made by varying with the three proposed wall layouts (core alignment, functional design and façade aligned wall layouts). The most successful wall layout was found to be highly dependent on the geometry of the original structure that the extension was put on top of. The effect of wall layouts on the spare capacity utilization found at element level were visualized to show which columns can become critical in different geometrical configurations of both the original structure and the extension.

Varying with the extension grid shows significant differences in spare capacity utilization as well, but overall the effect is smaller in magnitude than the differences made by varying with wall layout and the differences show less dependency on the geometry of the original structure.

When looking at the utilizations in the vertical extension itself, failure tends to concentrate on the connections between the CLT panels and the CLT floors. Here, wall layouts B (functional design) generate the most extensions that fail.

Finally, it is concluded that the research, combined with the development of a parametric tool satisfied the main goal. The accuracy of the tool is shown with extensive validations regarding the transfer of horizontal loads from the extension to the original structure. Furthermore, the parameter study carried out with the parametric tool showed significant effects of the aforementioned parameters in extension design and the original structure on the extendibility of the building. Thereby showing that the model can show differences between different extension alternatives and can thus be used as a useful and effective tool in exploratory design stages where vertical extension is considered.

Preface

In front of you lies the product of the master thesis that I worked on for the last year. Here, I want to take a few sentences to thank some people who have helped me tremendously during this process.

I first came in contact with the subject of this thesis when brainstorming with Djonno in our first conversation. I have always been incredibly interested in the intersection of old and new buildings and vertical extension turned out to be an amazing way to delve deeper into that fascination. This conversation turned out to become the beginning of a very interesting but also challenging thesis. I also credit this process for helping me find out where my strengths and challenges lie in large projects and how I can use the subjects that interest me as a source of external motivation.

First and foremost I would like to thank the members of my thesis committee. Djonno Bresser from Van Rossum Raadgevende Ingenieurs, for your many helpful tips and unique insight into the practice of structural design. Maria Felicita for our many conversations about timber design and Marco Schuurman for your incredible structural insights which really helped me a lot. Last but not least I want to thank Christian Louter for chairing this committee and guiding me through this process.

I also want to thank Van Rossum for having me, thanks for all the info and data on Rotterdamse Laag buildings. Every time I walked through Rotterdam to go to the office, the many buildings made me feel like my thesis had come to life, which was a very inspiring feeling.

Then, of course, I want to thank my friends and family: Mom, Dad and Lotte for always supporting me and telling me, every couple of months, that 'de laatste loodjes' are the heaviest. They sure were heavy and there were a lot of them but I couldn't have carried them without you. I also want to thank our dog Koda for always being excited to see me.

I want to thank all my friends, I also want to thank some in particular: Geke and Amey, who had a large part in making this thesis happen, at times literally (thanks Geke for letting me borrow your charger, and thanks both for being my fashion committee). Also Lilly for taking many coffee breaks with me. And of course Marc and Martijn for just always being there. Finally, I want to thank Max, who told me, multiple times, that the only way through the process is to stop resisting the process, which (annoyingly) turned out to be true.

*With sincere gratitude,
Rik Kwakman*

Table of contents

Timber on Top.....	1
Abstract.....	2
Preface.....	4
Table of contents.....	5
Chapter 1 - Introduction.....	8
1.1 Background	8
1.1.1 Extension as an urban densification measure	9
1.1.2 CLT.....	10
1.2 Problem definition	11
1.3 Research content.....	12
1.4 Methodology	15
1.5 Scope	16
Part 1 – Analysis	17
Chapter 2 - State of the art of vertical extensions	18
2.1 Case studies.....	19
2.1.1 55 Southbank boulevard - Melbourne.....	19
2.1.2 Glitne Housing	20
2.1.3 Ray 1 – Vienna	21
2.1.4 Strassburger Strasse 40 - Berlin.....	22
2.1.5 St. Jobsveem – Rotterdam	23
2.2 Comparison of projects.....	24
2.3 Conclusions	24
Chapter 3 – Structural context.....	28
3.1 Introduction.....	28
3.2 Rotterdamse Laag	29
3.3 Structural characteristics of Rotterdamse Laag buildings	29
3.4 Spare Capacity	33
3.4.1 Assessing spare capacity	33
3.5 Building codes	34
3.6 Wind loads.....	35
3.7 Strengthening techniques	37
3.8 Conclusions	39
Chapter 4 – CLT.....	40
4.1 Introduction.....	40

4.2 CLT makeup and limitations	40
4.3 Connections.....	41
4.4 CLT shear walls	43
Part 2: Synthesis	53
Chapter 5 – Methodology	54
5.1 Introduction	54
5.2 Studied parameters: original building parameters.....	54
5.3 Studied parameters: extension parameters	56
5.4 Design constraints	60
5.5 Design assumptions	63
5.6 Loads	67
Part 3: Simulation	72
Chapter 6 – Parameter Study Setup	73
6.1 Introduction	73
6.2 Set-up of the first part of the parameter study	73
6.3 Set-up of the second part of the parameter study.....	74
6.3.1 Workflow of part two of the parameter study	75
6.3.2 Colibri.....	76
Chapter 7 – Parameter Study Results.....	78
7.1 Effects of parameters in the original structure	78
7.2 Extension design results.....	86
7.2.1 C1 (corner core) variants	86
7.3 C2 variants	98
7.4 C3 variants	100
7.5 Conclusion results	102
8 Discussion.....	103
8.1 Discussion of results.....	103
8.2 Discussion of the developed grasshopper tool	110
9 Conclusion and recommendations	113
Bibliography	Fout! Bladwijzer niet gedefinieerd.

List of appendices

Appendix A – Design exploration for spare capacity and code calculations (including wind)

Appendix B – Model result verifications

Appendix C – Input verifications for boundary condition reliant elements

Appendix D – Connections for CLT

Appendix E – Model validations

Appendix F – Results elaborations

Chapter 1 - Introduction

1.1 Background

The Netherlands is currently experiencing one of the largest housing crises in recorded history. The shortage of houses has reached a record high the country is currently estimated to be around 310.000 houses short. Due to the 'natural' languor of policy makers and the fact that this housing crisis came as a surprise to many in combination with housing taking time to plan and construct means that a short term solution is more or less out of the question. It is currently estimated that 100.000 new houses should be built every year in order for the housing shortage to decrease by 2024 (Boelhouwer & van der Heijden, 2022). This quota however, has not been reached in recent years since about 75.000 new houses are added to the housing stock annually (Ministerie van Binnelandse Zaken en Koninkrijksrelaties, 2021) and as a matter of fact, the current prognoses do not see this annual number being reached anytime soon, with a housing shortage of 3.1% being projected for 2031 (van Rein & Trappenburg, 2023). This annual shortage of new houses illustrates the need of action and calls for a dramatic increase in identification and/or construction of new housing opportunities.

One solution that has emerged is so-called urban densification: creating more housing in urban environments, where people are already living. The main focus remains on urban densification through the means of expanding on empty plots in the urban environment. PBL (Planbureau voor de Leefomgeving) says that roughly half of the housing demand by 2050 can be fulfilled by creating housing in urban environments, more specifically in vacant buildings and empty plots in cities (Claassens & Koomen, 2017). This would come down to 500.000 extra houses by 2050. It is clear that urban densification can offer a solution to the current housing crisis by adding new housing in existing urban areas. The urban densification potential of in-use buildings themselves, however, is often overlooked completely.

1.1.1 Extension as an urban densification measure

Buildings themselves can offer an alternative to empty plots for urban densification. The process of adding more volume to a building is called extension. Two types of extension exist: horizontal and vertical extension. Through horizontal extension, the building is expanded sideways (horizontally) into an unused plot of land, which means that the building's footprint increases. Vertical extension, on the other hand, means that new volume is added on top of the existing building, therefore not requiring any new area and not increasing the building's footprint. Vertical extension, however, is often limited by the structural constraints instead, i.e. is the structural capacity sufficient for more volume to be put on top of it?

Refurbishment through vertical extension is flagged as 'the best solution for sustainability' because it generally takes less time, space and resources than more traditional approaches (Artes, Wadel, & Martí, 2017). In a case study based in Barcelona, Artes identified 2500 buildings in Barcelona that are considered to have high vertical extension potential, this amounts to about 800.000 square meters of usable area. The process of vertical extension, therefore, seems to be a viable alternative solution for creating significant amounts of new housing in urban areas.

What makes vertical extensions challenging however, is the large variety in base constraints that make every building a different problem. The extension of existing structures is therefore often considered a unique challenge every time. With this combination of complexity and cost in mind, it is often deemed 'easier' to demolish the existing building and design something completely new on the same plot of land.

This means that, in spite of the fact that refurbishment of an existing building is often more sustainable than demolition of said building, demolition is still the go to practice for a lot of end-of-life buildings in the Netherlands. For example, in 2022 it was found that about 8000 social housing homes are demolished. All the while, the same article shows that renovation of those homes would have been cheaper, faster and more environmentally friendly (Hendriks, 2022).

When considering the urgency of the housing crisis, this suggests a need for a more methodical approach to the identification and design of potentially extendable buildings. This would allow more buildings to be extended and thus more housing opportunities in cities.

1.1.2 CLT

What makes vertical extensions challenging in most, if not all cases are the aforementioned structural constraints of the original building. If a building is going to be extended with little to no structural interventions in the original structure, it is very important that the added loads that come with the extension are within the limits of whatever capacity is still available in the main structure. In order to achieve this, the most efficient way to create a large amount of extension volume is by utilizing lightweight materials in the structure of the extension.

CLT is a material that is cherished for its lightweight properties and therefore, at first sight, very suitable for use in vertical extensions.

While timber has been used in structures for a very long time, in the 20th century, steel and concrete became more prevalent structural materials. This can be explained by the fact that concrete, for example, is more cost-effective and can be made, more or less, locally, whereas timber oftentimes needs to be imported (CEMEX UK, sd). Nowadays, however, climate change and global warming have made the construction industry realize that, while concrete and steel may be more practical materials in some cases, timber trumps both materials in terms of sustainability. Timber began to make even more of a name for itself as a modern construction material with the invention of cross laminated timber, or CLT, composite slabs of layers of timber planks that are at a 90 degree angle from each other, thereby creating mechanical properties that are more isotropic than timber that is not cross laminated (Borgström & Fröbel, 2019). The added sustainability of timber elements, combined with contemporary technological developments is something that is going to make timber as a construction material much more common than it is now.

There are some caveats to timber as a structural material, however. While timber grows naturally and the supply is virtually limitless (if produced and harvested in a sustainable way) (Sasaki & al, 2016), timber's mechanical properties can be less practical. Timber being a biological material makes it vulnerable for imperfections. Besides, timber is an anisotropic material, meaning it has different mechanical properties in different directions. Even when using CLT, where the mechanical properties are more homogeneous than in 'natural' timber, the material is still considered orthotropic, it has different properties in two directions. In addition to this, CLT is overall less stiff than concrete. This makes CLT elements more complex to work with and to design for than other construction materials like concrete and steel. Thus, stabilising a vertical extension using CLT panels is more of a challenge than when a more conventional material like concrete would be used.

1.2 Problem definition

While vertical extension is universally seen as an efficient and sustainable solution to the housing crisis that is now being faced by the Netherlands. Vertical extensions, however, are not being constructed at the rate one would expect. Even in urban areas that have vertical extension potential the go to option is demolishing the old and constructing entirely new buildings. In the meanwhile, vertical extension has been shown to be a more sustainable and cheaper alternative. The main problem here is that vertical extension can be a complex endeavour that calls for an entire structural analysis of the existing structure. This creates the appearance that each possible vertical extension is a completely unique project and as such, vertical extension projects are often treated as 'one-offs'.

The problem becomes more complex when the principle material of the vertical extension is considered to be CLT. While CLT is a lightweight and sustainable material, and therefore a very popular choice for many newly constructed buildings, its use in vertical extensions is a bit more complex. This is mainly due to the added wind loads, the use of CLT in a stabilising capacity being a relative unknown and its connection to the original structure. Meaning other, more conventional materials like concrete and steel would make for a less complex design process. These factors make the successful use of CLT in vertical extensions slightly questionable.

Studying the main parameters that govern vertical extension potential and vertical extension success can provide a much needed insight into the 'extendibility' of a variety of buildings, which can be very relevant in an early design context: the phase in which vertical extension of buildings is considered as an alternative among many. It will also show the extent to which CLT is a viable material to use in vertical extensions.

1.3 Research content

Main research objective

Identifying CLT vertical extension potential in existing buildings by creating a parametric tool that takes into account different types of structural constraints. Ultimately, contributing to informed decision-making practices in the sustainable and effective structural design of vertical extensions.

Secondary research objectives

Analysis goals

- Explore the influence of structural typological boundary conditions in existing buildings on their potential for vertical extension.
- Identify the key design parameters that govern the feasibility of vertical extensions in a structural context.
- Study the mechanical behaviour of CLT shear walls and determine the factors that govern CLT performance.

Synthesis goals

- Utilize parametric modelling to generate a variety of sets of boundary conditions
- Employ parametric modelling to simulate vertical extensions across the aforementioned sets of boundary conditions.

Simulation goals

- Assess the effect of the shear wall layout in vertical extensions on critical stresses in the original structure
- Investigate the compatibility of CLT with the different identified wall layouts
- Conduct a comprehensive parameter study to analyse the effects of the identified design parameters on the vertical extension capacity under various boundary conditions.
- Present comprehensive results from a specific case study to exemplify the research findings.

Research questions

The research questions are presented here in a similar fashion as the research objectives: following the structure of this thesis report. First, the main research question is presented. Subsequently, the sub research questions will be presented in the order in which they will be answered.

Main research questions

Four main research questions have been defined.

Main research questions:

‘How is the spare capacity within a Rotterdamse Laag structure influenced by its building typology?’

‘How is the utilization of spare capacity influenced by vertical extension design?’

‘To what extent does vertical extension design influence the utilization of elements in the vertical extension?’

‘How and to what extent can a parametric tool indicate vertical extension potential in an early design stage?’

These questions will be answered in chapter 9 of this report (the conclusion). Furthermore, the results and discussion chapters are roughly divided into parts that coincide with the first three questions:

- Effects of parameters in the original structure on the spare capacity in the structure
- Effects of parameters in the extension design on the spare capacity in the original structure
- Effects of parameters in the extension design on the utilization of elements in the extension

As for the final question, the entire report is written as a tool development cycle. This is explained further in section 1.4.

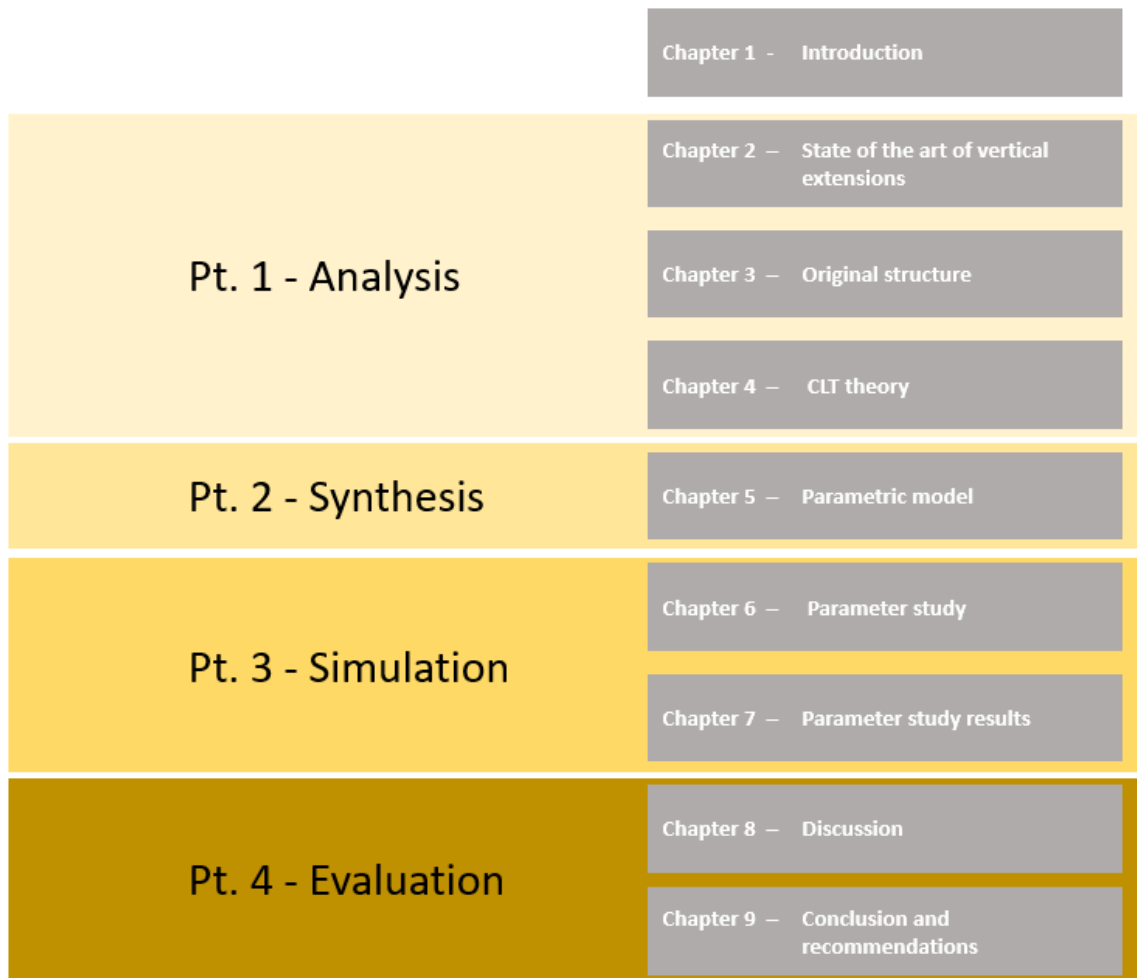


Figure 1.1 – The methodological setup of this thesis

1.4 Methodology

The methodological framework used for this thesis is based on the basic design cycle which consists of the following four phases:

- Analysis
- Synthesis
- Simulation
- Evaluation

This methodology framework was chosen because, at the centre of this thesis a parametric tool/model is developed. This framework corresponds with the stages of the basic design cycle. Please note, however, that while the structure of this report is framed around the design cycle, the main goal of this thesis is not to create aforementioned tool/model. The tool is merely, as the name suggests, a tool that helps with finding answers to the main research questions. Below, the four steps that were mentioned above and their role in this report are elaborated on.

Part 1: Analysis

In the analysis section of this thesis, the context of vertical extensions is analysed. A literature study will be carried out where the main goal is to review the state of the art in vertical extensions. Chapters 2-4 show the results of this literature study. In chapter 2 different types of existing vertical extensions and the methods used to achieve these. Then chapter 3 will focus on the structural boundary conditions used for this particular thesis. Subsequently, chapter 4 will focus on timber/CLT elements.

Part 2: Synthesis

For the synthesis section of this thesis, a tool will be created that is able to assess the added loads of different extension variants on varying original buildings. A design stage model will be created in Grasshopper using Karamba. The goal of the modelling stage is to create a parametric model that can take into account different configurations of structural constraints and where different grid and shear element solutions can be applied to each of these configurations. The modelling approach is elaborated on in chapter 5.

Part 3: Simulation

In the simulation, the tool will be used for a parameter study that involves different original buildings and vertical extensions. In this parameter study the model created in chapter 6 will be used on 27 different configurations of boundary conditions. The goal here is to find an optimal configuration of shear elements and an optimal grid solution for each set of boundary conditions. The extension variants deemed most successful will be assessed and analysed.

Part 4: Evaluation

Finally, in the evaluation the findings of the parameter and case study will be discussed and conclusions and recommendations will be given. Furthermore, the created tool will be reflected on and its possibilities and limitations will be discussed.

1.5 Scope

Finally, the scope of this thesis will be explained.

Building typology

The model that will be created in this thesis will be built for concrete skeleton buildings known as 'Rotterdamse Laag' buildings. Chapter 3 provides some insight as to the specific characteristics of this type of building.

For the extension, this thesis will look at CLT based structures. The stability is provided by CLT shear walls. The CLT shear walls are connected to the floors with holdowns and bracketed connections. For any further transfer of vertical loads, CLT columns are used that have pinned connections to the floor and ceiling. In this way, horizontal loads can only be transferred through the shear walls. The floors are also CLT. Between the original structure and the extension a 'transfer layer' made of steel beams will be placed.

Application

The research goal and questions, answered through the use of a parametric tool and parameter study are built for the initial stages of the design process. The goal is to create an efficient way for buildings to be assessed for vertical extension potential in combination with the effectiveness of different types of vertical extensions. The objective is not to deliver a tool that presents a fully designed vertical extension for any given building. This means that more detailed calculations involving the existing structure are not within the scope of this thesis. This includes capacity provided by reinforcement and rotational stiffness in the original structure. The work that lays before you is, therefore, explicitly intended to create a tool that identifies which element in a building pose the biggest challenges when vertically extending said building.

Part 1 – Analysis

Chapter 2 - State of the art of vertical extensions

Vertical extensions come in many shapes and sizes. In order to better define a scope for this particular thesis, it is important to have an idea of the state of the art of vertical extension in buildings, i.e. what are the possibilities and what is usually done in practice? To this end, a number of existing vertical extension projects from all around the world will be elaborated on here.

First, it has to be acknowledged that the term 'vertical extension' is a broad term that does not know a rigid definition. Vertical extension can be achieved in a large number of ways on almost any type of building.

In the book 'Building Additions in Steel', Daniel Stockhammer identifies three main structural types of vertical extensions (Stockhammer, 2019):

- Load transfer outside of the existing building structure
- Load transfer via parts of the existing building structure
- Load transfer through the existing building structure

It is interesting that Stockhammer includes load transfer outside of the existing building in his definition of vertical extension. While architecturally speaking this might be true, structurally speaking the two structures have nothing to do with each other and so, a structural vertical extension has to use the original structure to transfer (most of) its loads. For the purpose of this thesis, load transfer outside of the existing building structure is therefore not considered 'pure' vertical extension since the existing structure is not used. A vertical extension is defined here as any structure that is built on top of another structure where the loads of this new structure are transferred through the existing structure to an existing foundation. It is common practice however that certain structural interventions are introduced into the new and existing structure that increase spare capacity or ensure stability of the structure. The structural interventions that are taken into account here are elaborated on in Chapter 3.

Vertical extensions require extensive structural design and tend to rely on many different factors. The projects mentioned here will mostly centre on timber/CLT as the main material used. For each of the projects that will be covered here, a number of questions are answered:

- How many storeys were added?
- What was the original height of the building?
- What structural interventions were necessary to achieve this?
- What is the main material used?

Finally, the conclusions are condensed into the 6 main factors that influence vertical extensions.

2.1 Case studies

In this chapter five vertical extension projects with varying degrees of relevance will be looked into to determine the main parameters that influence vertical extension. The following projects are looked into:

- 55 Southbank Boulevard - Melbourne, Australia
- Glitne Housing - Umea, Sweden
- Ray 1 – Vienna, Austria
- Strassburgerstrasse 40 – Berlin, Germany
- St. Jobsveem – Rotterdam – The Netherlands

2.1.1 55 Southbank boulevard - Melbourne

55 Southbank is Australia's largest CLT extension, adding 10 storeys on top of the existing 7 storeys. This was made possible by a two structural interventions in particular. The existing cores were strengthened and a new steel core was added on a shallow foundation. Then, since the grid of the extension differs from the grid of the existing building, a large truss was placed on the 7th/8th storey that functions as a transfer layer. The main cause for this particular structural intervention is the fact that the extended part of the building was to become a hotel, meaning the structure was going to consist of relatively small CLT units. The change in function here imposed a challenge to the structural designers that was resolved by the transfer structure.

The idea of a transfer layer in vertical extensions is a relatively common one. Often the columns in the top storeys of a building are capable of carrying the extra loads that are added by extending the building. The beams at the top of the building, on the other hand, are designed to carry the roof structure, not an extra floor. This effectively means that demolishing the top layer of a building, and adding new beams (and possibly new columns) is necessary for a successful vertical extension. In the case of 55 Southbank boulevard, the grid of the extension differed significantly from the grid of the existing building. The effect of this is that new concentrated loads are introduced between the columns. This, in combination with the large amount of storeys added meant that an entire truss had to be constructed in order for the transfer layer to be effective.

One could imagine these structural interventions being much less drastic when the extension becomes smaller. However, the two main critical points remain the same: grid transfer and stability. (WoodSolutions, 2020).

Table 2.1 – 55 Southbank Boulevard Data

Storeys added	10
Original number of storeys	7
Structural interventions	New core, transfer structure for grid
Main material used for extension	CLT, steel
Building typology	Concrete skeleton with stability core

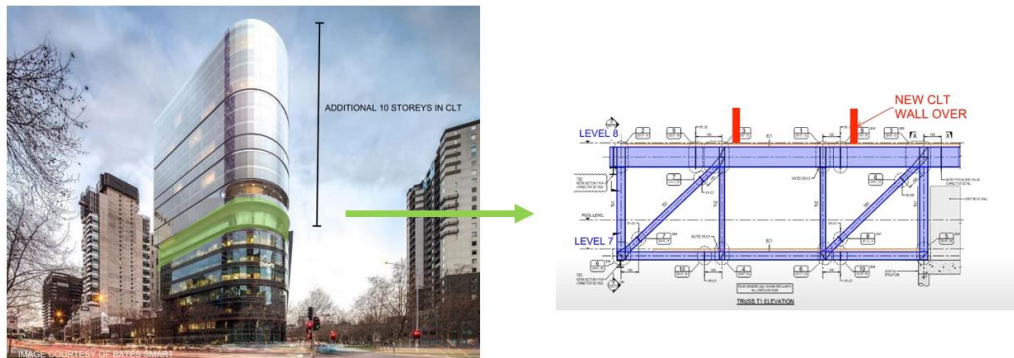


Figure 2.1 – Transfer layer in 55 Southbank Boulevard

2.1.2 Glitne Housing

The Glitne Housing project in Umea, Sweden shows that the concept of a transfer structure is often used in vertical extensions. Except here, it was a steel beam structure that was used to transfer the added loads, and the transfer structure was placed directly on top of the existing roof structure. The extension is often described as ‘snakelike’ and ranges from two storeys in some areas to four storeys in others (Bergqvist, 2021).

Sweden has a large history of building with timber and Glitne Housing uses this concept to vertically extend an existing mall using CLT elements. The timber elements are combined with steel frames in some spots with large spans with no supports, but overall the CLT panels are the main load bearing elements, providing stability as well.

One of the main challenges of this extension is created by the fact that the Utopia Mall, on which the housing project is situated, consists of three separate buildings. To make matters worse, each of these buildings are from a different time period and have vastly different foundations. One building has a shallow foundation while the others are founded on piles. To accommodate different settlements for these three different parts of the building, dilatation joints were added in Glitne to avoid large stresses due to uneven settlement.

Table 2.2 – Glitne Housing data

Storeys added	2-4
Original number of storeys	4
Structural interventions	Steel transfer layer
Main material used for extension	CLT
Building typology	Concrete skeleton

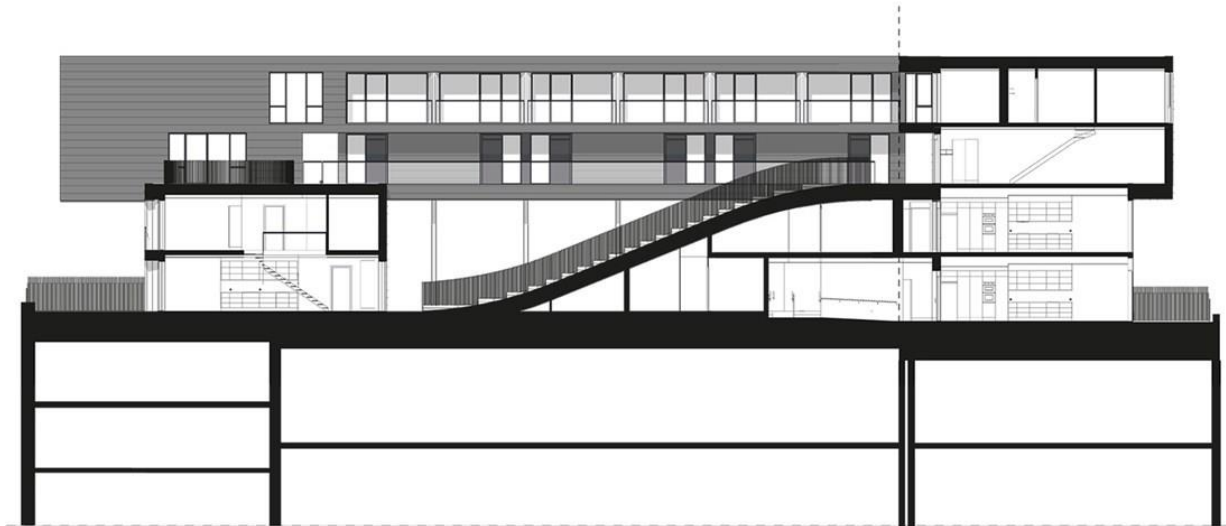


Figure 2.2 – Section of Glitne Housing in Umeå

2.1.3 Ray 1 – Vienna

Located in the city centre of Vienna, Ray 1 is a relatively small building addition, completely constructed out of steel. The relatively low vertical extension of Ray 1 is due to the constraint of architectural uniformity. The vertical extension was not allowed to rise above the existing line of facades (Frisch, 2008).

This project, once again, shows that the locations where the loads of the extension are brought into the existing building are an important design constraint. In the case of Ray 1, the new loads are primarily transferred to the two load bearing facades of the existing building. The rest of the building consists of a steel frame that was designed in a way where only a few columns were necessary in the extension itself.

Table 2.3 – Ray 1 data

Storeys added	2
Original number of storeys	
Structural interventions	Steel transfer layer
Main material used for extension	Steel
Building typology	Masonry

2.1.4 Strassburger Strasse 40 - Berlin

Like many cities in the Netherlands, Berlin is also experiencing a large housing shortage. This has caused the city to look into vertical extension as a viable solution that can add more housing opportunities in a rather quick manner. This apartment building in Berlin was extended with two extra storeys. The extension was constructed using clt panels and clt / concrete hybrid floors. The existing residential building consists of load bearing walls (Ryll, 2021).

The CLT walls on the first floor of the extension follow the same exact layout of the load bearing walls of the existing building. The same does not go for the second storey of the extension. Here the CLT walls do not follow the exact same grid. Here the first extended storey acts as a kind of transfer structure between the second story and the existing structure.

In this way, 23 new apartments were able to be created, with a cumulative added area of 1870 m².

Table 2.4 – Strassburger Strasse 40 data

Storeys added	2
Original number of storeys	6
Structural interventions	No large ones
Materials used	CLT walls and CLT hybrid floors
Building typology	Masonry

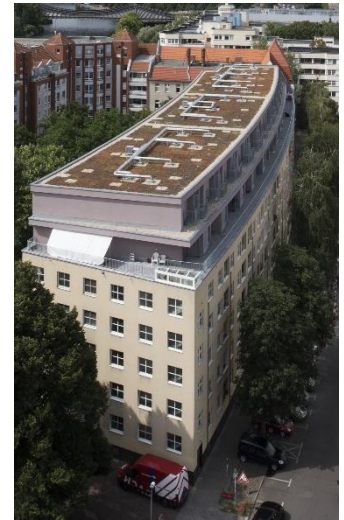


Figure 2.3 – Ray 1 Vienna (left) and Figure 2.4 – Strassburgerstrasse 40 Berlin (right)



Figure 2.5 – St. Jobsveem Amsterdam

2.1.5 St. Jobsveem – Rotterdam

The St. Jobsveem building remodel in Rotterdam consists of a little more than just an extension. The building was split into four parts by inserting three atriums. This of course has a large impact on stability and the four parts of the buildings had to be stabilised separately by steel braced frames. Originally the entire building was stabilised by the facade that consists of brick masonry.

The spare capacity of the foundation piles turned out to be the leading factor in vertically extending St. Jobsveem. Two storeys were able to be put on top of the existing structure. The existing cast iron columns were able to take the extra loads with no problems (Doomen).

The fact that this building was able to accommodate two extra storeys is due to the fact that its original function was that of a warehouse. Warehouse loads are significantly higher than loads for housing and therefore repurposing the entire building for housing creates a large spare capacity that can be used to add more volume to the building. In the new situation, all of the upper storeys have a residential function (109 apartments were created in the building), while the ground floor consists of shops (Jobsveem, sd).

Table 2.5 – St. Jobsveem, Rotterdam

Storeys added	2
Original number of storeys	5
Structural interventions	Large stabilizing trusses (not directly for the extension)
Materials used	Steel
Building typology	Concrete skeleton

2.2 Comparison of projects

Table 2.6 – Summary of case studies

Project	Structural Interventions	Added storeys	Materials used
55 Southbank Boulevard	Two new steel cores on new foundations, large transfer structure	10	Steel (cores) and CLT
St. Jobsveem	New steel stabilising frameworks throughout the building	2	Steel
Strassburgerstrasse Berlin	unknown	3	CLT
Glitne Housing	Steel transfer structure	2-4	CLT
Ray 1	Steel transfer structure	2	Steel

2.3 Conclusions

Looking at these existing vertical extensions the first thing that stands out is that without addition of a new stabilising core, most vertical extensions are a maximum of

2 or 3 storeys high. The reason for this is twofold: on the one hand, a new core is able to take new loads outside of the existing structure. On the other hand, the core stabilises the entire structure and therefore the wind loads that are newly introduced by the addition of extra storeys are taken care of right away.

This brings us to two main factors that have to be taken into account when designing vertical extensions that are built without large structural interventions, like a new stability core or strengthening of foundations. Stability of the entire system is important and because of the additional wind loads, an important part of vertically extending buildings is about introducing these horizontal loads into the existing structure. The other factor is spare capacity. Vertical extension potential is, in the basis, limited to the amount of extra loads the existing structure can handle. A building that is already utilizing its capacity to the maximum will not be able to absorb the loads of a vertical extension without significant structural interventions.

The projects that are covered in this chapter each deal with these two main problems in their own way. In CLT based vertical extensions like the Glitne housing project and Strassbourger Strasse in Berlin, stability can be ensured by CLT shear walls that also divide the building in residential units.

The conclusions drawn from this chapter are condensed in six factors that influence vertical extension potential. These factors are divided into two categories: boundary conditions and design factors. Boundary conditions are unchangeable, they are factors you have to work with. Design factors are factors that you can influence yourself.

The factors that are here concluded to play a large role in the vertical extension potential and vertical extension success will form the basis of the parametric model that is created in chapter 5.

2.3.1 Original structure factors

- **Original building grid** The grid the original building was built on influences the type of grid that can be put on top of the building. A very large grid will require a heavier transfer structure to bring the loads back to the original columns.
- **Building typology** The building typology of the existing structure influences where the stability of the building comes from and in what way the loads of the extension have to be introduced back into the substructure. In the case of Strassburgerstrasse in Berlin the original structure makes use of load bearing walls, which allowed the extended walls to be placed right on top. This becomes more complex with different types of building typology.
- **Spare capacity** Spare capacity of the existing structure usually relies on two factors: the building year and the functional typology. The building year influences what codes were used in the original design. The functional typology determines the types of loads that the building was designed for.

2.3.2 Design factors

- **Extension grid** The grid in which the extension is built influences the size of the transfer structure and the self-weight of the structure itself. A project like 55 Southbank Boulevard shows that with a change of grid a very heavy transfer layer may be necessary.
- **Extension stability** The location of the stabilising elements in the extension influence where horizontal loads are introduced into the existing structure. The stabilising elements have to be placed in such a way that the spare capacity of the original structure is used as efficiently as possible.
- **Lightweight design** By keeping the weight of the extension down, vertical reaction forces are kept down as well, resulting in a more efficient use of spare capacity.

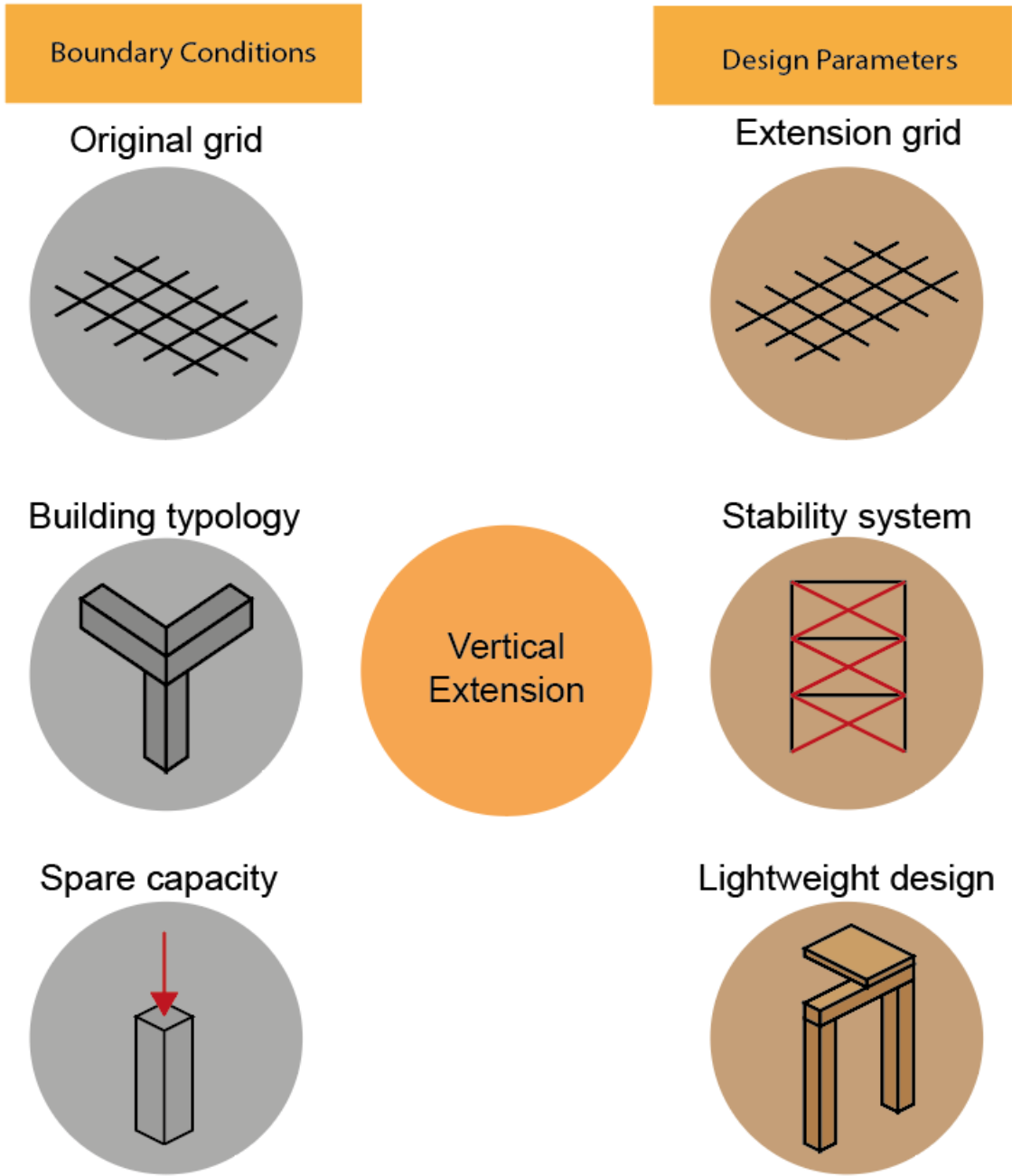


Figure 2.3 – The boundary conditions and design factors of vertical extension

Chapter 3 – Structural context

3.1 Introduction

Questions that are answered in this chapter

- *What defines the ‘Rotterdamse Laag’?*
- *What structural typology is typical for the Rotterdamse Laag?*
- *How can spare capacity be assessed?*
- *In what ways can spare capacity be created in Rotterdamse Laag buildings?*

Chapter 3 addresses the structural typology of the existing structure and its compatibility with vertical extensions. This chapter begins with an exploration of the concept of the ‘Rotterdamse Laag’, the definition of which will be expounded through some specific existing buildings. Subsequently, an analysis of the structural typology inherent to these types of buildings will be done. The relevant structural elements and their typical dimension will be shown.

Following this, an investigation into methodologies for assessing spare capacity is done in combination with two strategies that create additional spare capacity within these structures. Central to this pursuit is a comparative analysis between old and contemporary building codes. Finally, an overview of strengthening techniques for structural elements will be presented.

With the information presented in this chapter, the reader will have a clear view of the type of buildings that are at the heart of this thesis, the way spare capacity can be assessed and created in these types of buildings and the amount of strengthening that can be done in an existing structure.

3.2 Rotterdamse Laag

The scope of this thesis is framed around so-called 'Rotterdamse Laag' buildings. These are postwar concrete skeleton buildings that are quite common in the Rotterdam city center but can also be found in other urban areas in the Netherlands. The commonality of these buildings in Rotterdam is simply due to the fact that large parts of Rotterdam were bombed during the second world war, which instigated a necessity for new buildings from 1945 on. The end of the second world war and the subsequent building shortage, especially in Rotterdam, coincided with the rise of popularity of the large scale usage of reinforced concrete in buildings. While concrete had been invented in ancient Rome and reinforced concrete had been around since the 19th century, the material only really gained mass popularity in the fifties and sixties of the 20th century (White, sd)

This is how reinforced concrete came to be one of the most commonly used material for industrial/commercial buildings in postwar urban areas like Rotterdam.

When looking at 'Rotterdamse Laag' buildings, the thesis of this scope encompasses concrete skeleton buildings that fulfill the following requirements:

- Buildings that were constructed (roughly) between 1955 and 1975
- Buildings where the a reinforced concrete stability core may be present but where the columns and floors have been monolithically casted, therefore providing some stability within the frame itself
- Buildings that are 4 to 7 stories tall
- Buildings which primary use is that of an office building, possible with commercial spaces on the ground floor

Please note here that, while the term 'Rotterdamse Laag' implies that these buildings are only found in Rotterdam, the definition used within this thesis only includes the requirements mentioned above. The term is simply used as an umbrella term that includes buildings in all locations as long as these requirements are met.

3.3 Structural characteristics of Rotterdamse Laag buildings

Having explored the historical and functional context of buildings that are normally considered 'Rotterdamse Laag' buildings, the focus now shifts to the structural context of these buildings. In order to create an understanding of this structural context, two buildings that are typically considered 'Rotterdamse Laag' buildings were selected to show here: HUF, located in Rotterdam and Prinses Irenestraat 59 in Amsterdam (see figure 3.2). Two projects were selected here because the structural information for these types of buildings can sometimes be rather limited and multiple buildings are necessary to create a full understanding of their structures. The structure is being looked at here from the bottom up, first looking at the foundation piles and the stability core, then assessing the columns beams.

3.3.1 Concrete quality

Concrete quality determines the stiffness and capacity of the concrete elements used in a structure. When looking at HUF, it becomes clear that the concrete used for the stability core is one that reaches a maximum cube strength of 200 kg/cm^2 , whereas the columns and beams are cast using a stronger concrete that reaches 250 kg/cm^2 . The difference of concrete quality used among the two can bear large consequences because it effectively means that the stiffness of the concrete stability core is smaller than the stiffness of the column and beam structure surrounding it. Prinses Irenestraat 59, on the other hand, uses a concrete that reaches 300 kg/cm^2 homogeneously throughout the structure.

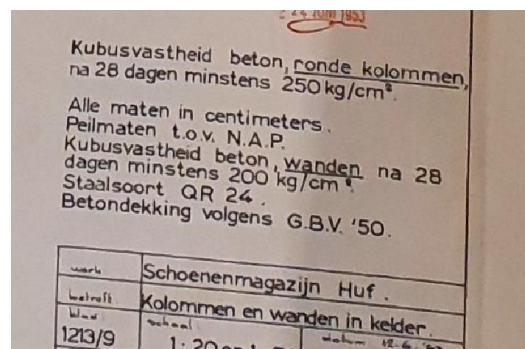


Figure 3.1 – Concrete quality used in HUF

3.3.2 Foundation piles

Normally, one column will be supported by multiple foundation piles. This is also the case in Rotterdamse Laag buildings. While detailed information of the exact pile plan in HUF is missing, the pile plan of Prinses Irenestraat 59 is available to use and shows how the piles are distributed over the building. It is important to note here that the amount of piles under one column is not homogeneous throughout the building. The amount of piles used per column varies between 4 and 5 piles near the edge of the building, while the pile groups underneath and close to the stability core have up to 6 piles. Figure 3.2 shows the piles groups found under Prinses Irenestraat 59.



Figure 3.2 – HUF, Rotterdam (left) and Prinses Irenestraat 59, Amsterdam (right)

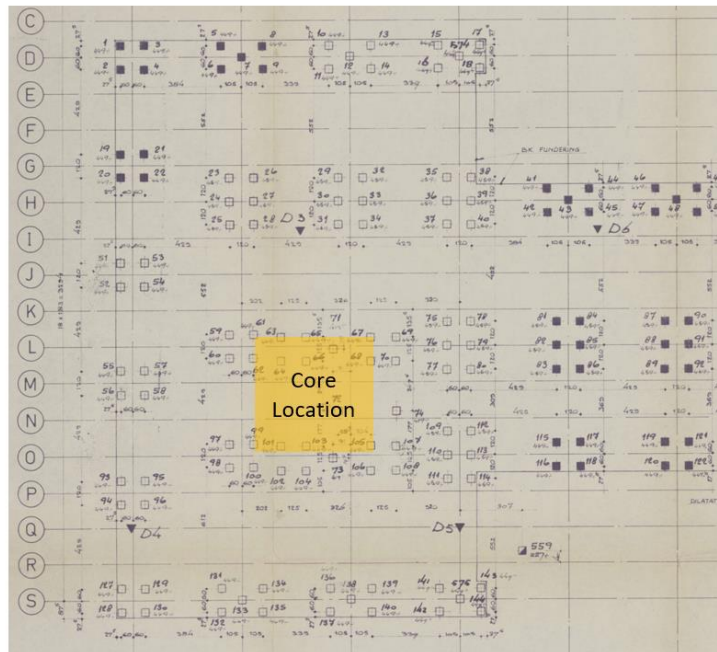
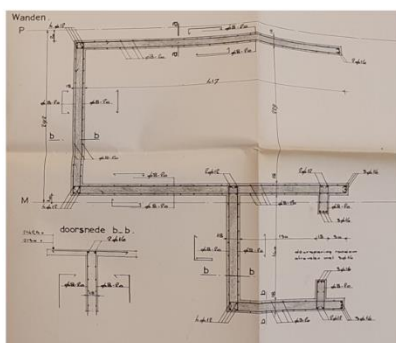


Figure 3.3 – core location in prinses irenestraat 59

3.3.3 Stability core

In both HUF and Prinses Irenestraat 59, a stability core is present, although at different locations. HUF contains a stability core in the far corner of the building, near the entrance, while Prinses Irenestraat 59 contains a stability core in the exact middle of the building. The cores are pictured in figure 3.4. While the cores range a bit in size, they are very irregular, containing multiple voids.

Stability core – HUF Rotterdam



Stability core – Prinses Irenestraat 59 Amsterdam

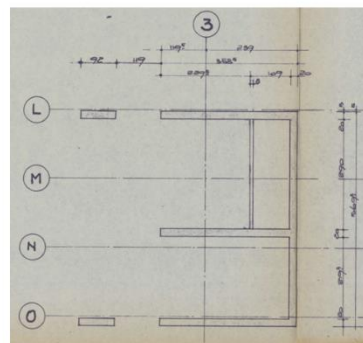


Figure 3.4 – Cores of HUF and Prinses Irenestraat 59

3.3.4 Columns, beams and floors

Beams and floors are consistently dimensioned homogeneously throughout the building in both buildings considered here. The beams found in HUF are 35x58 cm, while the beams found in Prinses Irenestraat range between 50 and 70 cm.

Columns, on the other hand, change diameter based on the floor they are on. At the Prinses Irenestraat, the ground floor columns are dimensioned 50x50 cm, whereas everything above is dimensioned round with a diameter of 45 cm. The columns in HUF show more variety, the columns change in dimension with 5 cm each floor, converging on a diameter of 40 cm for the two floors at the top. The floors are 35 cm thick.

3.4 Spare Capacity

Having established the structural typological characteristics of the buildings that lie within the scope of this thesis, the subsequent step is to gauge their spare capacity. The term 'spare capacity' refers to the amount of capacity that is still 'left' in a building, or the amount of loads that the structural elements could still theoretically handle without compromising safety or serviceability. Spare capacity is arguably the most important factor in the decision-making process for vertical extensions.

3.4.1 Assessing spare capacity

The spare capacity of a building can be determined in a number of ways, ranging in level of detail. It is, therefore, important to define the scope of assessment before starting a project. Assessment of spare capacity can, in principle, be as detailed as the structural engineer deems necessary. The German Federal Institute of Materials Research and Testing defines 6 levels of assessment of existing structures (Rücker, Hille, & Rohrmann, 2006).

Level 0 : Non-formal qualitative assessment:

A level 0 assessment is a non-quantitative assessment that is completely based on the experience of the structural engineer that assesses the building, it is therefore also completely subjective. Visual signs of damage are taken into account, but no further qualitative checks are carried out.

Level 1: Measurement based determination of load effect:

*Level 1 assessment is a code based assessment where the spare capacity is based on what loads are already acting on the building. **Threshold values.** No further structural analyses are carried out.*

Level 2: Partial factor method, based on document review:

For a Level 2 assessment, information is taken from original design documents and inspection documentation. Structural analyses are done here, but in a relatively simple way. Partial factors are used in the determination of spare capacity.

Level 3: Partial factor method, based on supplementary investigation:

Level 3 assessments differ from level 2 assessments in that a level 3 assessment takes additional information from non-destructive investigation methods on the structure.

Level 4: Modified target reliability, modification of partial factors:

Partial factors used in Level 4 assessments are modified specifically for the building that is to be assessed.

Level 5: Full probabilistic assessment

For a level 5 assessment, no partial factors are used. Instead, a structural reliability analysis is used for the assessment of structural elements.

The goal of assessing spare capacity in this thesis is to define vertical extension potential in an early design stage. It is, therefore, not desirable to use a very detailed

assessment method. *This means that for this thesis, a level 2 spare capacity assessment seems to be most realistic.* Structural analysis is carried out in a quantitative way, but no on-site (non) destructive investigations are carried out and regular partial factors are used to determine load-bearing capacity. SAMCO defines three steps that make up any model based structural assessment (which level 2 assessments fall under):

1. Acquisition of data of loading and resistance
2. Calculation of load effects on structural models
3. Safety and serviceability verification

In the case of a level 2 assessment that means that first, in step 1, data is acquired of the existing building and, most importantly, about the type of loading that the building is currently undergoing / the building was designed for. Then in step 2, the building can be structurally assessed with the loads of the extension. After which, in step 3, the safety and serviceability of the new situation is reviewed (Rücker, Hille, & Rohrman, 2006).

3.5 Building codes

The level 2 method found above to assess spare capacity requires an in depth comparison of the building code used to design the building in its original state and the building code used for restructuring. Rotterdamse Laag buildings were originally constructed between 1950 and 1975, meaning that for these buildings, the reigning building guidelines are the ‘technische grondslagen voor bouwvoorschriften 1955’ or TGB1955 in short.

3.5.1 Building code at time of construction (TGB1955)

The ‘technische grondslagen voor bouwvoorschriften 1955’ is an important set of building codes because it was created just after the second world war. Whereas contemporary building codes use safety factors at multiple times in the design process, the safety factor used in the TGB1955 is used only once and relies on the material used. For concrete structures this factor is 1.5 (Arends, 2021).

3.5.2 Building code at time of extension (NEN1990 and NEN8700)

The building code that should be referred to at present time is the current Eurocode. For newly constructed buildings, one should refer to NEN1990 and NEN1991 for the characteristic loads that a building should be designed for. This, of course, also goes for the extension of any vertically extended building. For the original structure that is extended, however, NEN8700 may be used. This code governs the structural safety of existing buildings and restructuring of buildings. NEN8700 defines some reduced safety factors that may be used in the design of a restructuring of a building. A reduction of safety factors is allowed here because the building has already structurally proven itself. Table 3.2 shows the relevant variable loads and load factors given in both NEN1990 and NEN8700 as well as for the original building code TGB1955.

Table 3.2 – Variable loads and load factors from different codes

	TGB1955	NEN1990	NEN8700
Function			
Commercial	3 ** kN/m ²	4	4
Office	2.5	2.5	2.5
Residential	1.5	1.75	1.75
Load factors			
Permanent	1.5	1.35	1.2 (6.10a)
Variable	1.5	1.5	1.3 (1.4 for wind loads)

One can clearly see here that while the functionality specific characteristic variable loads were lower in 1955 for both commercial functions and residential functions, the use of NEN8700 in the restructuring of a building that was designed according to 1955 will probably unlock some spare capacity because the safety factors are lower here. This means that spare capacity can be unlocked in an existing structure, using the building codes, in two ways:

- Spare capacity is already unlocked by restructuring a building that was built during the reign of TGB1955 using NEN8700, due to a significant difference in load safety factors
- Spare capacity can be unlocked by altering the functional layout of a building in such a way that the variable loads of the new function are significantly lower than the variable loads when originally designed with the original function in mind.

3.6 Wind loads

The addition of an extension creates an increase in the resultant wind load. And since wind loads, as determined using Eurocode, increase quadratically, a small increase in the total height of a building might result in a significant increase in wind loads. It is therefore important to know how wind loads can be determined as they were in the timeframe within the scope and how they can be determined now, for new buildings as well as for restructuring of buildings.

The method of determining wind loads according described in TGB1955 is rather straightforward and follows a simple formula. The Netherlands is divided into three sections, each of which receives a base wind load. The base wind load for Rotterdam is 0.4 kN/m². Then, a base height for the building is defined, which is 20m. To determine the wind load on a building one simply adds the base wind load and adds 0.01 kN/m² for every meter of the building height that exceeds the base height of 20m.

The determination of wind loads given in Eurocode is slightly more complex. The determination of wind loads on buildings is described in NEN1991. The Netherlands is divided into three main wind areas. Each of these areas is then assigned a base

wind speed that is used to further determine wind loads on a building. Rotterdam and Delft, for example, are in wind zone 2 with a base wind speed v_{b0} of 27 m/s. A full determination of wind loads according to Eurocode can be found in Appendix A.

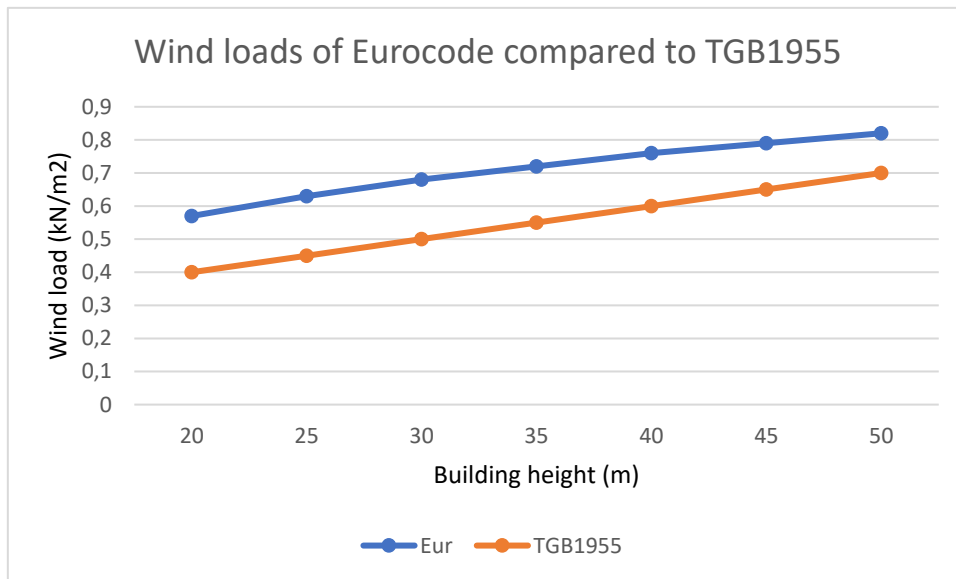


Figure 3.5 – Wind loads of eurocode and TGB1955

The wind loads according to TGB1955 and the most recent Eurocode were both determined at different heights. Graph 3.5 shows the results of this. It becomes visible here that the wind loads determined using NEN1991 are significantly larger compared to TGB1955.

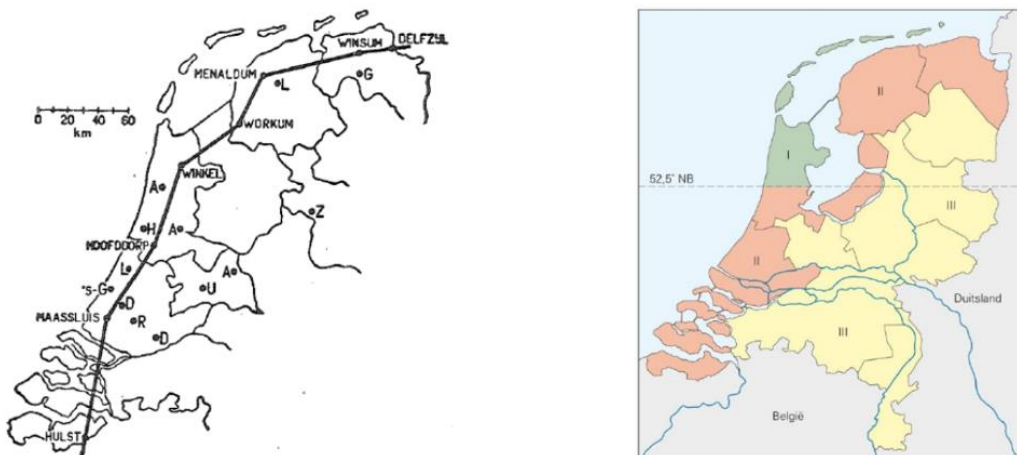


Figure 3.6 – wind area map of TGB 1955 (left) and wind area map of NEN1990 (right)

3.7 Strengthening techniques

A situation that might occur when vertically extending a building is that in some elements the spare capacity is exceeded, meaning that a column, for example, is overloaded. In that case, some strengthening might be required. An example of a project where strengthening was used is 55 Southbank boulevard, mentioned in chapter 2, where approximately 30% of columns had to be strengthened.

3.7.1 Columns

In some cases it can be necessary to strengthen existing columns, either to restore their original load bearing capacity (in case of damage) or to increase overall capacity. Reinforcement of existing columns can be necessary for the entire building, however, this would make for an expensive endeavour. This method is more realistic when only a certain amount of columns have to be strengthened, like in the case of 55 Southbank Boulevard, where 30% of columns had to be reinforced (WoodSolutions, 2020).

A few strengthening techniques are mentioned in (Heiza, Nabil, & Meleka, 2014). The type of strengthening applied on a column depends on what type of loads the column has to withstand. Where spare capacity is a limiting factor, the critical loads are often compressive loads. This means a strengthened column has to be able to withstand a higher compressive load than before. A traditionally popular method to achieve this is to increase the cross section of the column, also called 'reinforced concrete jacketing'. This can be done by applying extra reinforcement on the outside and then casting an additional layer of concrete. This increases both bending and compression strength of the column, however, it also takes up more space and adds more weight to the structure.

In some cases however, increasing the cross section of the column is far from practical. This is where techniques like steel jacketing and textile reinforced mortar jacketing come in (Triantafillou, 2016). Steel jacketing is commonly used when expanding the cross section of the column is not desirable. Here the steel sections are attached to the column on all sides. Another advantage of steel jacketing is that the increase in weight due to this strengthening technique remains quite low.

In a comparative study carried out (Vritesh & Asish, 2021) the relative increase in load carrying capacity of columns strengthened with these three different techniques were compared. The results of this study are shown in figure 3.5. Compressive load carrying capacity of the columns tested in this study went up by at least 35.2% for steel jacketing and 48% for reinforced concrete jacketing.

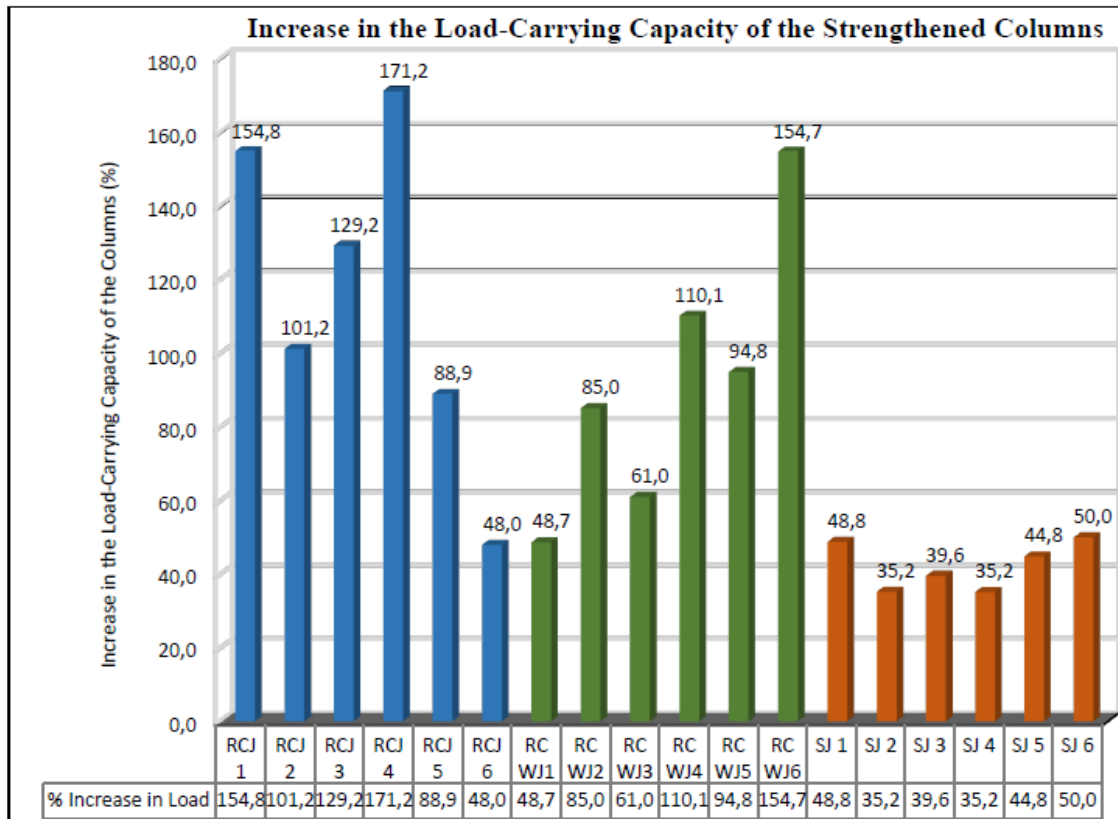


Figure 3.7 – Increase in load carrying capacity of columns strengthened in three ways where RCJ is reinforced concrete jacketing, RCWJ is reinforced concrete wire mesh jacketing and SJ is steel jacketing

3.8 Foundation piles

Alternatively, the foundation piles could also be the weak link in the structure. Methods for the strengthening of foundation piles do exist. One way of strengthening an existing foundation is by adding micropiles, or jet grouting (van der Stoel, 2001). However, the downside of these methods, and of foundation pile strengthening overall, is that it generally requires significantly more work than the strengthening of columns. The main reason for that is accessibility: columns are fully accessible parts of the structure and the strengthening techniques shown in section 3.7 do not require any large structural interventions. Micropiling, while proven to be an effective way to strengthen an existing foundation, is still expensive and requires a lot of space. Besides, the process of implementing micropiles creates noise and vibrations and ‘can damage adjacent structures’ (Pitroda, 2015).

Foundation pile strengthening would, per definition, require a complete overhaul of the structure to reach the piles in the first place. Especially when working in an urban context (as in this thesis’ scope), this could create very impractical situations and it can even be dangerous, since the capacity of pile foundations of adjacent buildings can be reduced (van der Stoel, 2001).

3.8 Conclusions

In this chapter the structural typology of the 'Rotterdamse Laag' buildings was shown, offering insights into their defining characteristics and historical context. It explored the concrete quality, foundation piles, stability cores, columns, beams, and floors of these structures, providing a comprehensive understanding of their structural elements. The assessment of spare capacity was shown to be a central theme, with various levels of assessment methods discussed and finally providing two manners of unlocking spare capacity in a Rotterdamse Laag building. The first of these methods is the change in building codes that provides a fortunate margin between safety factors. To this end, the difference between TGB1955 and contemporary Eurocodes was explored and it was found that a significant difference exists between the safety factors of both codes. It was also found that wind loads determined using Eurocode are higher than TGB1955 wind loads, under which the original buildings were designed. This might prove to be a limiting factor in the design of vertical extensions.

The second way of unlocking spare capacity is by changing the functional typology of the building to a function with a smaller variable load, thereby increasing the amount of loads that fit into the base capacity of the building.

Finally, some methods of strengthening existing columns were presented and it was found that an increase of at least 35% in load bearing capacity can be expected, proving that when spare capacity is reached in a structure, that does not automatically mean a vertical extension is not a possibility. Furthermore, it was found that, foundation strengthening, while possible, is most likely significantly more expensive than column strengthening and also a lot less practical.

Chapter 4 – CLT

In this chapter, first we will look at what exactly CLT is and what the specific limitations of the material are. Then we will talk about the relevance of connections in CLT panels and the different ways to connect these as well as the effect this has on structural performance. Subsequently, a look is taken into some different ways of determining the structural properties of CLT panels for modelling purposes and finally, the modelling approach will be explained and validated.

4.1 Introduction

Timber structural elements are universally seen as a sustainable alternative to less environmentally friendly construction materials like concrete and steel. This is currently leading to a surge in the usage of timber in structures all over the world. There is one major caveat, however: timber is, by nature, an anisotropic material. Due to the biological makeup of trees, the structural characteristics of the material are different in three directions: the longitudinal, radial and tangential axes. This means, effectively, that due to the configuration of the wood fibres, a timber specimen will react differently under loads with different locations and directions.

One way to (partially) bypass the anisotropic behaviour of timber, is to use combine different orientations of timber in the same element in order to create an element that has structural properties that are more equivalent in multiple directions. This can be done by cross laminating timber into panels. And is usually done by layering slats of timber in one direction with slats of timber with the grain perpendicular to the first layer.

Cross Laminated Timber (CLT) panels are deemed more sustainable than their concrete counterparts, have a relatively high load capacity and are versatile in the way they are used. This makes CLT a great material to use in modern structures (Borgström & Fröbel, 2019).

4.2 CLT makeup and limitations

CLT panels are made using individual sawn lamellae. These are first fingerjoined together lengthwise to create lamellae that are as long as required. Then, a CLT panel is made by gluing together a layer of lamellae with the woodgrain in one direction, and then a layer of lamellae perpendicular to the first layer. The CLT panel is then pressed and finished before it can actually be used in construction.

Due to the fact that the lamellae are fingerjointed together, a CLT panel can, in principle, be as large as one needs. There are, however, two main constraints: first is the size of the manufacturer's production facility and second is the means of transportation. In practice, transportation turns out to be the weakest link here. CLT panels have to be able to be transported in a large truck. One large CLT producer, Stora Enso, specifies a maximum panel size of 16x2.95 meters.

This means that if it is deemed necessary to have a CLT slab that is either higher than 16m or wider than 2.95m, the CLT panels have to be joined together using connections (StoraEnso, 2017).

Looking further into the range of thicknesses for CLT panels for well-known producers we find that Stora Enso provides a range of 60-320 mm thick panels, for which the panels with a thickness larger than 160 mm are more often used for floors and roofs, whereas the lighter panels are used more often as walls. Variants exist with 3, 5 or 7 layers of lamellae with varying thicknesses.

4.3 Connections

The stiffness of a CLT panel is mostly governed by its connections to the surrounding structure. The CLT slab is often considered rigid compared to its connections and it is incredibly important to make a good estimation of what connections can be used in CLT shear walls and floors and their respective stiffnesses (Shahnewaz, Alam, & Tannert, 2018)

Connecting CLT panels in-plane

When CLT panels are connected in-plane (whether it be for floors or for walls that have a 180 degree connection to each other), slotted connections are often used (Rothoblaas, 2019). Slots are designed to transfer shear stresses from one panel to the other. Figure 4.1 shows how slotted connections are used when connecting two or more walls. The determination of the stiffness of slotted connections can be found in appendix B.

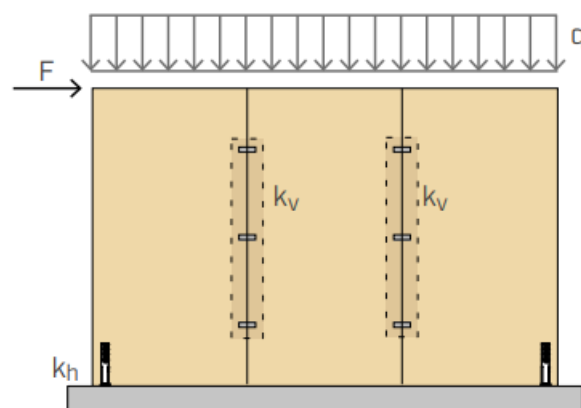


Figure 4.1 - Slotted connections (from the Rothoblaas catalogue)

Connecting CLT panels out of plane / perpendicular to each other

Panels connecting to each other on a 90 degree angle can happen in two situations:

- Floor to wall connection, where the floor can be concrete or CLT
- Wall to wall, where the walls connect in a 90 degree angle

For floor to wall connections, the most used connections are hold downs or angle brackets. These make for a non-rigid connection from floor to wall. When a concrete floor or foundation is present, the angle bracket is usually cast into the concrete and then screwed into the CLT wall panel. When the floor is also a CLT panel, the angle bracket will also be screwed into the floor.

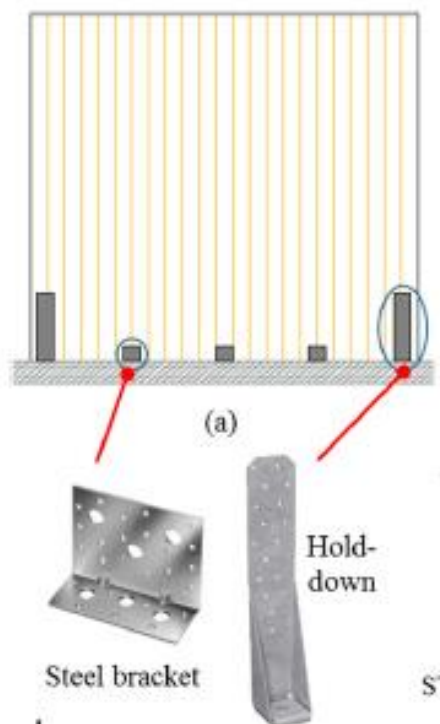


Figure 4.2 – Common types of connections for a CLT shear wall

Figure 4.2 shows a way CLT panels are normally connected to a floor (either concrete or CLT). At the ends, vertical forces are higher which warrants a longer holddown type connection, while in the middle the horizontal forces are transferred by wider steel brackets.

The stiffnesses of some of these connections can be found in appendix B.

4.4 CLT shear walls

The stiffness properties of cross laminated timber make CLT panels very suitable for shear wall applications. When CLT panels are used as shear walls generally, four modes of displacement have to be taken into account (Lukacs, 2019) two of these can be attributed to the material properties themselves, the other two depend on the connections.

- Bending (material)
- Shear (material)
- Sliding (connections)
- Rotation / Uplift (connections)

In research by (Znabei, 2020), this last mode of displacement increases significantly when multiple shear walls are placed on top of each other because a larger height is needed than the maximum logistical height possible (16 m according to Stora Enso). It is therefore not recommended to make shear walls out of CLT longer than 16 meters if it is not absolutely necessary.

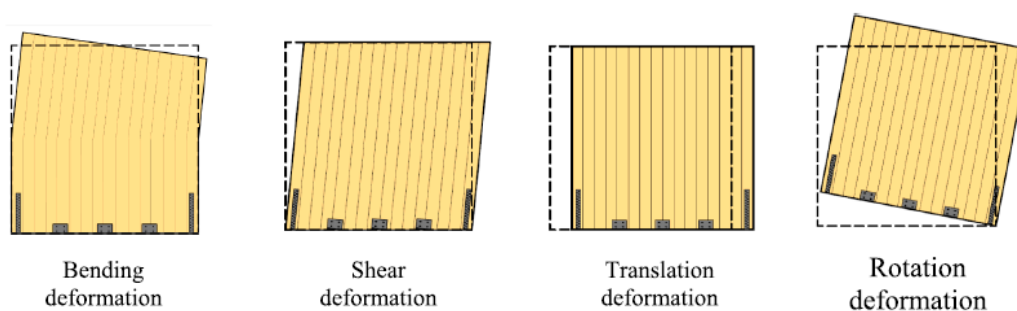


Figure 4.3 – The four different modes of displacement for CLT shear walls

The net section

The orthotropic nature of CLT panels makes it difficult to find the structural properties that govern the entire panel. When making structural calculations where the panel is loaded in the direction of the grain (as is the case with shear walls). A net section has to be used to make these calculations. This means that only the layers with the grain parallel to the load can be taken into account and the layers perpendicular to the grain have to be neglected.

In-plane stiffness of the CLT panel

The in-plane flexural stiffness of a CLT panel can be determined by using the net-section of the wall. Here, only the active lamellae are taken into account for the stiffness determination. This means that in a CLT panel with 5 layers, only the two layers where the grain is perpendicular to the horizontal load is taken into account for the determination of the stiffness of the panel in this direction (Lukacs, 2019). An argument for this negligence is given by (Bogensperger, 2016) where it is mentioned that gaps can exist between the different lamellae of one layer, meaning they cannot be assumed to work as one element to provide flexural stiffness in the direction parallel to their grain.

The effective bending stiffness of a CLT panel can be determined by taking the Young's modulus of the timber type used in the direction parallel to the grain and multiplying this by the moment of inertia of the net section (equation 4.1) (Lukacs, 2019).

$$EI_{ef} = E_0 * \frac{t_{ef} * w^3}{12}$$

Equation 4.1

Alternatively, the stiffness of a CLT panel in plane can also be determined by the 'k-method', proposed by Blass and Fellmoser (Blass & Fellmoser, 2004). Here, instead of only modifying the cross section, the Young's modulus of the CLT panel itself is adapted.

$$E_{m,0,ef} = E_0 * k_3$$

Equation 4.2

$$E_{m,90,ef} = E_0 * k_4$$

Equation 4.3

$$k_3 = 1 - \left(1 - \frac{E_{90}}{E_0}\right) * \frac{a_{m-2} - a_{m-4} + \dots \pm a_1}{a_m}$$

Equation 4.4

$$k_4 = \frac{E_{90}}{E_0} + \left(1 - \frac{E_{90}}{E_0}\right) * \frac{a_{m-2} - a_{m-4} + \dots \pm a_1}{a_m}$$

Equation 4.5

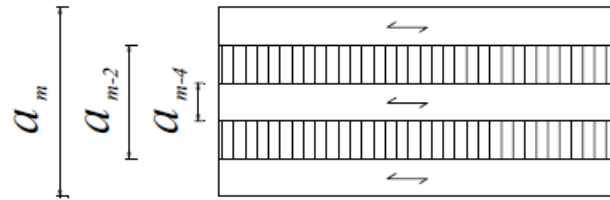


Figure 4.4 – Effective E-modulus of CLT according to Blass & Fellmoser

Here the bending stiffness is calculated using the entire thickness of the CLT panel, not just the net section (equation 4.4 and 4.5), using the k-factor depending on how the grain direction is relative to the load direction. The k- method takes into account not just the net section but modifies this by taking into account the ratio between the Young's moduli in the directions parallel to and perpendicular to the grain.

	k_i
	$k_1 = 1 - \left(1 - \frac{E_{90}}{E_0}\right) \cdot \frac{a_{m-2}^3 - a_{m-4}^3 + \dots \pm a_1^3}{a_m^3}$
	$k_2 = \frac{E_{90}}{E_0} + \left(1 - \frac{E_{90}}{E_0}\right) \cdot \frac{a_{m-2}^3 - a_{m-4}^3 + \dots \pm a_1^3}{a_m^3}$
	$k_3 = 1 - \left(1 - \frac{E_{90}}{E_0}\right) \cdot \frac{a_{m-2} - a_{m-4} + \dots \pm a_1}{a_m}$
	$k_4 = \frac{E_{90}}{E_0} + \left(1 - \frac{E_{90}}{E_0}\right) \cdot \frac{a_{m-2} - a_{m-4} + \dots \pm a_1}{a_m}$

Figure 4.5 – The k factors for different types of loading, k3 and k4 are relevant here

Like the Young's modulus, the shear modulus also has to be altered in order to give correct results when structurally analyzing CLT slabs.

In-plane stiffness for panels with voids

When a CLT panel with a window is considered the stiffness of the panel is considerably lower than that of a panel with no void. A method to reduce the stiffness of a CLT panel according to the size of its void was proposed by Shahnewaz (Shahnewaz & Shahria Alam, In-plane stiffness of CLT panels with and without openings, 2016) and is presented here in equation 4.6.

$$K_{opening} = K_{full} \left[1 - \frac{r_{o/w} \left(\frac{A_o}{A_w} \right)}{\sqrt{r_{o/w} + r_o \left(\frac{A_o}{A_w} \right)}} \right]$$

Equation 4.6

Here K_{full} is the original bending stiffness of the CLT panel. A_o is the original area of the wall with an opening and A_w the area of the wall without an opening. r_o is the aspect ratio of the void (so width/height or height/width, the largest number comes first) and finally, $r_{o/w}$ is the maximum aspect ratio of opening to wall. An example of a CLT panel with a window is shown in figure 4.6.

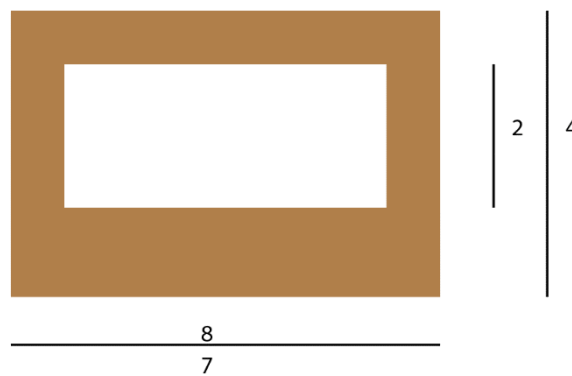


Figure 4.6 – Dimensions of a voided CLT panel

The voided wall presented here has total dimensions of 4x8 m and a void of 2x7 meters. Table 4.7 shows the calculation of the void factor for the bending stiffness.

Table 4.7 – Determination of stiffness reduction in voided CLT panel

A ₀	18 m ²
A _w	32 m ²

r0	7/2 = 3.5
r0/w	Maximum of 1/8 and 2/4 which is 2/4 = 0.5
Void factor	0.82

This means that this CLT panel with a void this size has approximately 80% of the stiffness of a CLT panel with no void.

While voids can be of relevance in this thesis, the method used here shows that a lot of information about the size and distribution of the voids is necessary to accurately determine the effective stiffness. It was therefore decided to neglect the presence of voids entirely.

Horizontal resistance of CLT shear walls

In calculating the strength of CLT walls (AKA the horizontal resistance of the CLT wall), it is universally assumed that the CLT panel itself can be assumed to be rigid. This means that the resistance comes from the connections, rather than the CLT panel itself. As mentioned before, two types of connections are regularly used in CLT walls. Holddown connections at the edges of the wall that are mainly used for transfer of vertical forces, and brackets in the middle section of the wall that transfer horizontal forces. Likewise, the resistance of a CLT wall to horizontal loads can be split in two different sections. On the one hand there is risk of 'overturning' or rotating. Overturning is ruled by the vertical strength of the holddown connection. On the other hand there is 'translation'. This is ruled by the horizontal resistance of the bracketed connections in the middle of the CLT wall. The horizontal resistance of the shear wall then becomes:

$$F_h = \min (F_R, F_T)$$

Equation 4.7

The resistance of the connections to translation can be determined by taking the horizontal resistance of each bracket and adding them together. The resistance to rotation is a little more complex to be determined and can be determined as proposed by Tomasi and described by Lucaks (Lukacs, 2019).

It is important to note that while brackets are designed to transfer horizontal forces, they do, in fact, transfer some vertical forces as well. Tomasi neglects this contribution to vertical load transfer by the brackets, instead assuming that all vertical tension is transferred to the foundation by the holddown connections. The design resistance of the holddowns and brackets can be found in appendix D.

Vertical resistance of CLT shear walls

CLT panels that are axially loaded need to be checked for out-of-plane buckling because they are relatively slender in this direction. Since Eurocode currently does not accommodate a buckling check for CLT specifically, a slightly different version

needs to be used. The method proposed here by (Brandner, 2016) uses the equivalent beam method.

$$\frac{N_d}{k_c * A_{net,ef} * f_{c,0,CLT,net,d}} \leq 1.0$$

Equation 4.8

Where k_c is the instability factor, which is calculated using the relative slenderness which itself is determined using the critical buckling load n_{cr} . It also becomes clear that for CLT as a material, buckling resistance is determined using the net section that was also used in determining the in-plane stiffness of the wall.

$$n_{cr} = \frac{K_{CLT,05} * \pi^2}{l_k^2 * \left(1 + \frac{K_{CLT,05} * \pi^2}{S_{CLT,05} * l_k^2}\right)}$$

Equation 4.9

Where $K_{CLT,05}$ and $S_{CLT,05}$ are the 5 percent quantiles of the bending stiffness and the shear stiffness respectively. l_k is the critical buckling length taken to be equal to the full length of the wall according to figure 4.8 .

$$k_c = \min \left[1.0 ; \frac{1}{k + \sqrt{k^2 - \lambda_{rel}^2}} \right]$$

Equation 4.10

$$k = 0.5 * (1 + \beta_c * (\lambda_{rel} - 0.3) + \lambda_{rel}^2)$$

Equation 4.11

Where β_c is equal to 0.1.

$$\lambda_{rel} = \sqrt{\frac{A_{net} * f_{c,0,CLT,net,k}}{n_{cr}}}$$

Equation 4.12

<i>Buckled shape of column</i>						
Theoretical value	0,5	0,7	1,0	1,0	2,0	2,0
Recommended design value	0,6	0,8	1,2	1,0	2,1	2,0

Figure 4.8 – Effective length factors for different types of supports

CLT Shear walls in buildings

Buildings made out of CLT elements generally come in two types: platform or balloon frames. The main difference is the method of construction used for the floors and walls. In platform frames, each story can be seen as a separate unit: the CLT wall is connected to the floor and the ceiling. The CLT wall above will be connected to the floor again, not to the wall below. This means that in a CLT building with four storeys, there will be four separate CLT panels above each other.

In balloon frame buildings, the walls extend to the top of the building. This means that instead of the wall connecting to the floor and ceiling and a new wall starting on the next floor, here the floors are connected to a continuous wall (see figure 4.9) (Shahnewaz, Performance of cross-laminated timber shear walls for platform construction under lateral loading, 2018).

Research suggests that balloon type construction reduces stresses perpendicular to the grain in the floor panels due to gravity loads. Balloon framing is therefore deemed a more efficient solution for CLT buildings. This however, is also influenced by some practical constraints that surround CLT panels. Since a CLT panel's length is limited by the means of production and transportation, balloon framing can only be done up to a certain point. As of now, CLT panels can reach a maximum length of 12-20 meters, often due to fact that larger panels are difficult to transport to the building site.

In this thesis, a platform type construction will be looked at because this allows for more width in shear walls. This also means however, that crushing checks will have to be performed at the interface of the shear walls and the floors.

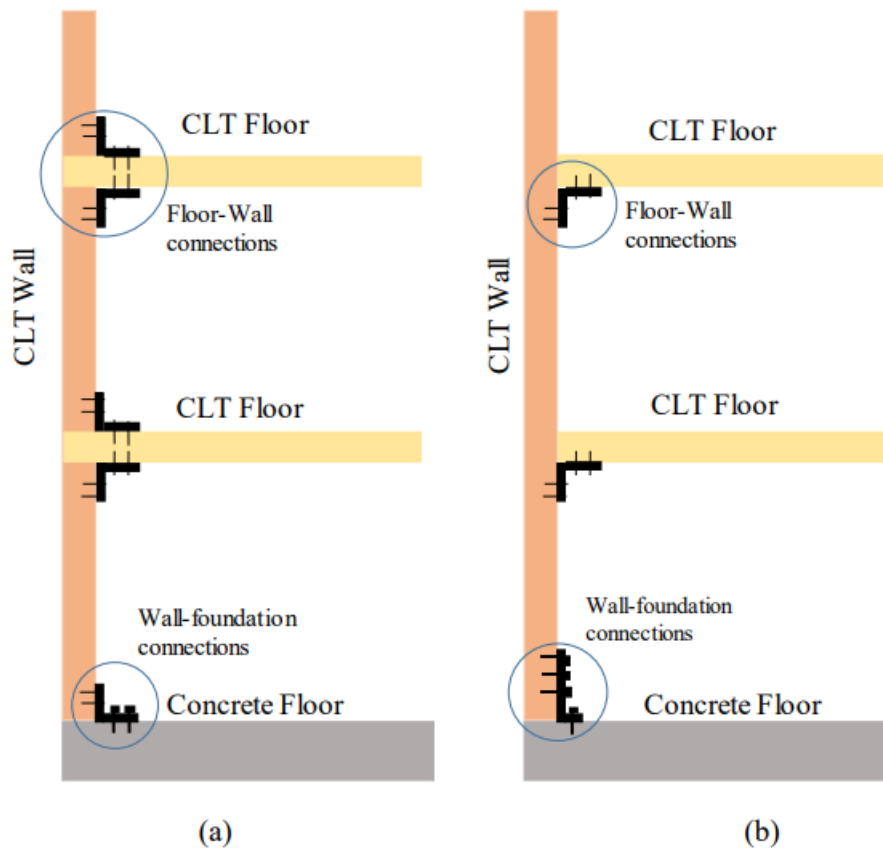


Figure 4.9 – a) platform construction and b) balloon construction

Modelling of the Shear wall

As mentioned earlier, the CLT shear wall itself is basically rigid in comparison to its connections to the surrounding structure. These connections, then, have to be modelled correctly if we want to accurately model the CLT shear wall as a stabilising element. It has already been established that a CLT shear element will be connected to the floors with two types of connections: holddown connections to transfer the large vertical forces at both ends of the wall, and angle bracket connections which are mainly to transfer the horizontal forces but also have some vertical load transfer capacity. According to Shahnewaz, (Shahnewaz & Shahria Alam, In-plane stiffness of CLT panels with and without openings, 2016), each of the connections can be modelled as a spring support. Here the holddown connections are modelled as pure vertical springs and the angle brackets as vertical and horizontal springs, see figure 4.10.

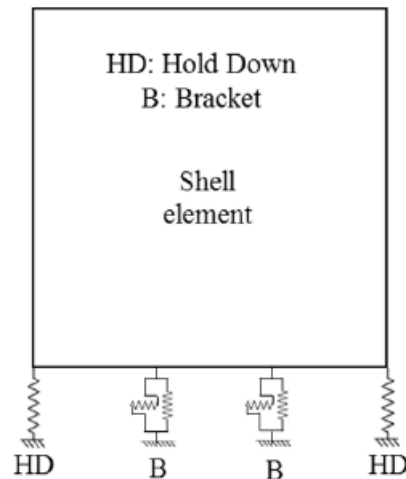


Figure 4.10 – Holddowns and Brackets as modelled by (source)

For the stiffnesses of these connections, Rothoblaas catalogue is used, this can be found in appendix D.

Modelling the CLT panel

In order for CLT elements to be put in the main thesis model, the properties given to the CLT element have to be verified. This is done by separately modelling the CLT panel using the Karamba plugin for Grasshopper. The model can be built using these four key concepts:

- Definition of the shell and its properties
- Modelling of the spring supports
- Loading

The composite method was used to find the structural properties of the CLT panel in both directions. Figure 4.11 shows how the CLT panel was modelled in Karamba. A shell element was created and like in Figure 4.10, four connections to the foundation were created. The supports themselves are assumed to be fully rigid, but to connect the panel to the supports, spring elements were used. The end supports were modelled as springs only in the vertical direction while the supports in between were modelled as springs both vertically and horizontally.

Appendix E contains a full validation of the accuracy of modelling CLT panels in this manner.

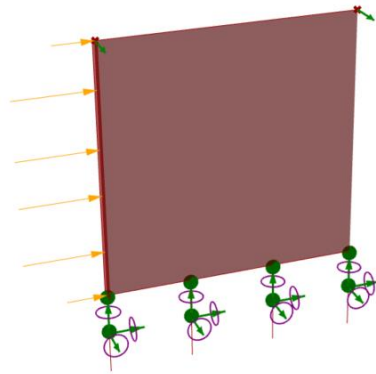


Figure 4.11 – CLT shear panel as modelled in Karamba

Part 2: Synthesis

Chapter 5 – Methodology

5.1 Introduction

As a result of the amount of parameters that will be studied and the fact that this will be done in a parameter study, a parametric model will be created. The advantage of using a parametric model is that all the research parameters can easily be applied to the model and the result of each change in parameters can be recorded. This can be done much quicker than in, for example, a regular FEM software package, where each change in parameters would result in a different model altogether.

In this chapter, the studied parameters will be explained. These are divided into two groups: parameters contained in the original building and parameters contained in the extension. Subsequently, the design constraints and design assumptions made in the modelling process will be explained. Finally, the model loading will be explained.

5.2 Studied parameters: original building parameters

As part of this thesis the effect of three parameters within the original building on the spare capacity of the original building is researched. In chapter 3, the characteristics of 'Rotterdamse Laag' buildings were presented. Some of these parameters will now be taken as the basis of the parametric model. The research parameters for the original structure are:

- The grid of the original structure
- The height of the original structure
- The location/presence of a stability core in the original structure

For each of these parameters, the parametric model can assign three options. Figure 5.1 shows which options exist for each parameter in the original structure.

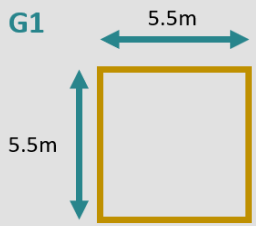
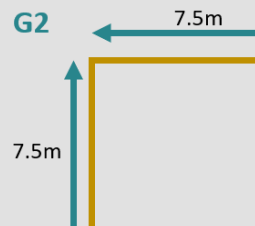
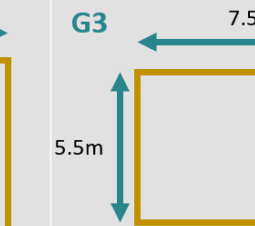
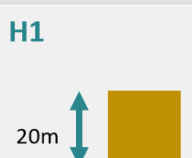
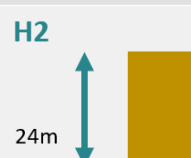
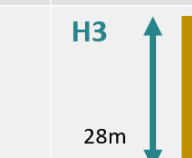
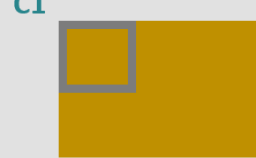

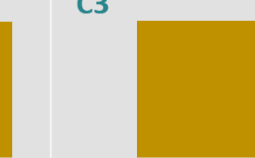
	V1	V2	V3
Grid of the original building	G1 	G2 	G3 
Height of the original building	H1 	H2 	H3 
Core position	C1 	C2 	C3 

Figure 5.1 – Original structure parameters and the options that are implemented in the model

5.2.1 Grid

The grid of the original structure can have a significant effect on the vertical extension potential of that structure. Since the way in which spare capacity is created in this thesis is largely rooted in the change of safety factors and variable loads that come from the change in building codes, the original grid can have a large effect on the spare capacity of a building. This is because the ratio between permanent loads and variable loads differs between construction grids.

5.2.2 Number of storeys in the original structure

As was shown in chapter 3, there is a significant difference in wind loads among the building codes looked at in this thesis. It is therefore very relevant to look not only at different heights of the vertical extension itself, but also at the height of the original structure. To account for this difference in wind loads and the quadratic increase of wind loads with height, three original building heights are included in the sets of original structures.

5.2.3 Stability core location

In chapter 3 it was found that the location of the stability core (and sometimes even the presence of a stability core) varies quite a lot among different Rotterdamse Laag buildings. It was therefore decided to explore the effect of the position and presence of a stability core on the distribution of spare capacity of the building.

The core dimensions will vary only with the original building grid. This is so that the stability core always makes up the same percentage by area of the building. The thickness of the core will be constant in each variant.

5.3 Studied parameters: extension parameters

In addition to the studied parameters in the original structure, this thesis also looks at the effect of parameters in the extended structure. These extension parameters are the following:

- The height of the vertical extension
- The location of shear walls in the vertical extension
- The construction grid of the vertical extension

5.3.1 Number of storeys in the vertical extension

Chapter 2 showed that in vertical extensions that do not make use of any significant structural interventions, the amount of storeys that can be added lies around 1 or 2 storeys. For this thesis, this range will be adopted, however, one storey will be added so that the possibility of 3 added storeys is not ruled out.

5.3.2 Shear wall layout

One of the main goals of this thesis is to study the influence of different shear wall layouts on the individual vertical support reactions and the displacements at the top of the extension. Three types of shear wall layouts are defined that are going to be used for each set of boundary conditions.

Layout option A: Core alignment

The point of departure for layout A is the idea that by aligning the shear walls more or less exactly with the existing stability core, the horizontal loads are more efficiently transferred into the substructure. This would, hypothetically, decrease the added loads and bending moments on existing columns while redirecting these forces to the existing stability core.

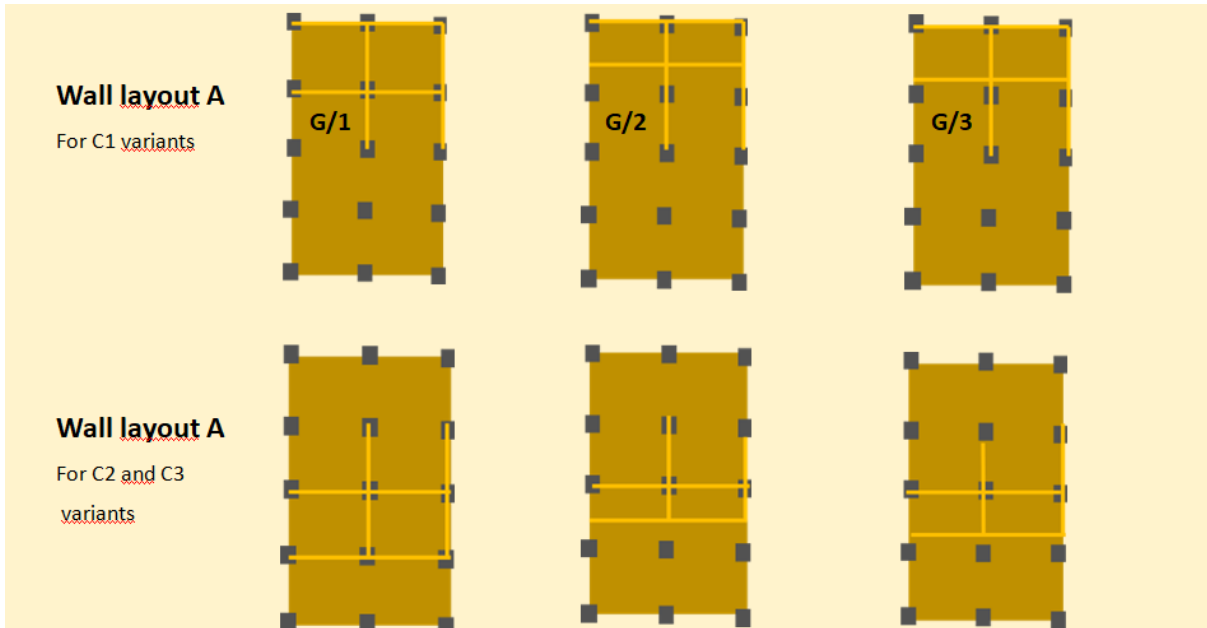


Figure 5.3 – Wall layout A: core alignment

Layout option B: Functionality

Layout option B is based on the subdivision of the space into functional units, or studio sized apartments. While subdividing the space like this is not optimal for the flexibility of the building (since structural elements are used to divide the spaces, one can't easily change the function of the extension in the future), this option is included because a significant part of contemporary residential CLT buildings are constructed this way.

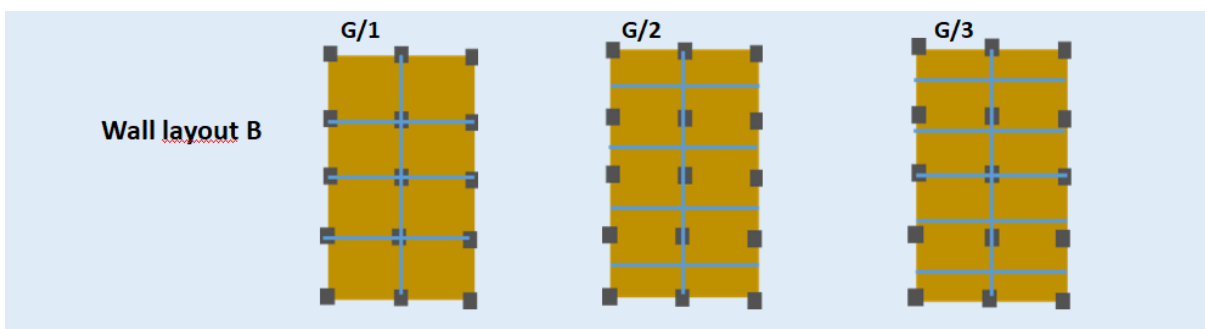


Figure 5.4 – Wall layout B: functionality

Layout option C: Façade

In the third and last layout option the shear walls are placed only in the façade of the extension. In doing this, flexibility of the building is ensured which makes the extension more future proof than, for example, option B. The downside is that by only using the façade, there is only so much space that can be used. Another disadvantage is that, depending on the number of walls needed, windows need to be considered as well. Adding a void into a shear wall drastically decreases its in-plane stiffness (see chapter 4).

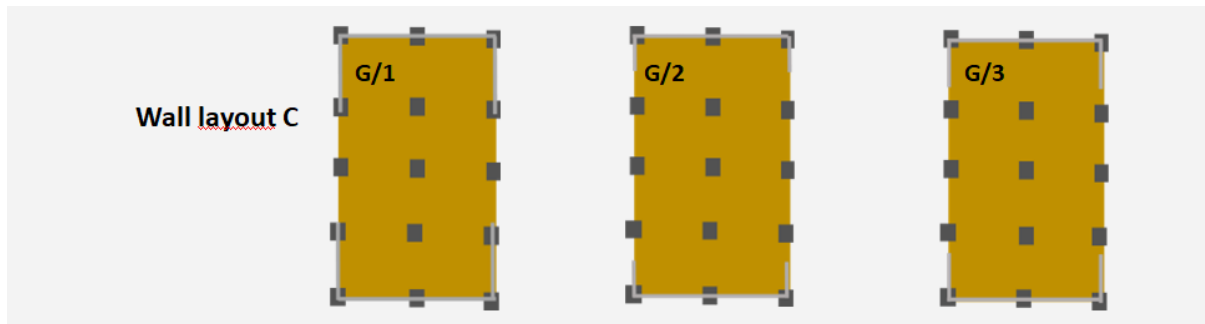


Figure 5.5 – Wall layout C: facade

5.3.3 Extension grid

Finally, the grid of the extension itself may differ from the grid that the original building is constructed with. The review of existing vertical extensions in chapter 2 showed that a transfer layer is often necessary in transferring the loads from the extension to the original structure. From this, it follows that the grid of the transfer layer does not have to fully adhere to the grid of the original structure. In the model, the extension grid can take three values:

- The extension grid is the same as the original grid
- The extension grid is half of the original grid
- The extension grid is one third of the original grid

Figure 5.6 shows how these three options look.










Extension parameter	V1	V2	V3
Number of storeys added	+ 1 storey 	+ 2 storeys 	+ 3 storeys 
Grid division	Original grid 	Original grid /2 	Original grid /3 
Wall layout	A core <u>aligned</u> 	B separation walls 	C facade only 

Figure 5.6 – The extension parameters and the values they can take

5.4 Design constraints

5.4.1 Load ratio

In chapter 3, it was shown that the manner of creating spare capacity in 'Rotterdamse Laag' buildings used in this thesis is by utilizing the difference in building functionality and the difference in building codes between the original situation and the new situation. Figure 5.7 shows how spare capacity in this thesis is first created and then utilized by extending the structure.

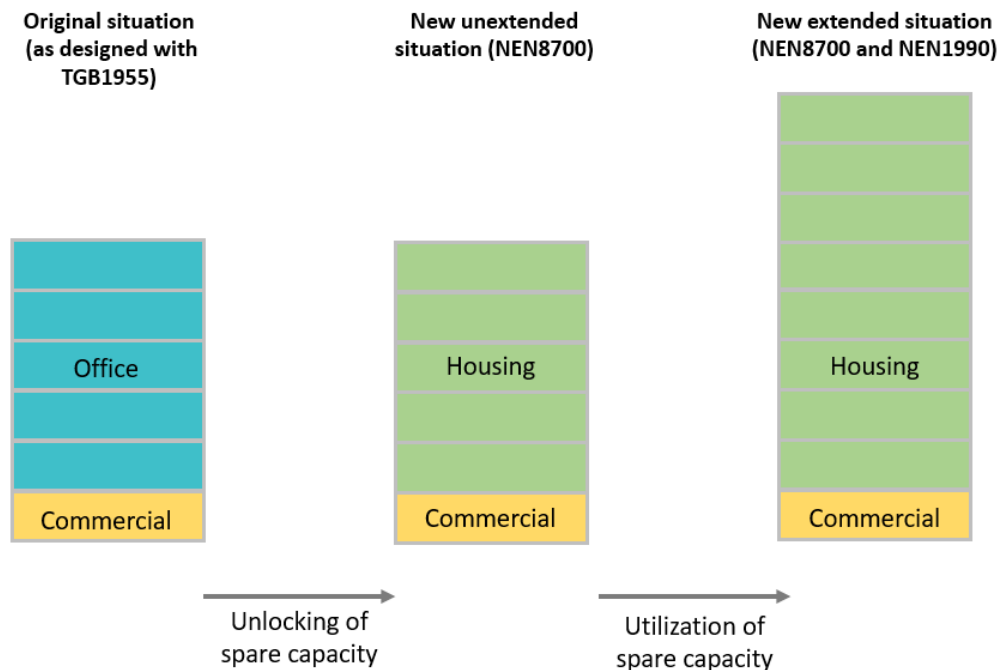


Figure 5.7 – Schematization of the process of creating spare capacity in a Rotterdamse Laag building

This mechanism can be explained more in detail by looking at how building codes work. This is done by schematizing both the loads and the resistance of the structure / structural elements as normal distributions. In the Eurocode, the loads that are acting on a certain structure and the resistance of that structure are assumed to be on a normal curve. The characteristic loads are then multiplied by a safety factor γ_s , which creates design loads, while the characteristic resistance is divided by a safety factor γ_R which creates a design resistance. The ultimate goal is for the design load to be smaller than the design resistance, otherwise the likelihood of failure is insufficiently low. *This is pictured in step 1 of figure 5.8.*

By switching codes from TGB1955 to NEN8700 (for the original structure), the safety factors on the load side are effectively decreased. Which creates more distance between the design loads and the design resistance. In addition to this, in this thesis,

the functional design of the building also changes. Where the buildings are assumed to have been used as office buildings, they will now be changed to residential buildings. As has been shown in chapter 3, the variable floor loads for office functions as per TGB1955 were higher than the variable floor loads for residential functions as per contemporary Eurocodes. This means that in addition to the lower value of the safety factor on the load normal distribution, the entire load distribution also shifts towards the left a little bit, since characteristic loads decrease. *This is pictured in step 2 of figure 5.8.*

Finally, it can be seen that the mechanisms used here create a significant space between the design load and the design resistance. This space is referred to as spare capacity and can be used to add more loads to the building, by vertically extending it. Here, the loads are increased again, but of course, the design load should never exceed the design resistance. *This is pictured in step 3 of figure 5.8.*

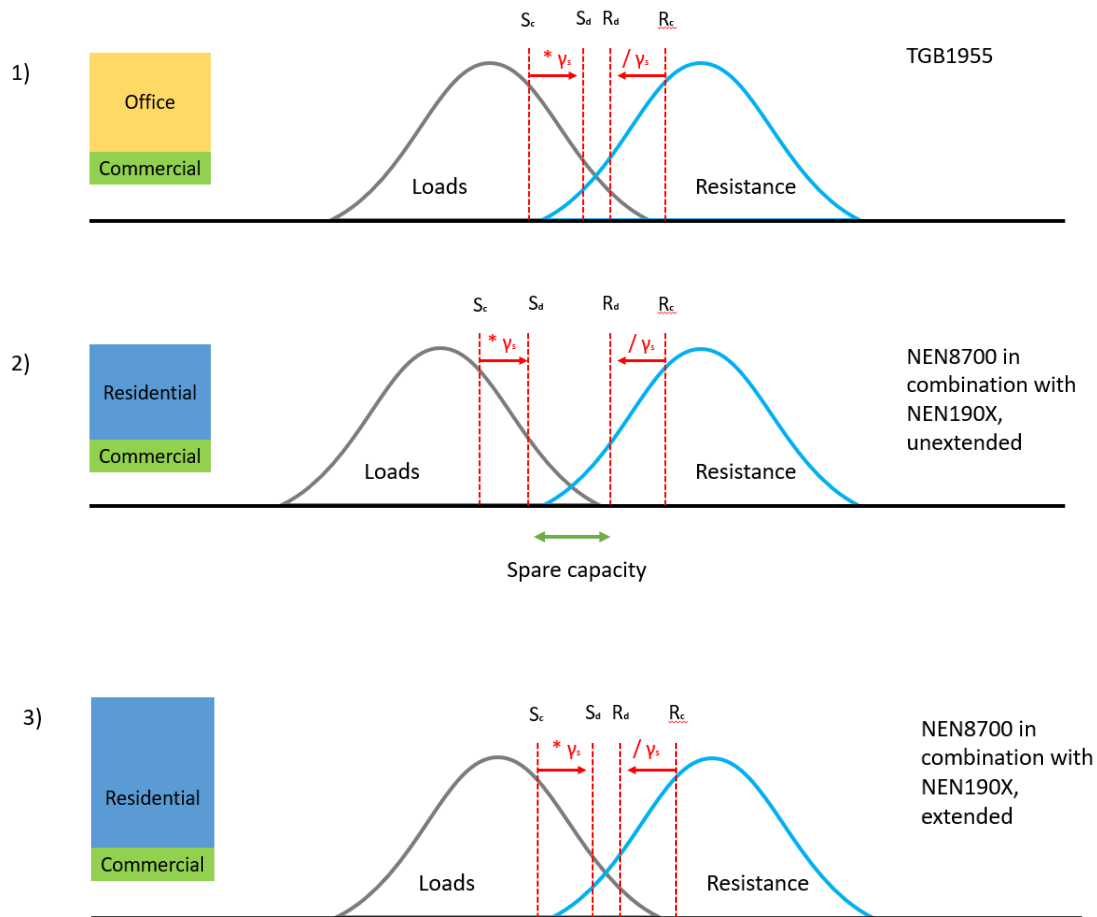


Figure 5.8 – Mechanisms of creating spare capacity

Spare capacity in the model is measured in terms of axial stress in the bottom columns and the reaction forces in the foundation piles. Equation 5.1 shows how the maximum and minimum axial stress in the bottom columns are determined in Karamba:

$$\sigma = \frac{N}{A} \pm \frac{M_y}{W_y} \pm \frac{M_x}{W_x}$$

Equation 5.1

5.4.2 CLT panel verification

Since Eurocode does not yet prescribe a method for verification of CLT panels, the CLT Handbook is used to verify these members. Checks will be done for in-plane compression (with buckling check) and shear capacity. The method of verification of CLT panels is shown in Appendix E.

5.4.3 Global deflection

As per Eurocode prescriptions, the maximum global deflection of any given building may not exceed 1/500th of the full building height. It is assumed that this requirement, given in NEN1990, is a limiting factor for the model (CEN, 2019).

5.5 Design assumptions

5.5.1 Foundation

The stiffness of the foundation piles is taken into account in the model. The stiffness of the foundation piles relies on the Young's modulus of the specific type of concrete used, the length of the pile and the area of the pile. Table 5.9 shows the values that were assumed for each of these, and the stiffness per pile. The soil stiffness, for this thesis, is assumed to be infinite.

Factor	Value
Pile cross section	20 x 20 cm
Pile length	12 m
Young's modulus	31476 MPa
Equivalent spring stiffness for one pile	N/mm
Equivalent spring stiffness for three piles	303727 N/mm

Table 5.9

As was seen in chapter 3, the pile to column ratio in a building is typically not equal to one, but larger. This means that for each column there are normally multiple foundation piles supporting that column. The number of piles under each column may vary among buildings and within a building. In chapter 3, it was shown that the amount of piles under each column is not typically homogeneously distributed over the floorplan. Since the number of piles under each column can differ per building and the amount of information is limited, the pile to column ratio is assumed to be homogeneous. Assuming a heterogeneous pile to column ratio would introduce uncertainty in the model. In this case, one will not be able to tell whether deformations or the distribution of loads can be ascribed to the structural typology itself or the difference in stiffness of the supports.

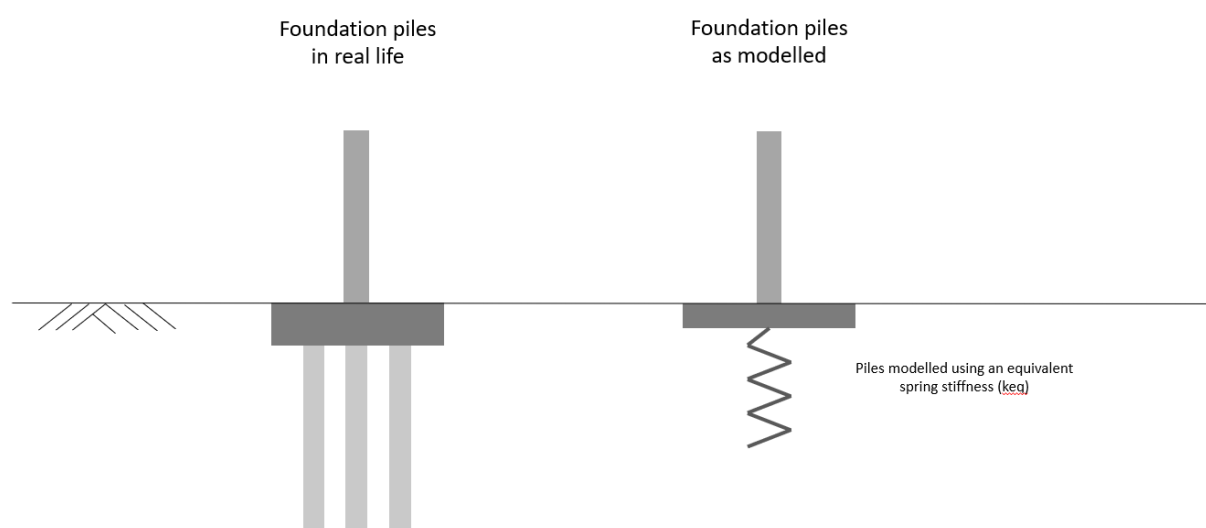


Figure 5.10 – Schematization of the way foundation piles are modelled

5.5.2 Stability core in the original structure

As was shown in chapter 3, the stability cores that are normally found in Rotterdamse Laag buildings tend to differ quite a bit, both in size and in make-up. In order to model these cores accurately, the core in the model can be made any size, but no voids can be added. It becomes, therefore, necessary to find an equivalent core size for the core that the user of the model wants to add. In the case of the parameter study that will be performed with the model later on in this thesis, the core of the Prinses Irenelaan building that was studied in chapter 3 will be modified to a perfect square. Since the parameter study will be looking at three construction grids, the core will, in each of these variants, take up half the grid in both directions. Table 5.11 shows the dimensions of the core in the Prinses Irenelaan building and the modified dimensions of the modelled cores.

Value	Prinses Irenelaan	Model (G1 = 5.5 x 5.5m)	Model (G2 = 7.5 x 7.5m)	Model (G3 = 5.5 x 7.5m)
Core thickness	180 mm	300 mm	300 mm	300 mm
Maximum core dimension X	2930 mm	2750 mm	3750 mm	2750 mm
Maximum core dimension Y	5000 mm	2750 mm	3750 mm	3750 mm
Iy	7.24 e12 mm ⁴	4.17 e12 mm ⁴	1.05e13 mm ⁴	

Table 5.11

5.5.3 Members in the original structure

Structural members in the original structure have mostly fixed dimensions that are based on dimensions found in 'Rotterdamse Laag' buildings (seen in chapter 3). Here table 12 shows the dimensions that were used for the columns at different storeys and the beams (which are assumed to be uniform in dimension, both over the floorplan and over the height).

Chapter 3 showed that the type of concrete used in Rotterdamse Laag buildings varies between a maximum cube strength of 200 kg/cm² and 300 kg/cm². For this thesis, the upper limit of that was chosen. Concrete with a maximum cube strength of 300 kg/cm² corresponds, in modern times, to C25/30 concrete. This type of concrete is used homogeneously to model both the columns and beams as well as the stability core. While this is not always the case in the buildings within the scope of this thesis, it

Table 5.12

Columns	Dimension
Columns 1 st and 2 nd floor	50 cm x 50 cm
Columns 3 rd and 4 th floor	45 cm x 45 cm
Columns 5 th , 6 th and 7 th floor	40 cm x 40 cm
Beams	50 cm x 30 cm
Floors	30 cm
Concrete quality	C25/30

5.5.4 Boundary condition reliant elements

The structural elements used in the vertical extension model are not fixed but change depending on the height and grid used in the vertical extension model. Table 5.13 shows the elements in the vertical extension that are reliant on the combination of design parameters used in the model. It also shows the range of dimensions used for these elements. Appendix C shows a full list of the dimensions for each of these elements and how they were determined for each combination of design parameters and original building parameters.

Tabel 5.13

Member	Dimensional range
Floors (CLT)	140 – 200 mm
Columns (CLT)	120 – 180 mm

5.5.5. Transfer layer

In chapter 2, the concept of a transfer layer and its purpose in existing vertical extensions has already been shown. A transfer layer is necessary in a vertical extension structure for three reasons:

The original top of the building (the roof) is not designed for full floor loads. The same goes for the beams supporting the roof. It is common practice in extensions to fully remove the roof structure (the beams and the roof itself) and replace it with a floor that is sufficiently capable.

A transfer structure is needed to support the CLT shear walls and transfer both vertical and horizontal forces from the shear walls to the original columns

A transfer structure is needed in structures where the extension grid differs from the original grid. Here vertical loads are transferred by CLT walls or columns to the transfer structure so the loads can be transferred to the original grid.

So even when the grid of the extension overlaps completely with the substructure grid, a transfer layer is necessary to support the CLT shear walls of the extension.

The transfer structure needs to be able to transfer horizontal and vertical loads to the existing columns. The beams are assumed to be discrete, not continuous.

The transfer structure consists of steel beams, that for the purpose of this thesis have been dimensioned as HEA beams. A validation of the beams used in each case can be found in Appendix C. The beams are divided in primary and secondary beams. The primary beams, which are supported by columns and span in two directions, and the secondary beams which are supported by primary beams (see figure 5.14, which shows how one grid of the transfer layer looks when the original grid of the building has been divided by 2).

1/2 GRID	+1 storey	+2 storeys	+3 storeys
G1 (5.5 x 5.5 m)			
G2 (7.5 x 7.5 m)			
G3 (7.5 x 5.5 m)			

Figure 5.14 – Transfer layer elements for a grid divided by 2 (G/2)

5.5.6 CLT panels

Stora Enso's CLT panel catalogue was used to select a CLT panel type to use in the extension part of the model. From the catalogue, the CLT panel with the largest cross section was selected. This is a 5 layered panel with a total thickness of 160 mm. CLT panels in the model have a height of 3.5 m and a width that relies on a combination of the original construction grid used and the extension grid. The mechanical properties of the CLT panel used are presented in chapter 4. The in-plane shear modulus was determined using the shear modulus reduction method proposed by Schickofer (Lukacs, 2019), the effective Young's modulus is determined through the effective area. Both methods can be found in chapter 3.

Tabel 5.15

CLT type	160C5s
Make-up	40-20-40-20-40
Effective Young's modulus E_x	9000 N/mm ²
Effective Young's modulus E_y	3000 N/mm ²
Effective shear modulus	350 N/mm ²
Area	0.16 m ² /m
Effective area A_x	0.75 A /m

5.5.7 Connection design

In chapter 4, the recommended connection design for CLT shear walls was presented. These connections are incorporated in the model in the following way:

- Holddowns are modelled at the ends of shear walls, so 2 holddowns are present per CLT panel
- Brackets are modelled each meter of the shear wall. For example: a shear wall of 5 meters has 3 brackets.

Both holddowns and brackets are modelled as springs in accordance with Lucaks (Lukacs, 2019). Holddowns are modelled as pure vertical springs and brackets as a horizontal and vertical spring. For out of plane forces, the same horizontal spring stiffness is assumed.

The specific spring types were selected according to the Rothoblaas connection catalogue. Because connection stiffness is not a studied parameter, a fixed stiffness was chosen for the connections.

Holddown: WHT620 – $K_{ser} = 13540$ N/mm
Bracket: TCN200 – $K_{ser} = 9600$ N/mm

The complete stiffness values of these connections can be found in appendix D.

5.6 Loads

For the structural analysis in Karamba, the self-weight of the structure, wind loads and variable floor loads are taken into account. Each of these loads are explained here and subsequently the load combinations that will be checked are shown. Where relevant, a distinction is made between Eurocode loads and TGB 1955 loads and partial factors.

5.6.1 Vertical loads – Self weight

The self-weight of the structure consists of two parts: the self-weight of the original structure and the self-weight of the extension. Here, the load values of each of the elements used in the model will be shown.

Any concrete elements are assumed to have a weight of 2400 kg/m³. This goes for the floors, columns, beams and core in the original structure and also for the concrete covers used for the timber floors in the extension.

The extension mainly consists of three materials: timber, steel and some concrete. Steel beams are used for the transfer layer, CLT is used for the floors and shear walls, Glulam timber is used for the columns and a small concrete cover is applied to the CLT floors. It should be noted that the self-weight from steel connections is not taken into account for the self-weight of the entire structure.

Table 5.16

Element	Weight (kN/m³)
Concrete elements (beams, columns, core, floors, cover)	24
Glulam (GL24h)	4.2
CLT	5.0
Steel	7.8

5.6.1.1 Permanent loads

Other permanent loads that are not included in the self weight (AKA permanent loads that do not come directly from structural elements but that are, in principle, present at all times in the structure) are the installations. For these a load of 0.5 kN/m² is assumed.

5.6.2 Vertical loads – Variable loads

In the original situation, the building is assumed to be calculated according to TGB 1955 standards. Here the ground floor is assumed to have been designed for commercial use and the floors above for office use. Table 5.17 shows the variable floor loads for office and commercial use according to TGB1955.

Table 5.17

Function	Load (TGB1955) (kN/m²)
Commercial	2,5
Office	2,5

In the extended situation, the building will consist of a commercial ground floor with the rest of the floors being residential in function. Table 5.18 shows the variable floor loads for residential and commercial functions according to Eurocode standards.

Table 5.18

Function	Load (Eurocode) (kN/m²)
Commercial	4
Residential	1,75

For variable floor loads, both Eurocode and TGB1955 allow for a reduction of variable floor loads for a number of floors. In Eurocode these are called momentaneous factors. These are to be used for all except the two floors that contribute the most to the total load, in this case those would be the bottom two floors. The rest of the floors can be multiplied by a factor of 0.7.

TGB1955 has a similar rule. The roof and the top floor need to be calculated with 100% of the variable floor loads. For every floor below this the percentage can be reduced with 10%, so the floor below the top floor is 90%, the floor below that 80% etc. Until 40% is reached, at which point all floors lower than that are calculated as 40%.

5.6.3 Horizontal loads

Wind loads are applied to the model in accordance with NEN1991 for the extended building and according to TGB1955 for the original situation. Wind loads are assessed in the two main axes of the building. Table 5.19 shows the factors necessary to determine the wind load according to Eurocode.

Table 5.19

Factor (Eurocode)	Description	Value
Wind Area	The wind area that the building is situated in.	2
V_{b0}	Fundamental value of the base wind velocity	27 m/s
C_{dir}	Directional factor	1
C_{season}	Seasonal factor	1
V_b		27 m/s
k_r	0.23	
Z_0	Base roughness length	1m
$Z_{0,II}$		0.05m
Z_{min}	Minimum height	10m
k_l	Turbulence factor	1
C_0	Orography factor	1
C_{p10}		0.8

A full wind load calculation can be found in Appendix A.

Wind load according to TGB1955 is a bit less complicated. For the area that Rotterdam is in a base wind load of 0.4 kN/m² is assumed. For buildings higher than 20m every extra meter adds 0.01 kN/m². For the windward side a coefficient of 0.9 is used, for the leeward side 0.4 is used.

Wind loads are considered in both principal directions of the building, in two separate load combinations (see figure 5.20)

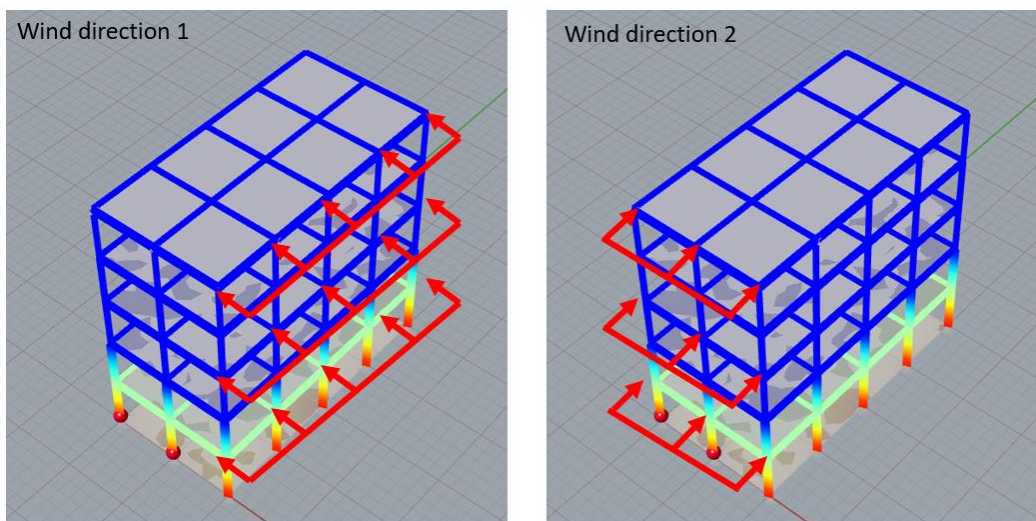


Figure 5.20 – The two wind directions that will be included in separate load combinations

5.6.4 Load factors

Here, the load factors for each of the three codes that are used (TGB1955, NEN-EN1990 and NEN8700) are shown:

Table 5.21

TGB1955		
Partial factor for concrete structures	$\gamma = 1.5$	
NEN-EN 1990		
Permanent loads	$\gamma = 1.35$	L.C. 6.10a
	$\gamma = 1.2$	L.C. 6.10b
Variable loads	$\gamma = 1.5$	L.C. 6.10a
	$\gamma = 1.5$	L.C. 6.10b
NEN8700		
Permanent loads	$\gamma = 1.2$	L.C. 6.10a
	$\gamma = 1.15$	L.C. 6.10b
Variable loads	$\gamma = 1.3$	L.C. 6.10a
	$\gamma = 1.3$	L.C. 6.10b

Here equation 6.10a is used.

5.6.5 Load combinations

The following load combination is used for the building in the original situation (TGB1955):

- $LC = 1.5 * PERM + 1.5 * VAR + 1.5 * WIND$

And the following load combinations were used for the building in the new situation.

ULS on the original building

For checks on elements present in the original building, NEN8700 may be used, in combination with load combination 6.10a.

Unity checks on elements will be carried out using ultimate limit state load combinations. For ULS, the normative load combination of the following three has to be used:

- $ULS1 = 1.2 * PERM. + 1.3 * VAR * \psi_0 + 1.4 * WIND$
- $ULS2 = 0.9 * PERM. + 1.5 * VAR * \psi_0 + 1.5 * WIND$ (for tensile stresses)

ULS on the extension

Since the extension is the new part of the building, regular NEN1991 standards have to be used to create load combinations.

- $ULS\ 1 = 1.35 * PERM. + 1.5 * VAR * \psi_0 + 1.5 * WIND$

These load combinations are used to check the member stresses in the extension. The wind will be checked for two directions (x-x and y-y). Each of these wind directions will be checked in a separate load combination, see figure 5.20. ψ_0 is taken to be 0.4 for both shopping areas and residential areas as per table NB.2 – A1.1 from the national annex to NEN-EN1990. (CEN, 2019)

SLS

For local and global deflections, serviceability limit state has to be used:

- $SLS = 1.00 * PERM + 1.00 * VAR + 1.00 * WIND$

Part 3: Simulation

Chapter 6 – Parameter Study Setup

6.1 Introduction

In chapter 5, the parametric model and the studied parameters were presented. Chapter 6 shows how these parameters are combined to create different extension variants that can be studied. The parameters are grouped into two groups: original structure parameters and extension parameters. The effects of these parameters are studied in two separate sections: the first part of the parameter study will study the effect of the original structure parameters on the spare capacity of the original structure. This is done without any vertical extension being added to the model yet. The second part of the parameter study will deal with both the original structure parameters and the vertical extension parameters. Here, the best combinations of original structure parameters with extension parameters will be studied as well as the effect of the extension parameters on the spare capacity utilization and the design constraints.

6.2 Set-up of the first part of the parameter study

The first part of the parameter study deals with the three original structure parameters which are:

- The original building grid
- The height of the original building
- The core location / presence of a stability core

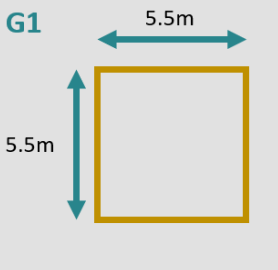
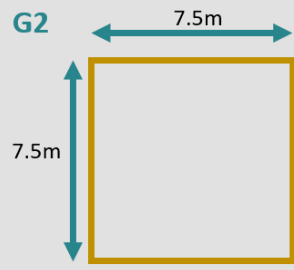
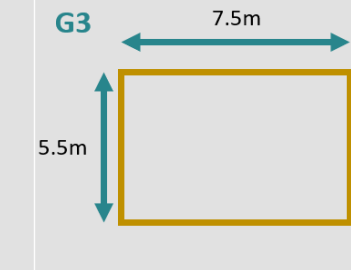


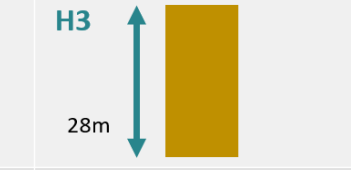
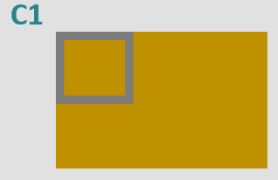


	V1	V2	V3
Grid of the original building	G1 	G2 	G3 
Height of the original building	H1 	H2 	H3 
Core position	C1 	C2 	C3 

Figure 6.1 – The original structure parameters and the values they can take

For each of these parameters, three values can be taken. These are shown in figure 6.1 In this part of the parameter study, the three parameters will all be combined so that every possible combination of parameter values is modelled. In total, that amounts to 27 sets of boundary conditions. Each of these sets will then be assessed on two counts:

- Overall spare capacity in structure
- Distribution of spare capacity in structure

The effect of each of the three parameters on these two design constraints is then analyzed.

6.3 Set-up of the second part of the parameter study

In the second part of the parameter study, the 27 sets of boundary conditions that were mentioned earlier are vertically extended by the model. As was shown in chapter 5, the three studied parameters in the vertical extension are:

- The number of storeys of the extension
- The extension grid
- The shear wall layout of the extension

Like the original structure parameters, the extension parameters can each also take three values, pictured in figure 6.2. Cumulatively, that means that, in total, the second part of the parameter study will create 27 combinations of vertical extension parameters that will be tested on each of the 27 sets of boundary conditions. In total,

that comes down to 729 unique combinations of original structures with vertical extensions.








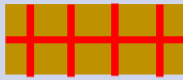

Extension parameter	V1	V2	V3
Number of storeys added	+ 1 storey 	+ 2 storeys 	+ 3 storeys 
Grid division	Original grid 	Original grid /2 	Original grid /3 
Wall layout	A core <u>aligned</u> 	B separation walls 	C facade only 

Figure 6.2 – The extension parameters and the values they can take

6.3.1 Workflow of part two of the parameter study

The second part of the parameter study consists of five separate steps. First, one of the 27 sets of boundary conditions will be created using grasshopper using the original structure parameters as pictured in figure 6.1. The specific parameters that are inputted here influence the elements of the extension that rely on the original structure parameters. This is talked about in chapter 5 and shown in appendix C. The next step is to create 27 extension variants that combine the extension parameters, as pictured in figure 6.2. Each of the created extension variants will then be structurally analyzed by Karamba in the third step. The outputs of this process are explained in chapter 5, under the section design constraints. After the structural analysis is completed and the output is generated, step four will begin. Step four uses grasshopper plugin Colibri to 'loop' steps 2 and 3. This means that each of the 27 extension variants will be tested on the same set of boundary conditions. Colibri then saves all the output and stores it in an excel file. The final step is to assess the variants that are saved in the excel files and to repeat this workflow for each of the 27 sets of boundary conditions. This last part is done by hand. The entire parametric workflow is pictured in figure 6.3.

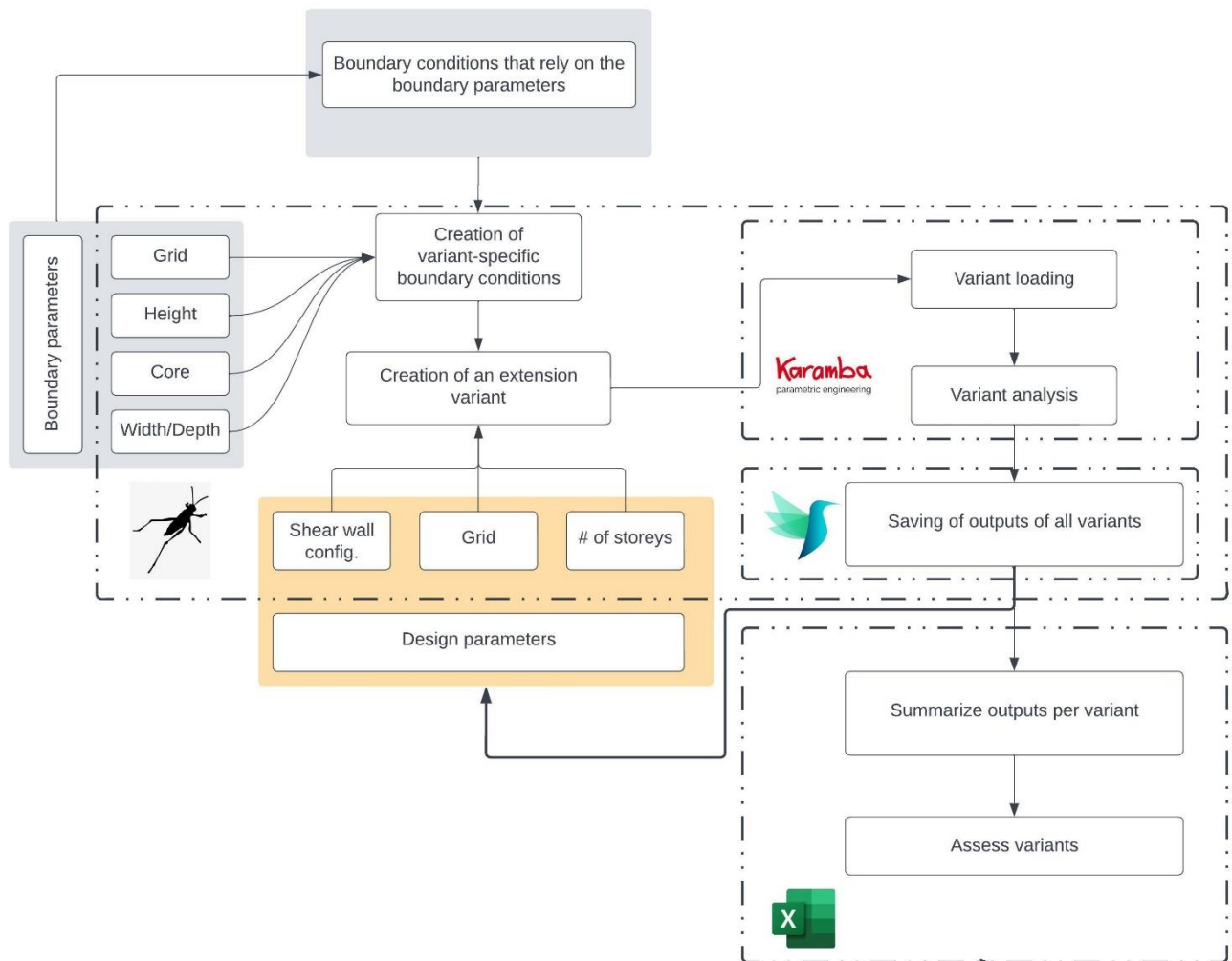


Figure 6.3 – The parametric workflow of the second part of the parameter study

6.3.2 Colibri

Since, in the parameter study, 729 variants will be created, a workflow needs to be created that allows for efficient summarization of each of these variants. In order to do that, the output of each variant has to be aggregated and ‘summarized’. The Grasshopper plugin Colibri is used for this. Colibri offers components that, together, are able to iterate through every design variant and aggregate the desired results into one excel sheet. Below, the three Colibri components that are used, are elaborated on. Figure 6.4 shows the placement of these components in the parameter study workflow.

The first component is the Colibri iterator. The iterator is connected to the design parameters and loops through every possible combination of these design parameters. In this thesis, there are three design parameters that are each regulated with a slider in the model:

- Number of storeys added
- Location of the shear walls
- Grid division

This means that Colibri will make sure that every possible combination of these three parameters is activated within the model.

The second component, the Colibri parameters component, 'catches' the different outputs. In combination with the boundary conditions that have already been put into the model beforehand, the design parameters complete the model which means the Karamba part of the script can be activated. The structural assessment results in a number of numerical results (increased column load, displacement, model mass, etc.) each of which is connected to the Colibri parameters component. This component summarizes the results.

Finally, the third component, the Colibri Aggregator, records the results of each of the combinations of design parameters made with the Colibri Iterator. It then converts these results to a CSV file that is subsequently read and processed in Excel.

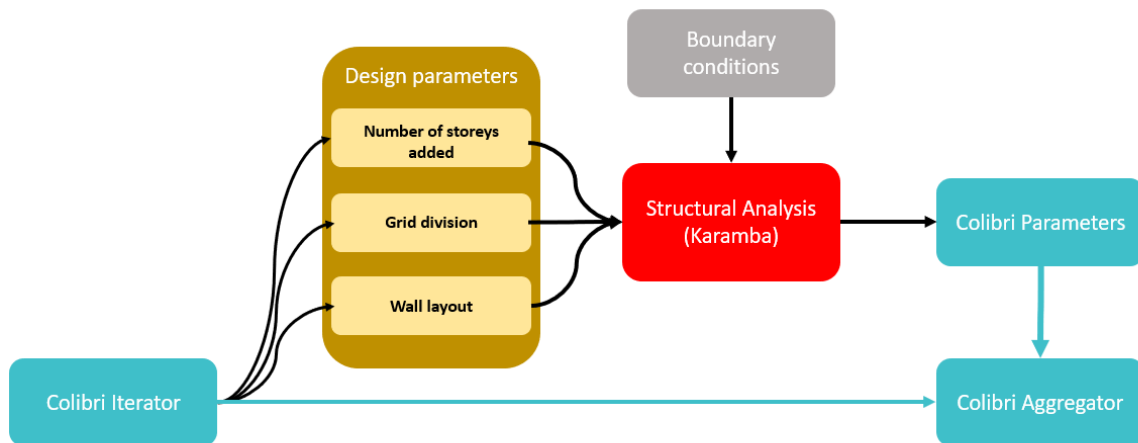


Figure 6.4 – The Colibri components and their placement in the parametric workflow

Chapter 7 – Parameter Study Results

Following the creation of a parametric model to facilitate the exploration of the effects of the studied parameters on vertical extension potential and vertical extension success, a parameter study is conducted to study these parameters. Chapter 6 showed the workflow of the parameter study, now chapter 7 will show the results of that parameter study.

The results have been split into two sections. First, the effects of the parameters present in the original structure on the spare capacity of said structure are explored. This is done by looking first at the effect of the presence and location of a stability core, then the effects of the building grid are shown and finally the effect of the original building height on the spare capacity is presented. It is important to realize here that at this point in the results the original building has not been extended yet.

Subsequently, in the second part of this chapter, the effects of the design parameters will be looked at. These are the studied parameters that influence the design of the vertical extension itself and therefore can have an impact on the success of the vertical extension and the utilization of spare capacity. They are the height of the vertical extension, the construction grid of the vertical extension and the shear wall layout of the vertical extension. In this section the utilized spare capacity is assessed, as well as the unity checks for elements in the extension. The results have been grouped into three parts C1, C2 and C3 variants. Of these, the C1 variants have been elaborately shown here, the C2 and C3 variants are summarized and graphs and sheets made for these variants can be found in Appendix F.

7.1 Effects of parameters in the original structure

First, the effects of the parameters present in the original structure are looked at. As shown in chapter 6, these three parameters were combined in each possible way to create 27 possible original structures. In this section of this chapter, the effect of each of the three parameters is looked at in regards to the spare capacity in the original structure and the distribution of the spare capacity in the original structure. The manner in which the results are compared is that for each parameter that is looked at, the other two parameters are kept fixed. This method allows for a comprehensive comparison between variants of one studied parameter.

The spare capacity is measured in two ways: first, the maximum occurring axial stress in the columns on the ground storey, which is assumed to be the critical set of columns. Second, the reaction forces in the foundation piles. The determination of the spare capacity is shown more elaborately in chapter 5.

7.1.1 Effect of the placement and presence of the stability core

The placement of the stability core can assume three different values (also see figure 6.1 in chapter 6):

- Core option 1 – Core in corner
- Core option 2 – Core in true middle
- Core option 3 – No stability core

Here, the effect of the location / presence of a stability core on the distribution of spare capacity is explored. The distribution of spare capacity through the structure is shown visually, in figures. One figure is made per core variant. The notation that is used in these figures denotes the spare capacity (as a percentage) on top, and the old maximum stress and the new maximum stress on the bottom, respectively on the left and right.

First, the variants of the original buildings with a stability corner in the core of the building are assessed. Figure 7.2 shows the distribution of spare capacity, presented in percentages.

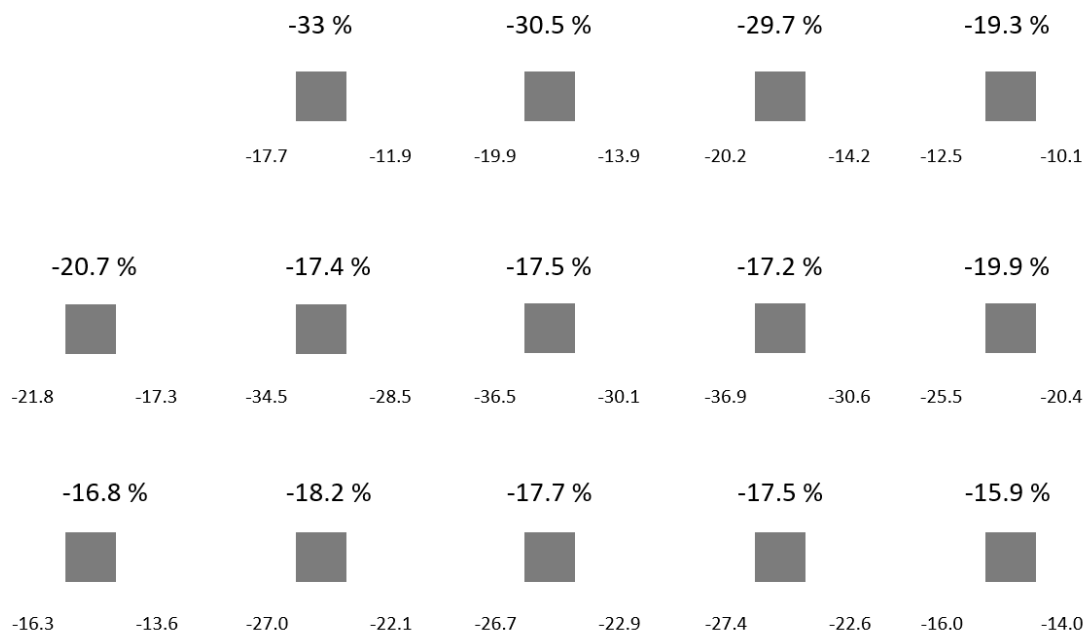


Figure 7.2 – Spare capacity distribution in MPa and in percentages for corner core variants

Since there is a stability core in the corner, no column is present in that location. What becomes clear from figure 7.2 is that the largest spare capacity is unlocked in the first row of columns (as seen from main wind direction). The smallest relative spare capacity is found in the corner diametrically opposite the stability core, column 15. Next, the original building variants with a stability core in the middle are looked at. Figure 7.3 shows the distribution of spare capacity over the floor plan.

Again, the first row of columns shows the largest relative spare capacity, whereas the last row of columns shows the least relative spare capacity.

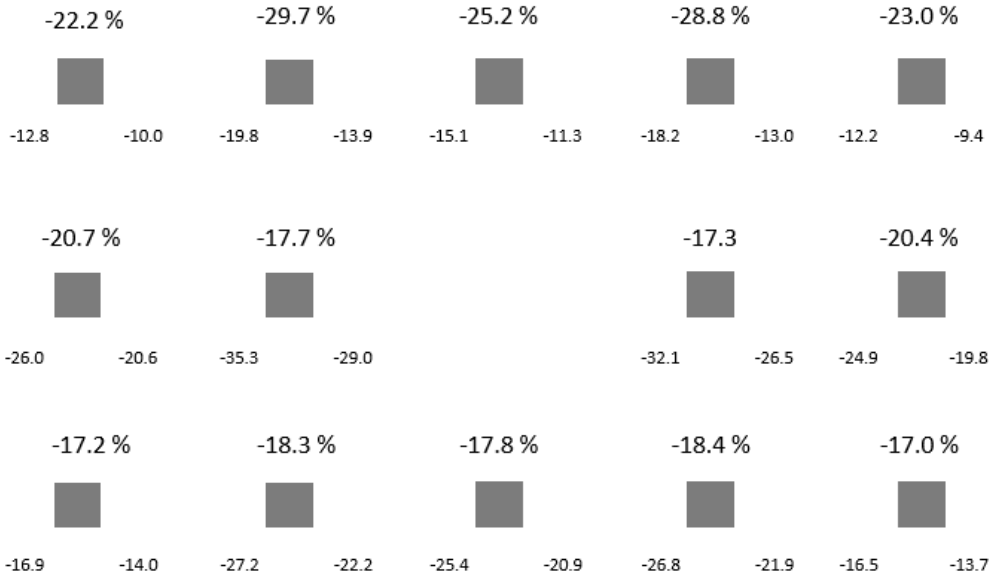


Figure 7.3 – Spare capacity distribution for C2 variants

Lastly, the original building variants with no stability core are studied in figure 7.4.

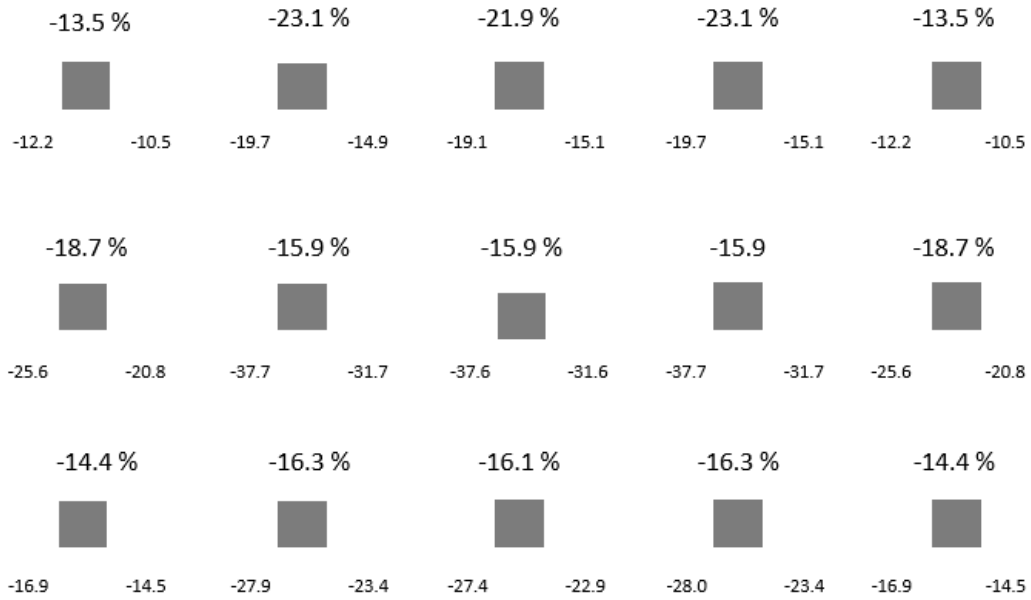


Figure 7.4 – Spare capacity distribution for C3 variants

The ranges of the relative spare capacity within each of the variants are shown in figure 7.5.

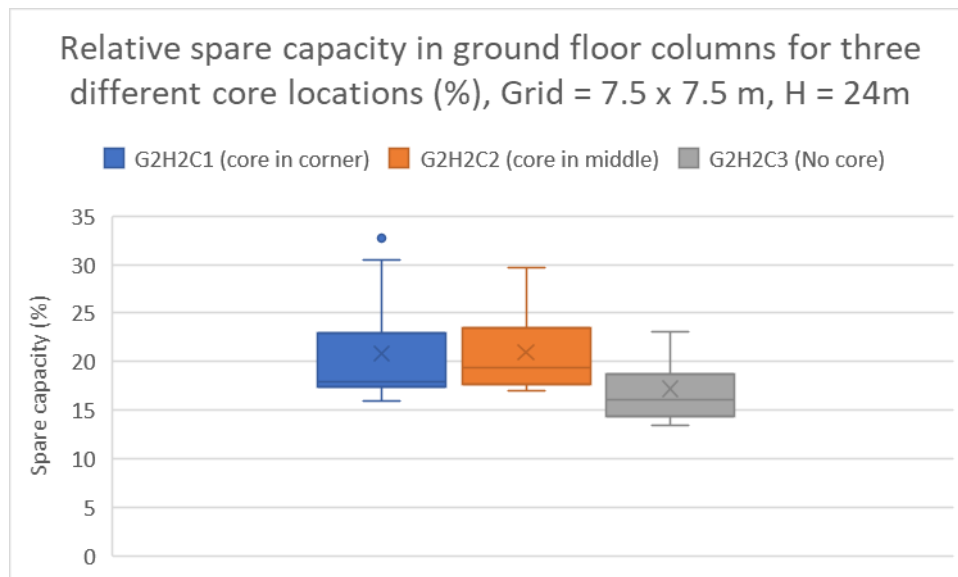


Figure 7.5 – Spare capacity distribution (%) for different core locations

Here it becomes clear that both the variants that possess a stability core show relatively similar spare capacities (the average relative spare capacity is very similar, 21% for both variants). The range of the spare capacity among columns in both variants, however is quite different. The variant with a stability core in the corner shows a range of 16.8 percent whereas the variant with a stability core in the middle shows a smaller range of 12.6 percent. The original building variant with no stability core at all, lastly, shows a range of only 9.7 percent and a significantly smaller average spare capacity than both variants that do possess a stability core.

7.1.3 Effect of the base construction grid

To assess the effect of the base construction grid, the average spare capacity utilization in the ground floor columns of the C1 variants (stability core in corner) was determined. When looking at the different spare capacity utilizations created by different construction grids, it becomes clear that construction grid 2 (7.5 x 7.5m) shows the largest spare capacity. This is presented in figure 7.6. Here, it is shown that the spare capacity utilization in the ground floor columns found in Grid 2, at a base structure height of 20m is 15% lower than the spare capacity utilization in the same columns in structures with smaller grid sizes.

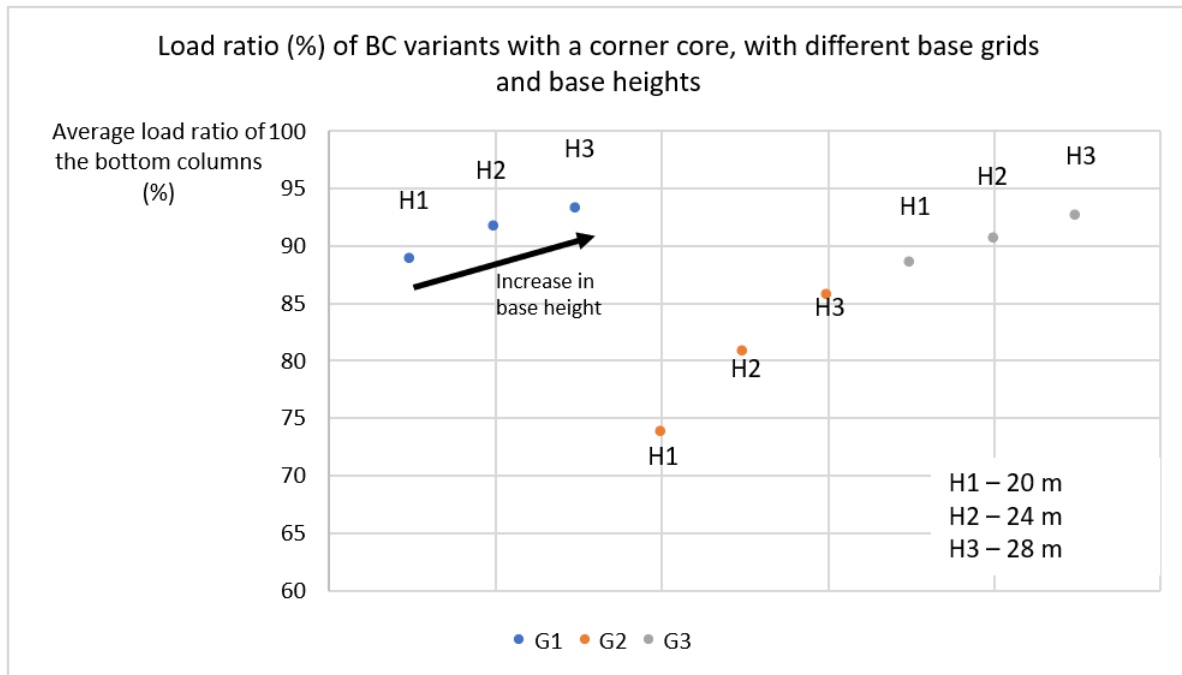


Figure 7.6 – Spare capacity utilization of sets of boundary conditions with a corner core, with different grids

However, it is possible that the shape factor has something to do with this. Since the model keeps a set amount of grids in both x and y direction (the building is always 4 x 2 grids), this means that the width and depth of the building automatically change when the gridsize is changed. To assess whether the difference seen in figure 7.6 is purely gridsize related or also has something to do with width and depth of the model, a separate model is created that is 3x3 grids large. By using this grid size, the shape is as good as corrected for because the G1 variant will be 16.5 x 16.5 m and the G2 variant will be 15 x 15 m. It should be noted that the dimensions are not exactly the same, but since they are close, this can give us a good idea of the direct influence of the original base grid. Figure 7.7 shows the two grid models and figure 7.8 shows the results.

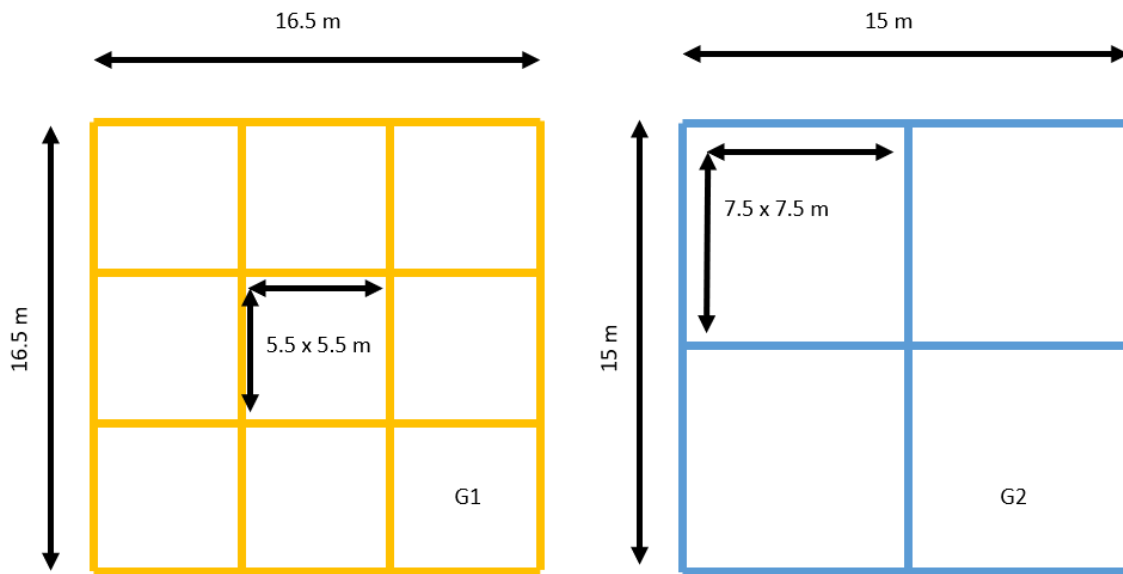


Figure 7.7 – Gridsize models with shape correction

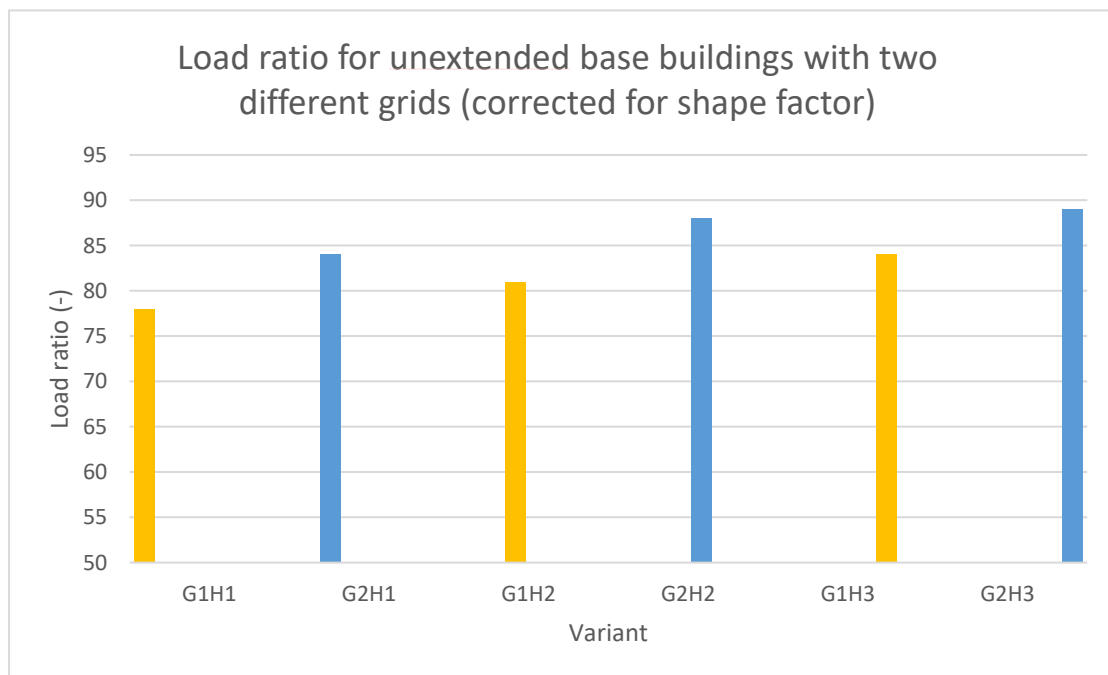


Figure 7.8 – Load ratios for the two different grids when corrected for shape

There is still a difference visible, but the largest difference is only 7% instead of 15%. That means that 7% of the abovementioned differences can be explained just by the grid and the other 7% come from the shape factor that also plays a role.

7.1.4 Effect of the number of storeys in the original structure

Lastly, the effect of the height of the original structure on the spare capacity is assessed. The three possible heights of the original structure are:

- H1 - 5 storeys – 20 m
- H2 - 6 storeys – 24 m
- H3 - 7 storeys – 28 m

Figure 7.9 shows the effect of the height of the original building on the spare capacity found in the columns. Here, the percentage of capacity still left in the columns is given in a box plot. In order to effectively compare only variants with different height parameters, the other parameters are kept the same within each comparison group. In this case, all variants have no stability core, while the grids are also varied with.



Figure 7.9 Height of the original structure vs. spare capacity left in the bottom columns (%) for variants with no stability core

Graph 7.9 shows that the amount of storeys present in the original structure has quite a large effect on the percentage of spare capacity left in the bottom columns. As becomes visible in table 7.1, where the average spare capacity is determined, the relative spare capacity in the bottom columns decreases by around 2 to 3 percent per extra storey in the original building. For larger grids like Grid 2, which is 7.5 x 7.5 m large, the steps seem to be larger, around 5% of spare capacity is lost per added storey. However, this effect is only partially due to the gridsize itself and also includes the influence of the shape factor.

Tabel 7.1 Percentage of spare capacity left in ground floor columns, based on maximum axial stress, for different base grids

	H1 = 20m	H2 = 24m	H3 = 28m
G1 (5.5 x 5.5m)	12,93 %	10,30 %	8,02 %
G2 (7.5 x 7.5m)	22,09 %	17,19 %	12,31 %
G3 (5.5 x 7.5m)	13,97 %	10,60 %	8,21 %

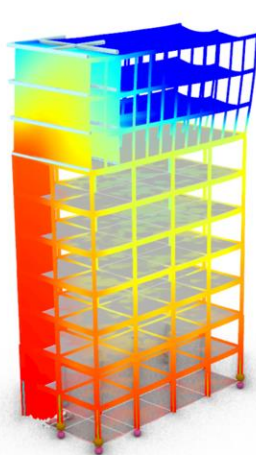
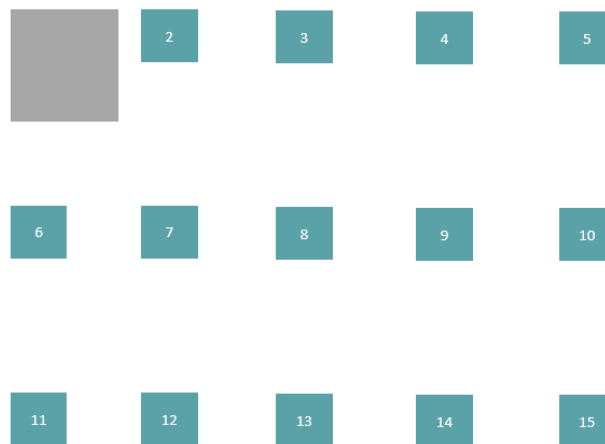
7.1.5 Observations of the effect of the parameters within the original structure

- Sets of boundary conditions that do not possess a stability core show a significantly smaller spare capacity than variants with a stability core. The range of the spare capacity found within the columns is also smaller, so the spare capacity is more evenly distributed.
- Sets of boundary conditions with a stability core in the corner and sets of boundary conditions with a stability core in the middle of the building show relatively similar average spare capacities, but the range of spare capacities found within columns differs more significantly. Sets of boundary conditions with a corner core show a larger range in column spare capacity than sets of boundary conditions with a middle core (16 vs. 12 percent).
- Sets of boundary conditions that possess a larger construction grid show significantly more spare capacity. It was found that the largest grid size looked at in this thesis possesses a spare capacity utilization that is about 15% lower than that of the same type of structure with smaller construction grids. However, this effect is due, in large part, to the shape factor. When two grids were compared with a correction for the shape factor, the largest difference was about 7%.
- Sets of boundary conditions that are higher show smaller spare capacities. The decrease in spare capacity per storey added ranges from 2 to 3% per storey, depending on the construction grid. Larger construction grids show a bigger decrease in spare capacity in the ground floor columns.

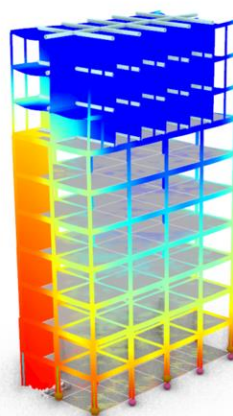
7.2 Extension design results

In this section, the results of the studied parameters in the vertical extension are presented. Three core locations were studied. In this chapter, the corner core (C1) variants are shown elaborately and a summary is given for the results of C2 and C3 variants. For more information on these latter two variants, one can refer to Appendix F, where the results for C2 and C3 are shown more elaborately.

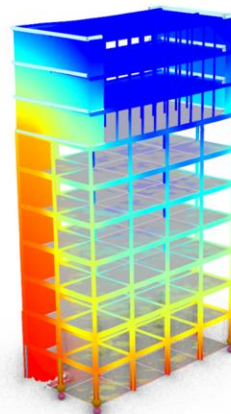
7.2.1 C1 (corner core) variants



Wall layout A
Core alignment



Wall layout B
Functional division



Wall layout C
Façade only walls

7.2.1 Effects of wall layout

First, the effect of wall layout was assessed. As mentioned before, three different wall layouts were tested on the 27 original structures that were parametrically created in Grasshopper. The effect of wall layout is assessed on three counts:

1. Capacity utilization, in the foundation piles, the columns at the ground floor and the columns at the top storey
2. Deflection of the entire building
3. Utilization of the CLT and connections in the extension

The effect of wall layout is looked at separately for the three corner positions, in the results, the parameter for grid size has been set to G1 (5.5 x 5.5 m grid). Wherever a change in base grid affected the results in a relevant way, this was mentioned in the text.

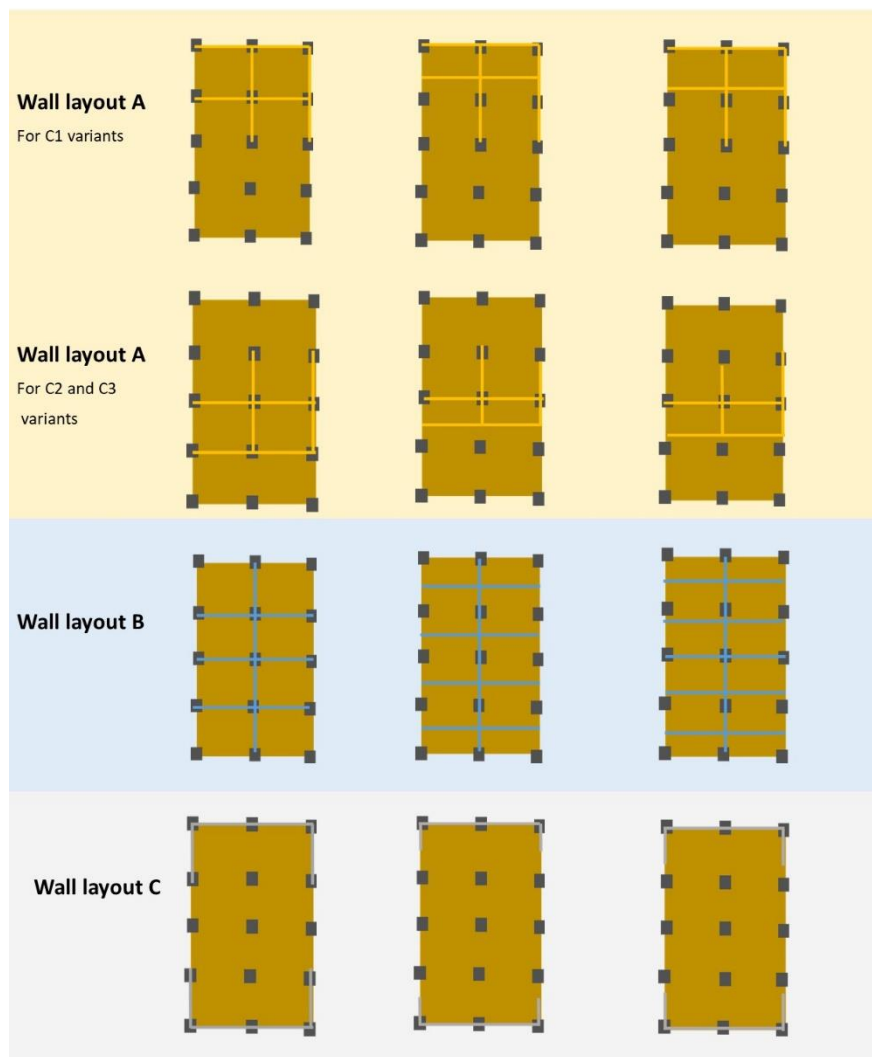
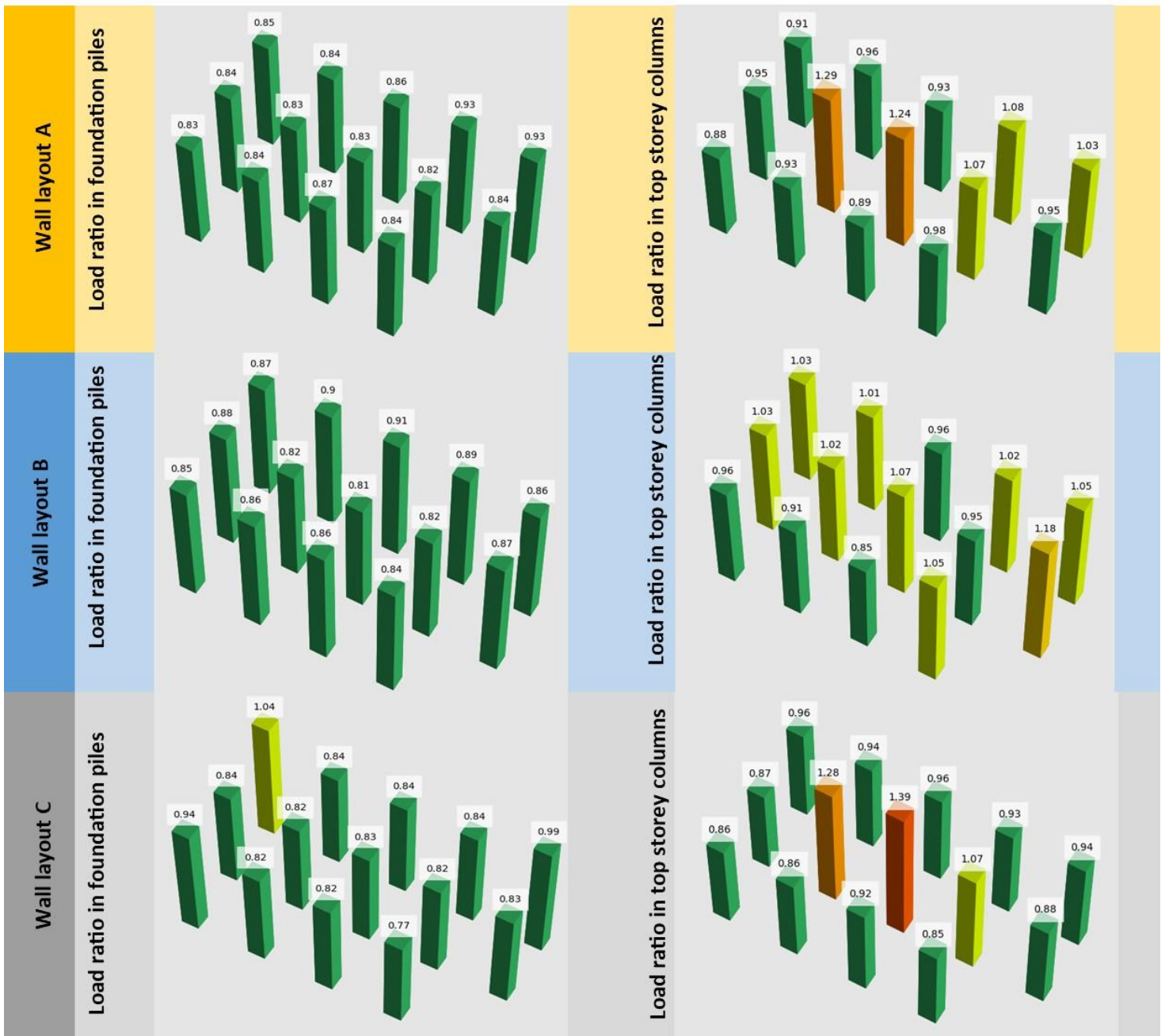
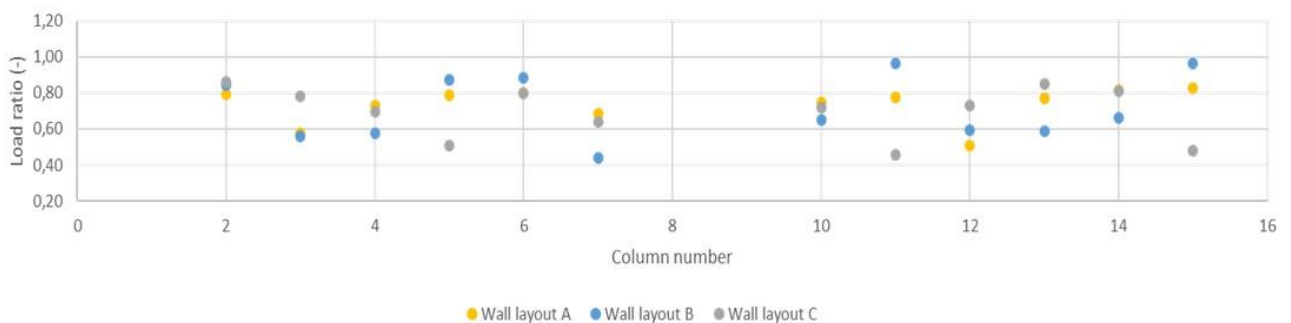


Figure 7.2.1

Load ratios for different wall layouts on a G1H3C1 variant (extension grid = G/1), 3 storeys added



Load ratio for tensile stress in the top storey columns for three wall layouts in a G1H3C1 variant
(G/1, 3 storeys added)



From the graphs above, it becomes immediately clear that a variation in wall layouts causes some significant differences in the foundation piles. Table 7.2 shows the largest percentual difference between wall variations found in the foundation piles. The variation in the front row foundation piles is smallest while foundation piles 8 and 15 show the largest range. In both these columns wall layout C shows the largest capacity utilization. Wall layout A especially affects the last row of foundation piles (11-15), showing a much larger capacity utilization in column 11 than in the following piles. Wall layout B shows a more 'stable' capacity utilization in this row of foundation piles. Finally, wall layout C shows a more symmetrical capacity utilization where column 11 and 15 are loaded much higher than columns 12-14.

Table 7.2 – Largest ranges in foundation piles found between wall layouts A, B and C

Foundation pile index		2	3	4	5
Range (%)		2,62	0,30	3,98	6,66
Foundation pile index	6	7	8	9	10
Range (%)	3,19	3,11	3,82	2,18	5,90
Foundation pile index	11	12	13	14	15
Range (%)	8,08	5,27	5,46	5,68	15,18

We also see that the effects in the compression in the top storeys are more pronounced than in the foundation piles. Here, we can see some clear effects.

The results show that the load ratio is significantly higher than for the ground floor columns or for the foundation piles, more than half of the columns exceed the capacity utilization limit of 1.0 for at least one wall variant. Some observations from figure 7.2.8:

- Wall layout A has a clearly concentrated effect on the core side of the structure. This effect also translates to the foundation piles.
- Wall layout B causes a large spike at column 6 that was only visible in a limited capacity at the ground floor columns. In addition to this wall layout B also causes large tensile stresses in columns 11 and 15 (the corner columns).
- Wall layout C shows a large peak in the middle of the structure (column 8 and 9), that is not visible when looking at the foundation piles. In addition to this, the tensile stresses at the top storey columns for wall layout C peak at column 13, but are very low at columns 11 and 15 (where a shear wall is located right on top of the column).

7.2.1.1 Tensile stresses in the ground floor

The columns on the ground floor are barely loaded in tension, while the columns on the top storey are much more prone to being loaded in tension. On the ground floor, column 11 is occasionally loaded in tension, while column 15 is loaded in tension most of the time. Figure shows the magnitude of capacity utilization based on minimum stress in these columns.

The relationship that follows here is that in terms of minimum stress, a higher main structure and a larger extension actually is a reducing factor. Extension variants with less extension storeys and original structure variants with less storeys show larger tensile stresses in the columns of the ground floor.

Figure 7.10 shows the capacity utilization of tensile stresses in columns 11 and 15 for variant G1H3C1, where the extension grid is G/1 (the same as the original structure). Column 11 shows to be loaded in tension considerably more by wall layouts B, which causes tensile stresses regardless of the amount of storeys added, whereas variants with wall layouts A and C are only loaded in tension for extensions where only 1 storey is added.

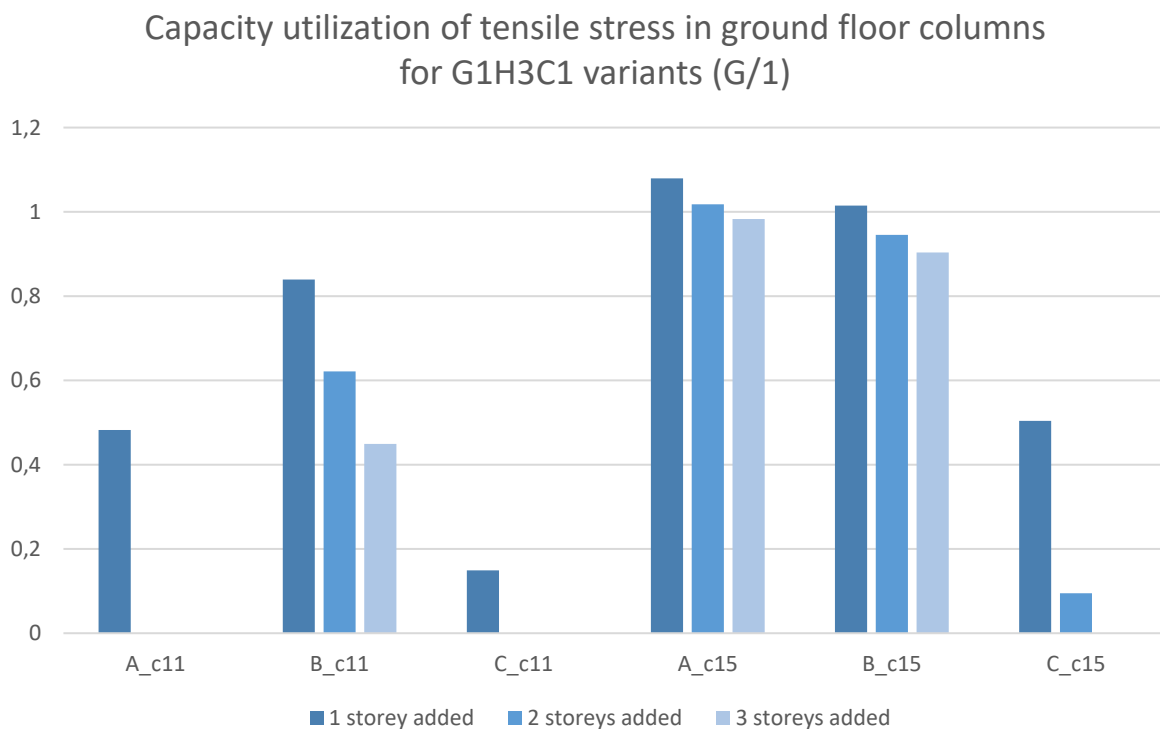


Figure 7.10

7.2.1.2 Overall capacity utilization observations for the effects of wall layouts in C1 variants

- Wall layout A shows larger capacity utilizations in the middle columns
- Wall layout B shows larger capacity utilizations in edge columns that are not corner columns
- Wall layout C shows the largest capacity utilizations at the corner columns and in the exact center of the building
- Columns at the ground floor are loaded less in tension than those at the top storey, but reach the capacity utilization limit earlier.
- At the ground floor, the columns that are most likely to develop tensile stresses are columns 11 and 15
- At the top storey, most columns develop tensile stresses, with the exception of columns 8 and 9
- Columns at the top storey tend to reach the capacity utilization limit earlier for compression stress
- In the foundation piles, the largest difference among wall variants is found in columns 11-15, with the peak difference being 15% at column 15.

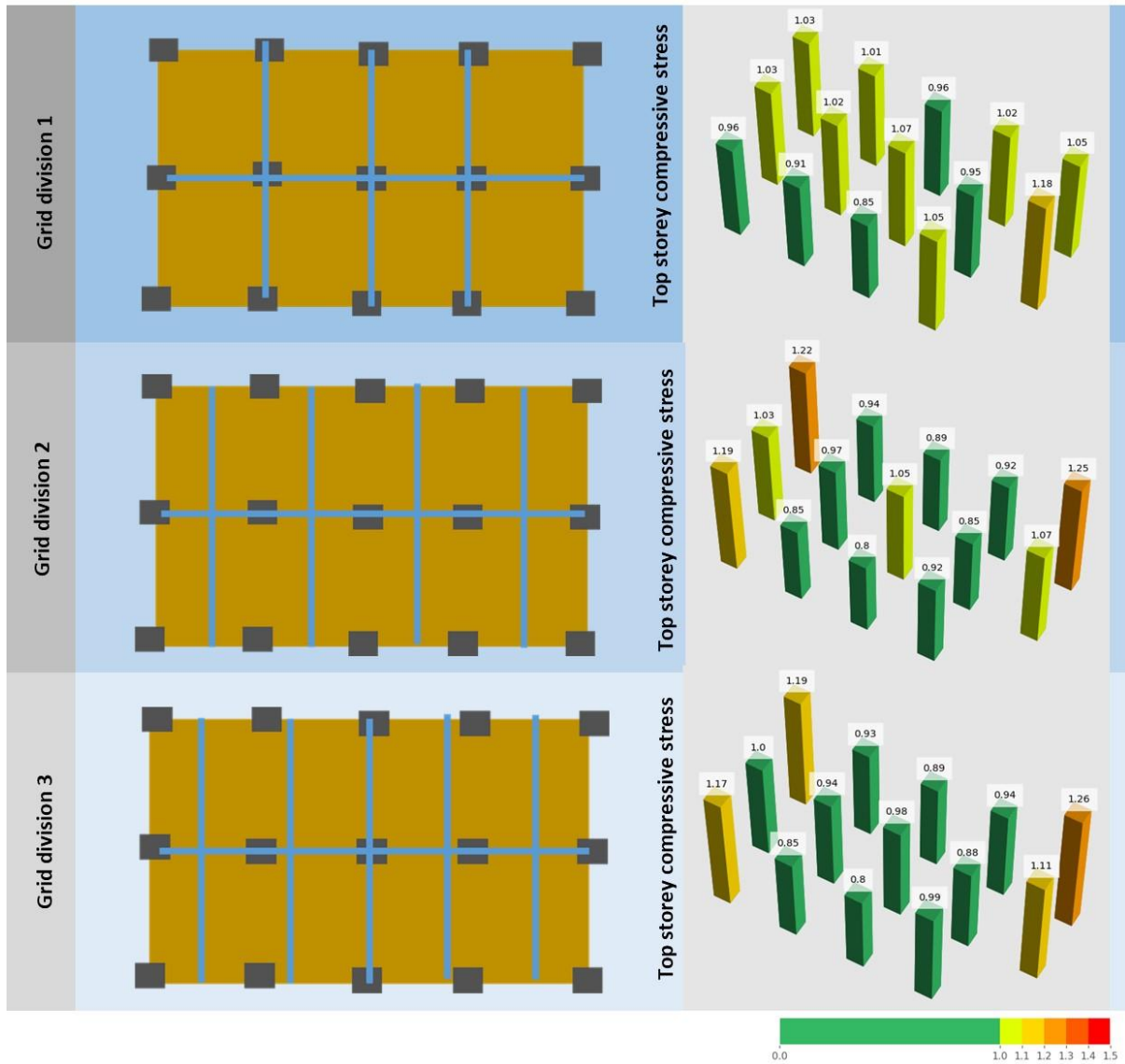
7.2.1.3 Effects of extension grid

To assess the effect of the extension grid on the spare capacity, now the wall layout will be the 'locked' parameter in each graph. This means that the three possible extension grids (G/1, G/2, G/3) will be compared against each other for only one wall layout at a time. Again, the main variant that is used here is G1H3C1.

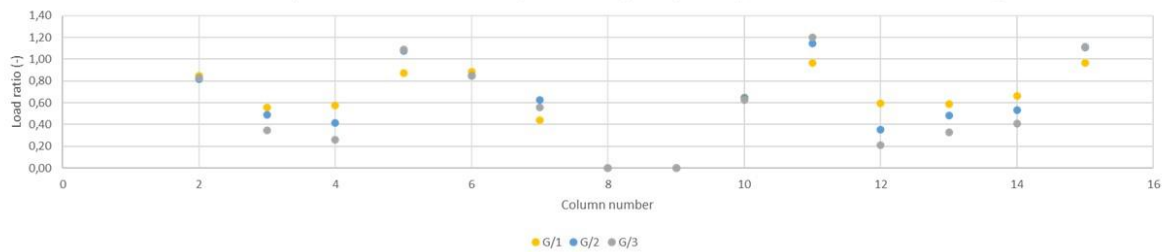
Like in section 7.2.1 , summary sheets are made that show the wall layouts and the compressive stresses in the top storeys. These can be found in Appendix F. Here, the sheet for different extension grids under wall layout B will be used (sheet pictured on the next page).

Here, it can be seen that a change in grid can bring out large differences in column loading. It is observed that G/1 variants with wall layouts B more evenly distribute the loads over all columns in the building. G/2 and G/3 variants, on the other hand, show an increased loading in columns 5, 11 and 15 (the corner columns). It can also be observed that in each variant, column 6 is loaded more than average.

Load ratios for different extension grids on a G1H3C1 variant (wall layout B: functional design), 3 storeys added



Tensile stresses in top columns in variant G1H3C1, with wall layout B, 3 storeys added for different extension grids



7.2.1.4 Deflection

The total deflection of the building, including the vertical extension, can be an important way to see how different wall layouts affect the stability of the extension. Figure 7.11 shows, for G1H3C1 variants, what deflection is found for different variants and the total building height.

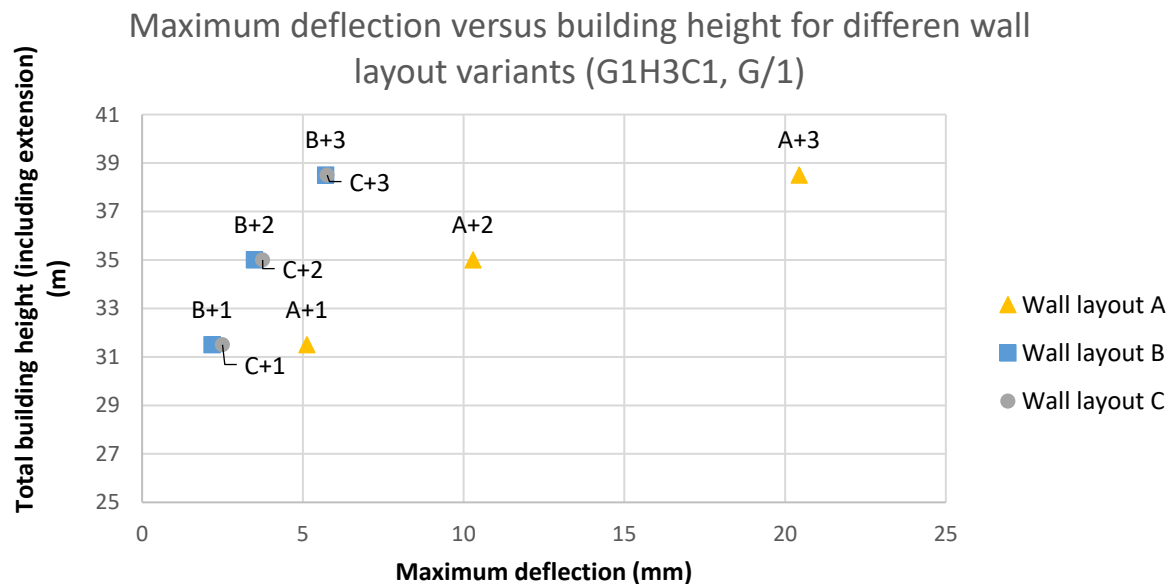


Figure 7.11 – Deflection versus building height

Wall layout A shows the largest deflections, diverging from wall layouts B and C with every storey that is added. Wall layouts B and C on the other hand show much smaller deflections than wall layout A and their deflections seem to converge with every added storey. It should be noted that, even though wall layout A variants show much larger deflections at the top of the building, these deflections still stay within the limits of deflection as defined by Eurocode ($h/500$ mm). Table 7.3 shows the U.C. values reached.

Table 7.3 – Deflection U.C.'s

Wall variant and added storeys	Total Height (m)	Deflection limit (mm)	Modelled deflection (mm)	U.C.
A+1	31,5	63	5,12	0,08
A+2	35	70	10,29	0,15
A+3	38,5	77	20,44	0,27
B+1	31,5	63	2,17	0,03
B+2	35	70	3,49	0,05
B+3	38,5	77	5,71	0,07

C+1	31,5	63	2,50	0,04
C+2	35	70	3,75	0,05
C+3	38,5	77	5,76	0,07

It follows that while all variants comply to Eurocode deflection limits, wall layout A shows the largest deflections.

7.2.1.5 Utilization of extension elements

Finally, we'll look at the utilization of elements in the extension. Here, we'll look at the CLT panels and the connections. Figure 7.12 shows the U.C. checks found in the CLT panels. What stands out here is that none of the CLT panels in the extensions fail. Wall layout B shows to have the highest fail rate in failures across the board. This is corroborated, in figure 7.13, by failure in the connections. However, in the connections, for G/1 grids, wall layouts A show higher U.C.'s.

The connections show, overall, much higher unity checks and cross over the critical U.C.'s in some cases. This is the case for only wall layouts A and B, never for wall layout C. In addition to this, connections seem to mostly fail in extension of three storeys. From this, it can be concluded that connections are much more likely to fail in the extensions on C1 structures. What also stands out is that overall, the U.C. values seem to be largest in G/1 variants, where the grid of the extension is the same as that of the original structure.

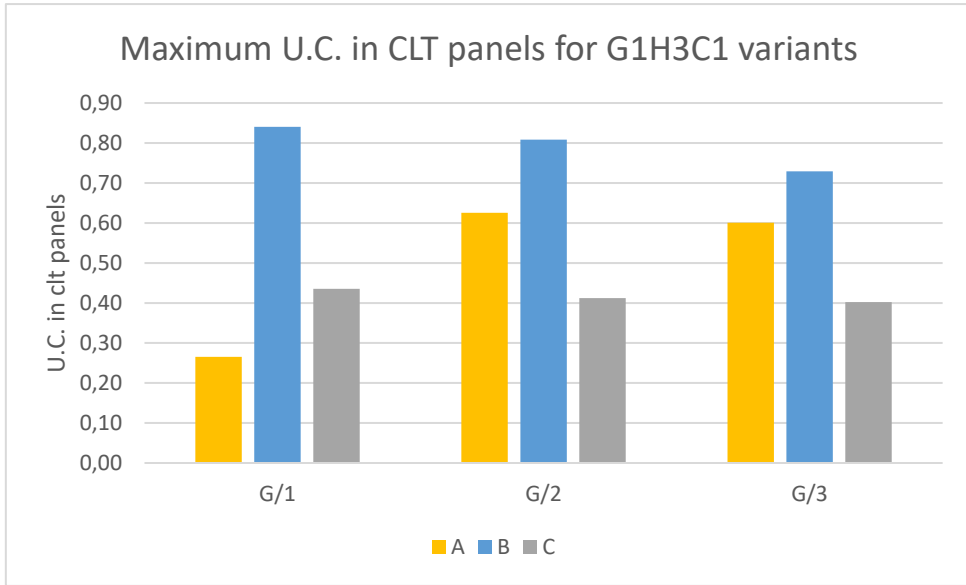


Figure 7.12

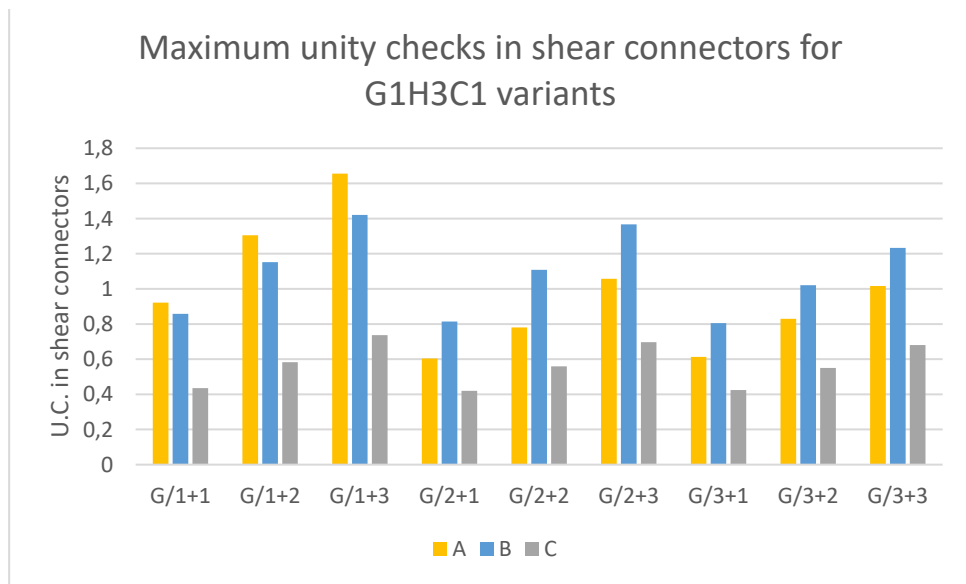


Figure 7.13

7.2.1.6 Conclusion C1 variants

In conclusion, some ranges are shown as to illustrate the magnitude of the effect caused by varying wall layouts and extension grids.

Two numbers are determined: the average range and the maximum range. The average range is the average percentual difference between individual elements of multiple studied variants. For example, when the average range in the top storey columns is determined the range in load ratios for each individual column is determined and from all of those ranges an average is calculated. The maximum range is the largest range that is encountered, and therefore it belongs to a single element.

Figure 7.14 shows the ranges found in C1 variants. The first three groups show the ranges between extension grids. These are found within groups of the same wall layouts. The fourth group shows the different amongst wall layouts. What becomes clear from this figure is that the effect on load ratios in elements of the original structure created by varying wall layout is overall larger than the effect caused by varying the extension grid. Especially when looking at varying the extension grid within wall layouts B and C. However, wall layout A shows some local and global ranges that are larger than those found in wall variations.

We also see that, especially when looking at tensile stress in the top storeys, the maximum range can be quite large, whereas the average range stays behind a bit. This implies that the local effects of both variations in extension grids and variations in wall layout can have very large local effect (on individual element level), whereas the average effect never goes above 22%.

In addition to see, we can observe that while overall the local effects brought by extension grid can be as large as those brought by varying wall layout, this is less so the case in elements lower in the structure. The foundation piles and ground floor columns are significantly more susceptible to changes in wall layout than to changes in extension grid.

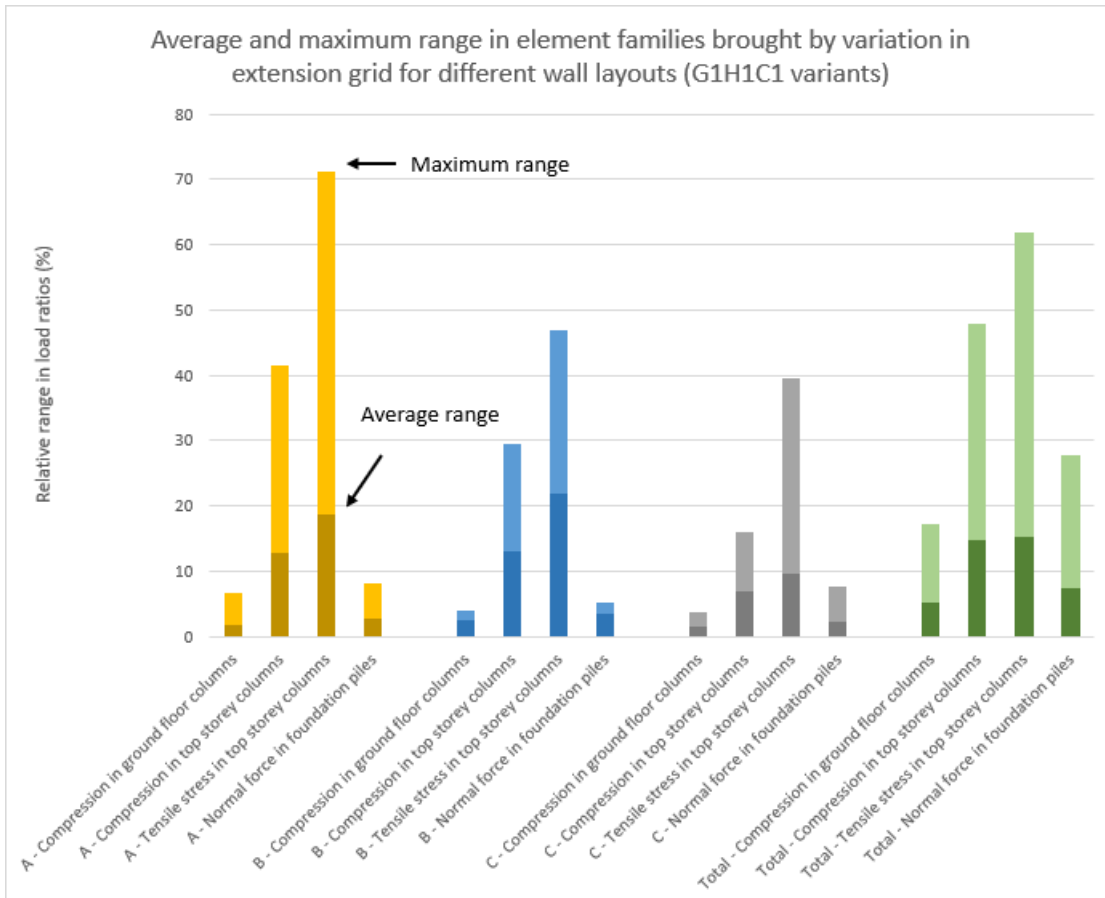


Figure 7.14

7.3 C2 variants

7.3.1 Spare capacity usage

In C2 variants, the core is now present in the middle of the structure (see figure 7.2.1). This has some effect on the different wall layouts that are used. Wall layouts B and C remain the same, but since wall layout A is intended to align with the stability core, the walls are now situated in the middle of the structure (also shown in figure 7.2.1). Elaborate graphs can be found in appendix F.

In the foundation piles it is shown that wall layout C shows an overwhelming increase in load ratio on columns 1, 5, 11 and 15, which are the corner columns. While wall layout A shows the smallest load ratios at most other columns. Wall layout B shows smaller load ratios on the middle row of columns (columns 6-10).

When looking at the tensile stresses in columns, it becomes clear that in C2 variants, no tensile stresses occur in the columns on the ground floor. This is in stark contrast to C1 variants where the two columns opposite the core did, in fact, experience tensile stresses. In the top storey, however, all columns experience tensile stresses. The windward corner columns experience the largest tensile stresses under wall layout A and the leeside corner columns do so under wall layout B. Overall, the load ratio shows a significant drop in column 13, the column just behind the stability core. Especially for wall layout A (core alignment), here the load ratio is equal to 0.

Finally, the compressive stresses in columns are assessed. Here it is observed that the distribution of compressive stresses in top storey columns are quite different from those at the ground floor. For example, in column 3, a 'peak' is found in the load ratios for wall layouts B and C in the top storeys whereas this becomes a 'dip' when looking at the ground floor columns.

For each of the elements discussed, the range between wall variants and grid variants was determined to show the magnitude of the effect, this is shown in figure 7.15.

7.3.2 Deflection

When looking at the effect of wall layout on deflection, it is observed that wall layout A causes, by far, the largest deflections, at three storeys added this deflection is 8mm while wall layout B and C both range between 3 and 4 mm.

When looking at the effect of the extension grid, on the other hand, it is observed that the differences made here are much smaller. When looking at different extension grids using wall layout C, the deflections are all the same. In wall layouts B, deflections under G/1 are 0.5 mm higher than those of G/2 and G/3. Finally, in wall layout A, the differences are a bit bigger, where G/3 variants show the highest deflection (8 mm), while G/1 variants show the lowest deflection (6.5 mm).

7.3.3 Utilization of Extension elements

Again, the U.C. checks of the CLT panels do not exceed 1.0 in any of the variants looked at within the C2 family. However, the shear connectors between the CLT panels and the floors do, at times, reach critical U.C. values. A clear trend is visible here between the type of extension grid and wall layouts. It is observed, for example that, in total, the critical U.C. is exceeded in 5 variants, 3 of which have wall layout A and 2 have wall layout B. Variants with wall layout C never exceed a U.C. value of 1 in the shear connectors. We also see that wall layouts B show a higher U.C. value for extension grids G/2 and G/3, while wall layouts A show a higher U.C. value for extension grids G/1 and G/2. While U.C. values in wall layouts A and B show a dependence on the extension grid, this is not the case for U.C. values in wall layouts C, these stay remarkably consistent.

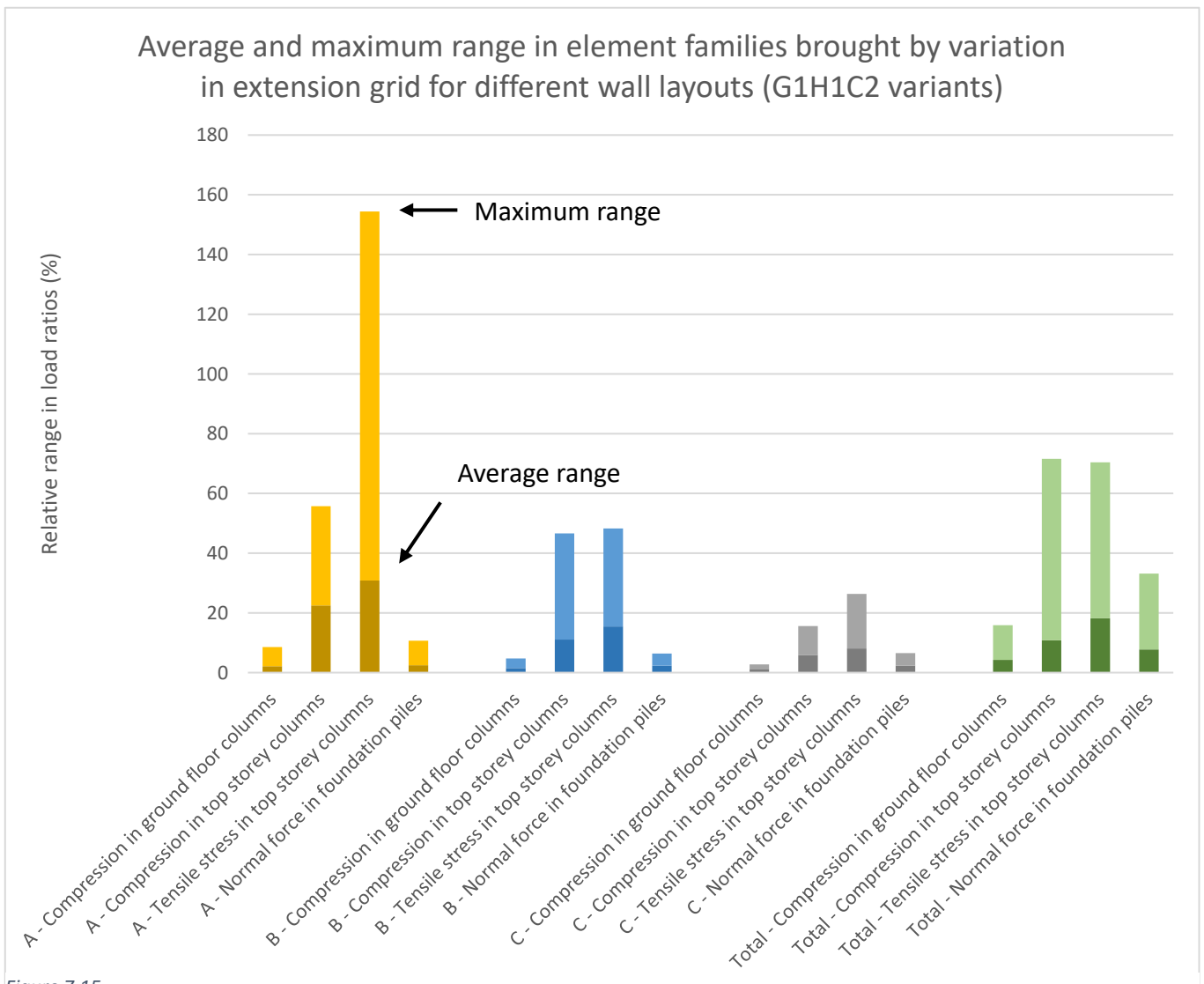


Figure 7.15

7.4 C3 variants

Finally, C3 variants are assessed. C3 variants were designed without a stability core in the original building. The same wall layouts are used as in the C2 variants. That means that, again, from C1 to C3 only wall layout A differs (shown in figure 7.2.1). Elaborate graphs can be found in appendix F.

7.4.1 Spare capacity usage

We observe, first and foremost, that the load ratios found in C3 variants are much higher than those found in C1 and C2 variants. This might already lead to some early conclusions on the extendibility of such building typologies.

When looking at the foundation piles, we see a very similar distribution to the one seen in C2 variants: wall layouts C show larger load ratios in the corner columns, while load ratios A and B show peaks in the middle of the structure. We see, however, that for wall layouts A and B, the average load ratio for all foundation piles is 5% higher in C3 variants than in C2 variants. Interestingly, for wall layouts C, the average load ratio in the foundation piles is the same in both C2 and C3 variants.

Then, looking at the tensile stresses in the ground floors. Most interestingly, the tensile stresses in the ground floor columns are significant. While tensile stresses in the ground floor columns did not occur as much in C1 and C2 variants, here we see that columns 1, 5, 6, 10 and the entire column row 11-15 are loaded exceed the load ratio of 1.0 for tensile stress for every base height of building used. This, again, indicates that buildings with no stability core are significantly more challenging to extend vertically.

Finally, the compressive stresses in the top storey and ground floor columns are assessed. Here we see that in the top storey, over half of the columns exceed a load ratio of 1 when 3 storeys are added, whereas in the ground floor columns every column exceeds the load ratio limit. This is an interesting insight because it shows an effect diametrically opposite to the one observed earlier in C1 and C2 variants, where the ground floor columns were *less* likely to exceed the load ratio limit than the top storey columns.

7.4.2 Deflection

First, it is observed that deflections for a structure with no stability core are significantly higher than those for structures that do possess a stability core. However, the critical deflection limit is not reached in any of the variants. The results show a trend similar to C2 variants, where wall layouts A show a larger deflection than wall layouts B and C. However, the maximum difference between wall layout A and B here is similar to the difference found in C2 variants. This implies that most of the deflection of C3 variants is due to the original structure and that the extension deflects more or less the same regardless of a stability core being present. One difference, however, is that wall

layouts C show a slightly larger deflection than wall layouts B in C3 variants, whereas the opposite is true in C2 variants.

7.4.3 Utilization of Extension elements

When looking at the utilization of extension elements, again, we see that critical U.C. values for the CLT panels themselves are never reached. Again, it is observed that the shear connectors are the only elements in the extension that reach a U.C. value of 1.0. They do so in C3 variants a lot quicker than in C2 variants. This implies the influence of the stability core. In the U.C.'s of connections, again, wall layouts A and B show failures in the shear connectors, while wall layouts C do not. What stands out in these results is that, whereas for C1 and C2 variants, the extension grid did not only influence the magnitude of the U.C. values (it also influenced which wall layouts showed failures), in C3 variants, the relationships between wall layouts A, B and C stay very similar throughout.

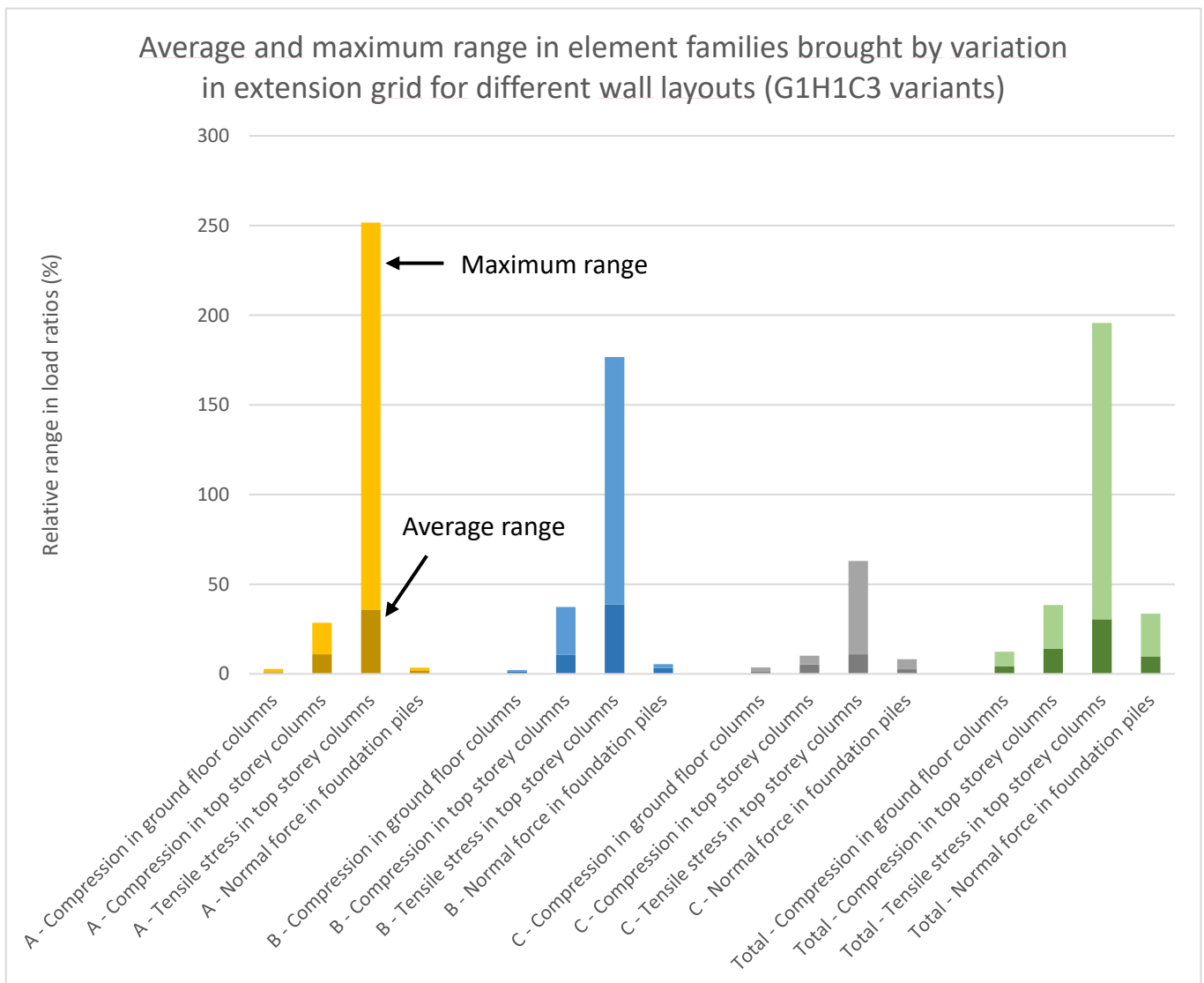


Figure 7.15

7.5 Conclusion results

In this chapter the results of the parameter study were shown. Using the same framework as earlier (original structure parameters and extension parameters), the effects of the studied parameters on specific aspects of the practice of vertical extension were shown. This was shown in both locally (where in the structure do certain parameters influence spare capacity and spare capacity usage) and globally (what is the magnitude of the effect of certain parameters). In doing this it was shown that the studied parameters in both the original structure and in the extension have major effects on the spare capacity and the usage of spare capacity.

Next, the results that were shown here are discussed.

8 Discussion

The discussion chapter of this thesis is split into two parts. First, the results of the parameter study are discussed and important observations are interpreted. Then, having shown how the trends seen in the results might be explained, the grasshopper tool itself will be discussed and reflected on. Here, the methodology, design assumptions and accuracy of the model will be discussed, as well as the intended place of use in the engineering design cycle.

8.1 Discussion of results

In the simulation phase of this thesis a parameter study was carried out. The results of this parameter study are discussed here. Some trends seen in the results are shown as well as interpreted. This part is split into two sections, the first section deals with the results of the studied parameters in the original building and the second section deals with the results of the studied parameters concerning extension design.

8.1.1 Original structure parameters

In this thesis, the effects of three parameters present in original 'Rotterdamse Laag' buildings on the spare capacity in the structure was assessed.

In general, it is observed that for unextended structures, the average load ratio lays consistently between 75 and 90%. This is an expected outcome when looking at the exploratory design calculation that was carried in appendix A. The average magnitude and the distribution of the load ratio amongst individual elements is highly dependent on the three studied parameters. Here, the effects of each of these three parameters are identified and interpreted.

8.1.1.1 Original building grid

It was observed that larger construction grids result in lower load ratios (a 7.5 x 7.5m grid shows a 15% lower load ratio than a 5.5 x 5.5m grid). In the results section, it was already shown that this effect is partially reliant on the 'shape factor' of the building. When the results were corrected for this shape factor, the larger grids still showed a lower load ratio, but the difference only showed to be 7% instead of the 15% that was observed when uncorrected for shape factor. The difference that is made by the shape factor is a combination of the following two mechanisms:

- G2 and G3 variants have a larger area that is exposed to wind forces, therefore they are loaded more than G1 variants.
- G2 variants have a broader base, which is beneficial for the absorption of horizontal loads because the 'moment arm' at the base is larger, therefore axial loads in ground floor columns are smaller.

When correcting for shape, these two mechanisms are effectively eliminated, only leaving the effects that are directly reliant on the area of the grid.

8.1.1.2 Original building height

To assess the effect on the amount of storeys or building height of the original structure, three different building heights were used as input in the model: 20m, 24m and 28m. Here, it was found that spare capacity decreases with height, by around 2,5% percent per storey added. It is important to note here that different base grids show a different rate of change in spare capacity with original building height. The reason for this different rate is related to the ratio between the structures self-weight (which larger per column/foundation pile for larger grids) and variable loads.

8.1.1.3 Core position

The placement of a stability core is observed to have to main effects on the spare capacity:

1. Core presence increases the spare capacity in the original building
2. Core location influences the distribution of spare capacity in the original building

To start with the first effect: it was observed that the presence of a stability core increased the average spare capacity in the bottom columns of the building with at least 5%, based on average load ratio alone. The reason for this might be that a portion of the wind loads are transferred to the stability core, which then leaves more spare capacity in the columns and foundation piles under the columns. As mentioned before, the spare capacity within the stability core is not analyzed in this thesis because the focus rests on the columns and foundation piles.

Then, for the second effect, it is seen that the distribution of spare capacity in the original structure is very reliant on where the stability core is situated. Corner core variants, for example, show a decreased spare capacity in the corner columns, but an enhanced spare capacity in the middle columns.

Figure 8.1 shows, for all parameters in the original structure, the amount of influence on the average spare capacity usage versus the influence on the distribution of spare capacity.

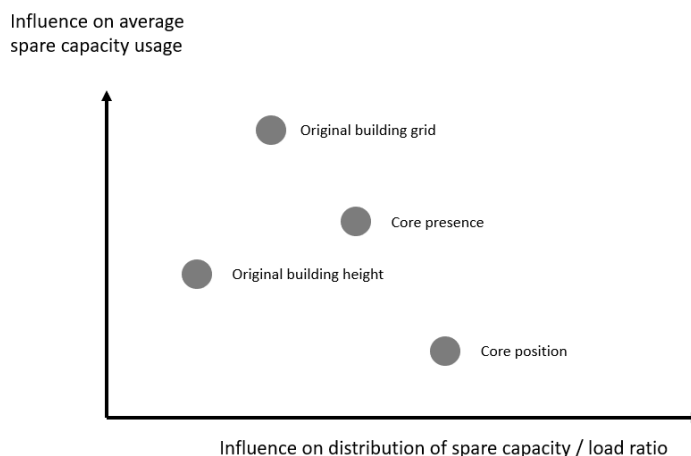


Figure 8.1 – Influence of parameters in the original structure

8.1.2 Extension design parameters

Next, the results for the studied parameters that govern the extension design will be discussed. This, is done in two parts: one for each studied parameter. First, the effects of the three studied wall layouts are discussed, then the effects of extension grid is discussed.

Some general trends are first discussed. It is observed, for example, that there is a rather large difference in the magnitude of the load ratios for elements at different locations in the original structure. Overall, it can be said that the foundation piles show the smallest load ratios as well as the some of the smallest ranges between different wall layout and grid variations (this means that the effect of implementing a different extension solution is rather small when looking at the foundation piles). This diametrically opposes the columns in the top storey, that are significantly more susceptible to changes in the extension design and are also much more likely to exceed the load ratio of 1.0.

Another effect that is observed in the results is that the magnitudes of the load ratios in the top storey columns do not always fully align with the magnitudes of load ratios at the bottom storeys and in the foundation piles. The differences that are visible here can possibly be explained by the fact that, in the top storey tensile stresses are much more likely to occur than in on the ground floor. On top of that, tensile stresses do not occur in the foundation piles at all. This implies that the columns higher up in the structure contain a bending moment that diminishes and redistributes when the bottom columns are reached. This redistribution of forces may be the cause of the difference seen in load ratios in the top storey versus the ground floor.

8.1.2.1 Effects of variations in wall layout

Variations in wall layout are shown to have a significant effect on individual and global element loading. The effect of wall layouts on the load ratios found in the original building is observed to be highly dependent on the structural boundary conditions within the original building. When looking at wall layouts that concentrate the spare walls and align them with the stability core (wall layouts A), it is observed that the columns around the core experience higher load ratios as well as the corner column diametrically opposite of the core, which can primarily be regarded as a torsional effect.

On the other hand, when looking at wall layouts B, load ratios are consistently more 'spread out' or evenly distributed over the structure. However, high tensile stresses are observed in the corner columns. The reason for this might be that wall layouts B are placed on the stiffest part of the original structure (the middle columns), leaving the corner columns, which are significantly less stiff, unincluded.

The opposite effect is seen in wall layouts C, where the walls are placed, not on the middle of the structure, but on the edges. The effect that is observed here is that by placing shear walls on the outer edges of the building, the columns in the middle experience higher load ratios. The answer to this conundrum might lie in the fact that the wall layout used here touches only the edge and corner columns. These columns are, per definition, less stiff than the columns in the middle. This might have, as a unintentional side effect, that, in combination with the torsion that is caused by the

eccentric core, the loads are redistributed towards the middle columns that are much stiffer than the columns on the edges and in the corners.

An overall observation that was made is that columns that are not directly under a shear wall are more likely to experience larger tensile stress load ratios. The reason for this might be twofold:

The shear walls pose a large concentrated vertical load on the column.

The shear walls increase the stiffness of the structure locally, which causes the less stiff parts of the structure to deform more, hence bending moments are more likely to occur here.

8.1.2.2 Effects of extension grid variation

Now, the observed effects of extension grid variation will be discussed. In the results section, it was observed that, while the effect of varying with extension grid within one wall layout is often smaller than varying with wall layouts, the effect is still significant.

One effect that deserves to be discussed is the observation that when the grid lines in the extension line up perfectly with the stability core (which is seen in G/2 variants), a favorable situation is created for the elements beneath the shear walls. This is because more of the loads will be transferred to the existing stability core.

The second effect that is discussed here is the effect of having shear walls located between columns. It is observed that moving the shear wall between two columns can lead to much larger load ratios in the other columns. This is seen with wall layouts B, where the load ratios in corner columns, which are never directly in touch with a shear wall become much higher when the shear wall from the adjacent column moves to the space in between the columns.

It becomes clear that by varying the extension grid, some (mostly subtle) alterations can be made to the load ratios of specific columns. This mechanism is clearly visible in wall layouts B. It can also cause much higher loads in some cases where the moment arm between walls is significantly decreased, in combination with the mechanism seen of shear walls on intermediary beams (Wall layouts A).

8.1.2.3 Effects on utilization of the extension elements

In this study, the utilizations of the CLT panels themselves were not found to be a limiting factor in the design of extensions. The connections, on the other hand, are observed to reach critical U.C. values in some cases. What seems to be the leading influential factor here is a combination of wall layout and the amount of storeys added in the extension, as well as the location of the stability core.

Extensions with wall layouts A and B (core aligned and functional design) are observed to create failure in the shear connectors of the extension in extensions that are three storeys high, in corner core variants specifically. Wall layouts A and B are two very different wall layouts, so what makes them so different from wall layout C? Figure 8.2 shows the internal moment arms of the vertical extensions. It is clearly visible that wall layouts C have the largest moment arms because the walls enclose the extension.

Wall layouts A have rather small internal eccentricity, especially in the G/2 variant. Wall layouts B have a medium sized moment arm between the transversal shear walls, but only have one shear wall crossing the longitudinal direction. In addition to this, the shear walls are somewhat removed from the stability core, this creates an eccentricity between the walls and the stability core that creates more torsion.

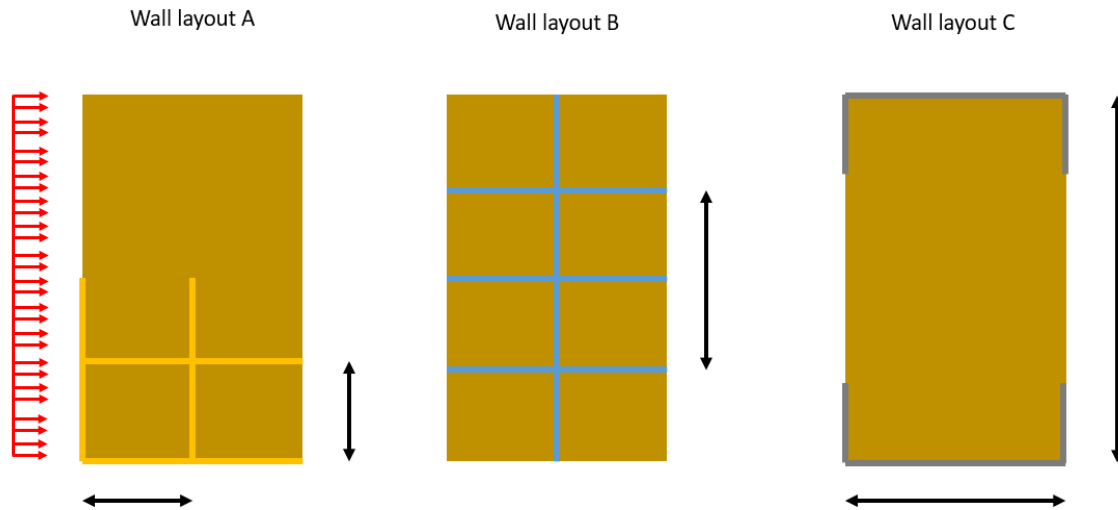


Figure 8.2 – Internal moment arms in different wall layouts

In terms of the utilization of the extension elements, it is seen that the grid division has little to no effect, especially when compared to the effect of wall layout. The failure of connections in the extension seems to be linked to the wall layout (only wall layouts A and B are shown to make connections fail) and the amount of storeys added to the extension.

8.1.2.4 Effects of wall layout and extension grid on deflections

In this study, deflection was found not to be a limiting factor in the design of the extensions. The U.C. value for deflection stays below 1.0 in all 729 variants.

When looking at extension grid and its effect on the overall deflection, the only significant change is between different grid variants of wall layout A of C1 variants (corner core). The reason for this is easy to imagine: in wall layout A, different grid variants directly influence the total width of the shear walls and thus the torsional resistance of the extension. A higher U.C. value for G/2 variants (which are the smallest in width) is therefore to be expected. This further confirms that the deflections in wall layout A, which are significantly higher than in wall layouts B and C, are mostly torsional in nature, and caused by the large eccentricity of the core aligned shear walls.

It was also observed that the deflections for C3 variants are significantly higher than those for C1 and C2 variants. This can be explained by the absence of a stability core. Since the difference between different wall layout variations stays roughly the same when looking at C2 and C3 variants (both are more or less symmetrical, so they serve as a good comparison), it is implied that the increase in deflection of the extensions in C3 variants is fully due to the absence of a stability core and the extension itself undergoes roughly the same deformation whether a core is present or not.

8.1.3 Remarks on the interplay between original structure and extension

The results of this research have been discussed and interpreted in this chapter. We've looked, extensively at both sides of the vertical extension question: the effect of the structural boundary conditions and the effect of extension design. Now, we can look at the interplay of both, and how the interpreted results can be used in practice.

With the results in mind, it becomes possible divide the elements in the original structure into categories based on their likelihood to exceeding the load ratio limit of 1.0, and their susceptibility to changes in loading by changes in extension design. The foundation piles, for example show much a much smaller susceptibility to large differences in added loads due to different wall layouts. Figure 8.3 shows the dependency of loading of different elements on different wall layouts and extension grids, plotted against the likelihood of that element exceeding a load ratio of 1.0. As is shown by the results, the piles in the foundation show the least likelihood of exceeding a load ratio of 1.0, as well as the smallest dependency on variations in extension grid and wall layout. On the other hand, it should be noted that while the likelihood of foundation piles exceeding a load ratio of 1.0 is small compared to other elements in the original structure, when the load ratio of 1.0 is reached, this could pose a significant challenge in the design of the structure because, as found in chapter 3, foundation piles are much more challenging and expensive to reinforce. To illustrate this aspect, the marking points in figure 8.3 were colored to show the challenge in reinforcing said element. Red markers are the most challenging, green ones are the least challenging. Here it is assumed that columns at the top storey pose the smallest challenge towards reinforcement, because in the worst case scenario, the columns of the top storey could be taken out entirely, in which case the extension would start one storey earlier. This cannot be done with the columns of the ground floor (since that would require taking down the entire building), so these elements are more challenging to reinforce. As mentioned before, the foundation is deemed the hardest to reinforce.

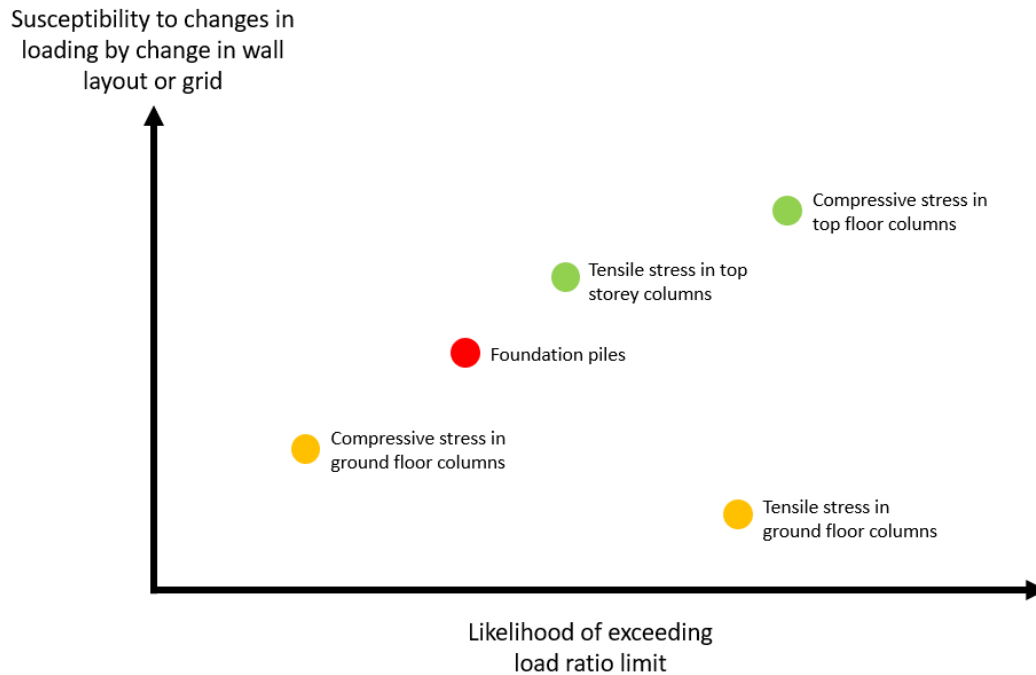


Figure 8.3 – Elements in the original structure and their susceptibility to changes in loading

It then becomes quite clear which elements in the original structure are likely to require the most attention in the design process: the foundation piles and the ground floor columns (specifically for tensile stress). Compressive stress in the ground floor columns is shown to rarely exceed the load ratio limit, and the top storey columns are quite easy to replace. This leaves the foundation piles, and tensile stress in the ground floor columns.

Another significant observation that can be made is that in some variants, the corner columns show a higher load ratio than others (this is especially the case in corner core (C1) variants, and is most visible in wall layouts B). It is important to realize that in this thesis, the assumption is made that all columns are designed equally, meaning that the columns in the corner are assumed to have the same capacity as the columns in the middle of the structure. While technical drawings of Rotterdamse Laag buildings that were utilized for this thesis support this insofar that the overall dimensions of these columns are often similar, no large amount of data was available on the reinforcement detailing of these columns. It might therefore not always be the case that all columns are created equally. It is important to realize that the data shown in this thesis, and data found using the tool that was created here is valuable as a jumping off point for further structural analysis of a building and explicitly not meant to show what extensions are possible on any given building.

8.2 Discussion of the developed grasshopper tool

Finally, the tool itself is reflected upon. To achieve the main goal of this thesis, a tool in grasshopper was developed. In this section, the methodology of the development of the tool, design assumptions, tool accuracy and the intended use range of the tool will be discussed.

8.2.1 Methodology of the tool development

The main mechanism that is used in this thesis to assess spare capacity is based on the differences between load factors and functional variable loads in TGB1955 and NEN8700/NEN-EN1990. This is shown in Chapter 5, figure 5.8. The main drawback here is that these alterations only happen on the 'load' side of the equation and not on the 'resistance' side. This means that, in this thesis, the resistance of structural elements is not considered. It is acknowledged, however, that there are some processes that influence the resistance of structural elements. For example, concrete strength is known to increase over time and design calculations are always made with the '28-day strength' of concrete in mind. This means that after 50-70 years, the strength of concrete will have increased significantly. In addition to this, it is important to keep in mind that, much like the strength of concrete, our knowledge of structural mechanics also increases over time. This means that nowadays, we have much more insight into the exact failure points of structural elements. In most cases, this means that these 50 to 70 year olds elements have been over dimensioned in the first place. It becomes clear, then, that while this tool offers a meaningful analysis of the loading of elements, it does not necessarily show the full picture of spare capacity in the structure. This should be kept in mind in further development of the tool.

In addition to this, it should be noted that this thesis assumes a configuration of functional spaces in the building that is based on the urban context and societal needs, as shown in chapter 1 and 3. It is possible to change the configuration of functional spaces to any desired configuration. However, the method of creating spare capacity that is used in this thesis partially relies on the change of function from office to residential. When this mechanism is altered, the existence of spare capacity, as defined in this thesis, cannot be guaranteed.

8.2.2 Design assumptions of the grasshopper tool

In the synthesis stage of the tool development, some assumptions have been made that may have a limiting effect on both the applications and outcomes of the model.

Starting with geometry, the tool was created for buildings of a rectangular shape and an evenly spaced out grid. While these are logical assumptions to make when creating a base tool, this is not a perfect reflection of reality. Many buildings that are part of the Rotterdamse Laag are irregularly shaped and, oftentimes as a result of an irregular shape, the grid used is not consistent over the whole floorplan. The consequence of this is that, as of now, the tool is a simplification of reality and can not be used for all

buildings. In further development of the tool, the base code could be adapted to allow for irregular grids and shapes.

Another one of these assumptions is the full rigidity of connections between concrete elements. While these connections are casts in situ in Rotterdamse Laag buildings, a connection is never fully rigid and always possesses some kind of rotational stiffness. This can have an effect on the deflection of the structure and the distribution of forces within the structure.

Looking at the extension design, it should be noted that the floor elements have been modelled to facilitate diaphragm action. However, as mentioned in chapter 4, the computational weight of the model made it impossible to model the CLT floor slabs as separate elements. While this has no significant impact on the results of the simulation phase, this does mean that the floor slabs in the model do not reflect reality accurately and no in-model verifications could be carried out. Instead, the floor slabs were verified beforehand by hand calculations, which are shown in appendix C.

Finally, it is important to take note that the CLT panels used as shear elements in this tool are modelled as solid slabs and are not modelled with voids. While this is not an entirely accurate representation of reality (CLT walls would naturally have doorframes and windows), the lack of data on the size, frequency and distribution of voids in CLT walls, they were taken out of the equation entirely.

These aspects should be considered when using the tool in grasshopper.

8.2.3 Tool accuracy

In order to substantiate the results of the simulation phase, model validations were done and are shown in appendix E for both CLT panels and the effect of the extension on the base structure. These show the accuracy of the tool. When looking at modelling the CLT panels that are used as the shear elements in the extension, it was found that stresses and deflections in the panels can differ 5 to 15% from hand calculations. The difference between real life stresses and deflections increases when stacked CLT panels are analyzed. This implies that there is a difference between the FEM calculated behavior of the connectors between CLT panels and the hand calculated behavior of CLT panels. In combination with this, a source of inaccuracy might also lie in the mesh resolution used in the FEM models. The mesh resolution could not be made too small because of the computational weight of the entire model. This might have an effect on the results of stresses within the CLT panels that are outputted in the Grasshopper tool. Therefore, it is recommended to always use separate FEM models to more accurately check the stresses within the CLT panels.

When looking at the support reactions under the shear elements, however, it is found that the results of the grasshopper tool line up within 5% with their hand calculated counterparts. This further highlights the recommendation that was made earlier: the tool presented in this thesis should be used to generate a global insight into the reaction of the base structure to different extension variants, but should not be used to check capacity utilizations of specific elements: further structural analysis should always be the next step in the design process.

8.2.4 Use range of the tool

With this in mind, it is important to mention that the tool that has been created in this thesis was developed with a very specific point in the design process in mind, which is the initial design stage. This means that this tool is particularly valuable when used as a means to identify the vertical extension potential in any given Rotterdamse Laag building. This is largely due to the parametric nature of the tool. The tool gives its user the possibility to quickly assess multiple extension variants and can give insight in the differences between extension variants. However, as mentioned before, this tool only tells a part of the story of spare capacity in a structure. The use of this tool should be confined to design explorations where, for example, the structural impact of different extension variants is identified, or where a rough estimation of the amount of layers that can be added to a building is made.

The place of this tool within the engineering design cycle is pictured in figure 8.4. The engineering design cycle is taken as defined by TU Delft (TU Delft, 2021).

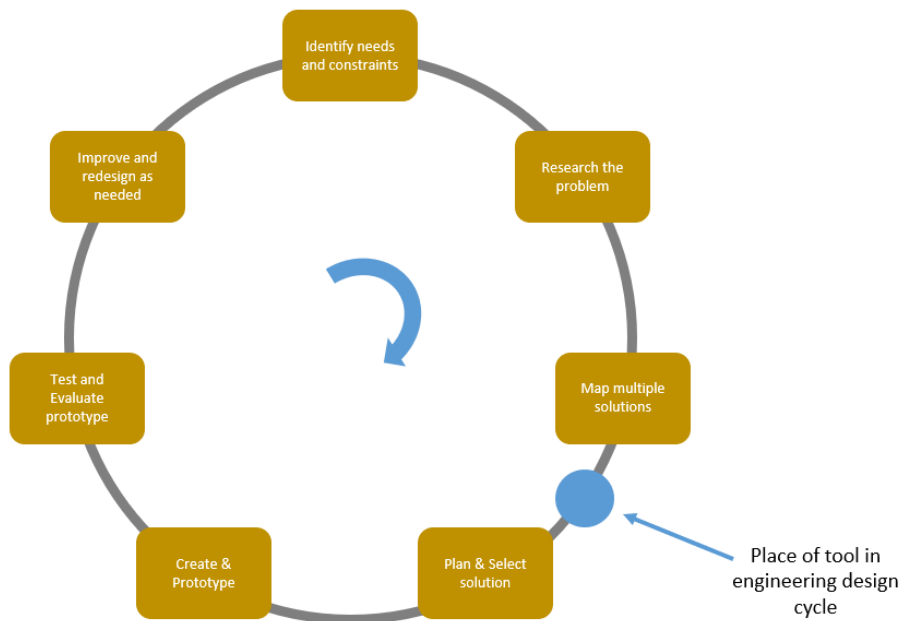


Figure 8.4 – Place of the grasshopper tool in the engineering design cycle

9 Conclusion

In this thesis, the influence of five parameters on vertical extension success in the Rotterdamse Laag was studied. The conclusion section of this report is structured by looking at the four research questions that were posed in the introduction of this thesis. First some conclusions will be made on the extendibility of Rotterdamse Laag buildings. Here, we'll look at the influence of the original structure and the influence of extension design. In the second half, some conclusions will be made that reflect on the overarching goal of this thesis, which was to create a parametric tool. Here, it will be shown that this thesis has contributed to an informed practice of decision-making by the means of the development of a parametric tool which has been validated and has been used to perform a parameter study with.

The following research questions will be answered throughout the conclusion:

- How is the spare capacity within a structure influenced by its building typology?
- How is the utilization of spare capacity influenced by vertical extension design?
- To what extent does vertical extension design influence the utilization of elements in the vertical extension?
- How, and to what extent, can a parametric tool be used to indicate vertical extension potential in Rotterdamse Laag buildings in an early design stage?

9.1 Effect of the studied parameters in the original structure on spare capacity

To answer the first research question that was posited at the beginning of this chapter:

“How is the spare capacity within a structure influenced by its building typology?”

It was observed that the three studied parameters (building height, building grid and core location) all have a significant effect on the spare capacity within a structure. For building grid and building height this effect is general (a change in these parameters influences the overall capacity of the building) whereas for the core location this effect is general as well as local (a change in this parameter also influences the distribution of spare capacity amongst structural elements).

It becomes obvious that the three studied parameters have a large impact on the 'extendibility' of a building, simply by having an effect on the spare capacity of a structure. This implies that, when looking at the specific effect of each parameter, an ideal candidate building for vertical extension can be defined. This 'ideal' building should have a large construction grid and should have a small height as well as a stability core. A similar thing can be said for a set of parameters that can be expected to have a low extendibility (hence a building that posits more of a challenge when considering it for vertical extension), this would be a very high building with a small construction grid and no stability core.

Studied parameter	Effect	Impact
Original construction grid	Larger construction grids show a larger spare capacity.	The effect of changes in extension grid between G1 and G2 base grids was found to be 7% when correcting for shape. However, shape is a factor that also has a lot of influence that might be relevant nonetheless.
Original building height	Higher buildings show less spare capacity.	2.5 – 5% decrease in spare capacity per storey added in the original building
Core location/presence	The presence of a core correlates with a larger spare capacity in columns and foundation piles. When a core is present, the location has a large effect on the distribution of spare capacity.	The average spare capacity diminished with 5% when no core was present. When a core is present, the distribution of spare capacity within the elements changes significantly based on the position / eccentricity of the core.

Table 9.1 Effects and impacts of the studied parameters in the original structure

9.2 Effect of vertical extension design on usage of spare capacity in elements in the original structure

To answer the research question that was posited at the beginning of this chapter:

“How is the utilization of spare capacity influenced by vertical extension design?”

Here it was observed that both studied parameters show a significant effect on mainly the distribution of loads to the original structure. Changes in wall layout were shown to have the largest effect on the use of spare capacity in the original structure, where changes in wall layout were shown to have an effect of sometimes over 15% on individual column loading. The effects show a large range depending on which element in the original is being analyzed: columns at the top storeys show larger susceptibility to changes in extension design than columns at the ground floor and the foundation piles also show a smaller susceptibility.

Changes in the extension grid show, overall, a smaller effect on the load ratios in the original structure. This especially concerns the elements that are located lower in the structure such as the foundation piles and the ground floor columns. The effect of extension grid variations can be said to be more local, being quite small overall while still showing significant differences in individual columns at the top storeys. This is further corroborated by the fact that variations in extension grid seem to have a large effect on the tensile stresses and compressive stresses in the top storey columns, while variations in wall layout have, by comparison, a larger effect on the bottom columns and foundation piles.

Furthermore, the largest range within extension grids are seen in wall layout A (core aligned). This is because wall layouts A have very concentrated shear walls (all more or less in one location). A variation in grid in these wall layouts can easily divert loads to another column. While wall layouts A were originally chosen to see if core alignment has a high extension potential. From the results, this shows not entirely to be the case. Wall layouts A produce a high degree of torsional stresses in the original structure.

Parameter	Effect	Impact
Wall layout: A, B or C (core aligned, functional design or façade aligned shear walls)	Varying with wall layout shows a significant effect on the distribution of loads towards the original structure.	Impact mainly depends on the element that is being looked at. The maximum difference between wall layout variants can be as big as 60% in top storey columns and as big as 25% in the foundation piles.
Extension grid	Varying the extension grid can enhance the effects that are created by choosing a specific wall layout. The change affects elements throughout the original structure.	The impact of varying with extension grid is more local than varying with wall layout. The largest effects are found in the top storey columns and can be up to 60%). The impact in the foundation piles, on the other hand, is smaller, only around 10% at its largest.

Table 9.2 – Effects of the studied parameters in the extension

9.3 Effect of extension design on utilization of elements in the vertical extension

Next, the third research question is answered:

“To what extent does vertical extension design influence the utilization of elements in the vertical extension?”

This study found that, when using cross laminated timber in the vertical extension, the CLT itself is often not the ‘weakest link’ of the extension structure. As a matter of fact, the shear connectors are significantly more likely to fail. Using the assumptions that were made in this thesis for the amount of connections in the structure, some relationships were found between the U.C.’s in these connections and the design of the vertical extension. First and foremost, failure always occurred as a result of wind loading along the widest façade and failure in the connections tends to happen more often when 3 storeys are added. Failure in the connections occurred solely in wall layouts A and B, never when wall layout C was utilized. The reason for this is thought to be the fact that wall layout C effectively creates a large moment arm that encompasses the entire building. Wall layout A has a much smaller moment arm and wall layout B only has one wall perpendicular to the critical wind load, which might cause a large concentration of loads in this particular wall. From the results in this section of the thesis, it can be concluded that wall layout C has the highest potential for usage in vertical extensions.

When looking at the extension grids for the different wall layouts, it becomes clear that there is little to no effect found in the variation of extension grid. This implies that failure in the connections has more to do with the overall design of the extension, and that effect cannot necessarily be subdued with subtle changes in the extension grid.

9.4 Conclusion on the creation of a parametric tool in Grasshopper

Finally, the fourth research question, which deals with the overall creation of a tool, is answered:

“How, and to what extent, can a parametric tool indicate vertical extension potential in an early design stage?”

Using the answers to the preceding research question in combination with validations we find that vertical extension potential in Rotterdamse Laag buildings can be indicated successfully when using this tool in an early design stage. The vertical extension potential can be indicated in two ways:

1. By the overall load ratios found in structural elements, which indicate whether the theoretical capacity of any given element has been reached. Thereby indicating on a global level, the amount of layers that can be added as well as the amount of elements that potentially exceed a critical load ratio, as well as the degree to which they exceed the critical load ratio.
2. By the effect of different vertical extension variants, which show a significant influence on the degree to which the load ratio increases in individual elements. Thereby indicating, on a local level, which elements are most likely to exceed a critical load ratio and how extension design can influence those likelihoods.

The effectiveness of the grasshopper tool was illustrated by performing a parameter study in the simulation phase and which are corroborated by model validations (see appendix E). From this, it can be concluded that a successful parametric tool has been created that can indicate vertical potential in Rotterdamse Laag buildings.

9.4 Concluding remarks

The main goal of this thesis was formulated as such:

“Identifying CLT vertical extension potential in existing buildings by creating a parametric tool that considers different types of structural constraints. Ultimately, contributing to informed decision-making practices in the sustainable and effective structural design of vertical extensions.”

To this end, a tool has been developed in grasshopper. This tool shows to be helpful in the quick assessment of vertical extension variants on existing structures and, as such, has the potential to be a valuable tool for identifying CLT vertical extension potential.

Furthermore, to conclude, it can be said that some significant steps have been taken towards a more general and efficient approach to vertical extensions in the Rotterdamse Laag. By comparing different real life parameters found in Rotterdamse Laag structures and combining them with various CLT extension solutions, the effect of the structural boundary conditions and vertical extension design on the spare capacity in buildings was assessed. It was observed that the design of the vertical extension can have a significant effect on the loading of individual elements in the original structure. This implies that in real life Rotterdamse Laag buildings, and possibly in other types of building typologies as well, vertical extension practices can be made more efficient by designing the vertical extension with the strengths of the original structure in mind. The tool that was developed in this thesis proves to be an efficient way to show how design choices in the vertical extension can affect loads in the original structure. This thesis therefore proposes a valuable tool that is intended to be used during the initial design stages of vertically extending a building.

9.5 Recommendations for further research and further tool development

This thesis encompasses a large amount of studied parameters. This large width of scope has its benefits: it lets us study the interaction between different configurations of an array of parameters and it helped create a tool that incorporates a large number of aspects in its workings. On the other hand, however, it means that the specific effects of some of these parameters could benefit from more research.

It was found in this thesis that the location and presence of a stability core has a very significant effect on the spare capacity in a building (both the magnitude of the spare capacity and its distribution). In this study, three iterations of this parameter were studied: corner cores, middle cores and no core at all. These iterations were chosen because of real life encounters with these types of core typologies in Rotterdamse Laag buildings. However, for further research, it might be interesting to look at stability cores that exist on more of a spectrum instead of the binary: middle or corner. Furthermore, some other stability systems could be included in future research. It was found, for example, that Rotterdamse Laag buildings are sometimes partially stabilized by masonry walls. This option was not included in this thesis because masonry comes with its own set of structural boundary conditions which would make it harder to generalize results. In future research, alternative stability systems could also be included and their effect on spare capacity could be taken into account as well.

In terms of tool development, some further developments could be made that make the tool helpful in more situations. One part of this is the aforementioned stability systems. This thesis has shown that the placement of stabilizing elements has a significant influence on load ratios in the original building. The next step of the Grasshopper tool could be to incorporate more types of stabilizing systems into the extension design, like steel bracings.

In addition to this, the tool that has been created can potentially be developed to play a role in the optimization of the extension design. A feature like this could perform two important optimizations:

1. Optimization of the placement of shear elements / stability elements. The stabilizing elements can be optimized to be placed in such a way that the overall load ratio's stay as low as possible, thus creating more potential room for extensions.
2. Optimization of materials. By incorporating a weight optimization into the Grasshopper tool, the extension could be optimized to be as light weight as possible. This was initially a goal of this thesis, but it was dropped due to time constraints. Even so, incorporating an optimization like this could potentially be very helpful because it would allow the user to find which element dimensions can create the largest extension with the least amount of material used.

Finally, one more aspect can be incorporated in the model: sustainability. Incorporating life cycle assessments into the model could create an option where multiple extension variants can be compared based, not only on their effect on the original structure, but also on their respective environmental impacts.

Bibliography

- Arends, J. (2021). *Compendium van relevante artikelen uit de TGB 1955 en de Eurocode 1 t.b.v. BK4TE5 onderdeel Draagconstructies*. TU Delft.
- Blass, J., & Fellmoser, P. (2004). *Design of Solid wood panels with cross layers*. Karlsruhe: University of Karlsruhe.
- Bogensperger, T. (2016). *Verification of CLT-plates under loads in plane*. Graz: Graz University of Technology.
- Borgström, E., & Fröbel, J. (2019). *The CLT Handbook*. Stockholm: Swedish Wood.
- Brandner, R. (2016). *ULS Design of CLT Elements*. Graz: Graz University of Technology.
- CEMEX UK. (sd). *Concrete vs Steel & Timber*. Opgehaald van [cemex.co.uk](https://www.cemex.co.uk): <https://www.cemex.co.uk/concrete-vs-steel-timber>
- CEN. (2019). *Nationale bijlage bij NEN-EN 1990+A1:2006+A1:2006/C2:2019 Eurocode: Grondslagen van het constructief ontwerp*. CEN.
- Heiza, K., Nabil, A., & Meleka, N. (2014). *State-of-the-Art Review: Strengthening of Reinforced Concrete Structures - Different Strengthening Techniques*. Menofia University.
- Hendriks, P. (2022, October 24). *Oude huurwoning krijgt vaak de sloopkogel, maar renovatie is de nieuwe trend*. Opgehaald van Follow the Money: www.ftm.nl/artikelen/slopen-van-woningen-is-kapitaalvernietiging
- Lukacs, B. T. (2019). *Strength and stiffness of cross-laminated timber (CLT) shear walls: State of the art of analytical approaches*. As: Norwegian University of Life Sciences.
- Pitroda, J. (2015). *Micro-Pile: Recent advances and future trends*.
- Rothoblaas. (2019). *Plates and Connectors for Timber*. Rotho Blaas Srl.
- Rücker, W., Hille, F., & Rohrmann, R. (2006). *Guideline for the Assessment of Existing Structures*. Berlin: Federal Institute of Materials Research and Testing (BAM).
- Sasaki, N., & al, e. (2016). *Sustainable Management of Tropical Forests Can Reduce Carbon Emissions and Stabilize Timber Production*. *Frontiers in Environmental Science*.
- Shahnewaz. (2018). *Performance of cross-laminated timber shear walls for platform construction under lateral loading*. University of British Columbia.
- Shahnewaz, & Shahria Alam, T. P. (2016). *In-plane stiffness of CLT panels with and without openings*. Vienna: World conference on timber engineering.

- Shahnewaz, Alam, & Tannert. (2018). *In-Plane Strength and Stiffness of Cross-Laminated Timber Shear Walls*. University of British Columbia.
- Stockhammer, D. (2019). *Building Additions in Steel*. PARK BOOKS.
- StoraEnso. (2017). *CLT by Stora Enso*. Stora Enso Wood Products.
- Triantafillou, T. (2016). Strengthening of existing concrete structures: Concepts and structural behavior. In T. Triantafillou, *Textile Fibre Composites in Civil Engineering* (pp. 303-322).
- TU Delft. (2021, Januari 4). Lecture: The Engineering Design Cycle. Delft.
- van der Stoel, A. E. (2001). *Grouting for pile foundation improvement*. Delft.
- van Rein, E., & Trappenburg, N. (2023, Juli 12). Onderzoek: woningtekort loopt op, forse bouwdip verwacht. *Financieel Dagblad*.
- Vritesh, & Asish. (2021). *A Comparative Analysis on the Methods of Strengthening Isolated Reinforced Concrete Columns*. Redit: University of Mauritius.
- White, J. (sd). *Concrete*. Opgehaald van 20th Century Architecture: <http://architecture-history.org/schools/CONCRETE.html>
- WoodSolutions. (2020, September 4). Case Study: 10 Storey Vertical Building Extension (Timber Over Existing Building) (Webinar).
- Znabei, T. (2020). *A Post-tensioned Cross-Laminated Timber core for buildings*. Delft: Delft University of Technology.

Appendix A – Code comparison calculation and wind load calculations

In order to assess the differences between the three building codes that are relevant for vertical extensions within the boundaries of the scope of this thesis, an example calculation was made. The total loads of the same building are calculated here for the three building codes:

- TGB 1955 (aka the original building code the building was constructed under)
- NEN1990 (aka the Eurocode that would normally be used for newly constructed buildings)
- NEN8700 (aka the Eurocode that is used for reconstruction of existing buildings)

This appendix will consist of the following subchapters:

- Explanation of case and dimensions
- Self weight of the structure
- Functional change + code comparison
- Wind loads
- Combination of everything

The case

The case that is used to compare these three codes consists of a concrete building on a 4.5 x 4.5 grid that is 5 storeys high. The bottom storey is used as a shop (commercial area) and the top 5 are used as offices. The new function of the building will consist of shops on the ground floor and residential area on the top 5 floors. The building was constructed according to TGB1955 regulations.

This calculation takes into account the vertical loads on one single column. Material properties and dimensions can be found in table A.1.

Table A.1

Element	Dimensions
Columns	0.5 x 0.5 m
Beams	0.5 x 0.3 m
Floors	0.3 m

Determination of self weight of the structure

Based on the dimensions mentioned above and the density of concrete, the weight of the existing structure will be estimated. This is done per column, this means that the lowest column will carry the weight of:

- 6 columns
- 6 floors
- 6 sets of beams

Table A.2 shows how much the load on the lower column is due to the weight of the structure itself.

Table A.2

Element	Volume	Weight/storey	Weight in kN
Column	$0.5 \times 0.5 \times 3 = 0.75$ m ³	$2300 \times 0.75 = 1725$ kg/ storey	16.91 kN/storey
Floor	$0.3 \times 4.5 \times 4.5 = 6.075$ m ³	$2300 \times 6.075 =$ 13972.5 kg / storey	136.93 kN/storey
Beams	$0.5 \times 0.3 \times 4.5 = 0.675$ m ³	$2300 \times 0.675 =$ 1552.5 kg/storey	15.21 kN/storey
Total/storey			169.05 kN/storey
Total			1014.3 kN

So the total self weight of the structure due to just the existing structure is 1014.3 kN on one column. This does not yet include the variable floor loads and variable horizontal loads. It also does not include any of the added loads due to the extension. The next step is to look at the weight of the extension structure per storey.

Functional change and comparison of codes

Like mentioned in the introduction of this case, the function of a large part of the existing building will be changed from office to residential. This means that the variable floor loads will be changed. The difference between the original variable floor loads that the building was designed for using TGB1955 and the new loads according to NEN1990 and NEN8700 can be used as spare capacity.

NEN1990 defines variable floor loads in different use classes. Here residential functions fall under class A, office functions under class B and commercial areas fall under class D. These categories are then split up even further, the following values are used:

- For residential areas, loads according to A1 for floors are used: 1.75 kN/m²
- For office areas, loads are according to class B: 2.5 kN/m²

- For commercial areas, loads are according to class D2 for larger shopping areas: 4 kN/m²

TGB1955 uses the following variable floor loads:

- For residential areas, a load of 2 kN/m² is used
- For office and commercial areas a load of 2.5 kN/m² is used

It is good to realize that for commercial areas and office areas, the same load is used in TGB1955.

Not yet taking into account any load factors the total variable loads are given in table A.3.

Table A.3

Loads	TGB1955 old situation	NEN1990 old situation	NEN1990 new situation
Commercial	2.5 kN/m ²	4 kN/m ²	4 kN/m ²
# of storeys	1	1	1
Office	2.5 kN/m ²	2.5 kN/m ²	2.5 kN/m ²
# of storeys	5	5	0
Residential	2 kN/m ²	1.75 kN/m ²	1.75 kN/m ²
# of storeys	0	0	5
Total weight on foundation	303.75 kN	334.125 kN	258.19 kN

It already becomes clear that just by changing the functions of the existing building, a considerable amount of spare capacity is 'unlocked'. Now the load factors for both codes, and the load factors for NEN8700 are added. Table A.4 shows how, using NEN8700 the design loads for the same building decrease significantly when different building codes are used.

Table A.4

	TGB1955 old situation	NEN1990 old situation	NEN1990 new situation	NEN8700 new situation
Variable load (kN)	303.75	334.125	258.19	258.19
Load factor for variable loads	1.5	1.5	1.5	1.3
Design variable loads (kN)	455.63	501.18	387.29	335.64

Lastly, the structure's own weight will also be added, with the respective load factors.

Table A.5

	TGB1955 old situation	NEN1990 old situation	NEN1990 new situation	NEN8700 new situation
Permanent load (kN)	1014.3	1014.3	1014.3	1014.3
Load factor for permanent loads	1.5	1.15	1.15	1.1
Design permanent loads (kN)	1521.45	1166.45	1166.45	1115.73
Total design loads (kN)	1977.08	1667.63	1553.73	1451.37

Table A.5 shows that the total design loads can be reduced by 25% by using NEN8700 in combination with a functional change on a typical Rotterdamse Laag building.

Wind loads

Wind loads according to Eurocode are determined using the fundamental windspeeds representing each of the three wind areas in The Netherlands. In wind area 2, the fundamental windspeed is 27 m/s. The base windspeed is then converted to the base windspeed according to equation 4.1 in NEN1990.

$$v_b = v_{b,0} * c_{dir} * c_{season}$$

Where c_{dir} is a wind direction factor and c_{season} is a seasonal factor. Both factors are taken as 1.0 in accordance with Eurocode recommendations.

Next, the base windspeed is used to determine the average wind speed at any given height: $v_m(z)$. The equation used here makes use of a terrain roughness factor, given in equation x and an orography factor which is taken to be 1.0 in line with Eurocode recommendations.

$$v_m(z) = c_r(z) * c_o(z) * v_b$$

$$c_r(z) = k_r * \ln \frac{z}{z_0}$$

$$k_r = 0.19 * \left(\frac{z_0}{z_{0,II}} \right)^{0.07}$$

Where z_0 is the length of roughness, $z_{0,II}$ is 0.05, k_r is the terrain factor and z is the height at which average wind speed is assessed. For heights lower than the minimum height z_{min} , the average windspeed should always be determined using the value of z_{min} . Table x, from Eurocode, shows the values for z_0 and z_{min} for

different terrain categories. Terrain type VI is chosen for urban areas, meaning z_0 is equal to 1.0m and z_{min} is equal to 10m.

Terreincategorie	z_0 m	z_{min} m
0 Zee of kustgebied met wind aanstromend over open zee	0,003	1
I Meren of vlak en horizontaal gebied met verwaarloosbare vegetatie en zonder obstakels	0,01	1
II Gebied met lage begroeiing als gras en vrijstaande obstakels (bomen, gebouwen) met een tussenruimte van ten minste 20 obstakelhoogtes	0,05	2
III Gebied met regelmatige begroeiing of gebouwen of vrijstaande obstakels met een tussenruimte van ten hoogste 20 obstakelhoogtes (zoals dorpen, voorstedelijk terrein, blijvend bos)	0,3	5
IV Gebied waar ten minste 15 % van de oppervlakte is bedekt met gebouwen met een gemiddelde hoogte boven 15 m	1,0	10
De terreincategorieën zijn toegelicht in A.1.		

Figure A.6

The last factor of importance is the wind turbulence at any given height. The wind turbulence factor can be determined by taking the standard deviation of the turbulence and dividing it by the average wind speed determined in equation x.

$$I_v(z) = \frac{\sigma_v}{v_m(z)}$$

$$\sigma_v = k_l * v_b * k_r$$

The wind turbulence factor should be determined for the height for which it is assessed, except when this height is smaller than the minimum height z_{min} , where the turbulence factor should be determined by using z_{min} in the equation instead of the actual height.

Finally, the extreme pressure per square meter at any given height can be determined using equation x.

$$q_p(z) = (1 + 7 * I_v(z)) * \frac{1}{2} \rho * v_m^2(z)$$

Combination of all of the above

Table A.7 shows the combination of all loads when the three situations are assessed. It is, once again, important to realize that while the loads of the original building may be assessed using NEN8700, the added loads of the extension are computed using NEN1990 safety factors. The wind loads that would already count for the original structure are factored according tot NEN8700 and the wind loads that are added because of the height of the extension are factored according to NEN1990 load factors.

Table A.7

	NEN1990	TGB1955
Self weight of original structure (characteristic load)	1014.30 kN/column	1014.30 kN/column
Variable loads in original structure (characteristic load)	258.19 kN/column	303.75 kN/column
Wind loads on original structure (characteristic load)	111.87 kN/column	115.2 kN/column
Total design loads on original structure from NEN8700	1596.8 kN/column	2149.88 kN
Spare capacity	533 kN / column	

Table A.8

	1 storey added	2 storeys added	3 storeys added
Total design load of original structure (NEN8700)	1596.8 kN	1596.8 kN	1596.8 kN
Added design permanent loads (NEN1990)	29.23 kN	58.48 kN	76.28 kN
Added design variable floor loads (NEN1990)	81 kN	162 kN	243 kN
Added design wind loads (NEN1990)	75.30 kN	166.71 kN	274.89 kN
Total design loads	1822.85 kN	2065 kN	2323.91 kN
UC	0.84	0.96	1.08

Appendix B – Model verifications

In this appendix, the model verifications are shown. U.C. checks were created for both the CLT panels and the connections.

CLT panels were checked for in-plane compression stresses (with buckling) and in-plane shear stresses. U.C.'s were determined for walls in X direction and walls in Y direction. The highest occurring U.C. check out of these is shown in the tables below.

The U.C. of the connections was determined based on shear forces occurring in the connections. Here, some variants show to have a U.C. larger than 1.0, these variants are still taken into account in the main results section of this thesis. The reason for this is that, while a set amount of connections was used in this model, the amount of connections could easily be increased.

GRID	HEIGHT	CORE	WALLS	STOREYS	GRID	Deflection U.C.	Maximum U.C. in CLT	Critical U.C.	Maximum U.C .connections
G1	H1	C2	A	1	1	0,025	0,343	UCX_sh	0,580
G1	H1	C2	B	1	1	0,013	0,358	UCY_sh	0,605
G1	H1	C2	C	1	1	0,011	0,207	UCX_sh	0,350
G1	H1	C2	A	2	1	0,050	0,447	UCY_sh	0,755
G1	H1	C2	B	2	1	0,026	0,504	UCY_sh	0,853
G1	H1	C2	C	2	1	0,022	0,288	UCX_sh	0,487
G1	H1	C2	A	3	1	0,099	0,453	UCY_sh	0,766
G1	H1	C2	B	3	1	0,047	0,650	UCY_sh	1,100
G1	H1	C2	C	3	1	0,042	0,373	UCX_sh	0,630
G1	H1	C2	A	1	2	0,024	0,360	UCY_sh	0,608
G1	H1	C2	B	1	2	0,012	0,382	UCY_sh	0,646
G1	H1	C2	C	1	2	0,012	0,204	UCX_sh	0,346
G1	H1	C2	A	2	2	0,054	0,417	UCY_sh	0,705
G1	H1	C2	B	2	2	0,023	0,493	UCY_sh	0,834
G1	H1	C2	C	2	2	0,023	0,285	UCX_sh	0,482
G1	H1	C2	A	3	2	0,107	0,503	UCY_sh	0,851
G1	H1	C2	B	3	2	0,040	0,601	UCY_sh	1,017
G1	H1	C2	C	3	2	0,043	0,365	UCX_sh	0,618
G1	H1	C2	A	1	3	0,030	0,398	UCY_sh	0,674
G1	H1	C2	B	1	3	0,012	0,377	UCY_sh	0,638
G1	H1	C2	C	1	3	0,012	0,206	UCX_sh	0,348
G1	H1	C2	A	2	3	0,063	0,444	UCY_sh	0,752
G1	H1	C2	B	2	3	0,022	0,447	UCY_sh	0,756
G1	H1	C2	C	2	3	0,023	0,280	UCX_sh	0,474
G1	H1	C2	A	3	3	0,118	0,534	UCY_sh	0,903
G1	H1	C2	B	3	3	0,037	0,532	UCY_sh	0,901
G1	H1	C2	C	3	3	0,044	0,358	UCY_sh	0,606

GRID	HEIGHT	CORE	WALLS	STOREYS	GRID	Deflection	U.C.	Maximum U.C. in CLT	Critical U.C.	Maximum U.C .connections
G1	H2	C2	A	1	1	0,032		0,42	UCX_sh	0,70
G1	H2	C2	B	1	1	0,018		0,39	UCX_sh	0,66
G1	H2	C2	C	1	1	0,016		0,23	UCX_sh	0,39
G1	H2	C2	A	2	1	0,062		0,46	UCY_sh	0,77
G1	H2	C2	B	2	1	0,036		0,53	UCY_sh	0,89
G1	H2	C2	C	2	1	0,029		0,32	UCX_sh	0,54
G1	H2	C2	A	3	1	0,119		0,51	UCY_sh	0,87
G1	H2	C2	B	3	1	0,062		0,69	UCY_sh	1,16
G1	H2	C2	C	3	1	0,054		0,41	UCX_sh	0,69
G1	H2	C2	A	1	2	0,031		0,46	UCY_sh	0,78
G1	H2	C2	B	1	2	0,018		0,42	UCY_sh	0,72
G1	H2	C2	C	1	2	0,016		0,23	UCX_sh	0,39
G1	H2	C2	A	2	2	0,067		0,54	UCY_sh	0,90
G1	H2	C2	B	2	2	0,031		0,51	UCY_sh	0,86
G1	H2	C2	C	2	2	0,030		0,32	UCX_sh	0,53
G1	H2	C2	A	3	2	0,130		0,64	UCY_sh	1,08
G1	H2	C2	B	3	2	0,052		0,61	UCY_sh	1,02
G1	H2	C2	C	3	2	0,055		0,40	UCX_sh	0,68
G1	H2	C2	A	1	3	0,039		0,49	UCY_sh	0,82
G1	H2	C2	B	1	3	0,018		0,39	UCY_sh	0,66
G1	H2	C2	C	1	3	0,016		0,23	UCX_sh	0,39
G1	H2	C2	A	2	3	0,079		0,54	UCY_sh	0,92
G1	H2	C2	B	2	3	0,030		0,46	UCY_sh	0,77
G1	H2	C2	C	2	3	0,030		0,31	UCX_sh	0,53
G1	H2	C2	A	3	3	0,144		0,64	UCY_sh	1,09
G1	H2	C2	B	3	3	0,049		0,54	UCY_sh	0,91
G1	H2	C2	C	3	3	0,056		0,40	UCY_sh	0,67

GRID	HEIGHT	CORE	WALLS	STOREYS	GRID	Deflection	Maximum	Critical	Maximum
						U.C.	U.C. in	U.C.	U.C
						U.C.	CLT	U.C.	.connections
G1	H2	C3	A	1	1	0,04	0,49	UCX_sh	0,83
G1	H2	C3	B	1	1	0,03	0,46	UCX_sh	0,77
G1	H2	C3	C	1	1	0,02	0,26	UCX_sh	0,44
G1	H2	C3	A	2	1	0,06	0,53	UCX_sh	0,89
G1	H2	C3	B	2	1	0,04	0,55	UCX_sh	0,92
G1	H2	C3	C	2	1	0,03	0,34	UCX_sh	0,57
G1	H2	C3	A	3	1	0,11	0,57	UCX_sh	0,96
G1	H2	C3	B	3	1	0,07	0,66	UCY_sh	1,11
G1	H2	C3	C	3	1	0,05	0,42	UCX_sh	0,71
G1	H2	C3	A	1	2	0,04	0,57	UCY_sh	0,96
G1	H2	C3	B	1	2	0,02	0,50	UCY_sh	0,84
G1	H2	C3	C	1	2	0,02	0,26	UCX_sh	0,43
G1	H2	C3	A	2	2	0,07	0,63	UCY_sh	1,07
G1	H2	C3	B	2	2	0,04	0,58	UCY_sh	0,99
G1	H2	C3	C	2	2	0,03	0,34	UCX_sh	0,57
G1	H2	C3	A	3	2	0,12	0,72	UCY_sh	1,22
G1	H2	C3	B	3	2	0,06	0,68	UCY_sh	1,14
G1	H2	C3	C	3	2	0,05	0,42	UCX_sh	0,70
G1	H2	C3	A	1	3	0,05	0,58	UCY_sh	0,97
G1	H2	C3	B	1	3	0,03	0,45	UCY_sh	0,76
G1	H2	C3	C	1	3	0,02	0,26	UCX_sh	0,44
G1	H2	C3	A	2	3	0,08	0,62	UCY_sh	1,05
G1	H2	C3	B	2	3	0,04	0,49	UCY_sh	0,83
G1	H2	C3	C	2	3	0,03	0,33	UCX_sh	0,56
G1	H2	C3	A	3	3	0,13	0,72	UCY_sh	1,21
G1	H2	C3	B	3	3	0,06	0,56	UCX_sh	0,95
G1	H2	C3	C	3	3	0,05	0,41	UCX_sh	0,69

GRID	HEIGHT	CORE	WALLS	STOREYS	GRID	Deflection	Maximum	Critical	Maximum
						U.C.	U.C. in	U.C.	U.C
							CLT	.connections	
G1	H1	C1	A	1	1	0,07	0,46	UCX_sh	0,77
G1	H1	C1	B	1	1	0,03	0,42	UCY_sh	0,71
G1	H1	C1	C	1	1	0,03	0,20	UCX_sh	0,34
G1	H1	C1	A	2	1	0,15	0,68	UCX_sh	1,15
G1	H1	C1	B	2	1	0,03	0,60	UCY_sh	1,02
G1	H1	C1	C	2	1	0,05	0,29	UCX_sh	0,49
G1	H1	C1	A	3	1	0,31	0,89	UCX_sh	1,50
G1	H1	C1	B	3	1	0,06	0,76	UCY_sh	1,29
G1	H1	C1	C	3	1	0,07	0,38	UCX_sh	0,64
G1	H1	C1	A	1	2	0,11	0,28	UCX_sh	0,48
G1	H1	C1	B	1	2	0,03	0,40	UCY_sh	0,67
G1	H1	C1	C	1	2	0,03	0,19	UCX_sh	0,33
G1	H1	C1	A	2	2	0,35	0,43	UCX_sh	0,72
G1	H1	C1	B	2	2	0,05	0,56	UCX_sh	0,94
G1	H1	C1	C	2	2	0,05	0,28	UCX_sh	0,47
G1	H1	C1	A	3	2	0,84	0,56	UCX_sh	0,95
G1	H1	C1	B	3	2	0,08	0,70	UCX_sh	1,18
G1	H1	C1	C	3	2	0,07	0,35	UCX_sh	0,60
G1	H1	C1	A	1	3	0,10	0,30	UCX_sh	0,51
G1	H1	C1	B	1	3	0,03	0,39	UCY_sh	0,66
G1	H1	C1	C	1	3	0,03	0,19	UCX_sh	0,33
G1	H1	C1	A	2	3	0,26	0,44	UCX_sh	0,74
G1	H1	C1	B	2	3	0,04	0,50	UCX_sh	0,85
G1	H1	C1	C	2	3	0,05	0,27	UCX_sh	0,45
G1	H1	C1	A	3	3	0,56	0,55	UCX_sh	0,93
G1	H1	C1	B	3	3	0,07	0,61	UCX_sh	1,04
G1	H1	C1	C	3	3	0,07	0,34	UCX_sh	0,58

GRID	HEIGHT	CORE	WALLS	STOREYS	GRID	Deflection	Maximum	Critical	Maximum
						U.C.	U.C. in	U.C.	U.C
							CLT		.connections
G1	H2	C1	A	1	1	0,07	0,50	UCX_sh	0,85
G1	H2	C1	B	1	1	0,03	0,46	UCY_sh	0,78
G1	H2	C1	C	1	1	0,04	0,23	UCX_sh	0,39
G1	H2	C1	A	2	1	0,17	0,75	UCX_sh	1,26
G1	H2	C1	B	2	1	0,04	0,65	UCY_sh	1,11
G1	H2	C1	C	2	1	0,05	0,32	UCX_sh	0,54
G1	H2	C1	A	3	1	0,33	0,97	UCX_sh	1,64
G1	H2	C1	B	3	1	0,07	0,83	UCY_sh	1,41
G1	H2	C1	C	3	1	0,08	0,42	UCX_sh	0,70
G1	H2	C1	A	1	2	0,12	0,30	UCY_sh	0,51
G1	H2	C1	B	1	2	0,03	0,44	UCX_sh	0,74
G1	H2	C1	C	1	2	0,03	0,22	UCX_sh	0,37
G1	H2	C1	A	2	2	0,37	0,46	UCX_sh	0,78
G1	H2	C1	B	2	2	0,06	0,60	UCX_sh	1,02
G1	H2	C1	C	2	2	0,05	0,31	UCX_sh	0,52
G1	H2	C1	A	3	2	0,89	0,62	UCX_sh	1,04
G1	H2	C1	B	3	2	0,09	0,75	UCX_sh	1,27
G1	H2	C1	C	3	2	0,08	0,39	UCX_sh	0,67
G1	H2	C1	A	1	3	0,10	0,33	UCX_sh	0,57
G1	H2	C1	B	1	3	0,03	0,43	UCX_sh	0,73
G1	H2	C1	C	1	3	0,03	0,22	UCX_sh	0,37
G1	H2	C1	A	2	3	0,27	0,48	UCX_sh	0,82
G1	H2	C1	B	2	3	0,05	0,55	UCX_sh	0,93
G1	H2	C1	C	2	3	0,05	0,30	UCX_sh	0,51
G1	H2	C1	A	3	3	0,59	0,61	UCX_sh	1,03
G1	H2	C1	B	3	3	0,08	0,67	UCX_sh	1,13
G1	H2	C1	C	3	3	0,08	0,38	UCX_sh	0,65

GRID	HEIGHT	CORE	WALLS	STOREYS	GRID	Deflection	Maximum	Critical	Maximum
						U.C.	U.C. in	U.C.	U.C
							CLT	.connections	
G1	H3	C1	A	1	1	0,08	0,54	UCX_sh	0,92
G1	H3	C1	B	1	1	0,03	0,51	UCY_sh	0,86
G1	H3	C1	C	1	1	0,04	0,26	UCX_sh	0,44
G1	H3	C1	A	2	1	0,15	0,77	UCX_sh	1,31
G1	H3	C1	B	2	1	0,05	0,68	UCY_sh	1,15
G1	H3	C1	C	2	1	0,05	0,34	UCX_sh	0,58
G1	H3	C1	A	3	1	0,27	0,98	UCX_sh	1,66
G1	H3	C1	B	3	1	0,07	0,84	UCY_sh	1,42
G1	H3	C1	C	3	1	0,07	0,44	UCX_sh	0,74
G1	H3	C1	A	1	2	0,12	0,36	UCY_sh	0,60
G1	H3	C1	B	1	2	0,04	0,48	UCX_sh	0,81
G1	H3	C1	C	1	2	0,04	0,25	UCX_sh	0,42
G1	H3	C1	A	2	2	0,29	0,46	UCX_sh	0,78
G1	H3	C1	B	2	2	0,07	0,66	UCX_sh	1,11
G1	H3	C1	C	2	2	0,05	0,33	UCX_sh	0,56
G1	H3	C1	A	3	2	0,65	0,63	UCX_sh	1,06
G1	H3	C1	B	3	2	0,10	0,81	UCX_sh	1,37
G1	H3	C1	C	3	2	0,08	0,41	UCX_sh	0,70
G1	H3	C1	A	1	3	0,11	0,36	UCX_sh	0,61
G1	H3	C1	B	1	3	0,03	0,48	UCX_sh	0,80
G1	H3	C1	C	1	3	0,04	0,25	UCX_sh	0,42
G1	H3	C1	A	2	3	0,22	0,49	UCX_sh	0,83
G1	H3	C1	B	2	3	0,06	0,60	UCX_sh	1,02
G1	H3	C1	C	2	3	0,05	0,33	UCX_sh	0,55
G1	H3	C1	A	3	3	0,45	0,60	UCX_sh	1,02
G1	H3	C1	B	3	3	0,09	0,73	UCX_sh	1,23
G1	H3	C1	C	3	3	0,08	0,40	UCX_sh	0,68

Appendix C – Model Input Verifications

This appendix shows how the CLT input elements throughout the model were verified and what mechanical assumptions were made in the process. First, the methods of verification are explained, then the relevant members are verified.

CLT floors

Compression perpendicular to the grain

The extension structure is a platform structure, meaning that the floors are in between the walls and therefore have to transfer the vertical and horizontal loads from the wall on top to the wall at the bottom. Here the vertical load transfer will be checked. The vertical loads may not exceed the out of plane compression resistance of the CLT.

In addition to k_{mod} and y_m , the characteristic out of plane compression strength of the CLT is now also multiplied by $k_{c,90}$. This factor considers that for elements that are loaded only on a part of the surface area higher resistances can be used and depends on the specific loading situation and configuration of the lamellae within the CLT panel (Brandner, 2016). Values for $k_{c,90}$ are given by Brandner for a load situation like in figure C.1, where a CLT panel is sandwiched between two walls and the grain of the outer layers is perpendicular to these walls.

A distinction is made between load introduction and load transmission. Since load transmission values for k_{c90} are lower thus more conservative and the compression in the structure is highest at the bottom (where the load is transmitted, not introduced), the transmission values for k_{c90} are used here.

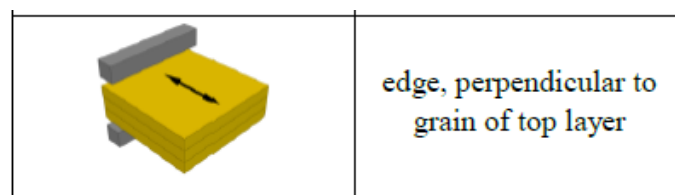


Figure C.1

Table C.2

Number of layers	Kc,90 Transmission	Kc,90 Introduction
3	1.05 – 1.10	1.09 – 1.19
5	1.07 - 1.15	1.13 – 1.28
7	1.13 - 1.20	1.23 – 1.36

The following formula can then be used to determine whether the floor panel can resist the compression transmitted from wall to wall:

$$\sigma_{c,z,d} = \frac{F_{z,c,d}}{A_{ef}} \leq f_{c,90,xlay,d} = k_{c,90} * k_{mod} * \frac{f_{c,90,xlay,k}}{\gamma_M}$$

Equation C.1

Bending capacity (out of plane)

The bending capacity of the floor slab is governed by the design bending strength of the CLT panel. The bending stress is determined by dividing the bending moment by the net moment of resistance:

$$W_{x,net} = \frac{2 * I_{net}}{h_{CLT}}$$

Equation C.2

$$\sigma_d = \frac{M_d}{W_{x,net}} \leq f_{m,d}$$

Equation C.3

Shear capacity (perpendicular to the plane)

The variable floor loads and self weight of the floor panels will result in shear forces perpendicular to the plane that will be largest at the edge of the floor panel. The panels resistance to shear force is sufficient when the shear in the middle layer of the panel does not exceed its shear resistance and when the rolling shear in the layer above and below the middle layer does not exceed these layers' rolling shear capacity.

Shear in the middle layer

For shear in the middle layer, the following equation must be fulfilled:

$$\tau_{v,xz,d} = \frac{S_{x,net} * V_{xz,d}}{I_{x,net} * b_x} \leq f_{v,090,ylay,d}$$

Equation C.4

Where $V_{xz,d}$ is the design shear force, $S_{x,net}$ is the static moment of the panel (an elaboration of cross sectional properties of the panel can be found in the model validations in appendix E), and $f_{v,090,ylay,d}$ is the characteristic shear strength of the longitudinal boards (in the y direction).

Rolling shear in the layers surrounding the middle layer

For the rolling shear in the layers perpendicular to the span, the following equation should be met:

$$\tau_{Rv,yz,d} = \frac{S_{R,y,net} * V_{yz,d}}{I_{y,net} * b_y} \leq f_{v,9090,xlay,d}$$

Equation C.5

Here $V_{yz,d}$ is the shear force, $S_{R,y,net}$ is the static moment of the panel and $f_{v,9090,xlay,d}$ is the characteristic rolling shear strength of the boards.

Deflections (SLS)

The vertical loads acting on the floor panels result in deflections. These deflections may not exceed the length of the panel divided by 300 (L/300 mm).

For the deflection of CLT one has to consider both the deflection due to bending and the deflection due to shear. The panels are considered to be simply supported. For bending, the deflection of the panel is determined according to formula C.6, the deflection due to shear is determined using formula C.7.

$$w_m = \frac{5 * q * L^4}{384 * E * I_{net}}$$

Equation C.6

$$w_s = \frac{q * L^2}{8 * GA_s}$$

Equation C.7

The total deflection amount to the sum of deflections due to bending and shear and should not exceed L/300 mm.

Vibrations

In addition to the deflection of the CLT floor panels, the eigenfrequency also has to be checked. Eigenfrequencies lower than 8 Hz are generally experienced as disturbing (Borgström & Fröbel, 2019). Equation C.8 is used to determine the lowest fundamental frequency of the floor panel:

$$f_1 = \frac{\pi}{2L^2} \sqrt{\frac{(EI)_L}{m}} \geq 8 \text{ Hz}$$

Equation C.8

Where f_1 is the lowest fundamental frequency, which should be greater than 8 Hz, L is the length of the panel, EI_L is the bending stiffness in the stiffest direction and m is the mass of the CLT panel in kg/m of span.

This is how the floors are dimensioned in the model. Deflection and vibrations tend to be the governing aspects of the structural analysis.

CLT floor panels input verifications

The following is the result of calculations according to the paragraphs above. For each base grid (G1, G2 and G3), the necessary floor length has been determined. Vibration checks were ultimately performed using calculatis, the CLT tool created by Stora Enso which has also been used in some of the validation checks in appendix E.

Table C.3

Grid	5.5 x 5.5 m
Span	5.5 m
Width of panel	2.75 m (two panels per grid)
CLT Panel type	160L5S (40-20-40-20-40)
U.C. Compression perp. to the grain	0.33
U.C. Deflection (SLS)	0.47
U.C. Bending	0.28
U.C. Vibrations	0.92 (with calculatis)
U.C. Longitudinal shear	0.04
U.C. Rolling shear	0.21

Table C.4

Grid	5.5 x 7.5 m
Span	5.5 m
Width of panel	2.5 m (three panels per grid)
CLT Panel type	160L5s (three panels per grid)
U.C. Compression perp. to the grain	0.44
U.C. Deflection (SLS)	0.47
U.C. Bending	0.28
U.C. Vibrations	0.94 (with calculates)
U.C. Longitudinal shear	0.04
U.C. Rolling shear	0.21

Table C.5

Grid	7.5 x 7.5 m
Span	7.5 m
Width of panel	2.5 m (three panels per grid)
CLT Panel type	260L7S (80-30-40-30-80)
U.C. Compression perp. to the grain	
U.C. Deflection (SLS)	0.34
U.C. Bending	0.21
U.C. Vibrations	0.96 (with calculatis)
U.C. Longitudinal shear	0.04
U.C. Rolling shear	0.14

As observed here, the increase of span from 5.5 to 7.5 m has a large effect on the type of CLT panel that can be used. The critical factor in all situations are the smallest

own frequency of the CLT panels, which have to be above 8 Hz to be used in residential buildings.

CLT Columns input verifications

Columns are assumed to be CLT columns. The column dimensions are determined per base grid and per extension grid, but is kept the same whether one, two or three storeys are added. The critical situation is always taken to be an extension of three storeys. This of course, results in over dimensioned columns in extensions of one storey, but since the columns are only a very limited part of the extension it is assumed that the difference between an optimized column versus a non-optimized column does not add a significant weight and thus is not assumed to have a large effect on the model results. Column dimensions and their respective critical buckling checks are shown in table C.6. It is important to note that buckling was always observed to be the critical U.C. check. Since the columns are modelled as shuttle bars (hinged on both sides), they cannot transfer any loads other than normal forces. This means that only two failure mechanisms have to be checked: compression and buckling. Out of these, buckling is always the most critical.

Table C.6

Base Grid	Extension Grid	Dimensions (cm)	U.C. (buckling)
G1	G/1	30x15	0.75
	G/2	15x15	0.9
	G/3	15x15	0.6
G2	G/1	25x25	0.81
	G/2	20x20	0.76
	G/3	18x18	0.72
G3	G/1	20X20	0.59
	G/2	18X18	0.79
	G/3	18X18	0.53

Transfer beams – Input values when the extension grid = original grid

Here, the transfer layer is verified.

Table C.7

Variant	Type beam	Profile	UC – Bending	UC – Shear	UC – Deflection
G1 + 1 storey	Primary	HEA280	0.61	0.12	0.95
	Secondary	HEA280	0.61	0.12	0.95
G1 + 2 storeys	Primary	HEA300	0.59	0.12	0.86
	Secondary	HEA300	0.59	0.12	0.86
G1 + 3 storeys	Primary	HEA320	0.59	0.13	0.81
	Secondary	HEA320	0.59	0.13	0.81
G2 + 1 storey	Primary	HEA450	0.53	0.13	0.7
	Secondary	HEA320	0.56	0.12	0.77
G2 + 2 storeys	Primary	HEA450	0.63	0.15	0.84
	Secondary	HEA320	0.67	0.15	0.92
G2 + 3 storeys	Primary	HEA450	0.73	0.17	0.97
	Secondary	HEA340	0.69	0.16	0.88
G3 + 1 storey	Primary	HEA450	0.53	0.13	0.7
	Secondary	HEA450	0.53	0.13	0.7
G3 + 2 storeys	Primary	HEA450	0.63	0.15	0.84
	Secondary	HEA450	0.63	0.15	0.84
G3 + 3 storeys	Primary	HEA450	0.73	0.17	0.97
	Secondary	HEA450	0.73	0.17	0.97

Please note that, since the 1:1 grids here do not include extra intermediary beams, the primary and secondary beams are able to be dimensioned the same.

Transfer beams – Input values when the original grid is halved

Here the critical situation is used of CLT shear walls located on both the secondary and primary beams and the added wind load acting on the primary beam as well.

Table C.7

Variant	Type beam	Profile	UC – Bending	UC – Shear	UC – Deflection
G1 + 1 storey	Primary	HEA280	0.75	0.13	0.95
	Secondary	HEA280	0.61	0.12	0.95
G1 + 2 storeys	Primary	HEA300	0.75	0.14	0.86
	Secondary	HEA300	0.59	0.12	0.86
G1 + 3 storeys	Primary	HEA320	0.75	0.15	0.81
	Secondary	HEA320	0.59	0.13	0.81
G2 + 1 storey	Primary	HEA400	0.91	0.16	0.99
	Secondary	HEA320	0.56	0.12	0.77
G2 + 2 storeys	Primary	HEA450	0.88	0.18	0.84
	Secondary	HEA320	0.67	0.15	0.92
G2 + 3 storeys	Primary	HEA500	0.84	0.19	0.71
	Secondary	HEA340	0.69	0.16	0.88
G3 + 1 storey	Primary	HEA400	0.79	0.16	0.70
	Secondary	HEA450	0.53	0.13	0.7
G3 + 2 storeys	Primary	HEA450	0.97	0.19	0.84
	Secondary	HEA450	0.63	0.15	0.84
G3 + 3 storeys	Primary	HEA500	0.93	0.2	0.71
	Secondary	HEA450	0.73	0.17	0.97

Transfer beams – Input values when the original grid is divided by 3

Here the critical situation is used of CLT shear walls located on both the secondary and primary beams and the added wind load acting on the primary beam as well.

Table C.8

Variant	Type beam	Profile	UC – Bending	UC – Shear	UC – Deflection
G1 + 1 storey	Primary	HEA360	0.79	0.12	0.99
	Secondary	HEA280	0.61	0.12	0.95
G1 + 2 storeys	Primary	HEA400	0.81	0.14	0.88
	Secondary	HEA300	0.59	0.12	0.86
G1 + 3 storeys	Primary	HEA450	0.78	0.15	0.74
	Secondary	HEA320	0.59	0.13	0.81
G2 + 1 storey	Primary	HEA400	0.88	0.16	0.99
	Secondary	HEA320	0.56	0.12	0.77
G2 + 2 storeys	Primary	HEA450	0.86	0.17	0.84
	Secondary	HEA320	0.67	0.15	0.92
G2 + 3 storeys	Primary	HEA500	0.83	0.18	0.71
	Secondary	HEA340	0.69	0.16	0.88
G3 + 1 storey	Primary	HEA400	0.96	0.16	0.99
	Secondary	HEA450	0.53	0.13	0.7
G3 + 2 storeys	Primary	HEA450	0.94	0.18	0.84
	Secondary	HEA450	0.63	0.15	0.84

G3 + 3 storeys	Primary	HEA500	0.91	0.19	0.71
	Secondary	HEA450	0.73	0.17	0.97

Appendix D – Connection design

Two types of connections are looked at for the model:

- Floor/ ceiling to the shear wall (90 degrees connection)
- Shear wall to shear wall, or floor to floor connections (180 degrees connection)

Modelling of the floor and ceiling to the shear wall connections:

Floor to wall connections are usually done with holddowns and brackets.

Holddowns are connections specifically designed to resist vertical forces. They are usually not able to resist significant horizontal forces.

Each modelled shear wall will get two holddowns, each at one end of the modelled wall. Below are the connection stiffnesses for holddowns from the Rothoblaas connection catalogue. For this thesis, the WHT620 will be used (the stiffest holddown). The stiffness values mentioned in this appendix are all for CLT to CLT connections.

WHT type	configuration	fastening type Ø x L [mm]	n _v [pcs]	K _{1,ser} [N/mm]	
				GL24h	CLT
WHT340	• total fastening • without washer	LBA nails Ø4,0 x 60	20	-	3440
	• total fastening • with washer	LBA nails Ø4,0 x 60	20	5705	7160
	• partial fastening • with washer	LBA nails Ø4,0 x 60	12	-	5260
WHT440	• total fastening • with washer	LBA nails Ø4,0 x 60	30	6609	10190
	• partial fastening • with washer	LBA nails Ø4,0 x 60	20	-	8060
WHT540	• total fastening • with washer	LBA nails Ø4,0 x 60	45	-	11470
	• partial fastening • with washer	LBA nails Ø4,0 x 60	29	-	9700
WHT620	• total fastening • with washer	LBA nails Ø4,0 x 60	52/55	13247	13540
	• partial fastening • with washer	LBA nails Ø4,0 x 60	30/35	9967	10310

Figure D.1 – Stiffness properties of the WHT620 Holddown connector

WHT620 - with WHTW70 washer (M20)

configuration	R _{1,k} TIMBER				R _{1,k} STEEL		R _{1,d} CONCRETE					
	holes fastening Ø5			R _{1,k} timber [kN]	R _{1,k} steel		R _{1,d} uncracked		R _{1,d} cracked		R _{1,d} seismic	
	type	Ø x L [mm]	n _v [pcs]		[kN]	Y _{steel}	VIN-FIX PRO Ø x L [mm]	[kN]	EPO-FIX PLUS Ø x L [mm]	[kN]	EPO-FIX PLUS Ø x L [mm]	[kN]
<ul style="list-style-type: none"> total fastening washer WHTW70 M20 anchor 	LBA nails	Ø4,0 x 40	55	86,4	85,2	Y _{M2}	M20 x 240	57,15	M20 x 240	48,5	M20 x 240	24,2
	LBA nails	Ø4,0 x 60	55	106,2								
<ul style="list-style-type: none"> partial fastening washer WHTW70 M20 anchor 	LBS screws	Ø5,0 x 40	55	86,4	85,2	Y _{M2}	M20 x 240	57,15	M20 x 240	48,5	M20 x 240	24,2
	LBS screws	Ø5,0 x 50	55	106,2								
	LBA nails	Ø4,0 x 40	35	55,0								
	LBA nails	Ø4,0 x 60	35	67,6								
<ul style="list-style-type: none"> partial fastening washer WHTW70 M20 anchor 	LBS screws	Ø5,0 x 40	35	55,0	85,2	Y _{M2}	M20 x 240	57,15	M20 x 240	48,5	M20 x 240	24,2
	LBS screws	Ø5,0 x 50	35	67,6								

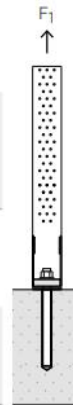


Figure D.2 – Strength properties for the WHT620 Holddown connector

Brackets are connections that are designed to resist horizontal forces. The shear walls in the model will receive three shear brackets each.

In a platform type structure, the same configuration of connections is used to attach the shear wall to the floor and the ceiling.

type	fastening type Ø x L [mm]	n _v [pcs]	K _{2/3,ser} [mm]
TCN200 + TCW200	LBS nails Ø5,0 x 50	30	9600
TCN240 + TCW240	LBS nails Ø5,0 x 50	36	10000

Figure D.3 – Stiffness properties of the TCN240 Brackets

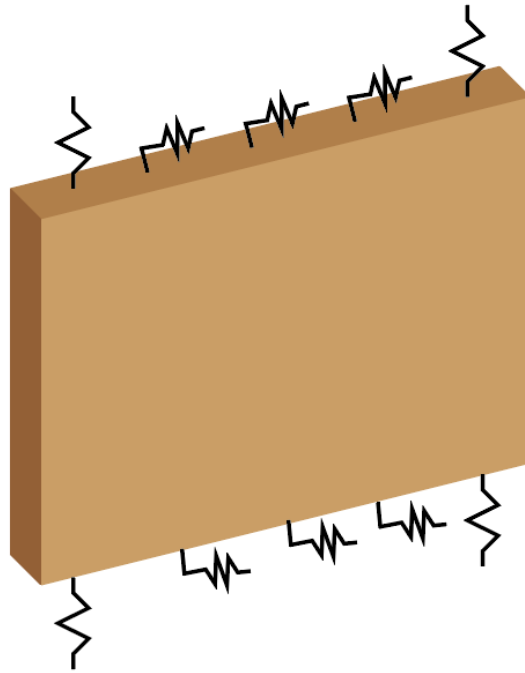


Figure D.4 – How the CLT shear wall connectors are modelled

As was previously shown in chapter 4 and 5, the CLT panel is modelled as shown in figure D.4. On both the bottom and top of the wall, spring elements are modelled. To simplify, it is assumed that bracket connections only transfer horizontal loads. They are modelled as springs with the spring stiffnesses derived from figure D.3. The holddowns are assumed to only transfer tensile forces and they are modelled with a spring stiffness derived from figure D.1.

Shear wall to shear wall (180 degrees connection)

For the connection of one shear wall to another, usually so-called 'slots' are used.

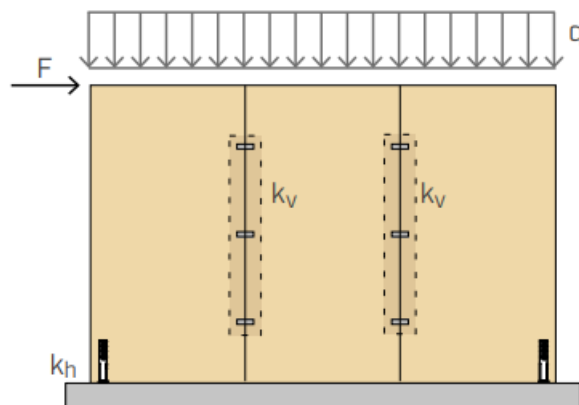


Figure D.5 – Slotted connections as used between shearwalls

The slots used in the connection of one CLT wall to another give a combined shear stiffness k_v in the y direction.

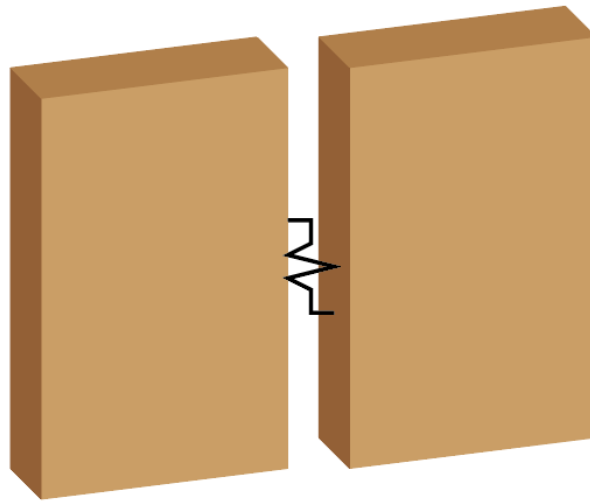


Figure D.6 – How slotted connections are modelled in karamba

Since the ‘springs’ work in parallel, the equivalent stiffness of all springs combined is equal to the stiffnesses of all springs combined:

$$k_v = \sum k_i$$

In the other directions (the x and z directions) the connection will be modelled to be completely rigid.

		$R_{v,k}$ [kN]	k_{ser} [kN/mm]
CLT ⁽⁵⁾	$\Sigma d_0^{(6)} =$ 40 [mm]	34.37	17,50
	45 [mm]	37.81	
	49 [mm]	40.57	
	50 [mm]	41.26	
	55 [mm]	44,70	
	59 [mm]	47.46	
	60 [mm]	48.15	
	69 [mm]	54.35	
LVL softwood	cross grain veneer ⁽⁷⁾	52.72	24,00
	parallel grain veneer ⁽⁸⁾	70.97	
LVL hardwood	cross grain veneer ⁽⁹⁾	125.71	48.67
	parallel grain veneer ⁽¹⁰⁾	116.59	
glulam ⁽¹¹⁾		68.13	25.67

Figure D.7 – Stiffness properties of slotted connections

For a CLT shear wall of one storey tall, four slots will be assumed. This adds up to a total k_v of $17.5 * 4 = 70$ kN/mm for the connection between two shear walls, connected in-plane.

Floor to floor connections

Like with the in-plane connections of shear walls, floor panels are also connected to each other in the same way. This, however, proves to be a problem. Since the model in grasshopper can only handle so much elements and connections before becoming unbearably slow and connecting every single floor panel in this manner is simply not a practical solution.

This problem was solved by creating a separate model that divides the floor in multiple larger pieces that are connected by the slotted connections mentioned above. An in-plane concentrated load is then put on this model as well as on a continuous model. The goal here is to match the deflection of the connected model to the continuous model by reducing the Young's modulus of the continuous model. In this way a reduction factor is created specifically for the model variant that can then model the effect of the slotted connections on stiffness in the continuous floor.

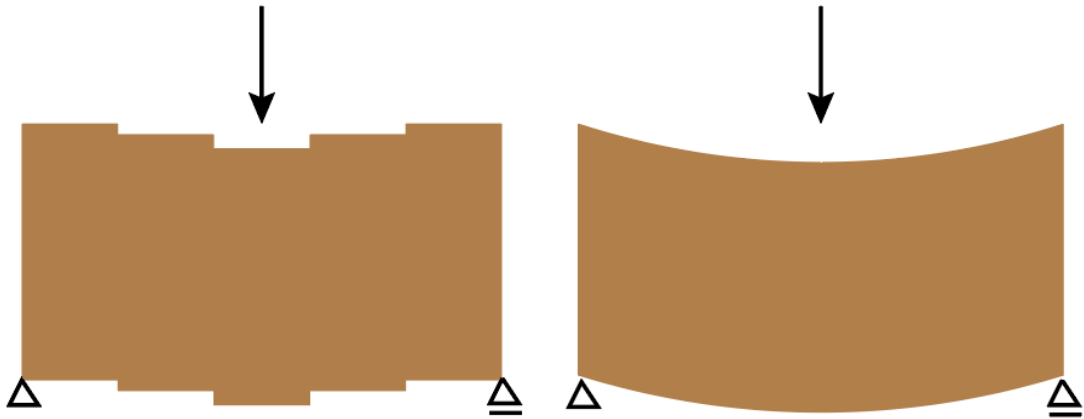


Figure D.8 – Schematization of equivalent floor stiffness modelling

Appendix E - Extension model validations

CLT Panel validations

This appendix shows how the model results of the CLT are validated. Since CLT is a material that is not often modelled using Karamba, validations are necessary to show that the results are indicative of the real life mechanical behavior of CLT and the connections between the CLT elements and the structure below.

As mentioned before, CLT is an orthotropic material, with different mechanical properties in its to principal directions. This means that two different Young's moduli have to be defined. For the shear modulus only one value is used.

Table E.1

Element	120C5S
Thickness	120 mm
E1 _{ef}	8000 MPa
E2 _{ef}	4000 MPa
G _{ef}	340 MPa
Self-weight	500 kg/m ³
Element	Hold down connection
K _{HD}	9070 N/mm
Element	Bracketed connection
K _B	6070 N/mm

The Young's moduli in the two primary directions are determined using the net section method described in chapter 4. An effective shear modulus is determined using the method described by Schikhofer. This is also elaborated on in chapter 4. For the effective shear modulus a lamella width of 150 mm was assumed.

For validations the following scenarios were looked at:

- Displacement of a single CLT panel (3x3m), pinned connections to the foundation, loaded vertically and horizontally
- Displacement of a single CLT panel (3x3m), using connections modelled as springs (as described in chapter 4), loaded vertically and horizontally
- Compression and shear stresses in a single CLT panel, using spring modelled connections, loaded vertically and horizontally
- Displacement for a stack of three CLT panels (3x3m each), using spring modelled connections, loaded vertically and horizontally
- Compression and shear stresses in a stack of three CLT panels (3x3m each), using spring modelled connections, loaded vertically and horizontally

Method of obtaining displacements and stresses with hand calculations

Displacement

As shown in chapter 4, displacement of a CLT panel that is connected with holddowns and brackets consists of four contributions: shear deformation, bending deformation, translation and uplift. The **Wallner Novak** method was used to determine the numerical value of each contribution with the following equations:

In scenario 1 where the CLT panel is modelled with pinned connections, the contributions made by translation and uplift are not taken into account (since these contributions solely rely on connection stiffness). In the subsequent scenarios where the connections are modelled as spring elements, these contributions will be taken into account.

Compressive stress

Compressive stress for pure vertical loads is determined using the following formula:

$$\sigma_{c,vertical} = \frac{F}{A_{ef}}$$

The compressive force is divided by the effective area to find the compressive stress in the structural part of the cross section. When a vertical load is combined with a horizontal load (as is done in the validations), the contribution made to the compressive strength by the formula above is augmented with the following contribution:

$$\sigma_{c,horizontal} = \frac{M}{W} = \frac{F_h * h}{W}$$

The horizontal force creates a bending moment in the CLT panel. This means a compressive stress and tensile stress are created in the cross section. The largest compressive stress is found by dividing the moment over the section modulus W.

In a scenario where both vertical and horizontal forces are acting on the CLT panel, the contributions of the vertical loads and horizontal loads can simply be superimposed to determine the maximum compressive stress in the CLT panel.

Shear stress

Shear stress is determined using the following formula:

$$\sigma_s = \frac{F_h}{A_{ef}}$$

The shear stress is determined by dividing the horizontal force over the shear area of the CLT panel, where, again, only the effective shear area is taken into account.

Interpreting Karamba results

Shell stresses in Karamba can be found using the 'shell sections' component. Here, however, the stresses are outputted in kN/m, not in kN/m² or N/mm². This is because Karamba returns stresses as if they are present on a one dimensional shell. To get to the correct stresses, these stresses have to first be divided by the width of the shell, in this case the CLT panel. Since, in a CLT panel, not every part of the cross section is assumed to contribute structurally, the stresses given by Karamba are divided by the effective area that is appropriate for the type of stress.

The 'shell sections' component requires a location within the shell to read the stresses from. For the validation of hand calculations, the best location to determine stresses is the middle of the shell. Reading stresses at the bottom of the shell will yield results that cannot be calculated by hand because it will show disturbances caused by the local stresses at the connections.

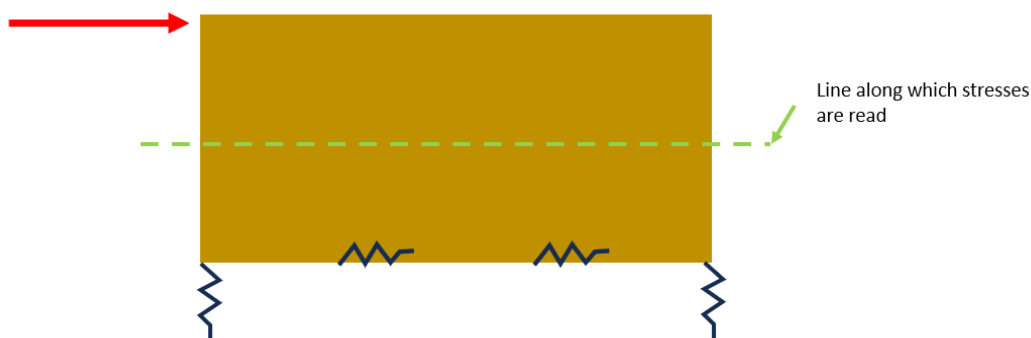


Figure E.2 – line along which stresses are read and positions of spring supports

Single CLT panel with horizontal load

The first scenario consists of a single CLT panel (3x3m) with pinned connections. The reason for not incorporating the stiffness of connections in this scenario is that it is important to know whether the mechanical properties assigned to the CLT panel in Karamba give accurate results and whether the shell is modelled correctly. The CLT panel was modelled as an orthotropic shell where the shell properties were determined as described in chapter 4, and as shown in table E.1.

The supports were placed as schematically shown in figure E.2.

Displacement

For three horizontal loads (30, 40 and 50 kN), the displacement of the modelled CLT panel in Karamba was compared to the displacement found using hand calculations made according to **REFERENCE THE METHOD**. Table E.3 shows the results:

Table E.3

Horizontal Load	Hand calculated deflection	Modelled deflection	Percentage difference
50 kN	10.91 mm	10.94	0.27%
40 kN	8.73	8.75	0.23%
30 kN	6.54	6.56	0.31%

The displacement found using Karamba is consistently about 0.3% higher than the one found using hand calculations.

Stresses

Now the compressive and shear stresses of the Karamba model are compared to the stresses according to hand calculations. Stresses are determined in the middle section of the panel (see figure E.2), since the stresses closer to the support will show localized disturbances that cannot be calculated by hand.

Table E.4

Horizontal load	Hand calculated shear stress	Modelled shear stress	Percentage difference
50 kN	0.208 MPa	0.205 MPa	1.6%
40 kN	0.167 MPa	0.164 MPa	1.8%
30 kN	0.125 MPa	0.122 MPa	2.4%

Table E.5

Vertical load	Hand calculated compressive stress	Modelled compressive stress	Percentage difference
10 kN/m	0.125 MPa	0.124 MPa	0.81%
7 kN/m	0.0875 MPa	0.087 MPa	0.57%
5 kN/m	0.0625 MPa	0.062 MPa	0.81%

Validation for stacked CLT panels

In Chapter 2, the theory behind deflections in CLT panels has already been elaborated on. It was shown that the deflection of a CLT panel that is loaded in plane consists of four contributing factors: shear, bending, translation and rotation (also referred to as uplift).

A structure with three stacked CLT panels will be considered here. The holddowns and bracketed connections are modelled in the same way they were for the singular CLT panel. These connections are modelled as small spring elements, which means that a space of 1 mm was held between the panels vertically to fit in these spring elements. This distance was found not to influence the total deflection.

The validation is done with hand calculations following the method described by **(wallner novak, from cltstrenght)**, which were also used for validation of the singular CLT panel. Here, however, some alterations have been made to account for the stacking of CLT panels.

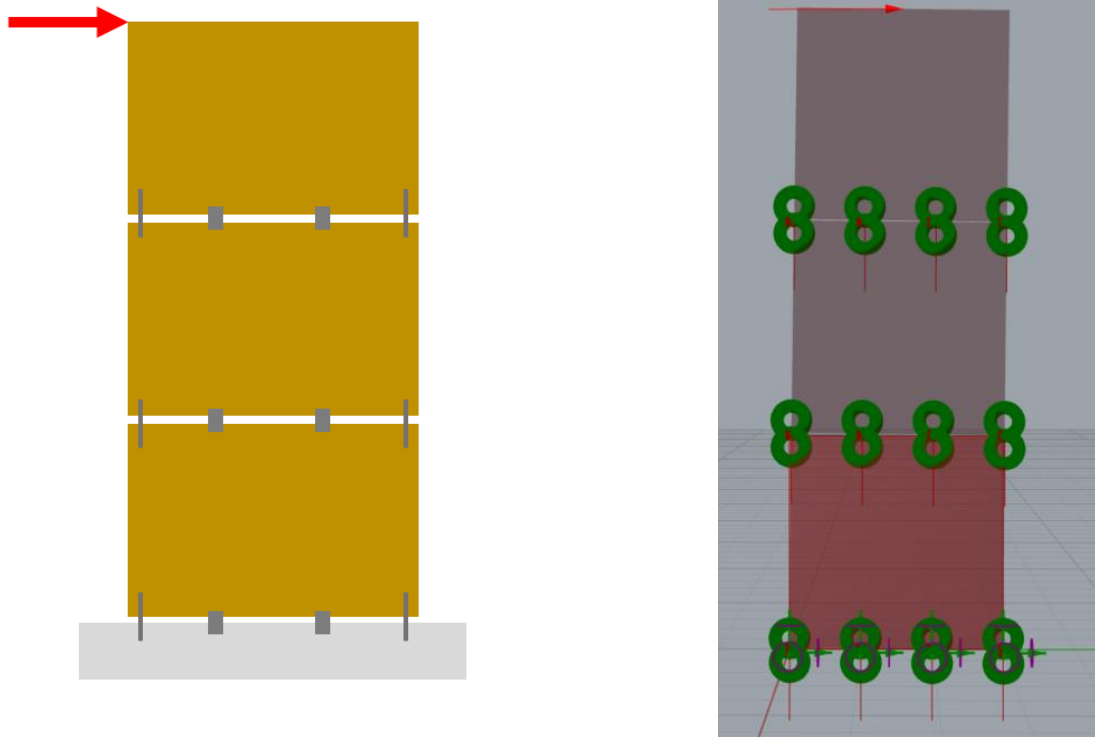


Figure E.6

The contributions made by shear and translation are straightforward to superimpose. The contributions can be calculated for one panel and multiplied by three to get the total deflection made by that contribution. This is because the deflection, for both of these contributions, increases linearly with height.

The equations to determine the contributions made by bending and uplift, on the other hand, have to be modified to obtain the correct deflection for the stack of CLT panels. This is because the deflections found here are governed by the bending moment found in the stack of CLT panels, and so, the height of the entire stack has to be taken into account.

For the deflections caused by uplift, the total deflection can be found by using equation X (note that, at this stage, vertical loads are not taken into account, this will be done at a later stage). Here, the vertical force in the holddown connection is determined according to the bending moment. Since uplift at the holddown connection is only caused by the panels above it, the contribution of uplift from the uppermost panel only takes the height of one panel into account whereas the contribution of uplift of the base panel takes the full height of construction into account (see figure E.7).

$$u_{uplift_{total}} = u_1 + u_2 + u_3$$

$$= \frac{F * h_1^2}{w^2 * K_{HD}^V} + \frac{F * h_2^2}{w^2 * K_{HD}^V} + \frac{F * h_3^2}{w^2 * K_{HD}^V}$$

In this equation u_n is the partial displacement brought by panel n (see figure E.7), F is the horizontal force, h_n is the height from the top of panel n to the location of u_n (see figure E.7), w is the width of the panels and K_{HD} is equal to the stiffness of the hold down connector.

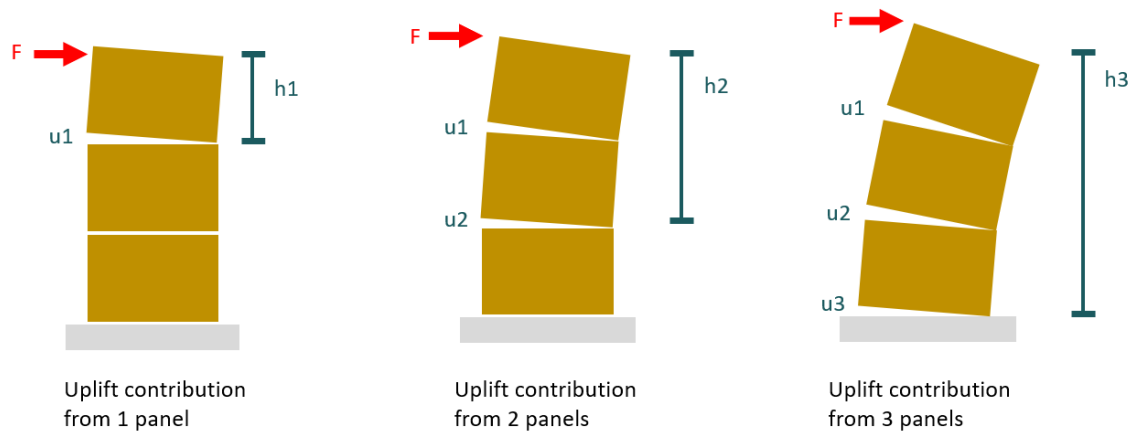


Figure E.7

Table E.8

Contribution		Deflection
Shear		3.13 mm
Bending	Bending 1 panel	0.42 mm
	Bending 2 panels	3.33 mm
	Bending 3 panels	11.25 mm
Translation		12.35 mm
Uplift	Uplift 1 panel	5.51 mm
	Uplift 2 panels	22,05 mm
	Uplift 3 panels	49.61 mm
Total deflection		107.97 mm

These hand calculations show that, the contribution of uplift increases significantly when considering stacked panels instead of a single panel. The contribution to the deflection made by uplift is now 77%.

When modelled in Karamba (as shown in figure E.6, on the right), the global deflection is as shown in table E.9. The difference in deflection between the hand calculated and modelled version is consistently about 8.4%. This makes the difference larger than seen with one singular panel. The range of this difference should be taken into account when interpreting the results from the model.

Table E.9 – Deflections for a stack of three panels

Horizontal load	Hand calculated deflection	Modelled deflection	Percentage difference
50 kN	107,97 mm	117,02mm	8,37%
40 kN	86,37 mm	93,61 mm	8,38%
30 kN	64,78 mm	70,2 mm	8,38%

Table E.10 – Shear stresses for a stack of three panels of three panels

Horizontal load	Hand calculated shear stress	Modelled shear stress	Percentage difference
50 kN	0.208 MPa	0.23 MPa	10.57%
40 kN	0.167 MPa	0.187 MPa	11.97%
30 kN	0.125 Mpa	0.14 MPa	12%

Table E.11 – Compressive stresses for a stack of three panels of three panels

Horizontal load	Hand calculated shear stress	Modelled shear stress	Percentage difference
50 kN	0.208 MPa	0.23 MPa	10.57%
40 kN	0.167 MPa	0.187 MPa	11.97%
30 kN	0.125 Mpa	0.14 MPa	12%

Finally, the shear and compressive stresses in a stack of three CLT panels are assessed. Average shear stresses were handcalculated by hand, by simply dividing the horizontal load over the effective area of the shear wall. In Karamba, the shear distribution is more detailed so the average of the Karamba shear stresses in one cross section was taken. The results for shear stresses are shown in table E.7, and a visible representation is shown in figure X. When stacking three panels, the difference between shear stresses and hand calculations are shown to be a bit higher than expected, at a maximum of 12% when a horizontal load of 30 kN is imposed. Again, this difference needs to be taken into account when interpreting the results of the main model used in this thesis, especially when considering variants that have multiple storeys versus variants that have one storey. Validations for a single panel (that is not stacked) show much smaller margins. The reason for this discrepancy might be that the connections between stacked panels have some effect on the redistribution of the horizontal loads.

Now, compressive stress due to the horizontal load is validated. Here, the approach that was taken is a bit different. The compressive stress due to a moment in a panel is challenging to calculate. So, instead, calculatis, a tool created by Stora Enso was used to compare the compressive stresses to. This is shown in table E.9. In the case that was assessed a 7.3% difference was found. The reason the difference is still significant is very probably because, in Calculatis the stack of CLT panels was modelled as a single panel (calculatis does not allow for intermediary connections, see figure X) and in addition to this, the connections were all modelled as pinned because Calculatis also does not allow for spring connections.

Table E.12 – Compressive stresses in calculatis versus Karamba

Horizontal load	Calculatis calculated stress	Modelled compressive stress	Percentage difference
75 kN	4.51 MPa	4.85 MPa	7.3%



Figure E.13 – Compressive stresses as determined in calculatis

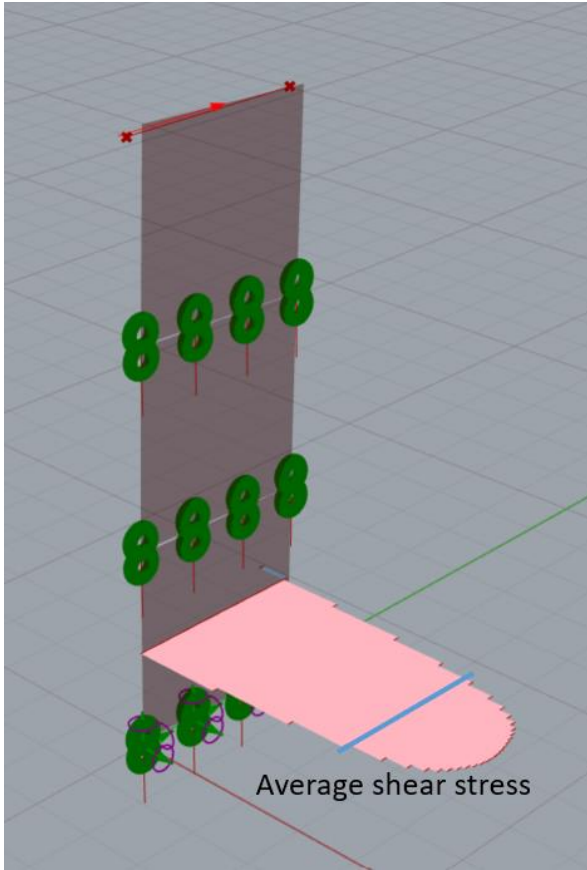


Figure E.14 – Shear stresses in a stacked panel

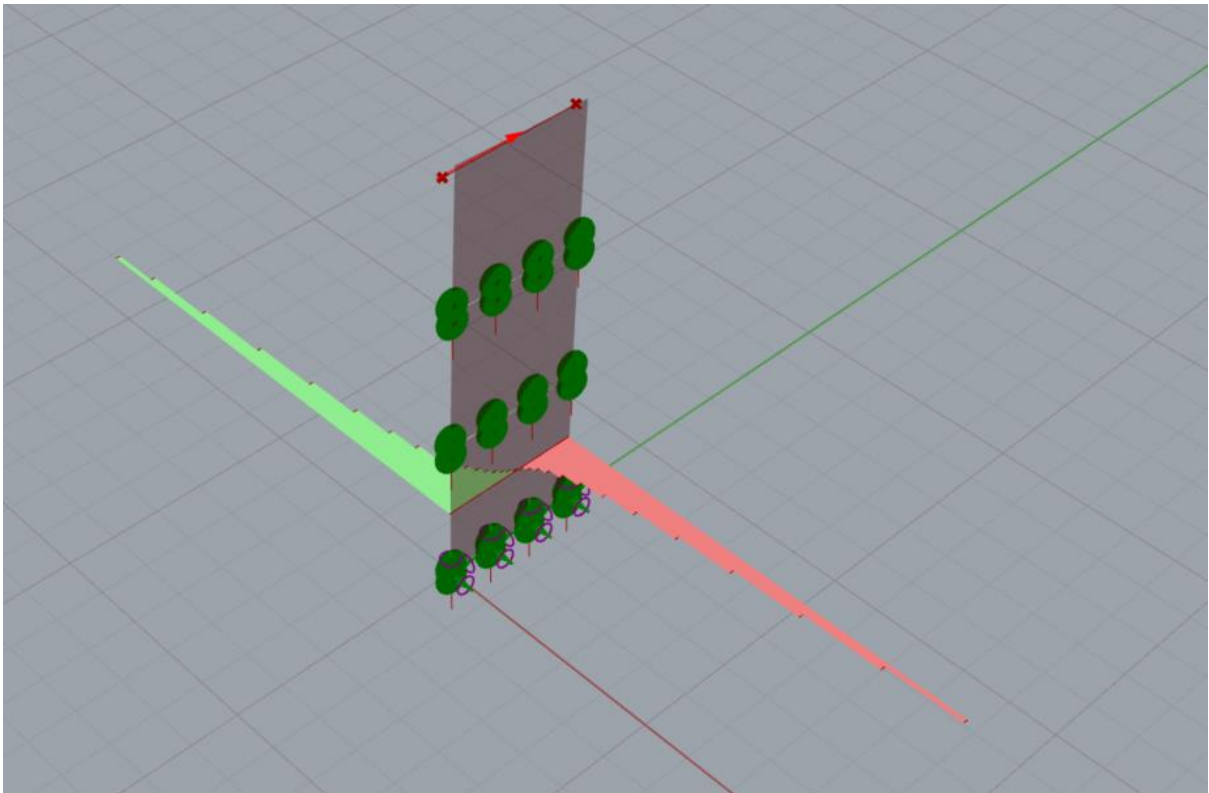


Figure E.15 – Compressive and tensile stresses due to horizontal load in a stacked panel

Model validations – Horizontal forces in the original concrete skeleton structure

To show the accuracy of the forces found in the model, a representative frame structure was modelled in matrixframe. This frame structure represents the middle cross section of the structure. A horizontal wind load was loaded on both the grasshopper tool model and the matrixframe model and the reaction forces were determined (see figure E.16). It can be seen that the matrixframe model shows a compression reaction force of 64.39 kN, while the grasshopper tool shows a reaction force of 62.48 kN, showing a difference of 2 kN, or 3 percent. The reason for the discrepancy might be that the stiffness of the structure is not uniform, and so the assumption that the wind load that is imposed on the structure is transferred specifically by this cross section might not be entirely correct. Still, an inaccuracy of 3% shows that the mechanical behavior of the concrete skeleton structure is representative of real life.

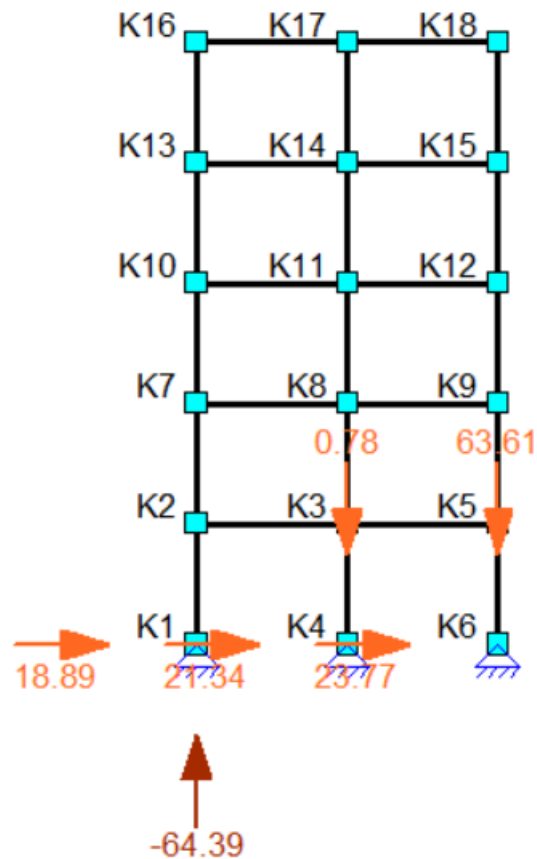


Figure E.16 - Reaction to an imposed uniform windload of 3.33 kN/m

Model validations – Column forces under shear walls

In addition to showing the accuracy of the modelled shear walls themselves (see the first part of this validation chapter), the accuracy of the model is also shown by looking at the forces found in the columns directly underneath the extension.

In order to find to what extent the model complies with hand calculations, a validation workflow was set up that consists of the following steps (also pictured in figure E.17): The equivalent stiffness of CLT panels is determined

A 2D model of the extension is constructed that uses the most eccentric wall layout (wall layout A), here the reaction forces in the CLT panels are determined. The reaction forces found when the CLT panels are represented as ‘supports’ shows us how much load is transferred to each CLT panel.

Then, the forces found in the CLT panels in the 2D model are placed on an unextended variant in the grasshopper tool. This is done so we can see how the horizontal forces in the shear walls are transferred to the original structure (here, we are looking at the reaction forces in the foundation piles).

Finally, the reaction forces in both models are compared to each other

The goal here is to show that the shear walls transfer the horizontal loads the way that they are expected to, as well as to show that these loads are transferred through the original structure as they are expected to.

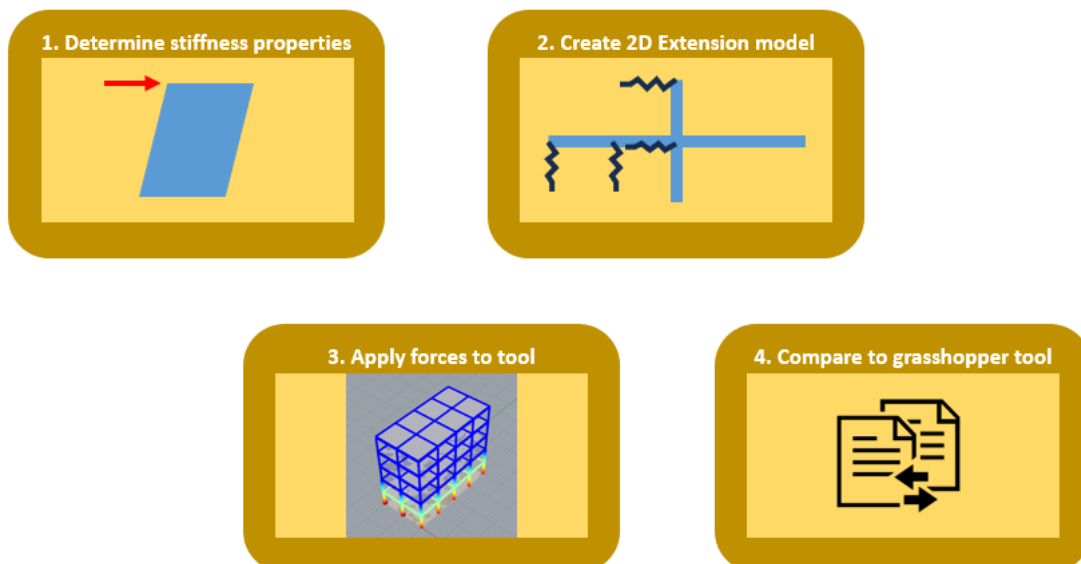


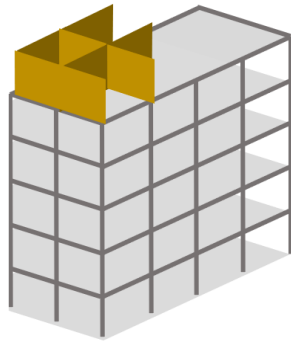
Figure E.17 – validation workflow

Step 1. Determination of equivalent stiffness of CLT panel

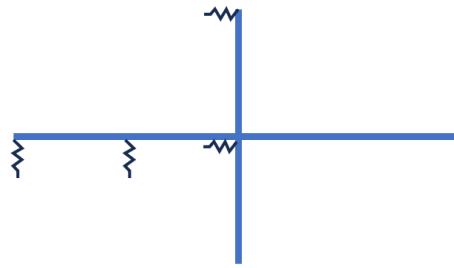
The equivalent stiffness of CLT panels can be determined by a simple pushover test, where a representative load is imposed on the panel and the maximum horizontal deflection is taken. By dividing the imposed load by the deformation, one arrives at the equivalent spring stiffness of the element. For the CLT panels this is done in Karamba, because Matrixframe does not allow for shell elements. Here, we find a deflection of 7.42 mm when a load of 50 kN is imposed on the panel (this load is representative of the wind load of half the façade and should therefore be able to create representative conditions to determine the equivalent stiffness of the panel). This translates to an equivalent stiffness of 6700 N/mm. This value will be used as the equivalent spring stiffness used to represent the CLT panels in step 2.

Step 2. 2D modelling the extension

The stiffness parameters found in step 1 are used in the modelling of the extension. In this step, the wind loads are imposed on an infinitely stiff cross shaped element that represents the floor. This element is supported by four supports, each of which represent a CLT wall in shear wall layout A. Figure E.18 shows how the wall layout translates to a schematization of the model, followed by the actual model in Karamba in figure E.19. Also note that the loads as imposed on the grasshopper tool model in step 3 are opposite to the reaction forces found in the validation model. This is because the reaction forces of the CLT panels to the wind are transferred to the main structure in the opposite direction.



Wall layout A



Schematization of shear walls



Figure E.18 (top) – Wall layout A and its modelled schematization

Figure E.19 (bottom) – Wall layout A as a 2D model in Karamba and the reaction forces

Step 3. Loading the unextended variant

In step 3, the reaction forces under the shear walls that were found in the previous step are now imposed, together with the appropriate wind load, on an unextended frame structure in the grasshopper tool. In the previous validation, it was already shown that the modelled concrete skeleton structure used in the grasshopper tool is sufficiently accurate. The reaction forces found here should, in principle, line up with the reaction forces that are found in an extended version of the model.

The support reactions that were found here are listed in table E.21.

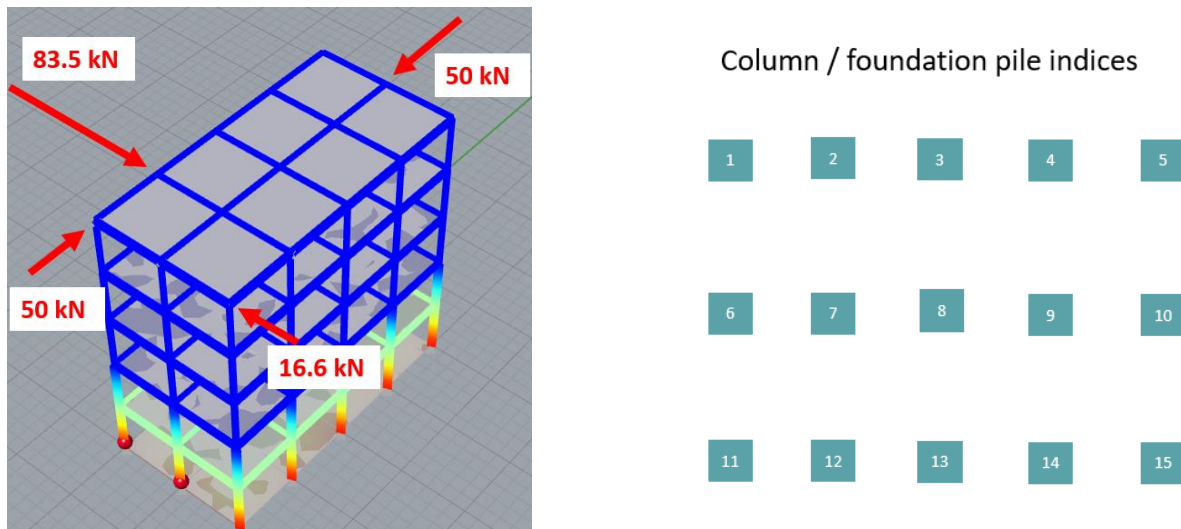


Figure E.20 – The reaction forces of step 2 imposed on the unextended structure (left), the column indices used (right)

Table E.21 – Reaction forces found in step 3

Column number	Reaction force validation model (kN)	Column number	Reaction force validation model (kN)
1	-82,53	9	-0,64
2	-94,22	10	0,08
3	-83,73	11	78,16
4	-85,95	12	95,20
5	-76,37	13	86,63
6	3,58	14	86,30
7	0,44	15	76,32
8	-3,25		

4. Comparison of hand calculations to grasshopper tool

Table X shows the reaction forces found in step 3 versus the reaction forces found in the extended model. Here, the absolute difference between the two is shown, the largest difference found is 5.2 kN, which translates to 5%.

Finally, the reaction forces found here can be compared against the ones found in the grasshopper tool. This is done in table E.22. One can see that the differences are 5% at most, meaning it can be concluded that the tool shows a sufficient accuracy for a model of which the main function lies in the initial design stages. Besides, this validation was done to show the accuracy of horizontal load transfer from the extension structure to the original structure. When the vertical loads are also taken

into account, the accuracy can be expected to increase because horizontal loading only makes up a part of the reaction forces.

Table E.22 – Reaction forces of the validation model and the tool model compared

Column number	Reaction force original model (kN)	Reaction force validation model (kN)	Absolute difference (kN)
1	80	82,5	2,7
2	89,63	94,22	4,59
3	88,33	83,73	4,59
4	88,46	85,95	2,51
5	77,94	76,37	1,57
6	0,03	-3,58	3,61
7	-0,06	-0,44	0,38
8	0,21	3,25	3,04
9	0,07	0,64	0,56
10	-0,06	-0,08	0,02
11	-79,73	-78,16	1,57
12	-89,97	-95,20	5,23
13	-88,34	-86,63	1,71
14	-88,42	-86,30	2,12
15	-77,97	-76,32	1,65

Overall conclusion validations

In this appendix, the accuracy of the grasshopper tool has been shown in two parts:

- The accuracy of deflections and stresses within the CLT panels were shown to strongly rely on whether one CLT panel or a stack of CLT panels was analyzed. When looking at single CLT panels, the differences were shown to range between 1 and 3%. However, when looking at a stack of CLT panels of three panels high, the differences increase to 7 to 12%.
- The inaccuracy of reaction forces in the original structure is shown to be, on average, 3.5%, with a maximum inaccuracy of 5%. When looking just at the reaction forces due to an imposed uniform wind load on the concrete skeleton structure, the reaction forces were found to be within a 3% margin with matrixframe validations.

Finally, it can be concluded that the accuracy of the grasshopper tool is sufficient, especially when looking at forces in the original structure. However, when looking at stresses in the CLT panels, the model shows some inaccuracies that can grow to an average of 10%. This should be taken into account when using the model and it is recommended to always use a separate FEM model for utilization checks in the extension elements.

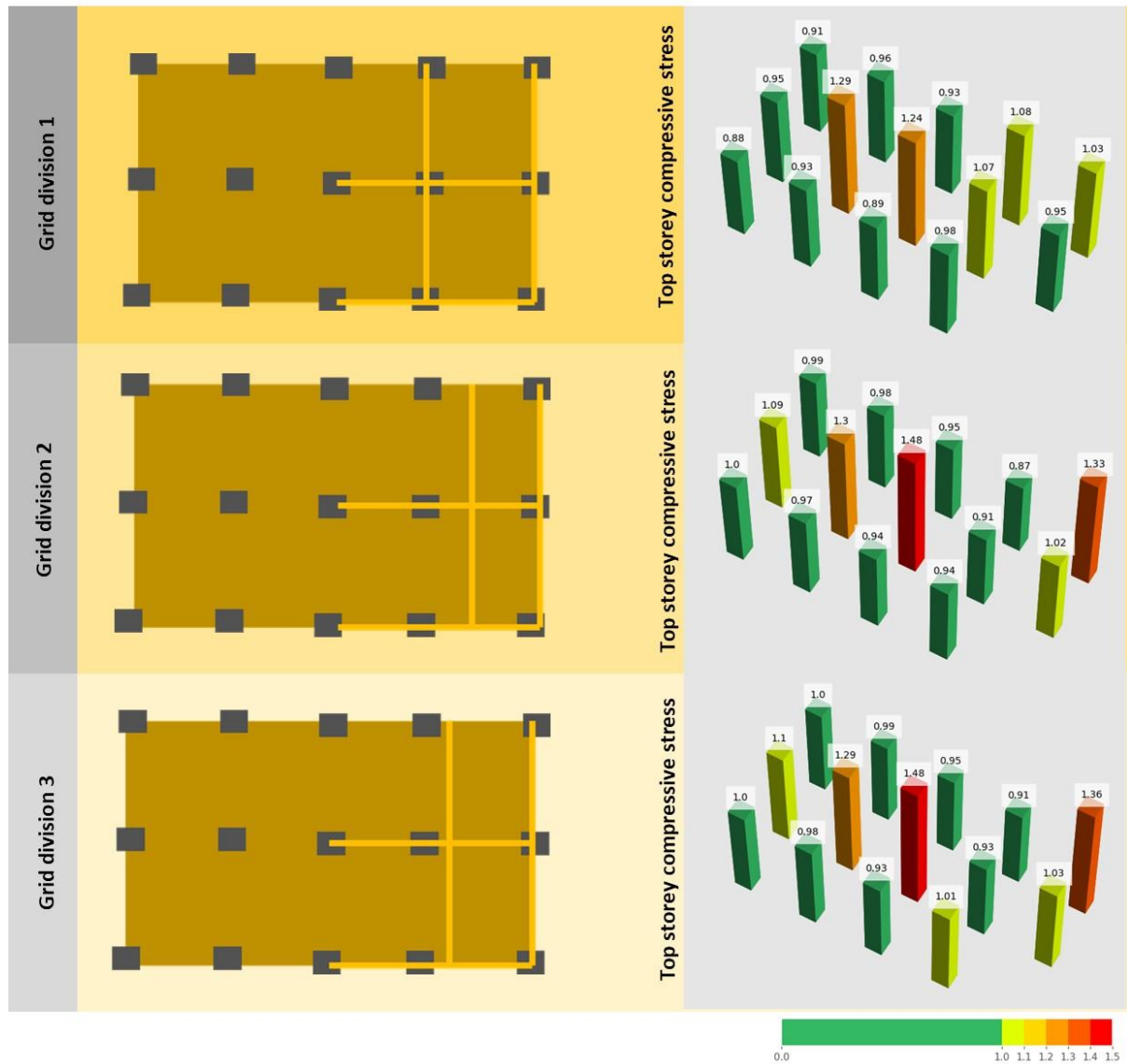
Appendix F – Result graphs

In this appendix some of the result graphs that are referred to in the main text can be found. In this appendix one can find:

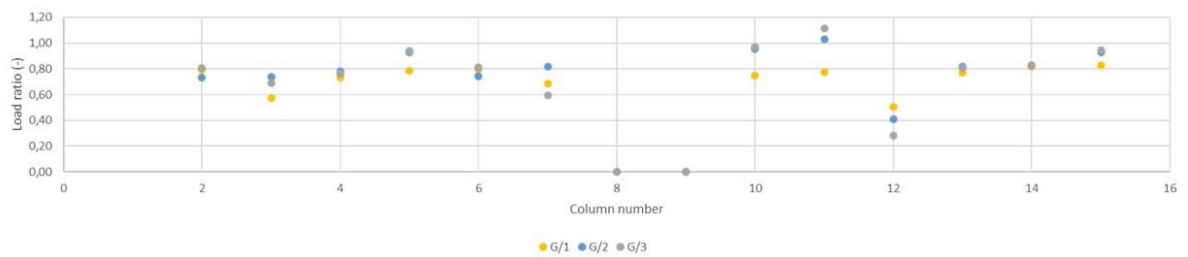
- C1 variants:
 - Overview sheets referring to the effects of extension grids
- C2 variants:
 - Overview sheets referring to the effects of wall layouts and extension grids
 - Graphs of load ratios in the original structure, deflections and unity checks in the extension
- C3 variants:
 - Overview sheets referring to the effects of wall layouts and extension grids
 - Graphs of load ratios in the original structure, deflections and unity checks in the extension

C1- SHEETS

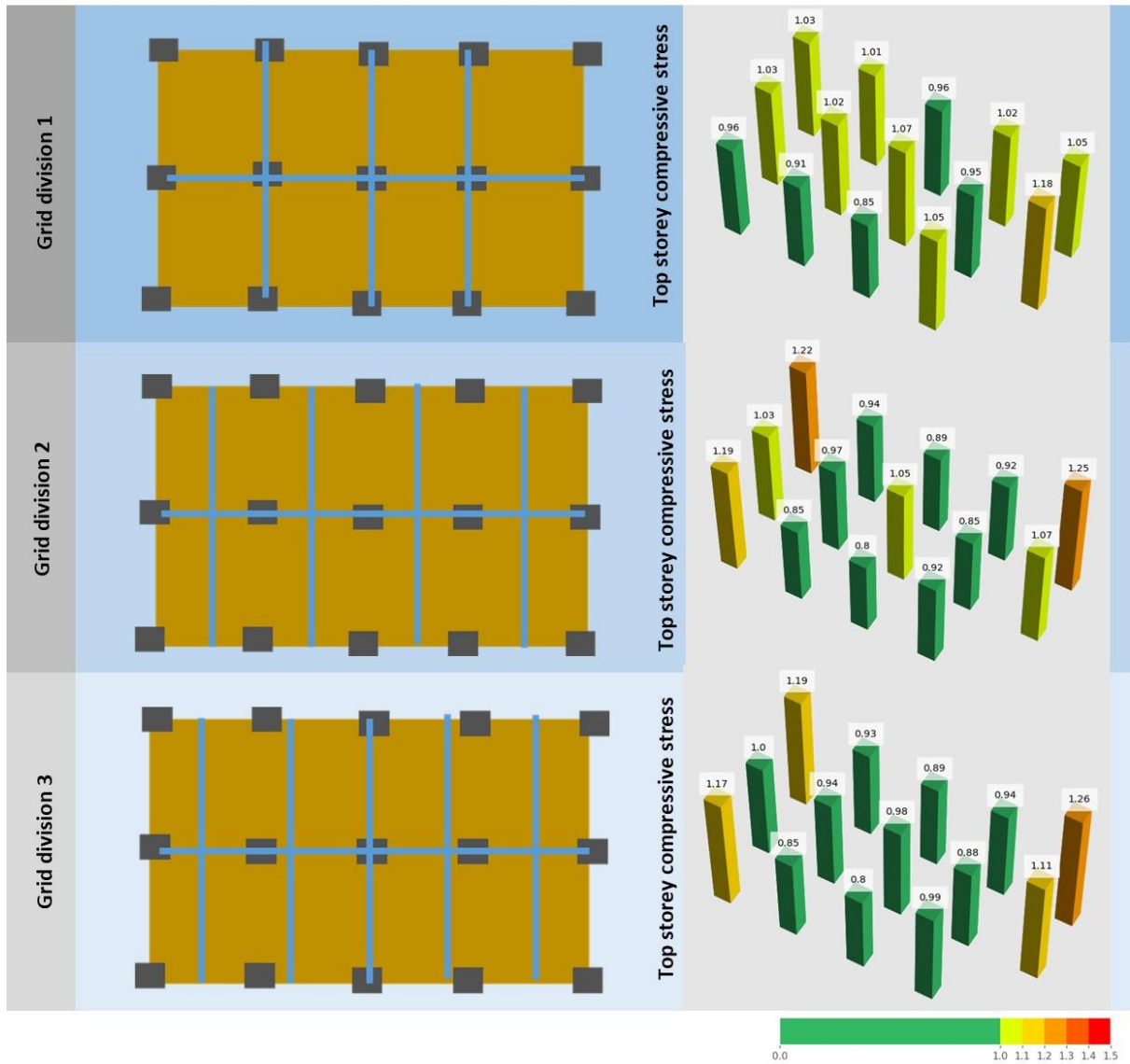
Load ratios for different extension grids on a G1H3C1 variant (wall layout A: core aligned), 3 storeys added



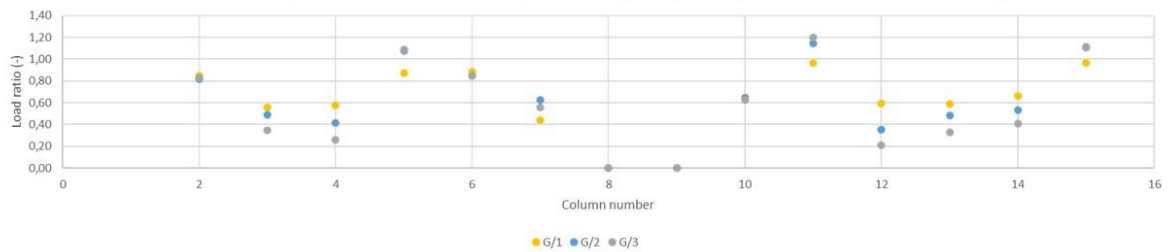
Tensile stresses in top columns in variant G1H3C1, with wall layout C, 3 storeys added for different extension grids



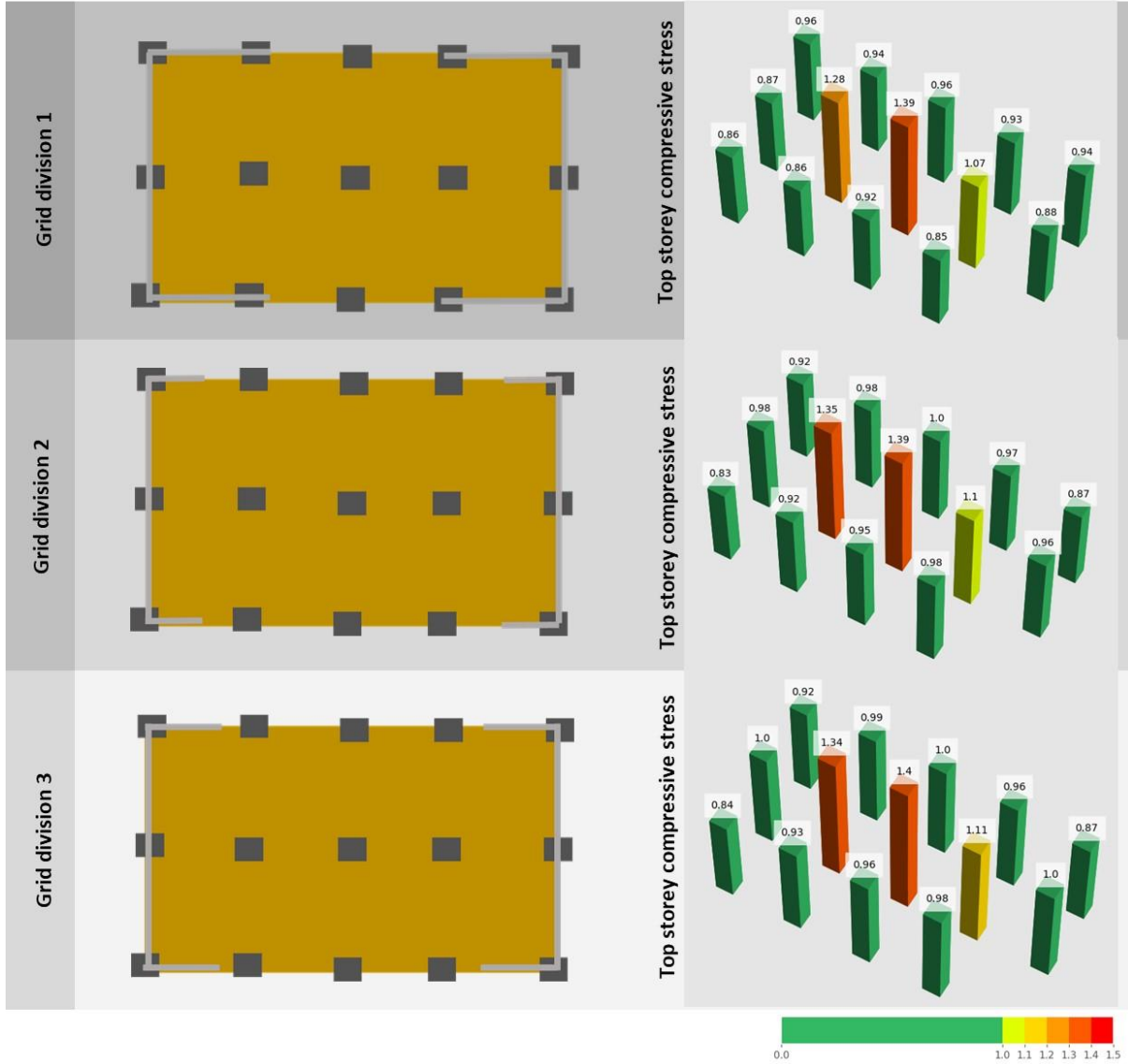
Load ratios for different extension grids on a G1H3C1 variant (wall layout B: functional design), 3 storeys added



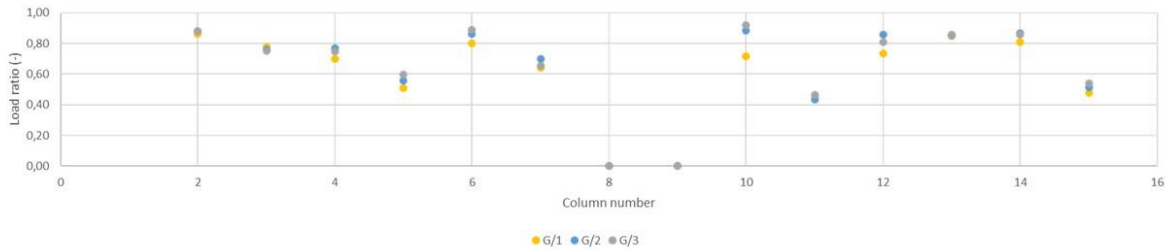
Tensile stresses in top columns in variant G1H3C1, with wall layout B, 3 storeys added for different extension grids



Load ratios for different extension grids on a G1H3C1 variant (wall layout C: facade aligned), 3 storeys added

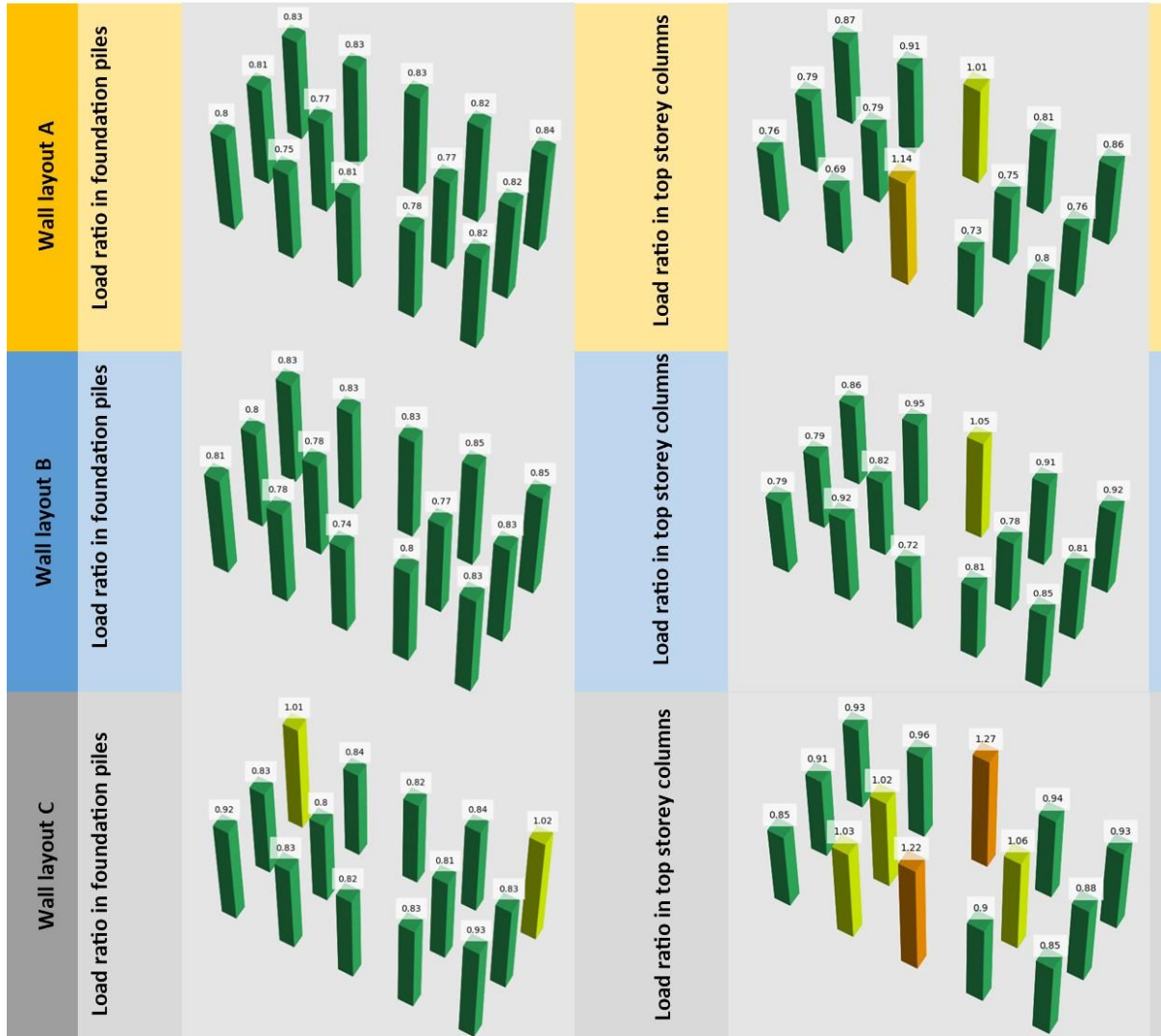


Tensile stresses in top columns in variant G1H3C1, with wall layout C, 3 storeys added for different extension grids

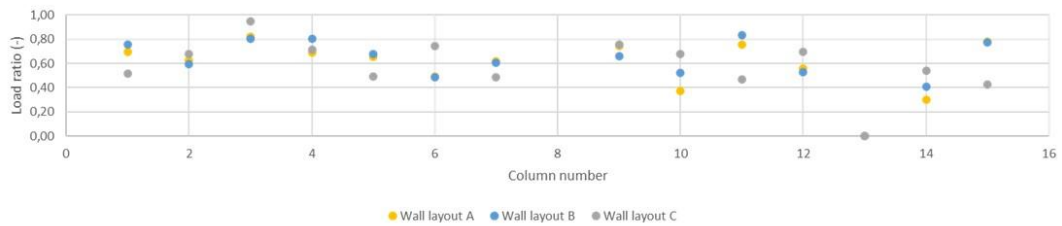


C2- SHEETS

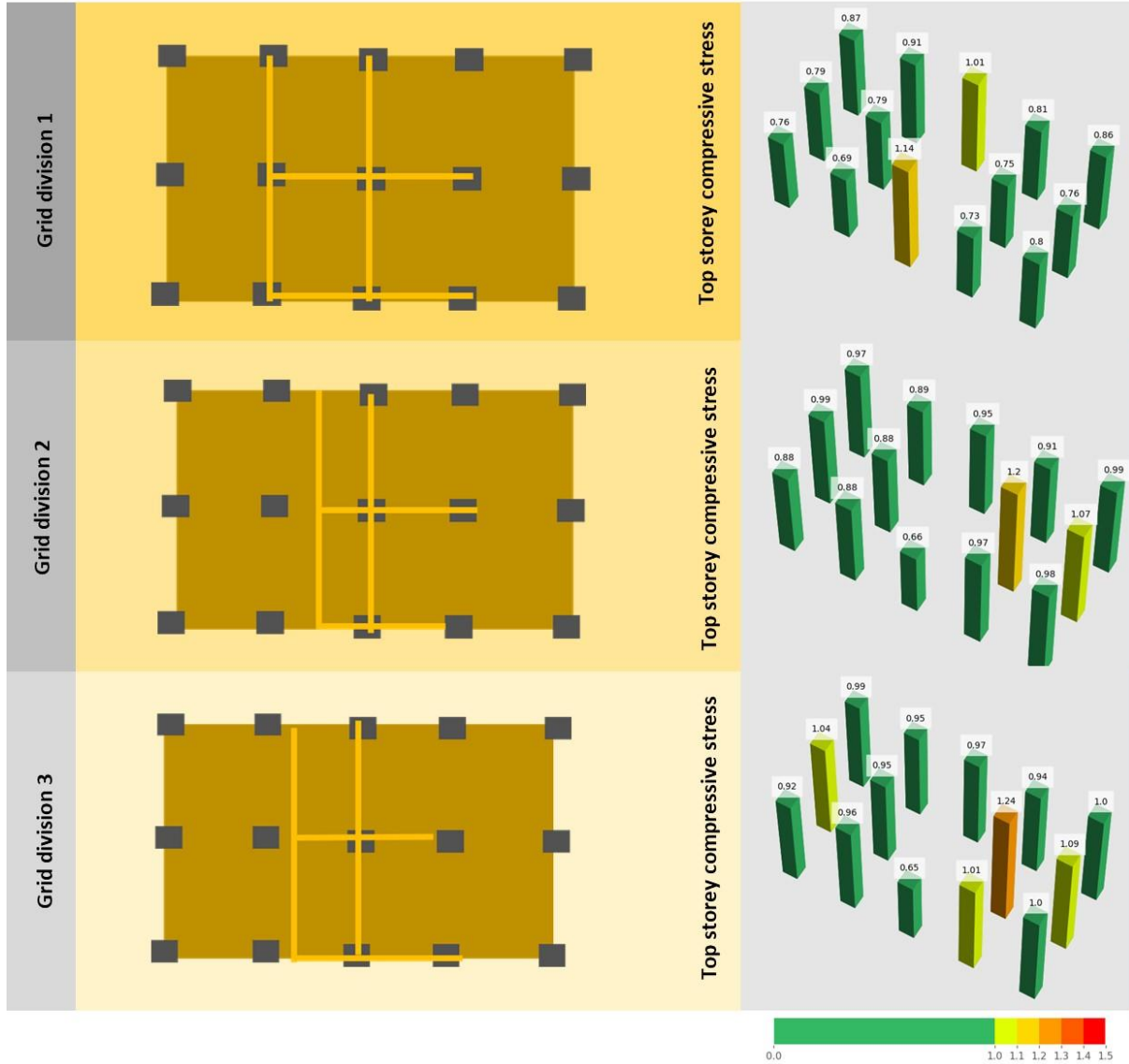
Load ratios for different wall layouts on a G1H3C2 variant (extension grid = G/1), 3 storeys added



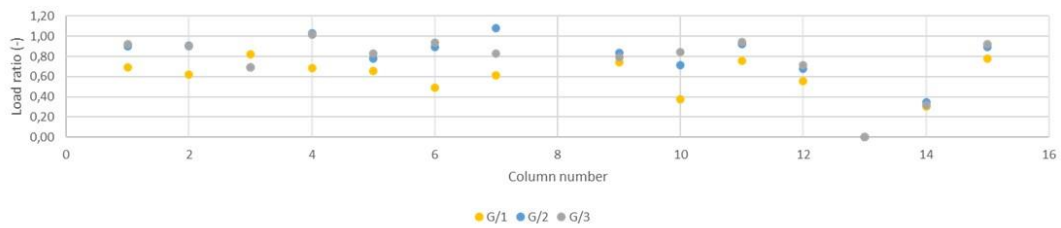
Load ratio for tensile stresses in the top storey columns for three wall layouts in a G1H3C2 variant (G/1, 3 storeys added)



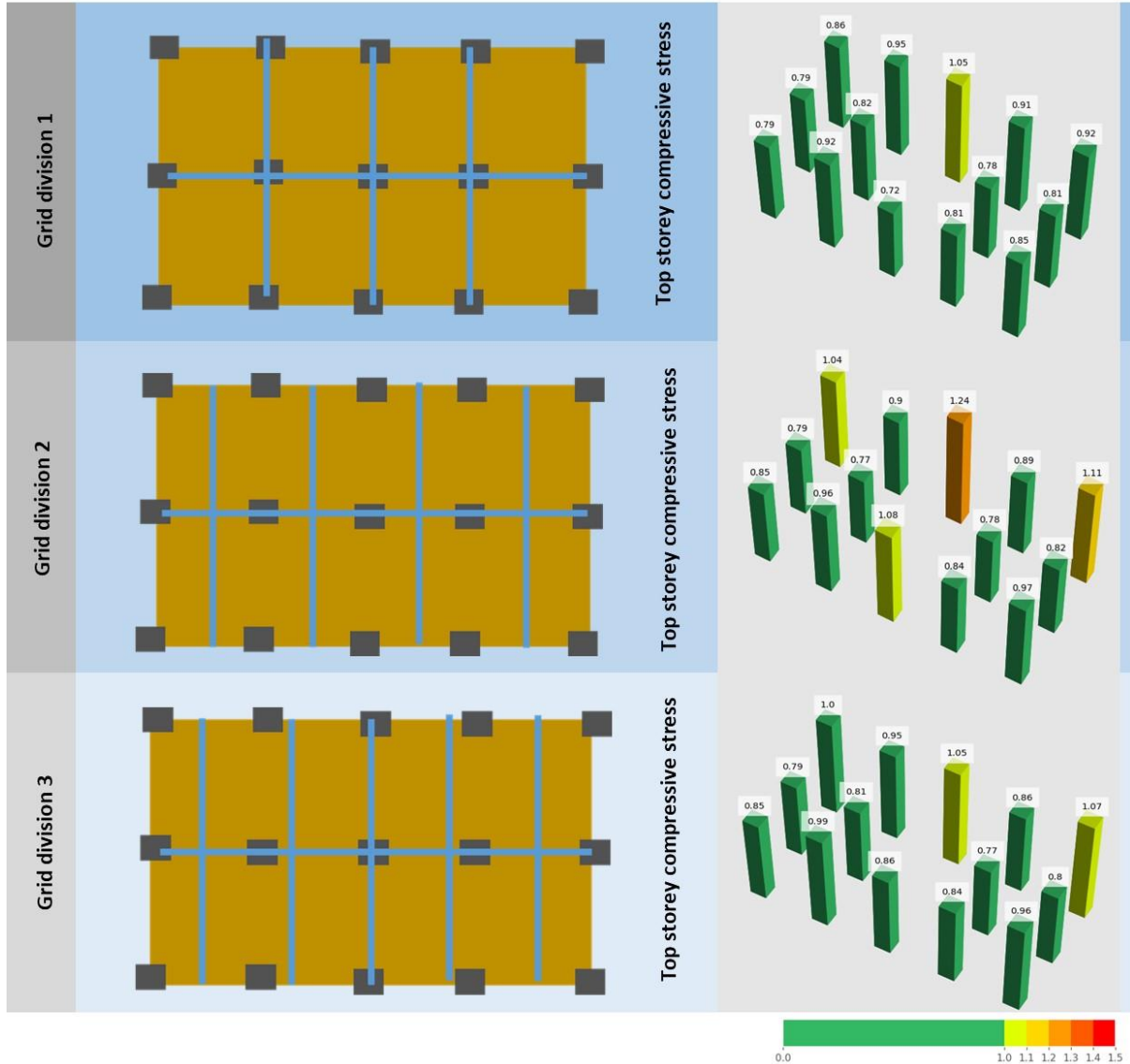
Load ratios for different extension grids on a G1H3C3 variant (wall layout A: core aligned), 3 storeys added



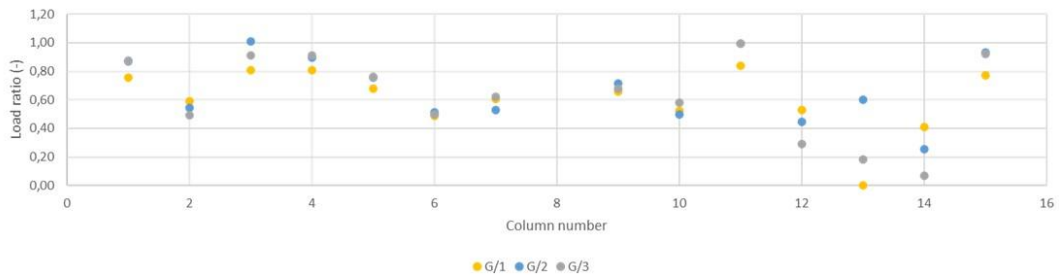
Load ratio for tensile stresses in the top storey columns for wall layout A for three extension grids in a G1H3C2 variant (G/1, 3 storeys added)



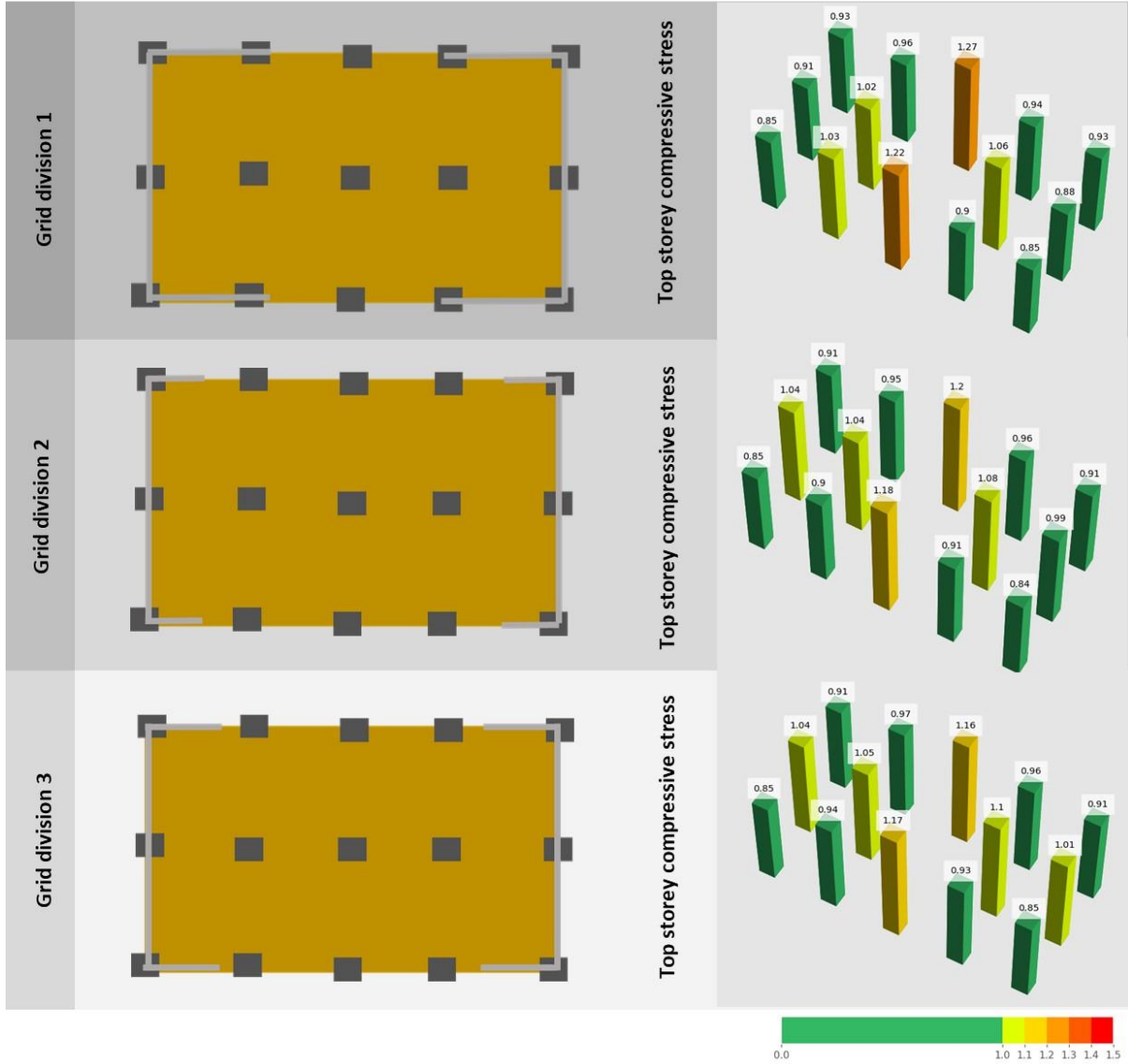
Load ratios for different extension grids on a G1H3C3 variant (wall layout B: functional design), 3 storeys added



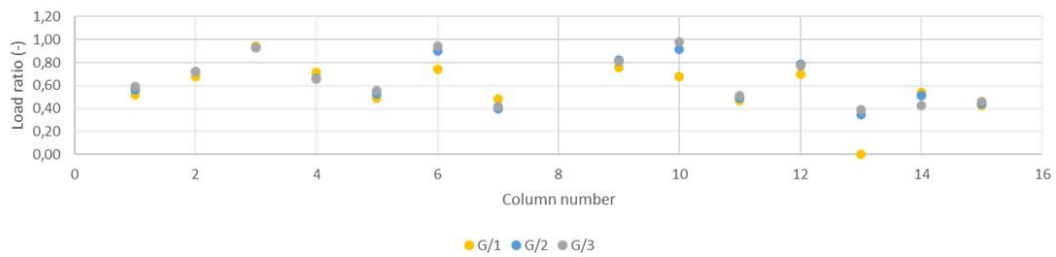
Load ratio for tensile stresses in the top storey columns for wall layout B for three extension grids in a G1H3C2 variant (G/1, 3 storeys added)



Load ratios for different extension grids on a G1H3C1 variant (wall layout C: facade aligned), 3 storeys added

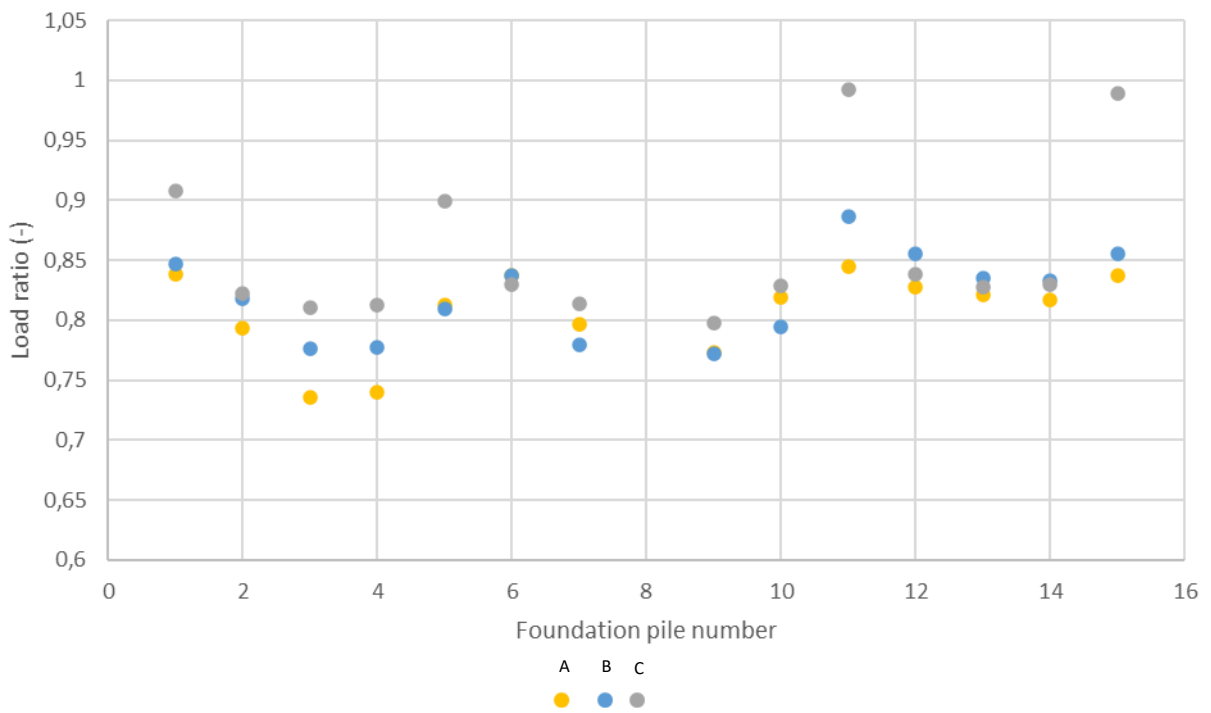


Load ratio for tensile stresses in the top storey columns for wall layout C for three extension grids in a G1H3C2 variant (G/1, 3 storeys added)

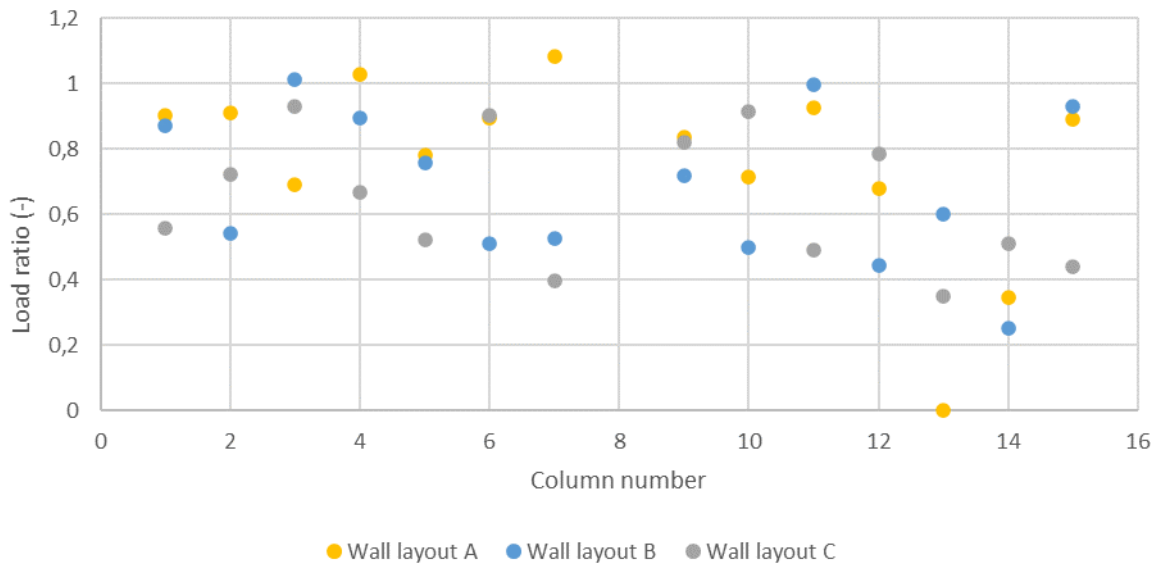


C2 – GRAPHS

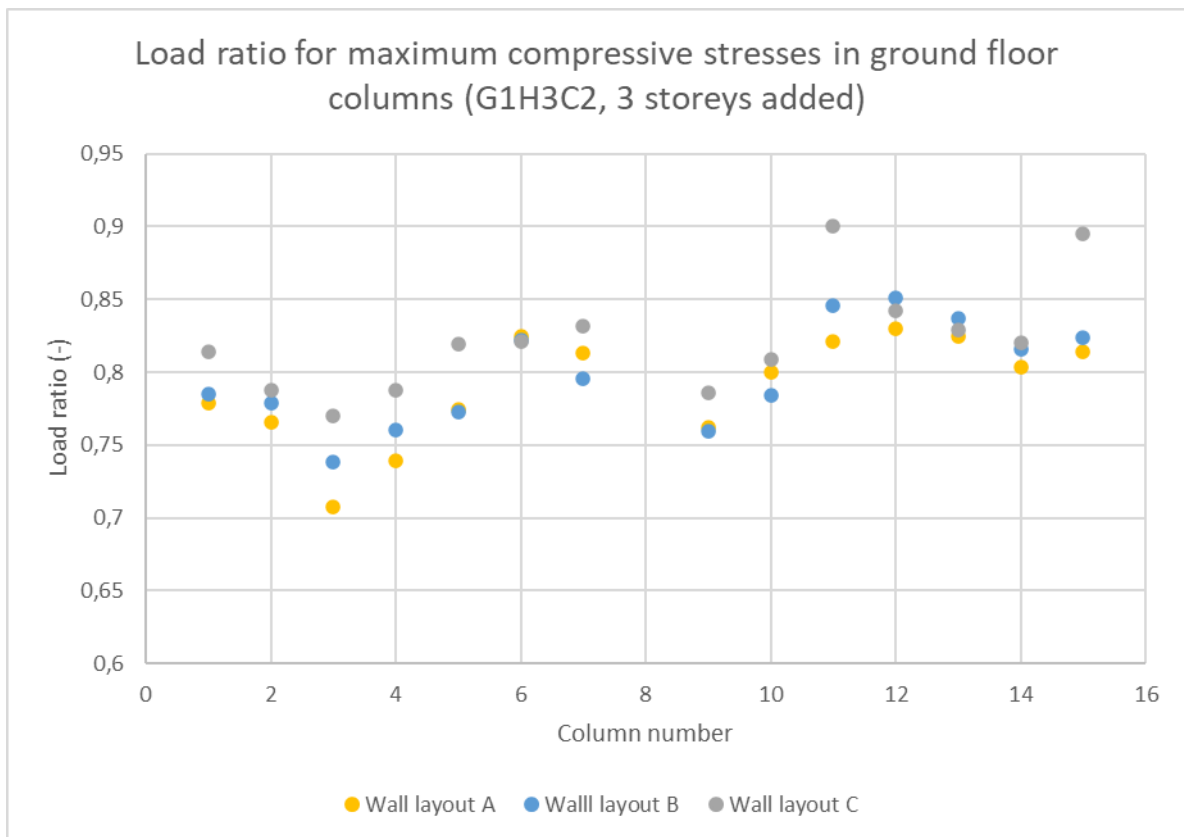
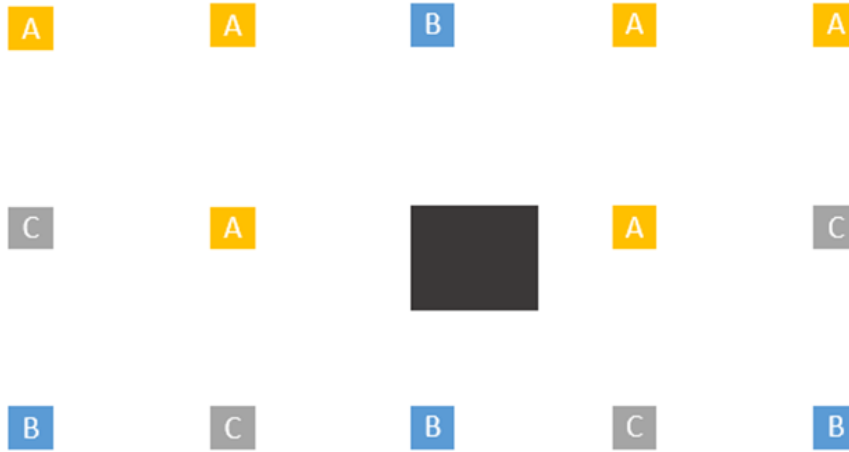
Load ratio for normal forces in foundation piles under columns
for variant G1H3C2, 3 storeys added (G/2)



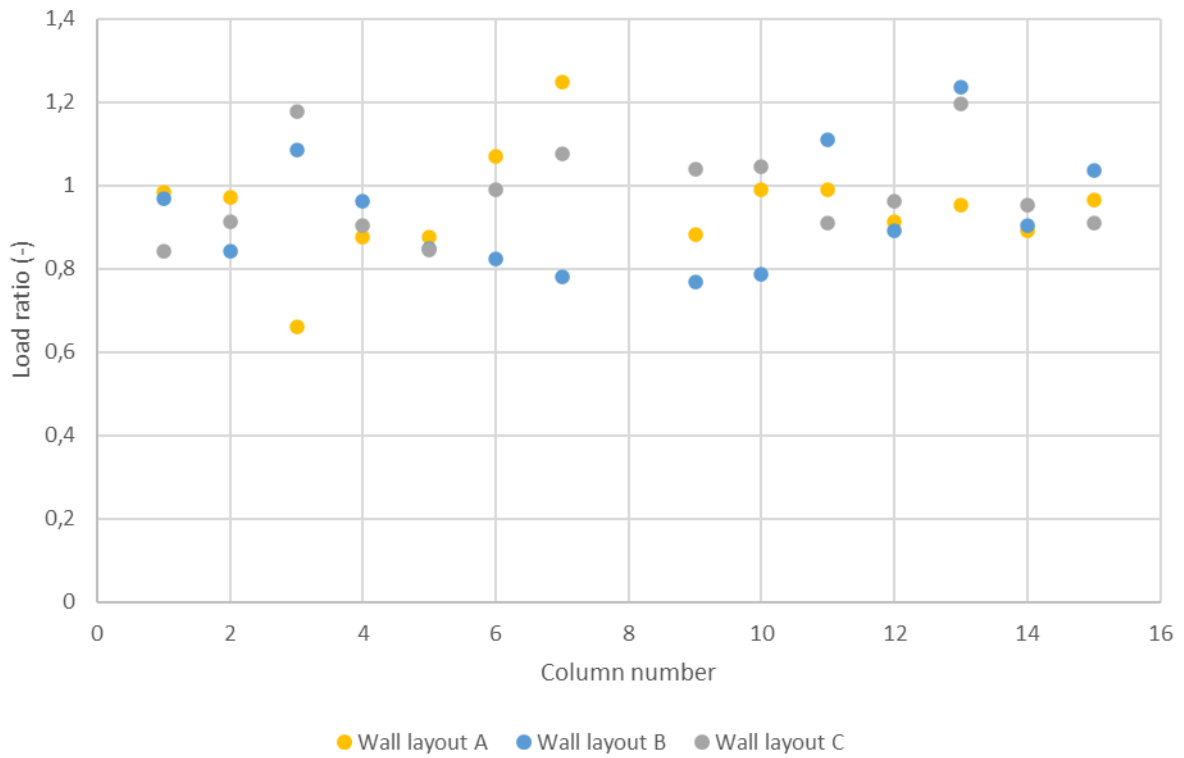
Load ratio for tensile stresses in top storey columns (G1H3C2,
3 storeys added, G/2)



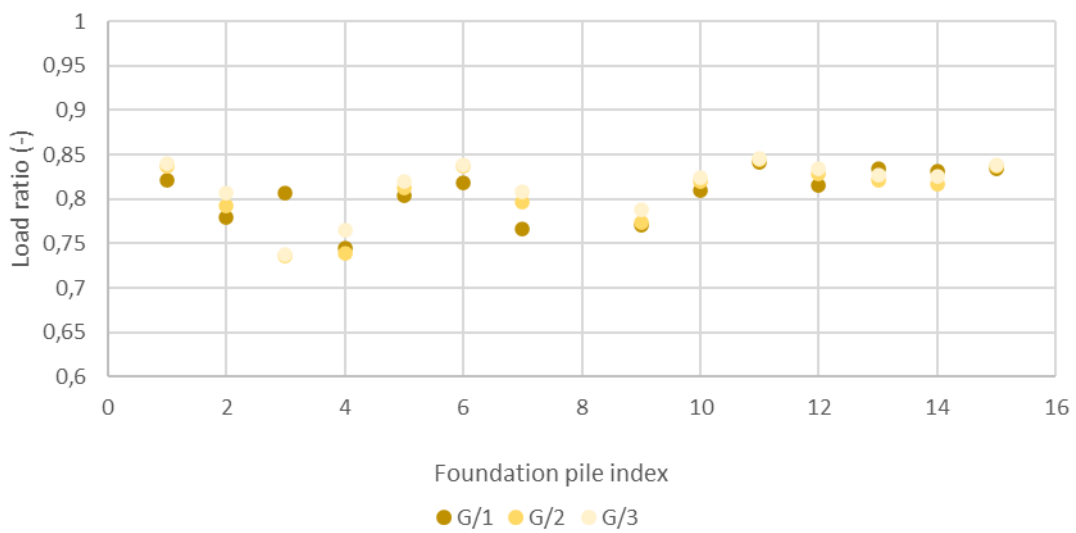
Wall layout that causes the largest capacity utilization in ground floor columns

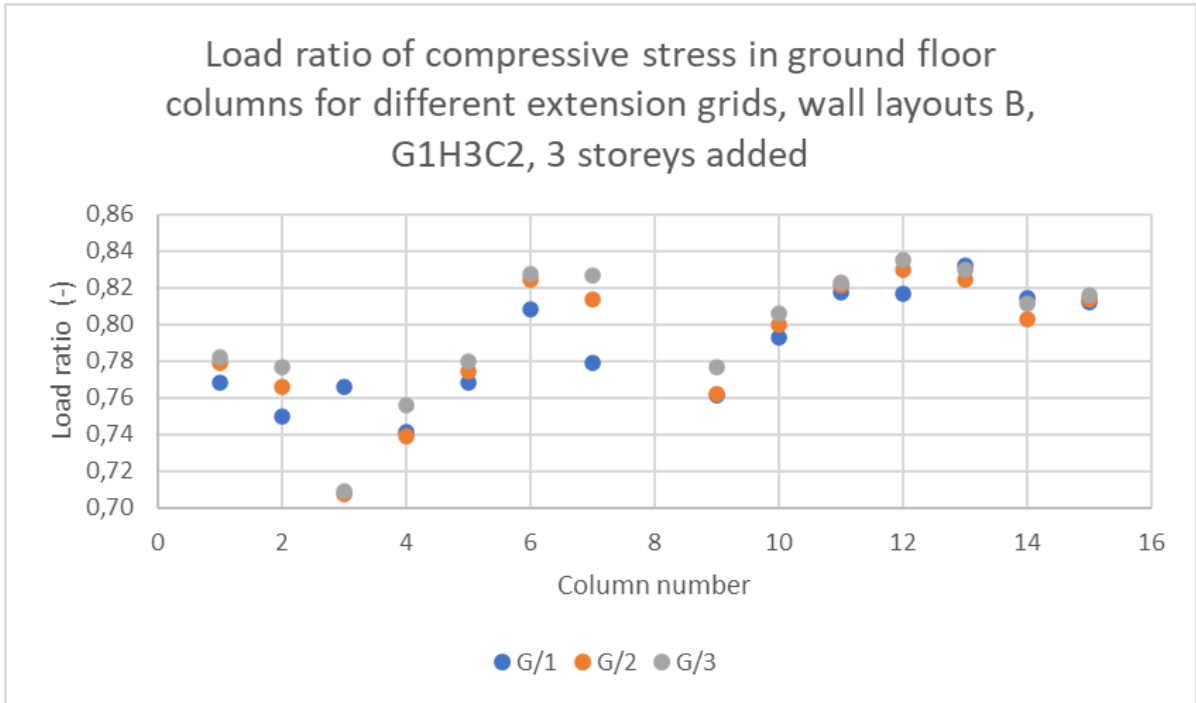
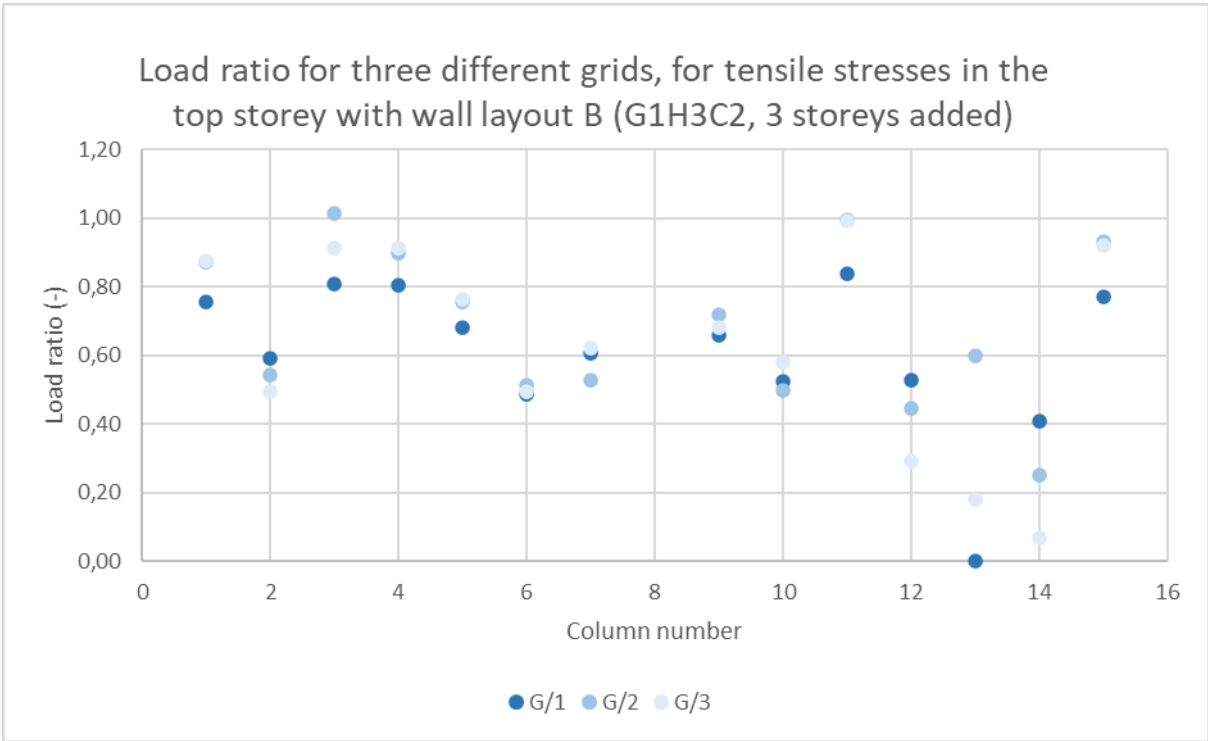


Load ratio for maximum compressive stress in top storey columns (G1H3C2, G/2, 3 storeys added)

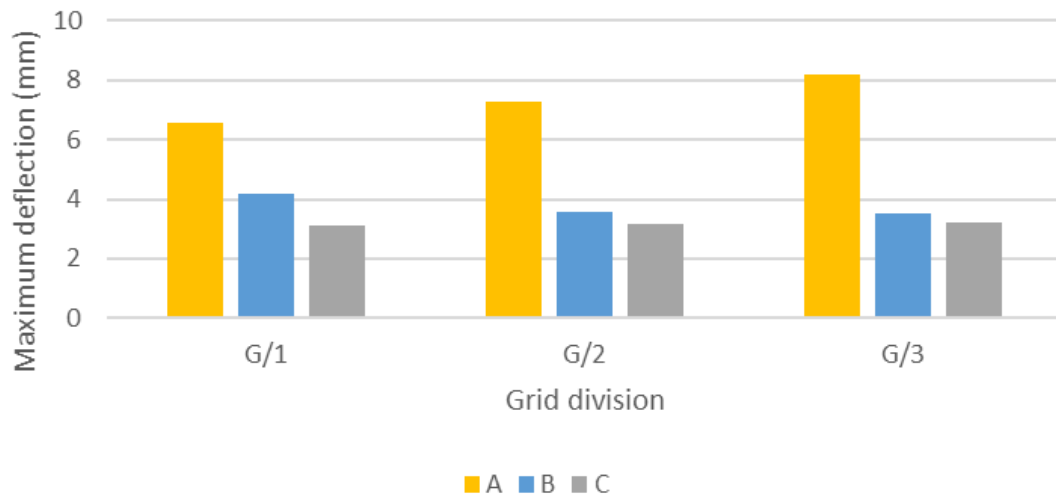


Load ratio found in foundation piles for wall variants A, G1H3C2, 3 storeys added

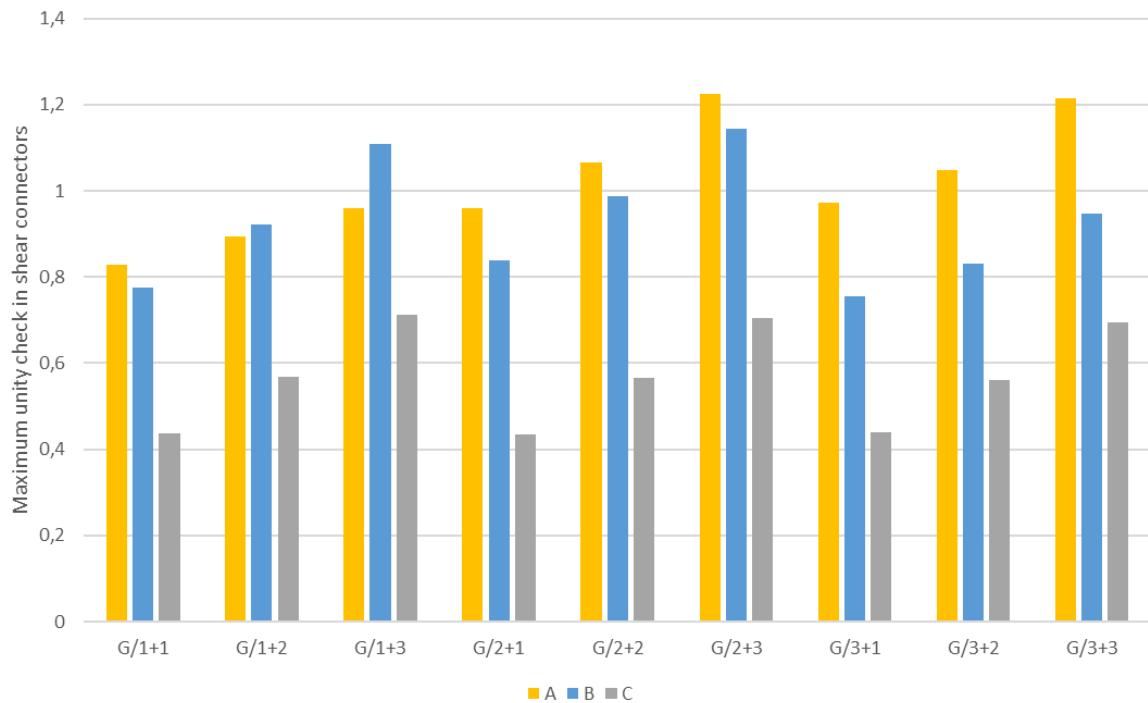




Maximum deflection for different wall layouts and extension grids (G1H3C2), 3 storeys added

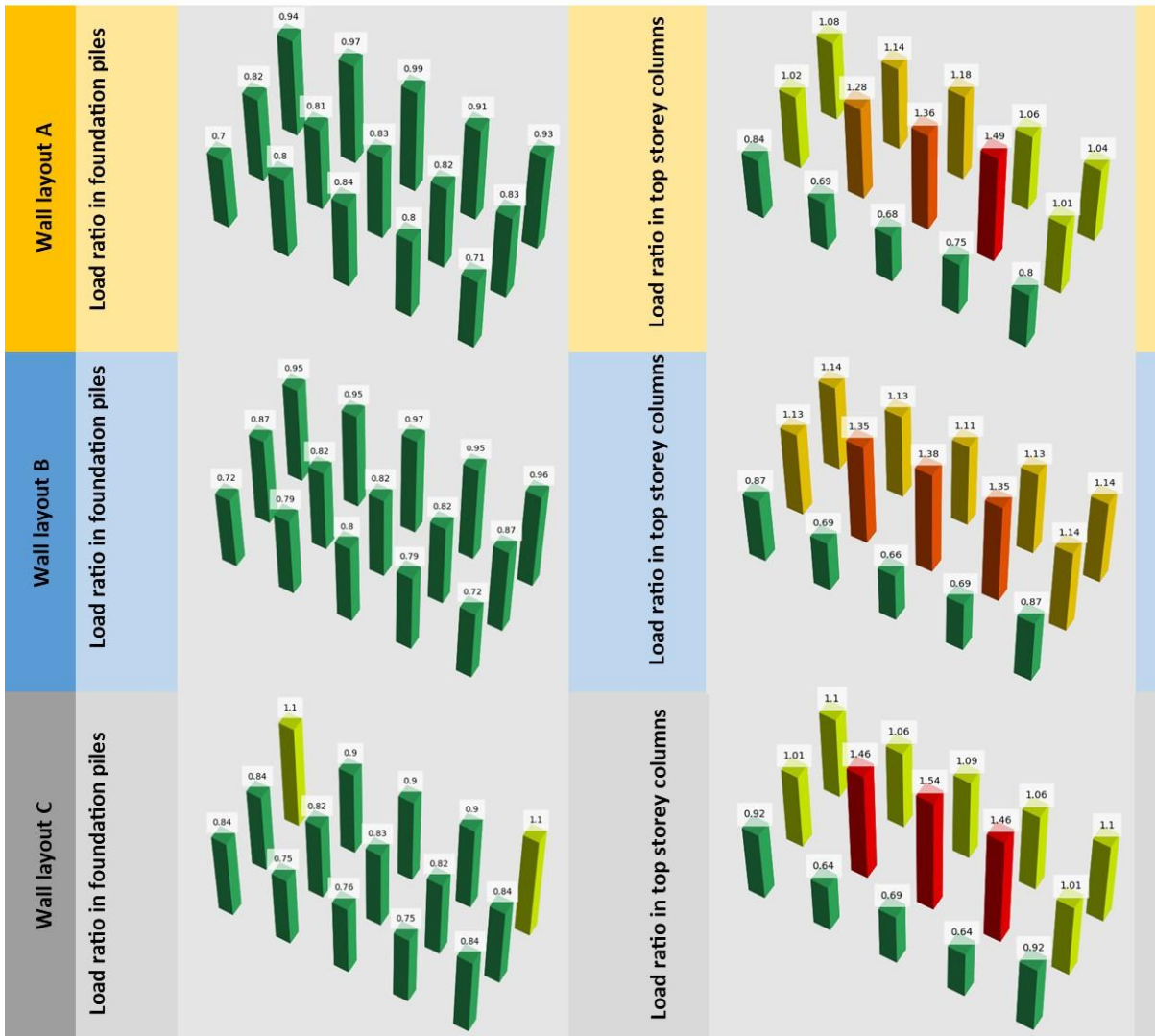


Maximum unity check in shear connectors for variant G1H3C2

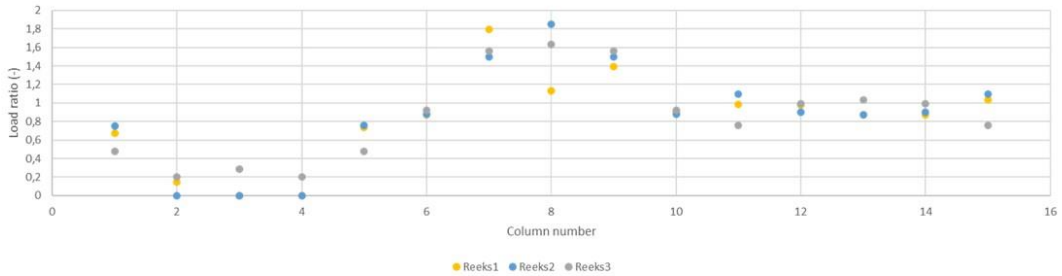


C3 – SHEETS

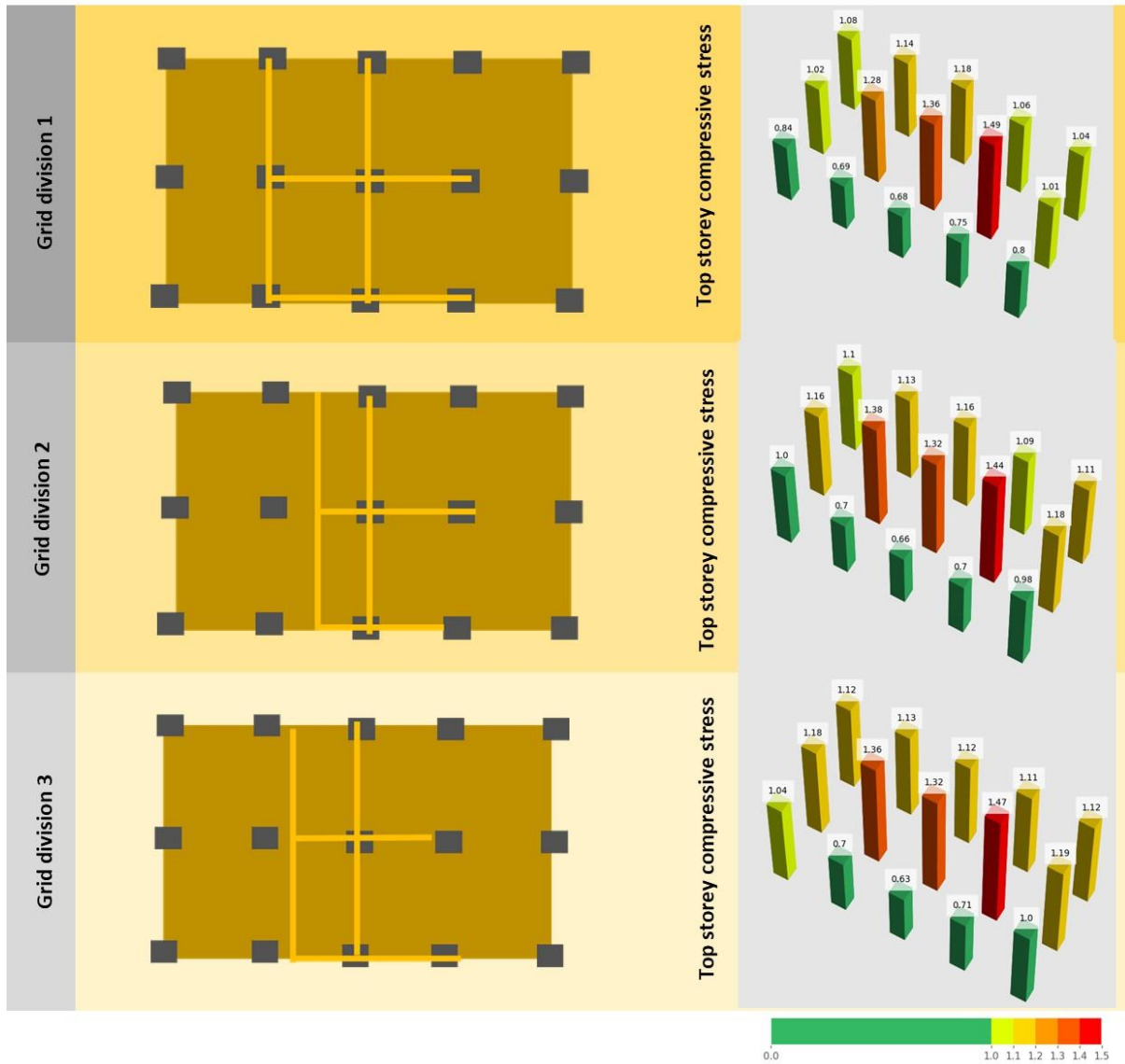
Load ratios for different wall layouts on a G1H3C3 variant (extension grid = G/1), 3 storeys added



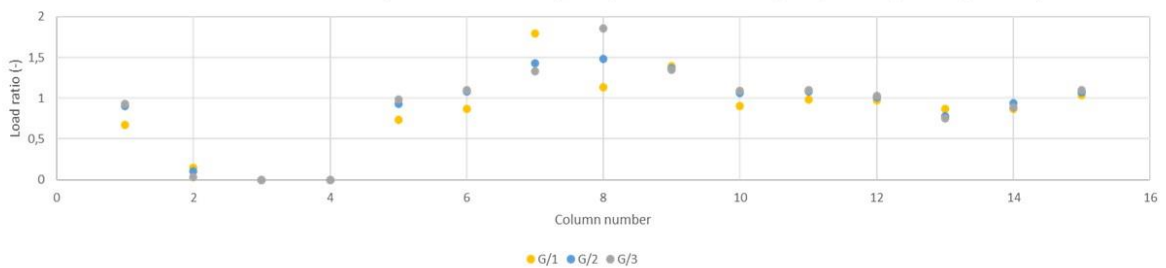
Load ratio for tensile stress in the top storey columns for three wall layouts in a G1H3C3 variant (G/1, 3 storeys added)



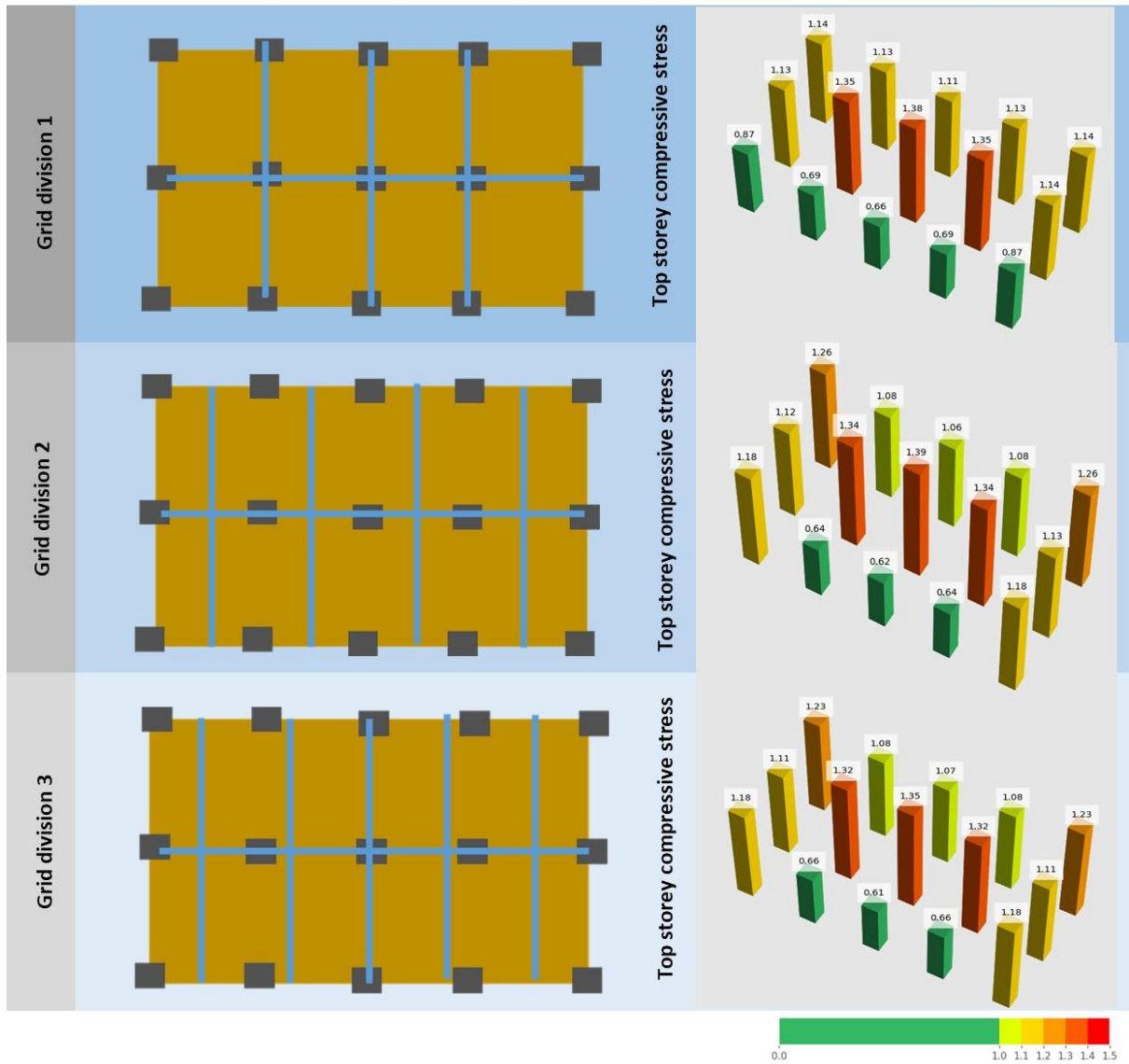
Load ratios for different extension grids on a G1H3C3 variant (wall layout A: core aligned), 3 storeys added



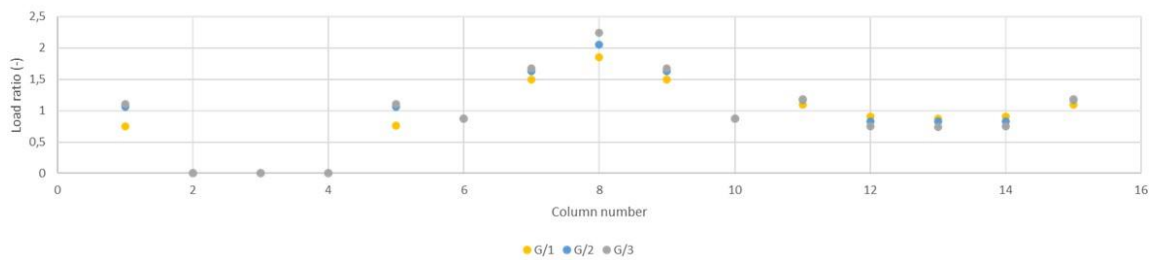
Load ratio for tensile stress in top columns for wall layout A, for three different grids (G1H3C3, 3 storeys added)



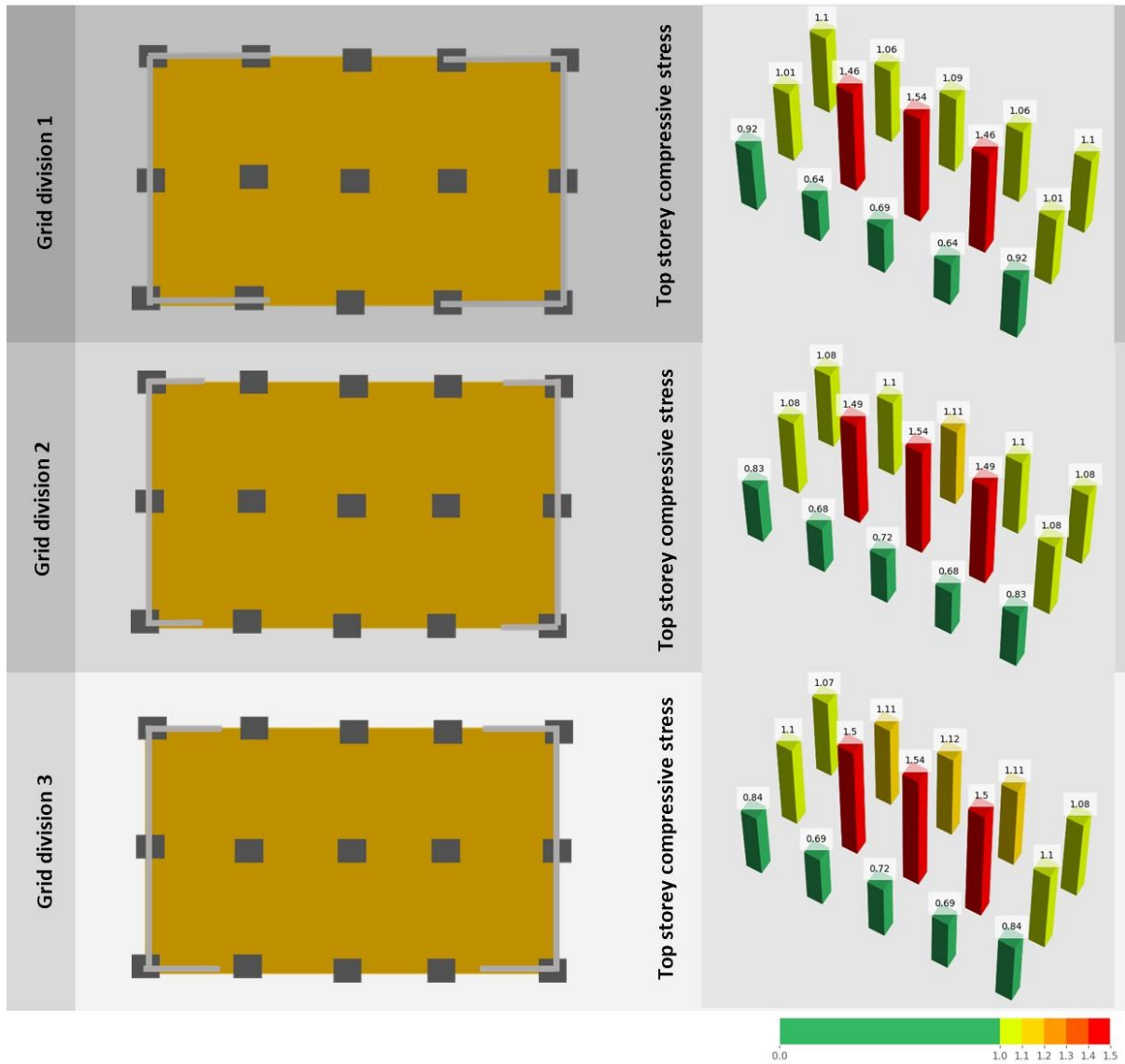
Load ratios for different extension grids on a G1H3C3 variant (wall layout B: functional design), 3 storeys added



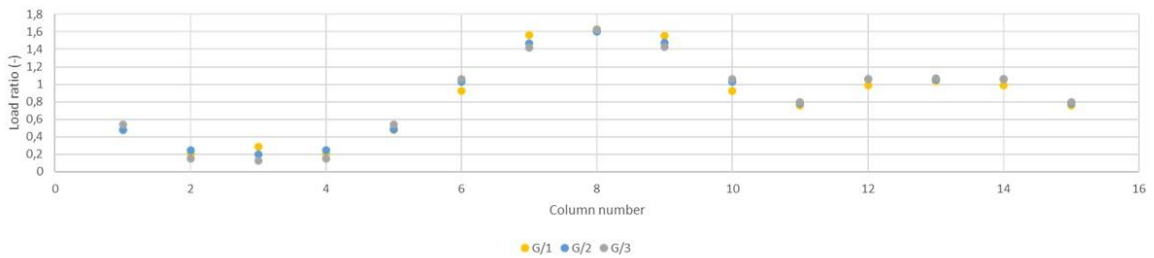
Load ratio for tensile stress in top columns for wall layout B, for three different grids (G1H3C3, 3 storeys added)



Load ratios for different extension grids on a G1H3C1 variant (wall layout C: facade aligned), 3 storeys added

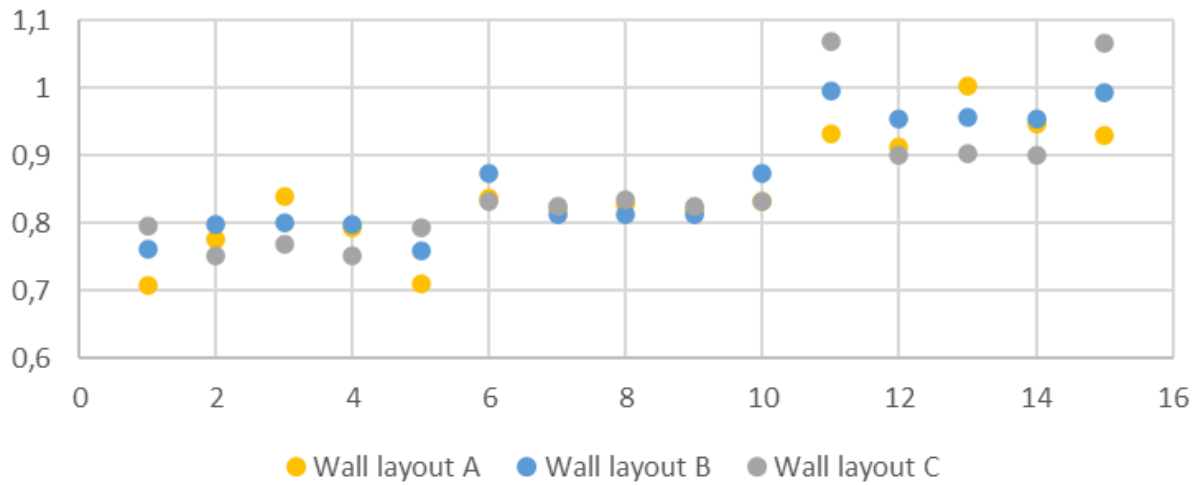


Load ratio for tensile stress in top columns for wall layout C, for three different grids (G1H3C3, 3 storeys added)

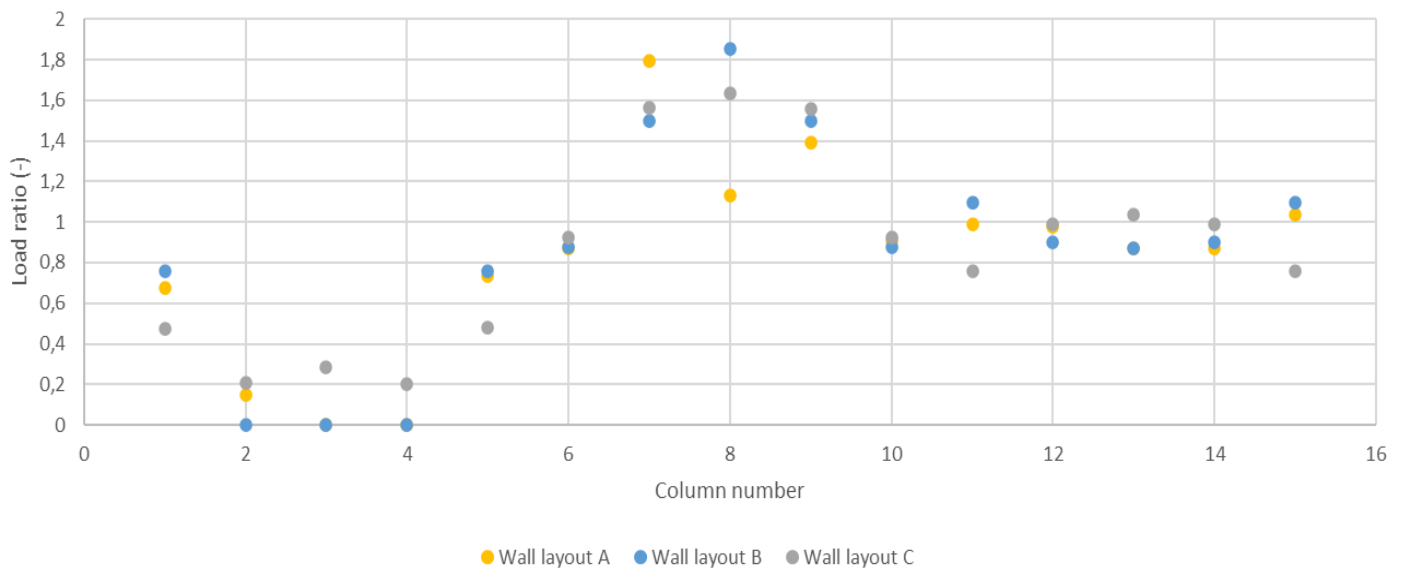


C3- GRAPHS

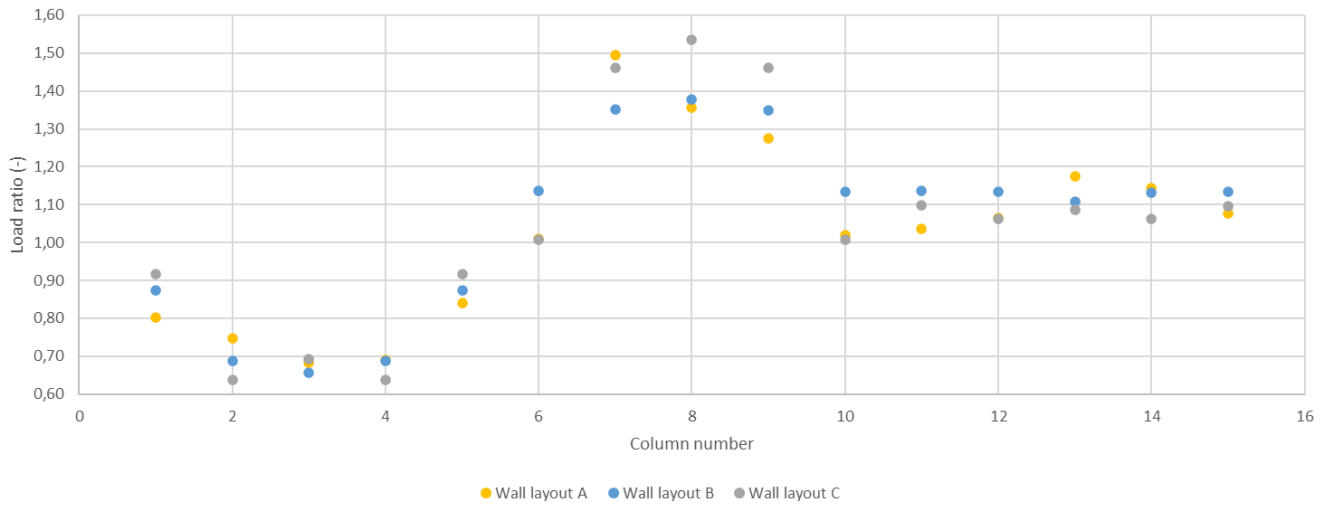
Load ratio for normal forces in foundation piles under columns for variant G1H3C3, 3 storeys added (G/2)



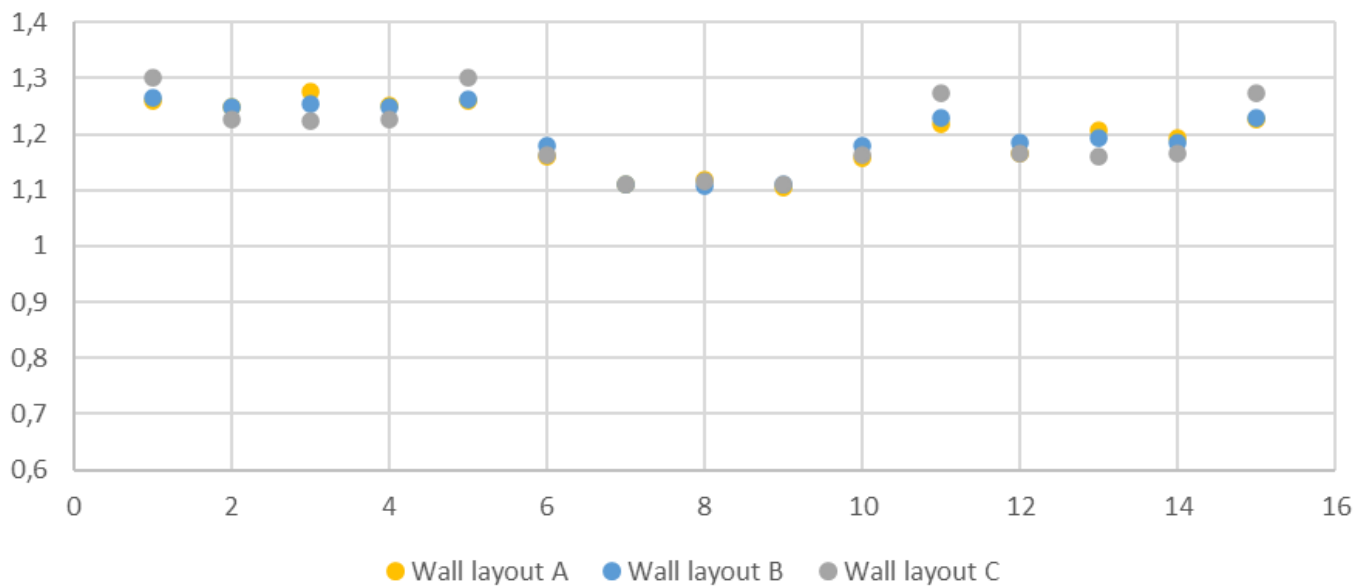
Load ratio for tensile stress in the top storey columns for three wall layouts in a G1H3C3 variant (G/1, 3 storeys added)



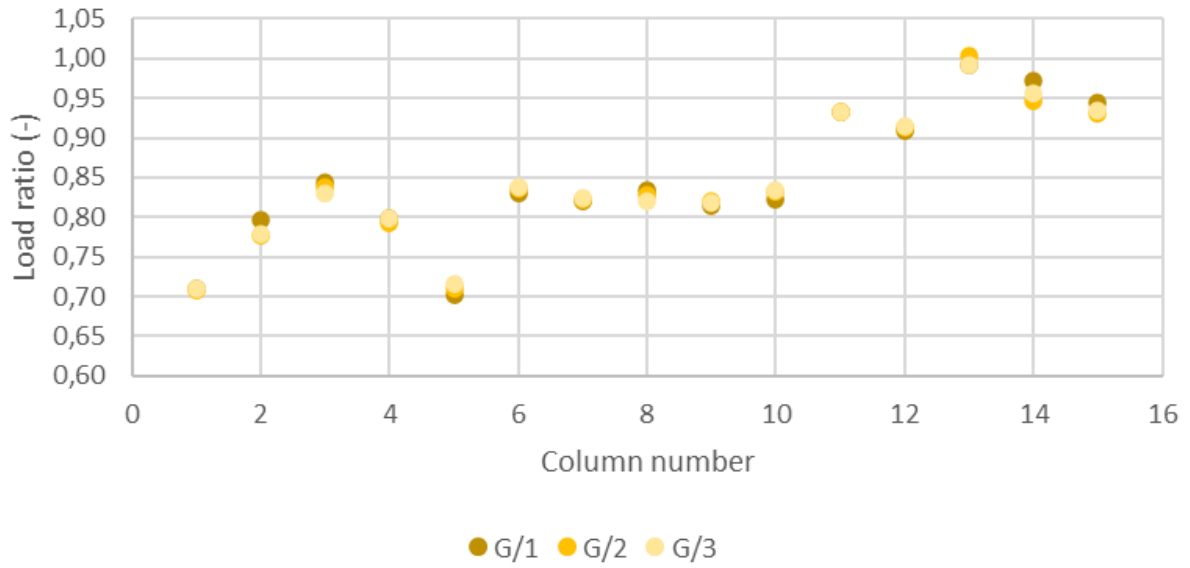
Load ratio for compressive stress in the top storey columns for three wall layouts in a G1H3C3 variant (G/1, 3 storeys added)



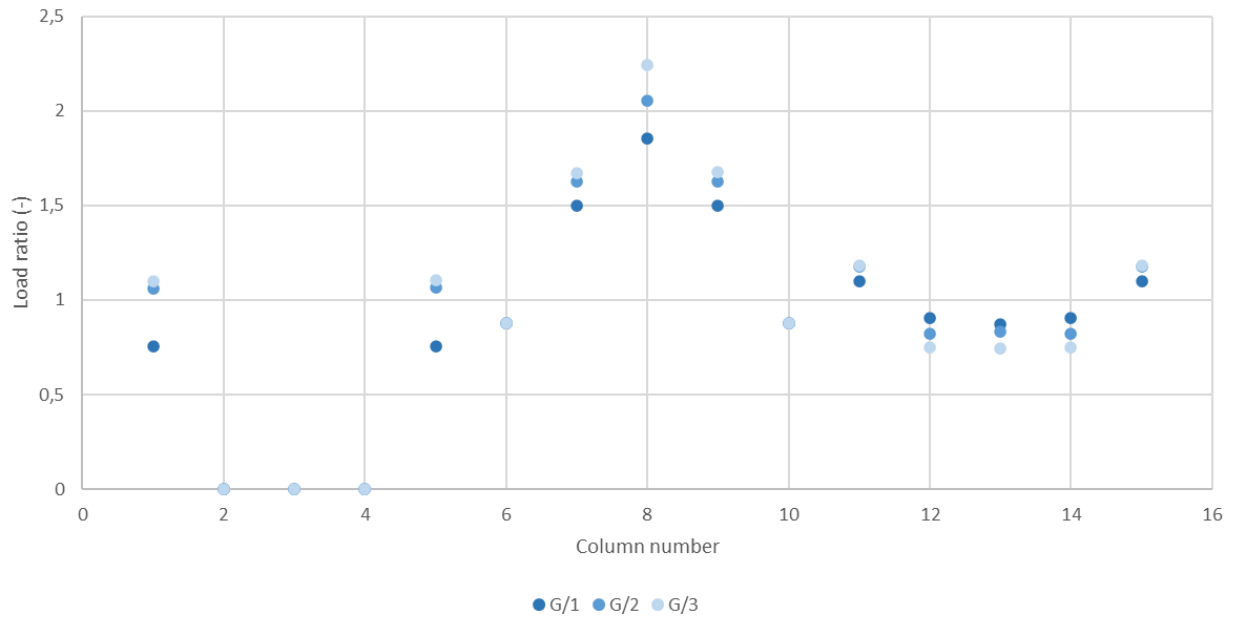
Load ratio for compressive stress in ground floor columns for variant G1H3C3, 3 storeys added (G/1)



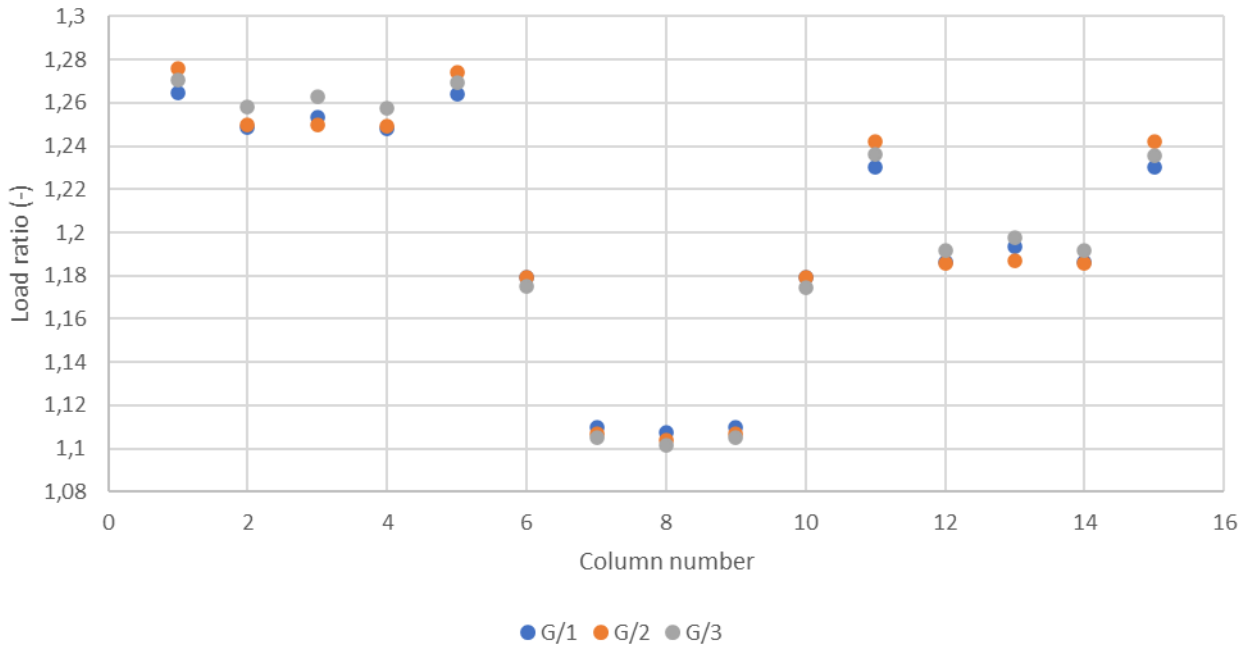
Load ratio in foundation piles for wall variants A, G1H3C3, 3 storeys added



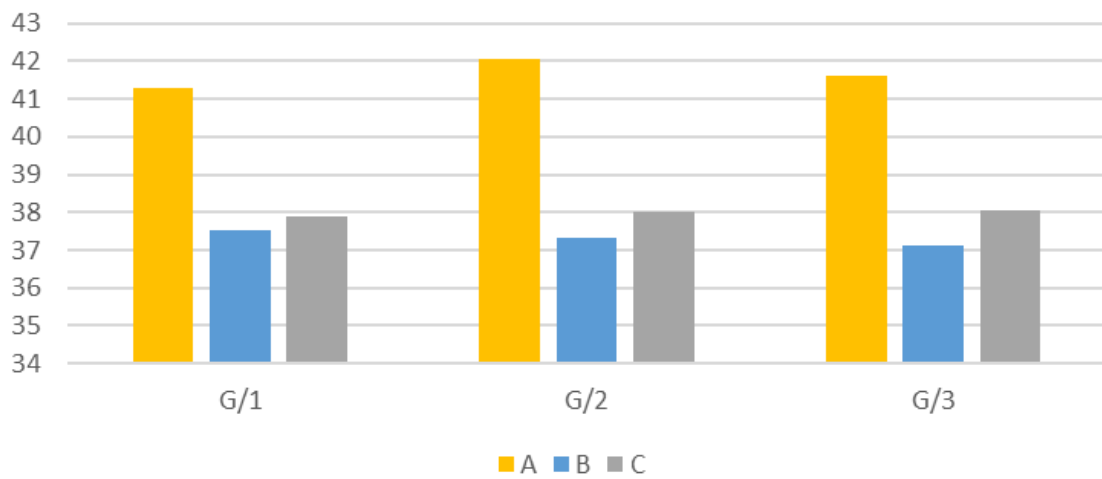
Load ratio for tensile stress in top columns for wall layout B, for three different grids (G1H3C3, 3 storeys added)



Load ratio for three different grids, for compressive stress in ground floor columns, wall layouts B, G1H3C3, 3 storeys added



Maximum deflection for different wall layouts and extension grids (G1H3C3), 3 storeys added



Maximum unity check in shear connectors for variant G1H3C3

